

426

STUDIES ON THE STRUCTURE AND REACTIVITY OF
BICYCLIC SYSTEMS

A Thesis presented for the Degree of
Doctor of Philosophy
in
The University of Stirling
by
Robert Charles Glen

December 1981

Graduation: June 1982



IMAGING SERVICES NORTH

Boston Spa, Wetherby

West Yorkshire, LS23 7BQ

www.bl.uk

BEST COPY AVAILABLE.

**TEXT IN ORIGINAL IS
CLOSE TO THE EDGE OF
THE PAGE**

DEDICATION

To my Father and Mother

ACKNOWLEDGEMENTS

I am indebted to all the research and technical staff who have contributed to this work.

At Glaxo Group Research, Ware, Hertfordshire, I would like to thank the staff of the analytical research department. In particular, Dr. Trevor Cholerton (for running and interpretation of n.m.r. spectra) and Leslie Larkins (for running the g.l.c. experiments). My special thanks go to Dr. Derek Reynolds for his instruction and advice in Organic chemistry and Dr. R. F. Newton, my industrial supervisor, for stimulating discussions.

At Stirling University, I would like to thank Dr. F. G. Riddell for running the ^{13}C n.m.r. spectra, Mr. Don Dance for running the mass spectra, and Chris Lilley for synthesising (29).

This work would not have been possible without the instruction, advice and encouragement of my principal supervisor, Dr. Peter Murray-Rust. For all his efforts, I thank him sincerely.

I am grateful to Mrs. Joan Weber for typing the manuscript. I am indebted to the Science and Engineering Research Council and Glaxo Group Research, Ware, Ltd. for a C.A.S.E. award.

ABSTRACT

Factors controlling the regio- and stereo-selectivity in small polycyclic molecules have been investigated by X-ray diffraction, reactions of model compounds and molecular-mechanics calculations.

The bicyclo[3.2.0]heptene system was investigated in detail. The products on addition of HOBr were isolated and characterised. Similarly, the analogous exo- and endo-epoxides were synthesised and reacted with hydrobromic acid. Product ratios were determined by g.l.c. and confirmed by isolated yields.

The compounds displaying high selectivity have the possibility of a transannular O...C=O interaction which could stabilise the transition state leading to the major product. Investigations of these interactions showed them to be a consequence of the molecular conformation. The energies involved are not sufficient to affect the product ratios.

One compound which displayed an enhanced O...C=O interaction due to the presence of two chlorines vicinal to the carbonyl crystallised as a 1:1 mixture of ring and chain forms in a single crystal. This is the first example of ring-chain tautomers (or reactant and product of a chemical reaction) being isolated in a crystal lattice.

The ground state structures of seven compounds were determined by X-ray diffraction and the transition states were modelled by molecular-mechanics calculations.

The stereoselectivity was explained by steric congestion around the double bond.

Regioselectivity depends on the preferred conformation. From the available data (n.m.r., X-ray structures, molecular-mechanics) the endo-envelope conformer of the bicyclo[3.2.0]heptane system is preferred to the exo-twist conformer. Assuming an antiperiplanar arrangement of the reacting species, this preferred conformation explains the observed regioselectivity.

The exo-bromonium ions and epoxides display higher selectivity than their endo analogues. This has been explained by conformational and steric factors.

CONTENTS

	<u>Page</u>
<u>Chapter 1</u>	
Introduction	1
References	13
<u>Chapter 2</u> Synthesis and reactions of bicyclo[3.2.0]heptane derivatives	15
2.1 Introduction	16
2.2 The formation and reactivity of the bromonium ion	18
2.3 The formation and reactivity of epoxides	21
2.4 Synthesis of compounds of interest	28
2.5 The reactions of synthetic intermediates and products	30
2.6 Conformational analysis of bicyclo[3.2.0]heptan-6-one derivatives by n.m.r.	36
2.7 Summary of results	41
2.8 Experimental	43
2.9 References	57
<u>Chapter 3</u> X-Ray crystallography	60
3.1 Introduction	62
3.2 The geometry and conformation of compounds studied by X-ray diffraction	63
3.2.1 2-(S)- <u>exo</u> -bromo-3-(S)- <u>endo</u> - hydroxybicyclo[3.2.0]heptan-6-one	63
3.2.2 7,8- <u>endo</u> -epoxy-2-oxatricyclo- [3.3.0.0 ^{4,9}]octan-3-one	67
3.2.3 2,3- <u>endo</u> -epoxybicyclo[3.2.0]- heptan-6-one-p-nitrophenylhydrazone	70
3.2.4 3- <u>exo</u> -methoxy-6,7- <u>endo</u> -epoxybicyclo- [3.2.0]octane	73
3.2.5 spiro{5- <u>exo</u> -hydroxy-3-oxatricyclo- [5.1.1.0 ^{4,9}]nonan-8-one-2-1'(4',5'- <u>exo</u> -epoxybicyclo[3.2.0]heptane)}	77

	<u>Page</u>
3.2.6 6- <u>endo</u> -methoxy-8- <u>trans</u> -N-methyl-N- p-toluenesulphonamide-2-oxabicyclo- [3.2.1]octan-2-one	81
3.2.7 2- <u>exo</u> -bromo-3- <u>endo</u> -hydroxy-7,7-dichloro- bicyclo[3.2.0]heptan-6-one	84
3.3 X-ray crystallography experimental	102
3.4 Appendix	
(A) Structure solution by the heavy atom method	118
(B) Direct methods of phase determination	121
(C) Anomalous dispersion	129
3.5 References	132
<u>Chapter 4</u> An investigation of regio-chemical control by transannular O...C=O interactions	135
4.1 Introduction	136
4.2 Review	139
4.3 Survey of O...C=O interactions involving 4-,5- and 6-membered rings	145
4.4 Discussion	151
4.5 References	162
<u>Chapter 5</u> Conformation and stereochemistry in bicyclo[3.2.0]heptane derivatives	164
5.1 Introduction	164
5.2 The conformation of bicyclo- [3.2.0]heptanes	164
5.3 Stereo-selectivity	174
5.4 Regio-selectivity	178
Appendix A. Molecular Mechanics	186
5.5 References	194

Appendix 1 X-ray Structural Data

Tables: bond lengths, bond angles, torsion angles, isotropic temperature factors, anisotropic temperature factors, structure factors.

CHAPTER 1INTRODUCTION

This project has been aimed at gaining a deeper understanding of the factors involved in the promotion of regio- and stereoselectivity in small polycyclic compounds.

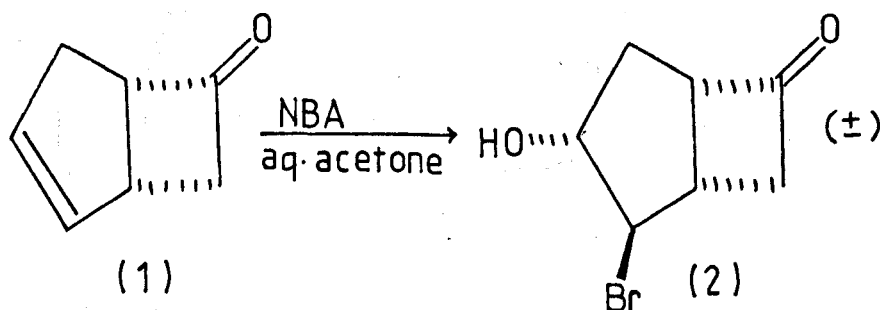
Bicyclic and tricyclic ring systems have been investigated in which the conformation and substitution pattern in one ring can profoundly influence the chemical reactivity of neighbouring rings. Transannular interactions in these coupled ring systems offer unique opportunities in the control of reaction stereochemistry. The bicyclo[3.2.0]-heptane ring system is particularly noteworthy in this respect.¹ The flexibility in stereochemical control is not seen in larger ring systems which are more flexible or in smaller ring systems which have more rigid conformations. Regio- and stereochemical control is especially important in natural product chemistry. The investigations undertaken here are particularly relevant to prostaglandin synthesis^{4-16,21,22}.

The natural prostaglandins are a family of hormone-like substances nominally described as oxidised derivatives of prostanoic acid characterised by a 5-membered ring with two side chains. In general they contain twenty carbon atoms in total^{2,3}. The wide range of biological activity and high potency exhibited by these compounds depends critically on their stereochemistry and this has stimulated pharmaceutical research into the synthesis of natural and analogous compounds⁴ using novel reactions with high stereochemical control.

A recent series of syntheses of prostaglandins

employing bicyclic and tricyclic intermediates utilises the inherent locked stereochemistry of such systems to define the regio- and stereospecificity of the syntheses^{5-16,21,22}. Central to this scheme is the regio- and stereochemical outcome of attack by various nucleophiles and electrophiles on derivatives of bicyclo[3.2.0]heptane⁵⁻¹⁷. (1).

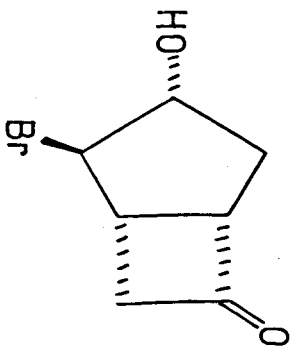
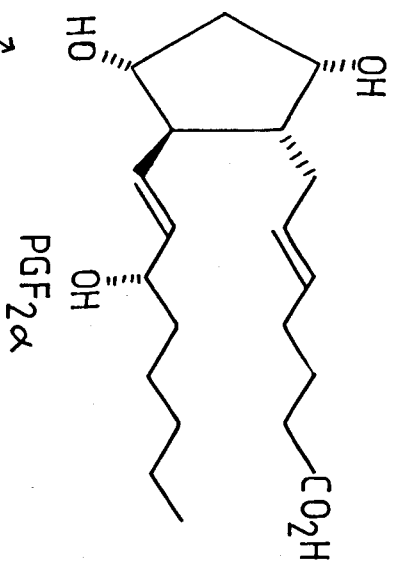
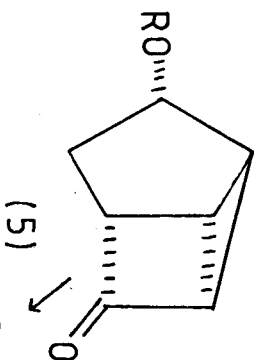
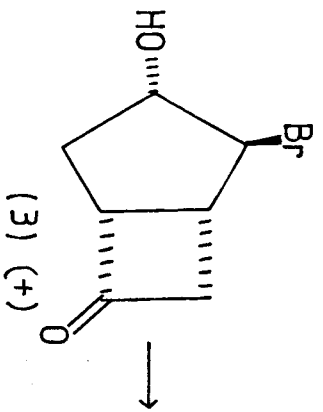
In particular, the addition of the elements HOBr to (1) gives the bromohydrin (2), a key synthon, in high yield via a regio- and stereoselective process^{6,23}.



The enantiomeric bromohydrins (3) and (4) may be obtained via a novel route involving yeast enzymes¹⁰. The enantiomer (3) can be converted to natural prostaglandins via the tricyclic ketone (5). The enantiomer (4) also gives natural prostaglandins via the epoxide (6) which is attacked regioselectivity by nucleophiles at C(2) exo to the cyclopentane ring.

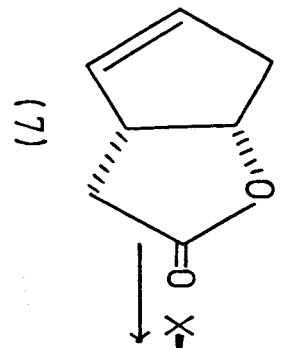
The regio- and stereoselectivity of (1) is in direct contrast to that of (7), which, under similar reaction conditions, gives an isomeric mixture of products⁶.

Analogous non-selective opening of the lactone (8) proved to be a serious flaw in an otherwise useful route to prostaglandins¹⁸.

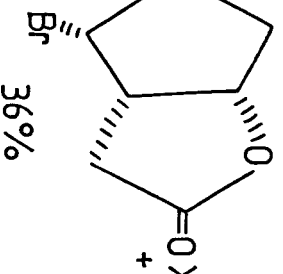


(4) (-)

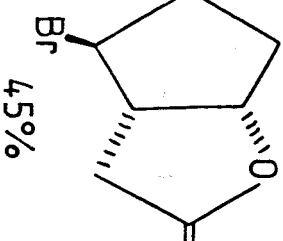
(6)



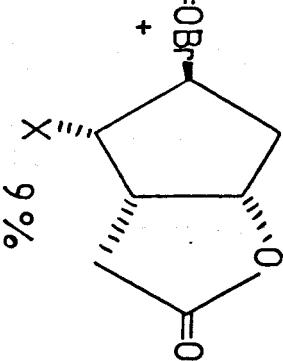
(7)



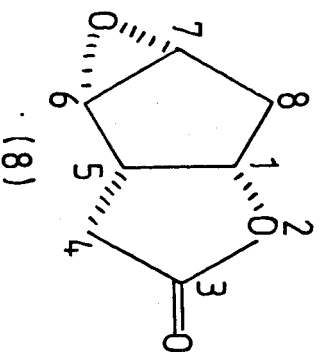
36%

X=CH₃OC(=O)-

4.5%



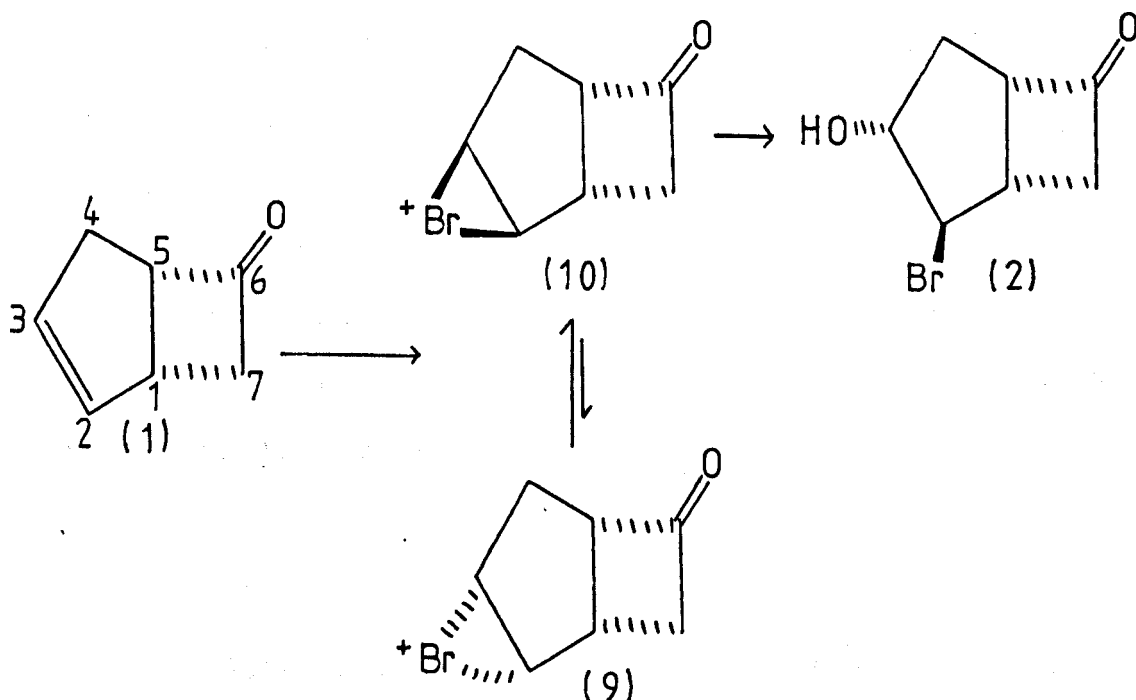
9%



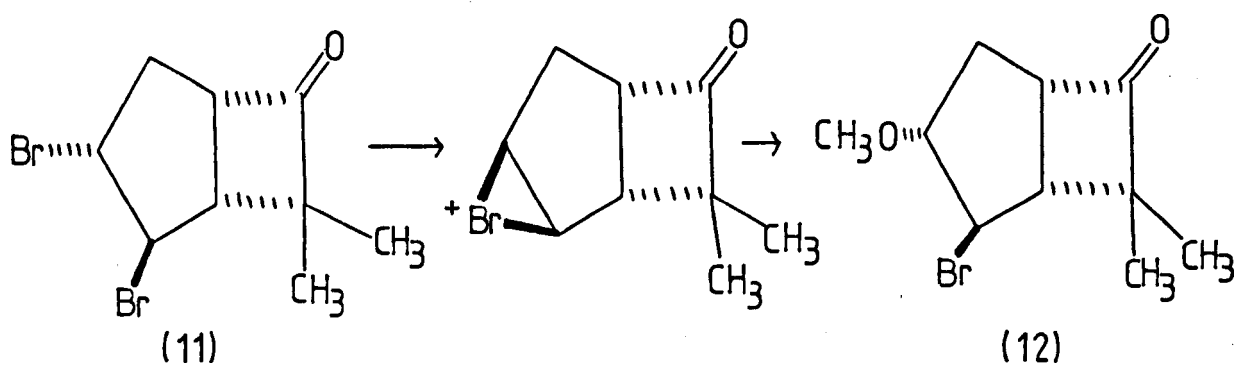
(8)

Several mechanisms have been invoked to explain the isomer ratios obtained in reactions of the type outlined above. In particular, the factors influencing the regio- and stereo-selectivity observed on addition of the elements HBr to (1) and its derivatives²⁰ in contrast to the non-selective reactions of (8) and analogous compounds under similar conditions have been investigated in detail and are reviewed below.

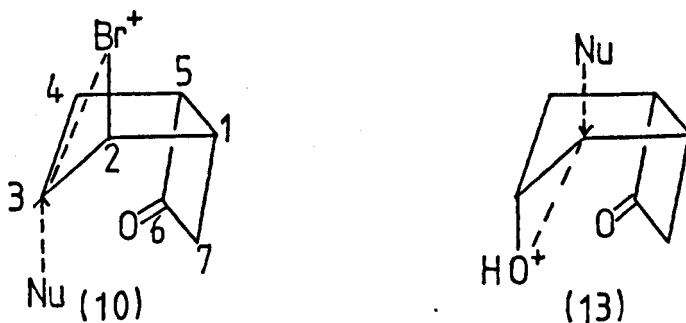
The initial step in bromohydrin formation from (1) is thought to be bromonium ion formation. It has been shown that in brominations in protic solvents involving N-bromoacetamide (NBA), bromonium ion formation is reversible and defines specificity¹⁹. Thus, formation of the endo-bromonium ion would appear to be a sterically disfavoured process due to the close proximity of the cyclobutane ring.



The marked preference for the formation of the exo- rather than the endo-bromonium ions is illustrated by silver tetrafluoroborate-promoted conversion of (11) to (12) in 70% yield¹⁷. The unreactivity of the more accessible bromine atom in the 2-exo position of the ketone is due to the inability of the neighbouring bromine atom in the 3-endo position to form an endo-bromonium ion.

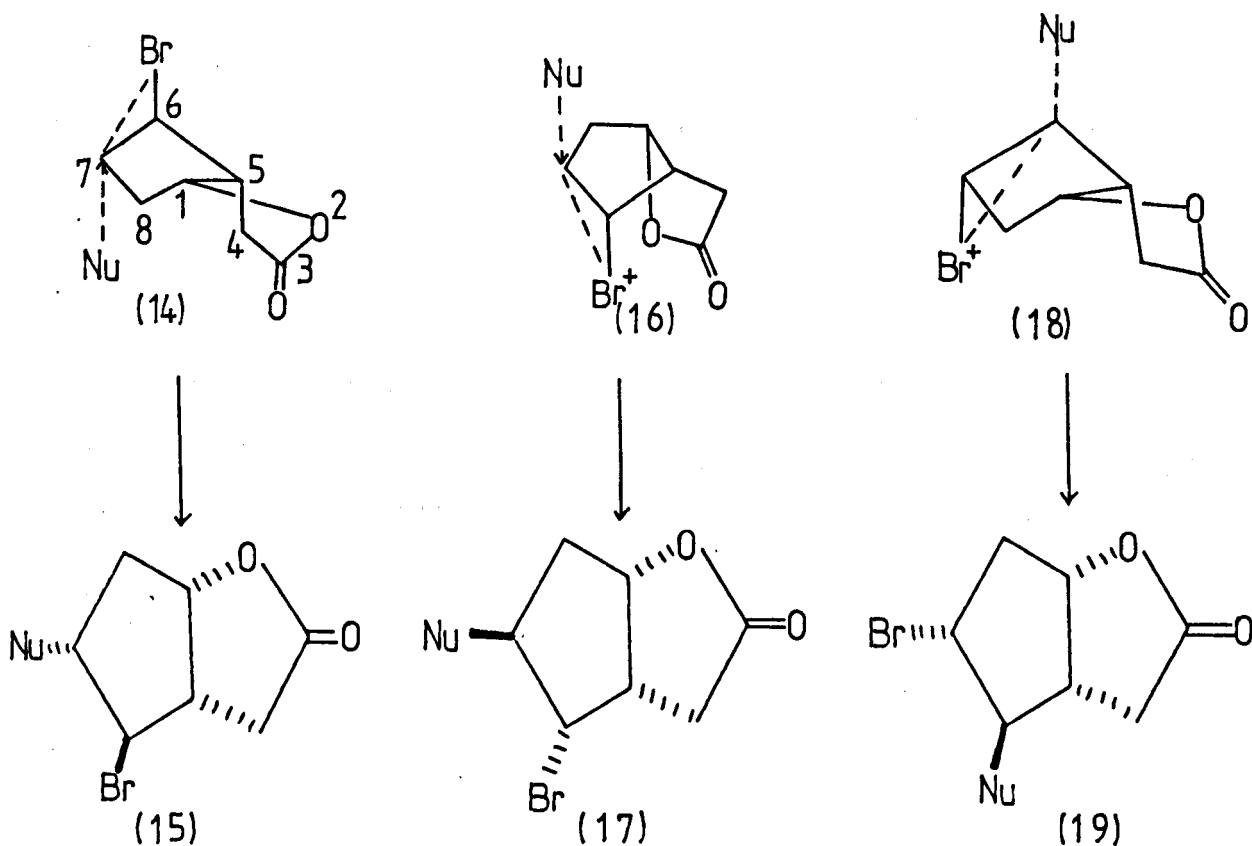


A number of possible transition states have been compared in a qualitative manner to explain the stereoselective bromonium ion opening of (10) and the analogous opening of the protonated epoxide of (6)^{17,20}. The cyclopentane ring was thought to exist preferentially in the endo-envelope conformation with the incipient 2-exo and 3-endo substituents trans orientated and coaxially disposed hence favouring the 2-exo-bromo-3-endo-hydroxy product (the nucleophile being OH^- in this case). Nucleophilic attack occurs at C(3) on the exo-bromonium ion (10) and at C(2) on the protonated epoxide (13).



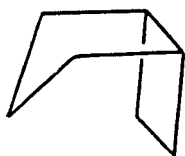
In contrast, molecular models suggested that the lactone (7) was more flexible and could more easily flip from the endo- to the exo-conformations thus promoting formation of endo- and exo-bromonium ions in more equal proportions. Hence formation of the exo-bromonium ion followed by selective attack at C(7) via the transition state (14) would give rise to the lactone (15).

Similarly, the lactone (17) may be formed from the endo-bromonium ion via the transition state (16) in which non-bonded interactions are minimised (from models). The endo-bromonium ion can also give rise to the minor product (19) via the transition state (18). This transition state has an unfavourable transannular interaction between the bromine atom and H-4endo.

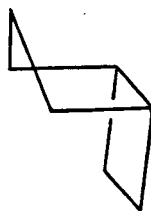


The influence of substituents on the conformation and reactivity of the bicyclo[3.3.0]octanone system has been investigated. The endo-bromonium ions and protonated exo-epoxides derived from (7) are attacked by nucleophiles at C(6) and C(7). The regioselectivity of attack is dictated to some extent by the nature and configuration of substituents at C(4) (e.g. bromine)⁶. These substituents influence the stereochemical outcome of the reaction by raising the energy of some of the possible transition states. Unfavourable transannular steric interactions and the alignment of dipoles (C-Br and C=O) appear to be the major destabilising factors.

Similarly, electrophilic brominations of (1) and several derivatives of (1) have revealed (utilising coupling constant data from nuclear magnetic resonance studies) that substituents on C(2) and C(7) can exert control over the conformation of the system¹⁷. The analysis of these data appeared to show that 7,7-dichloro substituted bicyclo[3.2.0]hept-2-ene-6-one derivatives have a twist in the cyclobutane ring of ca. 20°, while the 2-bromobicyclo[3.2.0]heptan-6-ones have an essentially planar cyclobutane ring. Also, the sole or major contributing conformation of the bicyclic system in such derivatives appeared to be the endo-envelope conformation (20) in preference to the exo-envelope conformer (21)¹⁷. In this conformation, the bulky groups at C(2) and C(7) (in the series of derivatives of bicyclo[3.2.0]heptane considered here¹⁷) are trans diaxial and eclipsing of bonds is minimised.

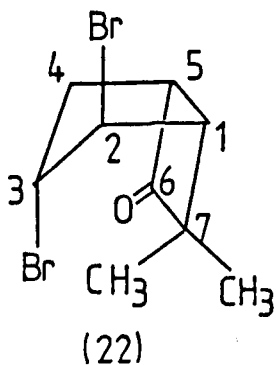


(20)

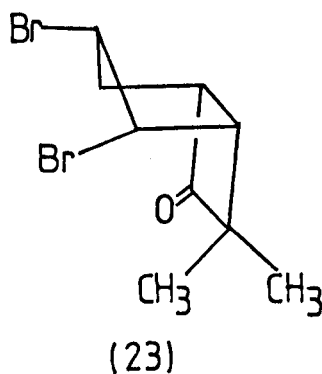


(21)

However, in the 2,3-dibromo-7,7-dimethylbicyclo-[3.2.0]heptan-6-one derivative (23), transannular steric interactions appear to push the cyclopentane ring into the exo-envelope conformation (23). Here, the steric factors present in less substituted rings are outweighed by the transannular interaction between the bulky endo-methyl substituent on C(7) and Br(3)endo (22).



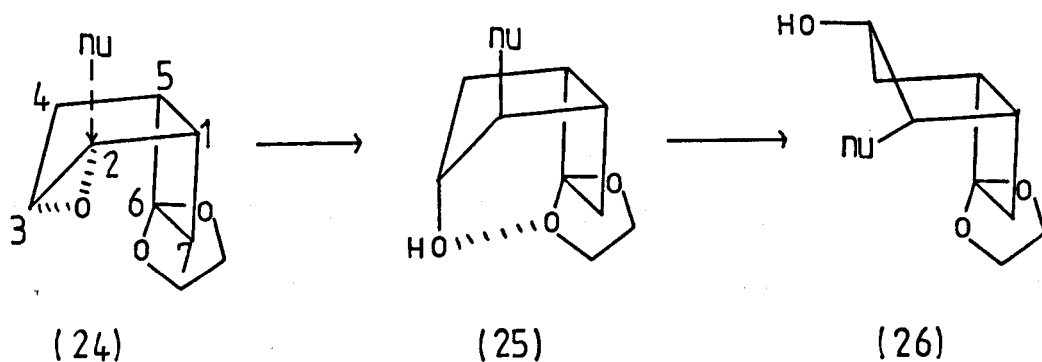
(22)



(23)

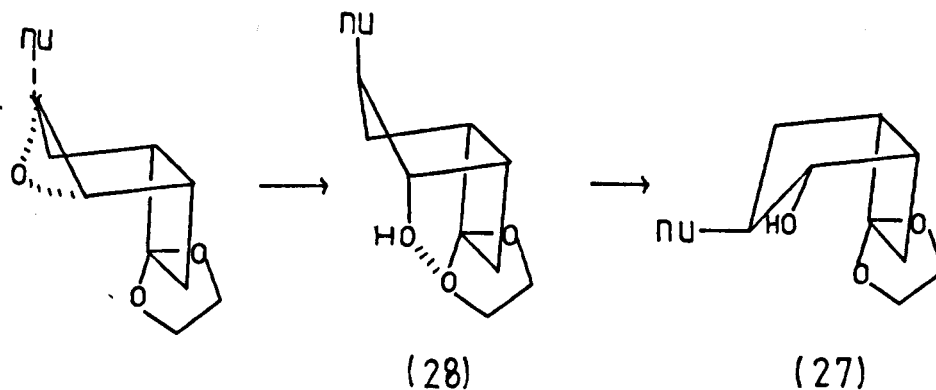
The endo-envelope conformation (20) may be further stabilised under favourable conditions by intramolecular hydrogen-bonding²⁴.

The ketal (24), a key intermediate in prostaglandin synthesis²⁴ reacts stereospecifically with organocuprate reagents preferentially forming the 3-endo-hydroxy product: 2-exo-hydroxy product in the ratio of 4:1.

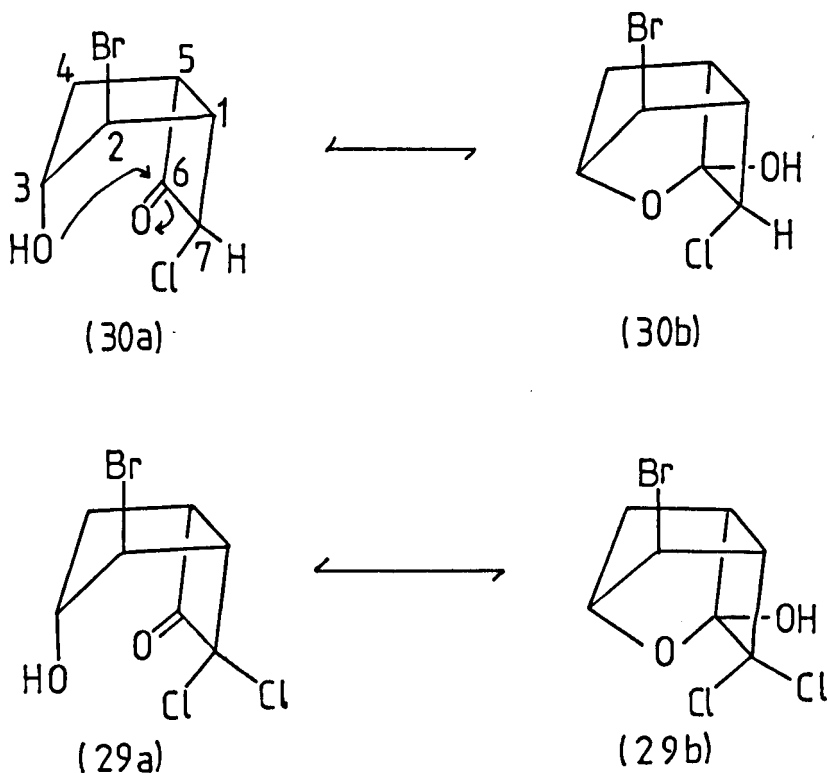


The hydroxy group at C(3) is intramolecularly hydrogen-bonded to the endo-ketal oxygen (from infra-red measurements; $\nu_{\max} = 3500 \pm 30 \text{ cm}^{-1}$, independent of concentration)²⁴. This supports the limiting endo-conformation and subsequent exo nucleophilic attack at C(2). In the alternative exo-envelope (26), intramolecular hydrogen-bonding is geometrically impossible.

The alternative 2-endo-hydroxy product (27), exhibits no intramolecular hydrogen-bonding (free OH at $\nu = 3590\text{-}3620 \text{ cm}^{-1}$)²⁴ indicating that the substituents at C(2) and C(3) are pseudo-equatorial with the cyclopentane ring in the endo-conformation. The absence of intramolecular hydrogen-bonding implies the absence of the exo-conformation, which could conceivably display hydrogen-bonding between OH(2)endo and the endo-ketal oxygen (O...O from models is ca. 2.4Å).

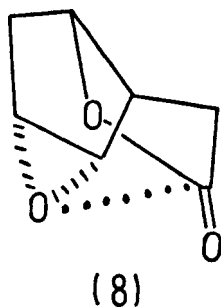


The possible role that transannular electronic effects could play in the stabilisation of particular reaction products was intimated by the observation of ring-chain tautomerism in derivatives of (1). In (30), the substitution of hydrogen at C(7) by chlorine increases the electropositive nature of the carbonyl carbon C(6). This effect, coupled with the close proximity of a hydroxyl group on C(3) results in transannular nucleophilic attack by the hydroxyl group, directed upon C(6)¹⁷.



In carbon tetrachloride solution, a tautomeric mixture of (30a):(30b) is observed in the ratio of 4:1. Disubstitution at C(7) by chlorine to give (29) further increases the electrophilic nature of C(6), the ratio of chain to ring forms being reduced to 1.1:1 ((29a):(29b)) in carbon tetrachloride.

The ring chain tautomerism observed in (29) indicated the possibility of an additional factor in the conformational stability of similar compounds. This is the non-bonded interaction of the type described by Bürgi, Dunitz and Shefter²⁶. This type of interaction has previously been observed in the lactone (8)²⁷. X-ray structure analysis showed a close transannular O...C=O contact of 2.992(2)Å. The observed endo-twist conformation of the cyclopentane ring could conceivably be stabilised by this interaction. (.....)



Many of the compounds described above have the possibility of such transannular interactions e.g. (4), and their observed stereoselective formation could be in part a consequence of the added stability conferred on the transition state and final product.

Three major approaches have been employed in the investigation of the regio- and stereochemical properties in compounds of the type described above.

Compounds of interest belonging to the bicyclo[3.2.0]-heptane system have been synthesised and their reactions with various nucleophilic reagents have been accurately quantified. The major reaction steps have been simulated by model systems specifically designed to elucidate the major processes controlling

the reactions overall.

X-ray structure analysis has been used extensively to obtain accurate information on the ground state geometries, conformation and flexibility of model compounds and by inference, the transition state geometries and their energies in reactions of interest. In particular, the role of transannular nucleophilic attack in regio- and stereoselective formation of particular products and subsequent stabilisation of their observed conformations has been investigated.

Molecular force-field calculations²⁸ have been employed to estimate the energies and conformations involved in the reaction pathways of interest. In these calculations it was hoped that information inaccessible by experimental methods would be available e.g. the energy and conformation of transition states.

REFERENCES

1. Ali, Mubarik S., Lee, T.V., Roberts, S.M., Synthesis, 1977, p.155.
2. Chemical Society Reviews, 1977, Vol.6, No. 4, p.489.
3. The Radiochemical Centre, Amersham, Technical Bulletin 76/5.
4. Caton, M.P., Tetrahedron, 1979, Vol.35, p.2705.
5. Newton, R.F., Roberts, S.M., Tetrahedron Report, 1980, No. 90.
6. Ali, Mubarik S., Crossland, N.M., Lee, T.V., Roberts, S.M., Newton, R.F., J.Chem.Soc.Perkin 1, 1979, p.122.
7. Grieco, P.A., J.Org.Chem., 1972, 37, p.2363.
8. Dimsdale, M.J., Newton, R.F., Rainey, D.K., Webb, C.F., Lee, T.V., Roberts, S.M., J.Chem.Soc.Chem.Comm., 1977, p.716.
9. Newton, R.F., Howard, C.C., Reynolds, D.P., Wadsworth, A.H., Crossland, N.M., Roberts, S.M., J.Chem.Soc.Chem.Comm., 1978, p.662.
10. Newton, R.F., Paton, J., Reynolds, D.P., Young, S., Roberts, S.M., J.Chem.Soc.Chem.Comm., 1979, p.908.
11. Reynolds, D.P., Newton, R.F., Roberts, S.M., J.Chem.Soc.Chem.Comm., 1979, p.1150.
12. Crossland, N.M., Roberts, S.M., Newton, R.F., J.Chem.Soc.Perkin 1, 1979, p.2397.
13. Chapleo, C.B., Finch, M.A.W., Lee, T.V., Roberts, S.M., Newton, R.F., J.Chem.Soc.Chem.Comm., 1979, p.676.
14. Finch, M.A.W., Lee, T.V., Roberts, S.M., Newton, R.F., J.Chem.Soc.Chem.Comm., 1979, p.677.
15. Ali, Mubarik, S., Finch, M.A.W., Roberts, S.M., Newton, R.F., J.Chem.Soc.Chem.Comm., 1979, p.679.

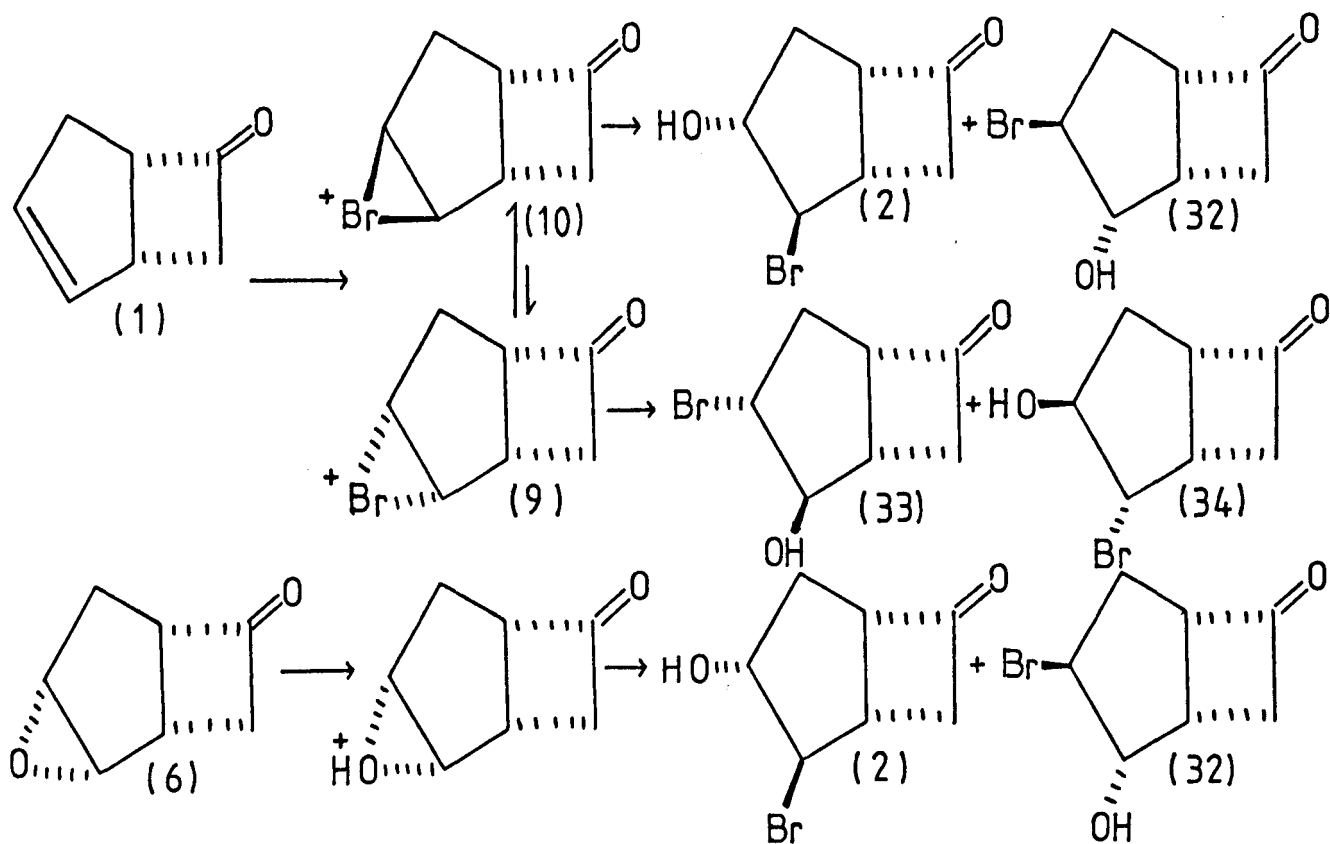
16. Chapleo, C.B., Roberts, S.M., Newton, R.F.,
J.Chem.Soc.Chem.Commun., 1979, p.680.
17. Grudzinski, Z., Roberts, S.M., J.Chem.Soc., Perkin 1,
1975, p.1767.
18. Corey, E.J., Nicolaou, K.C., Beames, D.J.,
Tetrahedron Letters, 1974, p.2439.
19. Ansselemi, C., Berti, G., Catelani, G., Lecce, L.,
Monti, L., Tetrahedron Letters, 1975, p.1215.
20. Berge, J.M., Roberts, S.M., Suschitzky, H., Kemp, J.E.G.,
J.Chem.Soc.Perkin 1, 1980, p.690.
21. Lee, T.V., Roberts, S.M., Dimsdale, M.J., Newton, R.F.,
Rainey, D.K., Webb, C.F., J.Chem.Soc.Perkin 1, 1978, p.1176.
22. Crossland, N.M., Roberts, S.M., Newton, R.F., Webb, C.F.,
J.Chem.Soc.Chem.Commun., 1978, p.660.
23. Roberts, S.M., J.Chem.Soc.Chem.Commun., 1974, p.948.
24. Cave, R.J., Howard, C.C., Klinkert, G., Newton, R.F.,
Reynolds, D.P., Wadsworth, A.H., Roberts, S.M.,
J.Chem.Soc.Perkin 1, 1979, p.2954.
25. Jackman, L.M., Sternhell, S., 'Nuclear Magnetic Resonance
Spectroscopy in Organic Chemistry', Pergamon, Oxford, 1979.
26. Bürgi, H.B., Dunitz, J.D., Shefter, E., Acta Cryst.,
1974, B30, p.1517.
27. Murray-Rust, P., Murray-Rust, J., Newton, R.F.,
Acta Cryst., 1979, B35, p.1918.
28. Allinger, N.L., Advances in Physical Organic Chemistry,
p.1976, 13, p.1.

CHAPTER 2Contents

- 2.1 Introduction
- 2.2 The formation and reactivity of the bromonium ion
- 2.3 The formation and reactivity of epoxides
- 2.4 Synthesis of compounds of interest
- 2.5 The reactions of synthetic intermediates and products
- 2.6 Conformational analysis of bicyclo[3.2.0]heptan-6-one derivatives by n.m.r.
- 2.7 Summary of results
- 2.8 Experimental
- 2.9 References

2.1 Introduction

A number of recent syntheses of prostaglandins have made use of the regio- and stereo-selectivity inherent in the reactions of some small polycyclic molecules.^{1,14} In particular, the addition of the elements HBr to (1) gives the bromohydrin (2) in high yield. Similarly opening of the epoxide (6) by nucleophile gives predominately the bromohydrin (2).



Previously, only those products of synthetic interest have been investigated.

A synthetic scheme has been devised to isolate and characterise those bromohydrins (32,33,34) not previously isolated from these reactions. The product ratios should indicate the ease of formation of each bromohydrin isomer and this can be correlated with subsequent molecular-mechanics

calculations and X-ray structure determinations of relevant molecules.

Similarly, the synthesis and reactions of exo- and endo-epoxide derivatives of the bicyclo[3.2.0] system have not previously been investigated in detail. Here, a number of these have been synthesised and the product ratios obtained when these compounds are reacted with various nucleophiles have been quantified.

Also, to further elucidate the nature of the bromonium ion intermediates (9,10) formed prior to nucleophilic attack, comparisons have been made with the mechanistically similar reaction of epoxide formation. Since nucleophilic attack on the bromonium ion and the protonated epoxide proceed by similar mechanisms, the opening of epoxides by nucleophiles can model nucleophilic attack on the bromonium ion intermediates.

Since much of this chapter is concerned with the formation and reactions of the epoxide and the bromonium ion, these aspects are reviewed briefly (Chapters 2.2, 2.3). The syntheses of compounds of interest are described (Chapter 2.4) as well as their reactions with various nucleophilic reagents (Chapter 2.5) in a series of solvents at various temperatures. The conformational properties of a number of bicyclo[3.2.0]-heptan-6-one derivatives isolated from these reactions have been investigated by n.m.r. (Chapter 2.6). Experimental details are given in Chapter 2.8.

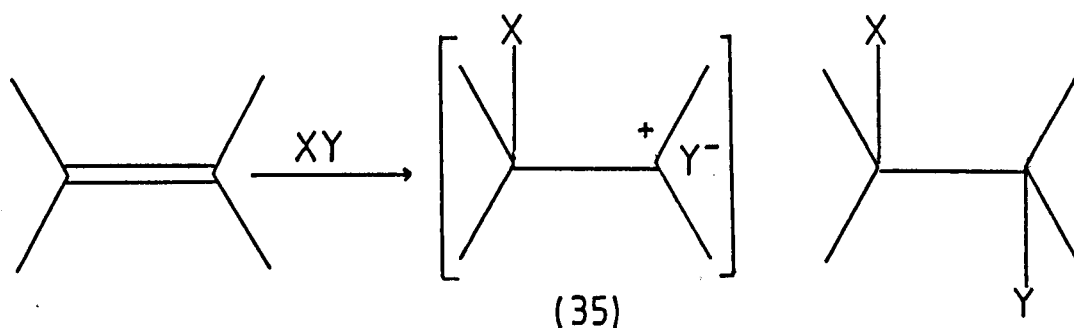
These reactions have provided a necessary experimental basis for subsequent theoretical discussion as well as compounds of use in later analyses.

The results and their significance are discussed in

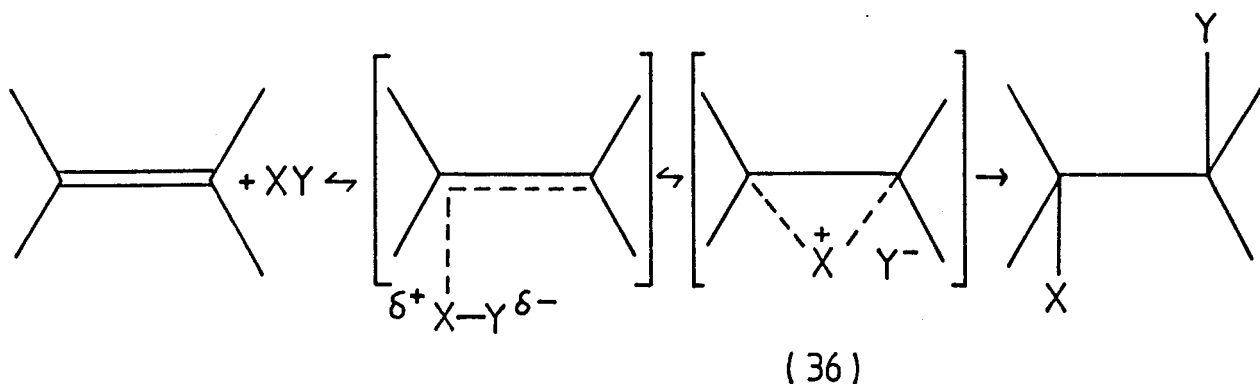
Chapter 2.7 and Chapter 5.

2.2 The Formation and Reactivity of the Bromonium Ion

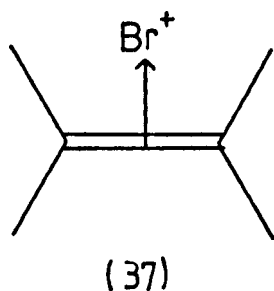
The majority of electrophilic additions to olefins are believed to occur by the so-called AdE_2 mechanism (addition, electrophilic, bimolecular) (using the notation of Ingold¹⁷), i.e. a cationic intermediate is formed¹⁵. The initial approach of the bromonium species is in general governed by steric factors, approach being along the path of least steric resistance. Two possible arrangements are generally assumed to describe the intermediate ionic species. The first is the formation of a negative halide ion and a positively charged organic ion (35).



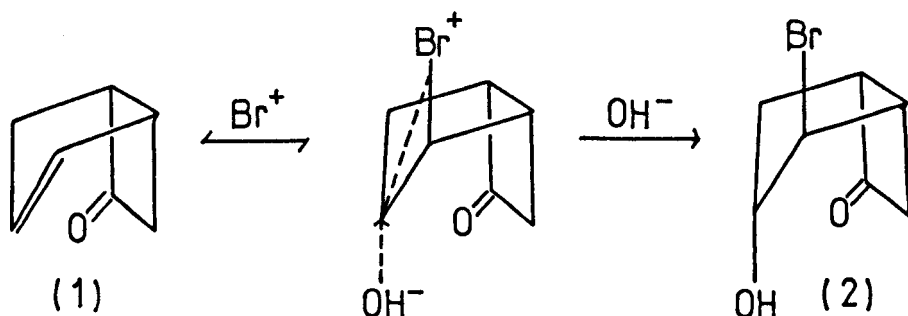
Free rotation about the C-C bond is not to be expected as one of the C^+ orbitals is empty and the Br atom has three orbitals occupied by pairs of electrons. The arrangement is such that a coordinate link will almost certainly be formed by the sharing of one of the pairs of the electrons of the halogen and the unoccupied orbital of the carbon¹⁵. Another possible structure of the ion intermediate is the bridged form (36) with the positive charge on bromine, i.e. it should have a structure similar to that of ethylene oxide¹⁵.



In bromination reactions involving simple olefins, there is a tendency for the predominant involvement of bridged ions¹⁶. This type of bromonium ion seems well established, and in special cases has been observed spectroscopically (n.m.r. studies of Olah and Bollinger)¹⁸; however, it does seem that both open and closed forms do contribute in varying degrees depending on the chemical environment¹⁹. The bridged description can be reformulated as a π -complex (Dewar)²⁰. This approach considers the problem in terms of molecular orbital theory. The intermediate ion can be represented as a dative π -complex (37) formed by an olefin acting as a π -donor, and the ion X^+ acting as an acceptor through its empty atomic orbital. Dewar²⁰ considers that reactions involving primary attack by Br^+ seem almost invariably to involve π -complex intermediates and to give trans adducts exclusively.



Thus, an important consequence of the AdE_2 mechanism for bromination of conformationally biased unconjugated olefins is that the diaxial adduct is obtained^{17,21}, e.g. in the formation of (2) from (1), presumably because of stereo-electronic



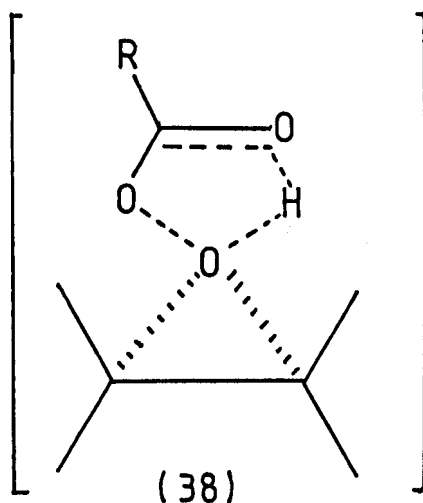
constraints on the opening of the bromonium ion¹⁶. The new atom or group is thought to approach one of the carbon atoms from the side opposite from the halogen already present. A bond to the carbon will be formed while the original C-Br bond is broken, with simultaneous neutralisation of the charges. This process will always lead to trans addition.

The stereo-selectivity of bromonium ion opening appears to depend mainly on substituents attached to the double bond, solvent, and the magnitude of the rate constant¹⁶. It is general that as the substituents at the double bond become more capable of stabilising the developing positive charge, without the assistance of bridging, then the lower is the stereo-selectivity of addition. More ionising solvents lead to lower stereo-selectivity and, in some cases, the solvent may compete for the intermediate ionic species (e.g. in bromohydrin formation from an aqueous solvent with N-bromosuccinamide, the products are formed by solvolysis of the cationic intermediate). If product

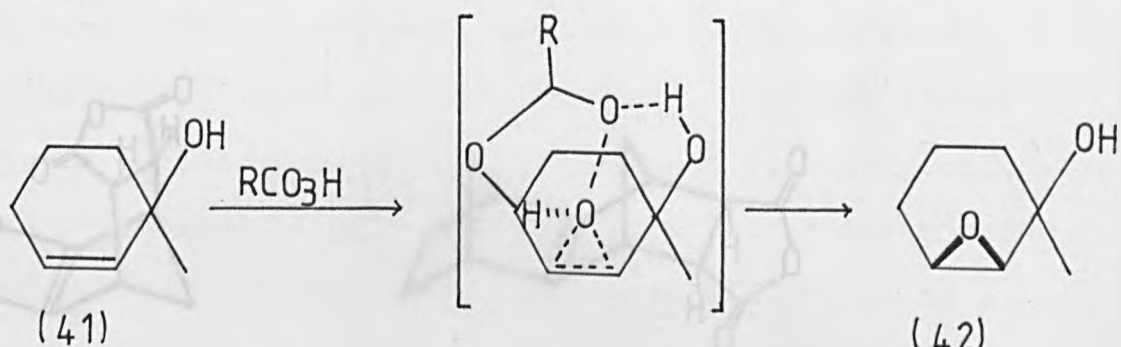
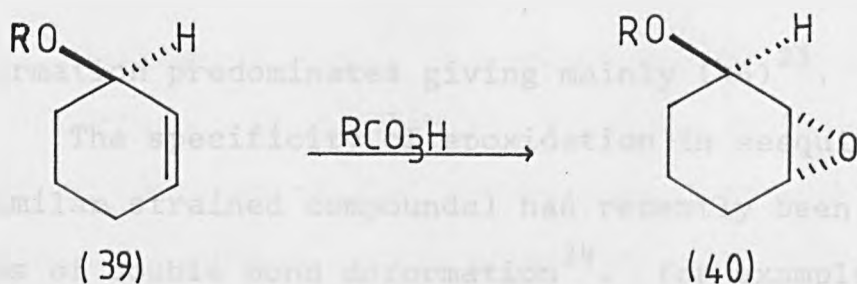
formation is slow, then bridging is encouraged and stereo-selectivity is governed by subsequent nucleophilic attack¹⁶. In bicyclic compounds of the type studied here, there are the additional complications of transannular effects of an electronic and steric nature.

2.3 The Formation and Reactions of Oxiranes

Probably the most widely used method for epoxide synthesis is the peroxy acid oxidation of alkenes. The high stereo-selectivity of addition indicates a cyclic transition state such as (38)^{16,21}.

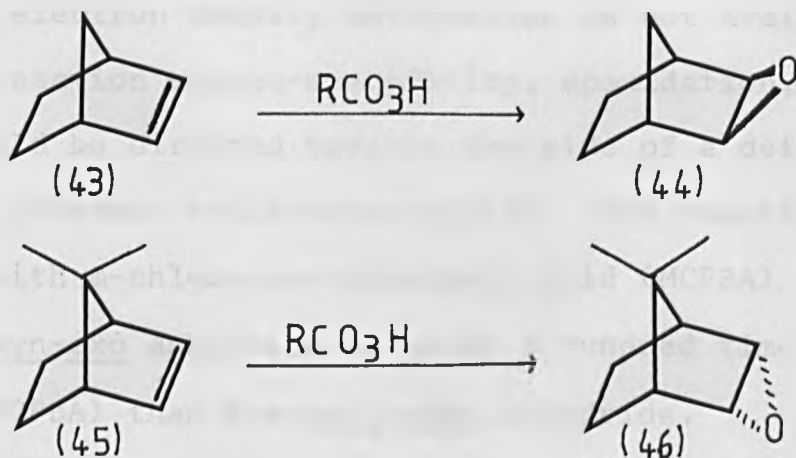


This is consistent with the view that peracids form intermolecular hydrogen-bonds and also that epoxidation is slower in ether solvent (which can form intermolecular hydrogen-bonds with the peracid) than in a hydrocarbon solvent where intramolecular hydrogen-bonding remains intact, i.e. the transition state is more polar than the reactants. The direction of attack by the peracid on the double bond may be influenced by hydrogen-bonding²¹, e.g. in the cyclohexene derivative with a



3-methoxy or 3-acetoxy substituent (39) attack is directed trans to give predominately (40), while in cyclohex-2-ene-ol (41), attack is directed cis to give (42).

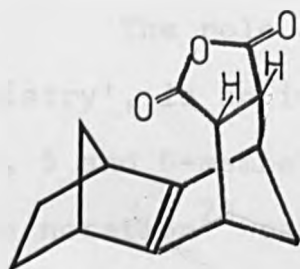
In compounds devoid of polar groups steric effects are very important, e.g. the epoxidation of norbornene (43) gives mainly the exo-epoxide (44) (exo:endo 94:6)²².



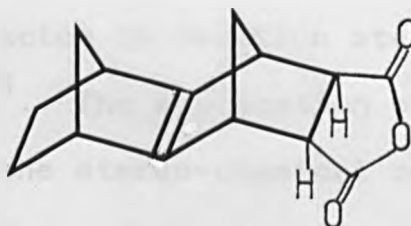
One view is that the endo-hydrogens at C(5) and C(6) hinder endo-attack. Substitution at C(7) by a gem-dimethyl group (45) provides even greater hindrance to exo-attack, here

endo-formation predominates giving mainly (46)²¹.

The specificity of epoxidation in sesquinorbornene (and similar strained compounds) has recently been interpreted in terms of double bond deformation³⁴. For example, in (47)³¹



(47)



(48)

a 'normal planar' double bond length is observed (ca. 1.326Å) and the interplanar angle around the double bond is ca. 180°.

However, in (48) the interplanar angle of 163.6° indicates a significant departure from planarity. This indicates that there is a shift in π -electron density to the region above the plane of the double bond. Unfortunately, deformation electron density studies of sufficient accuracy have not yet been performed on these systems and so quantitative data on the degree of electron density deformation is not available. In terms of reaction stereo-specificity, epoxidation, as described above, would be directed towards the side of a deformed double bond with greatest π -electron density. The reaction of (47) and (48) with *m*-chloro-peroxybenzoic acid (MCPBA) indicates that the syn-exo anhydride is about a hundred times more reactive (towards MCPBA) than the anti-endo anhydride.

Polar substituents (even when removed by several rings) can also direct epoxidation; the effect is solvent dependent, being more pronounced in non-polar media²¹.

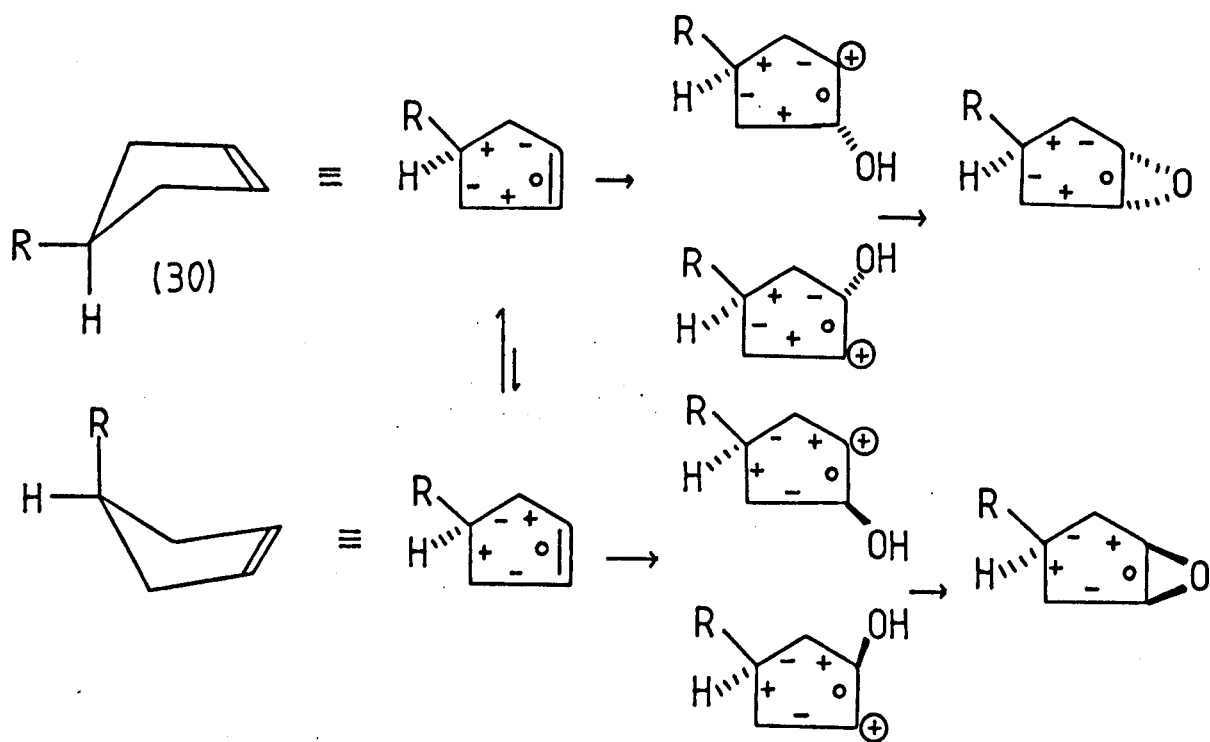
In flexible cyclic molecules able to take up a number of different conformations, the product ratios may be rationalised in terms of the conformational populations of the ground state. Flexible cyclic molecules like cyclohexane derivatives are particularly well described by this treatment¹⁶.

The role of conformational control, 'dynamic stereochemistry', is an important factor in reaction stereo-specificity of 4, 5 and 6-membered rings²⁸. The application of the torsion angle notation²⁹ can predict the stereo-chemical course of a number of reactions where conformational factors predominate. The essence of this method is embodied in the concepts of least conformational change and the maintenance of orbital overlap during the course of a reaction (which leads to the axial orientation of the reactive species at a double bond in the transition state).

Briefly, the torsion angle notation is applied as follows. A number of conformations may be assigned to the reactant and product. The reaction is thought to follow the path of least conformational change. The stepwise cis-addition to the double bond of a low energy conformer is assumed to proceed via perpendicular addition to one of the trigonal atoms. The important point is that there is only one direction of approach to the double bond which satisfies the torsion angle sign sequence and hence the torsion angle sign sequence can predict the direction of addition.

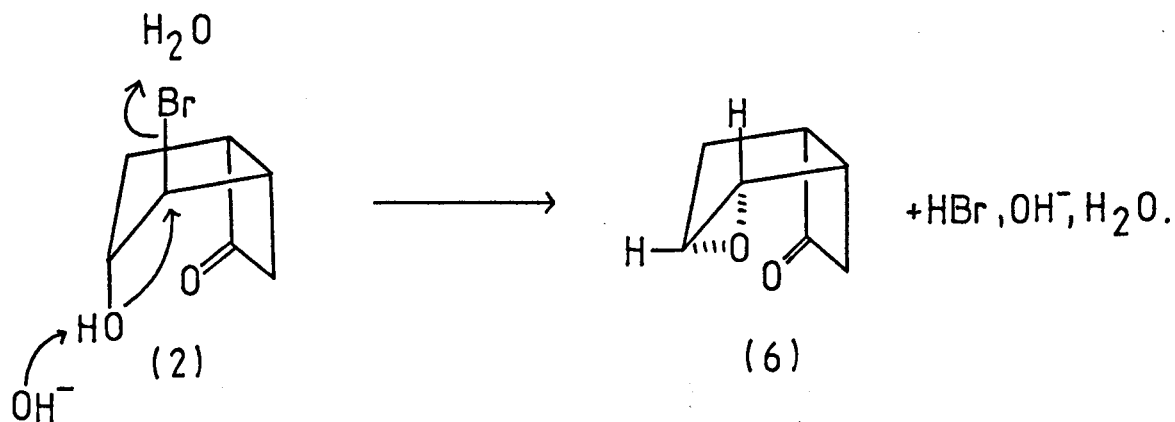
For syn addition to a double bond on a ring, a torsion angle sequence of +0- on the double bond favours addition above the mean plane of the ring while a sequence of -0+ favours addition below the mean plane, e.g. the epoxidation of (30)

proceeds from the preferred conformation with the substituent equatorial via addition of the epoxide below the plane of the ring (torsion angle sequence -0+)²⁸.



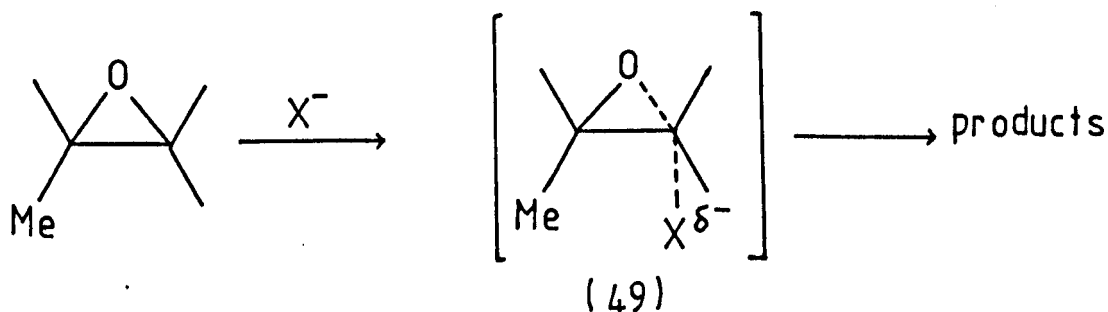
These ideas follow closely the epoxidation of 4-methylcyclopentene³⁰. The general principles of conformational control of epoxide formation are also applicable to bromonium ion formation.

Another important method for production of epoxides is a 1,3-elimination of an alcohol possessing a leaving group in the alpha position. The stereo-electronic requirement for such a reaction is that the 4 centres involved can take up an anti-coplanar arrangement. The halohydrin route is used here in a number of synthetic steps (2.4, 2.5), e.g. the conversion of (2) to (6).



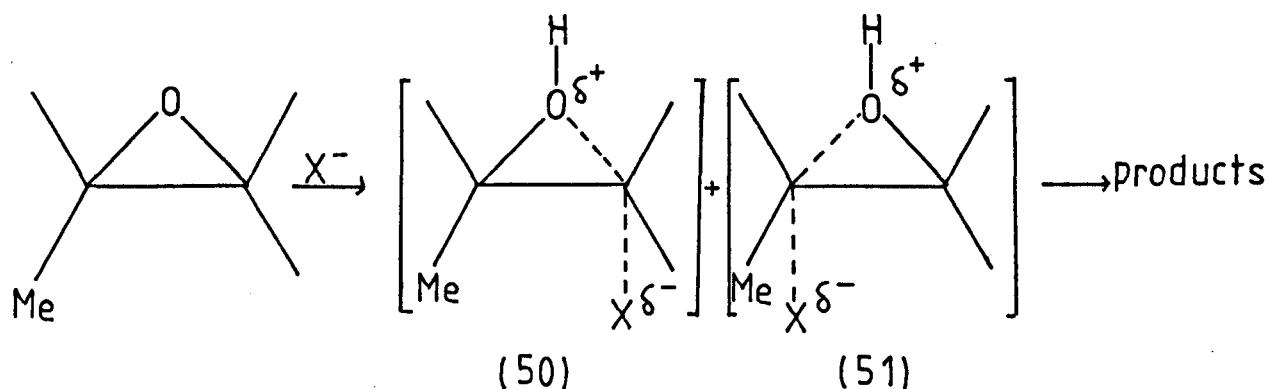
The opening of epoxide rings can be complicated. However, the epoxides of most alkenes open in a stereo-specific trans fashion analogous to opening of the cyclic bromonium ion¹⁵.

Steric, polar and resonance effects can influence the direction of opening in unsymmetrically substituted epoxides¹⁶. Under basic or neutral conditions, the oxygen of the epoxide is unprotonated (49), and nucleophilic attack occurs at the least substituted carbon so here steric factors are of greatest importance. The reaction may be regarded as having essentially S_N2 character, although bond breaking assumes greater importance than usual due to strain in the 3-membered ring.



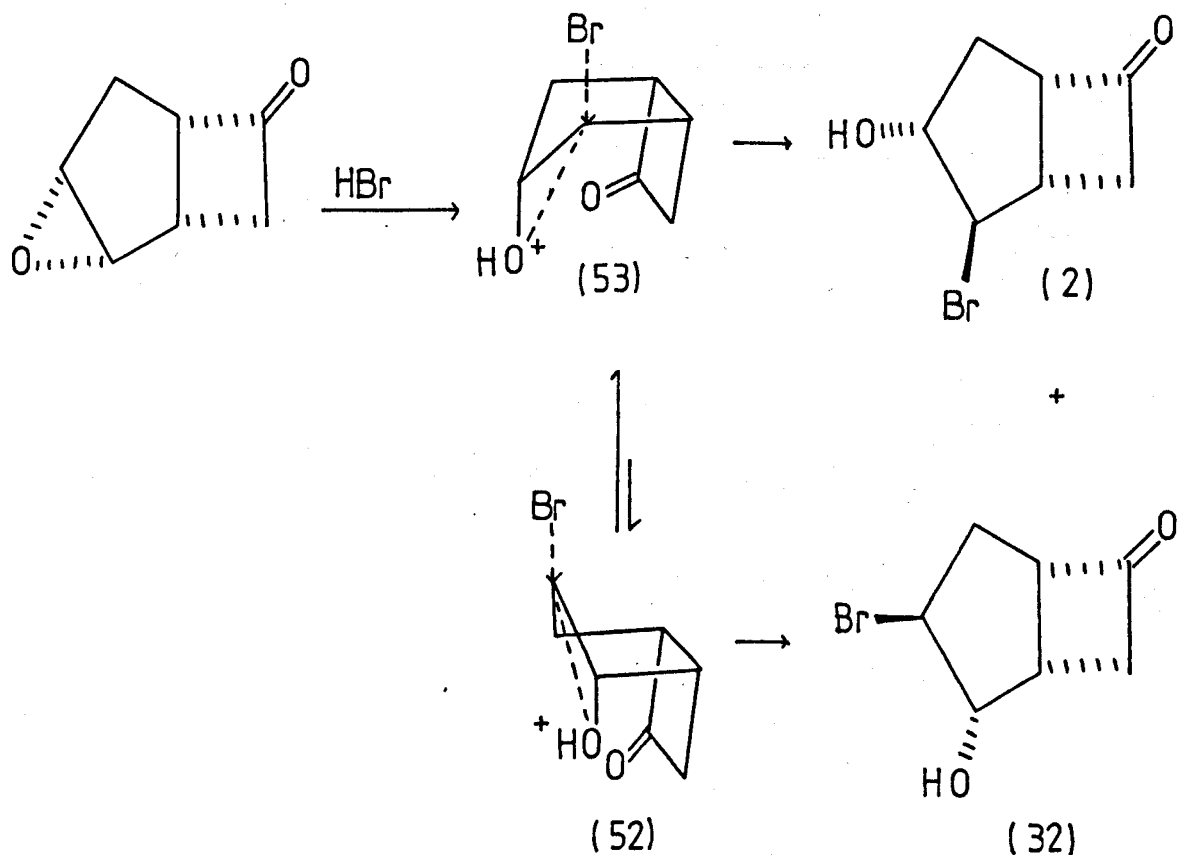
Under acidic conditions, kinetic data and product ratios indicate nucleophilic attack predominantly takes place on the protonated epoxide^{23,24} (50 and 51). In the transition states for attack, bond breaking has progressed to a greater

extent resulting in a partial carbenium character for the carbon at the reaction centre. Thus, an increase in nucleo-



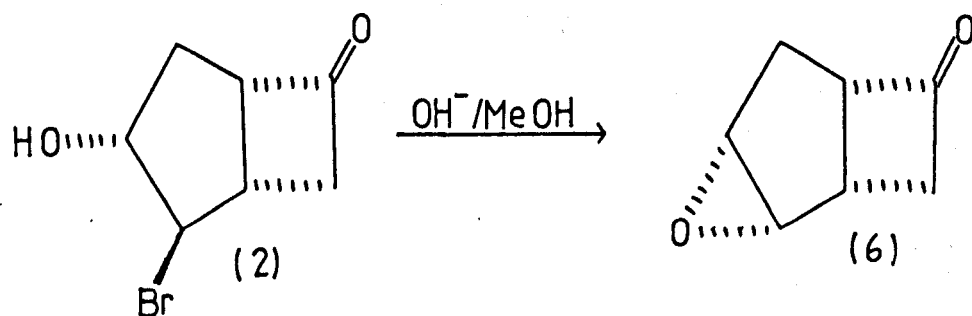
philicity of the nucleophile (which would tend to direct attack to the carbon with the greatest charge) and stabilising factors for the positive carbenium charge e.g. substituent alkyl groups (which would effectively reduce accumulation of charge on a carbon, and hence reduce the probability of nucleophilic attack at that carbon) will affect the product ratio.

The stereo-chemistry of reactions of epoxides on rings is constrained by the properties of the ring system. However, the course of these reactions may be understood in terms of the requirement for anti-parallel attack by the nucleophile along the axial direction, and on the relative energies of the transition states of the various ring opening possibilities¹⁶, e.g. one way of rationalising the product ratios on attack of the epoxide (6) by nucleophile is to consider the relative stability of the exo- and endo-envelope conformers (52) and (53) which undergo nucleophilic attack to give the bromohydrins (2) and (32).



2.4 Organic Synthesis

Scheme 1

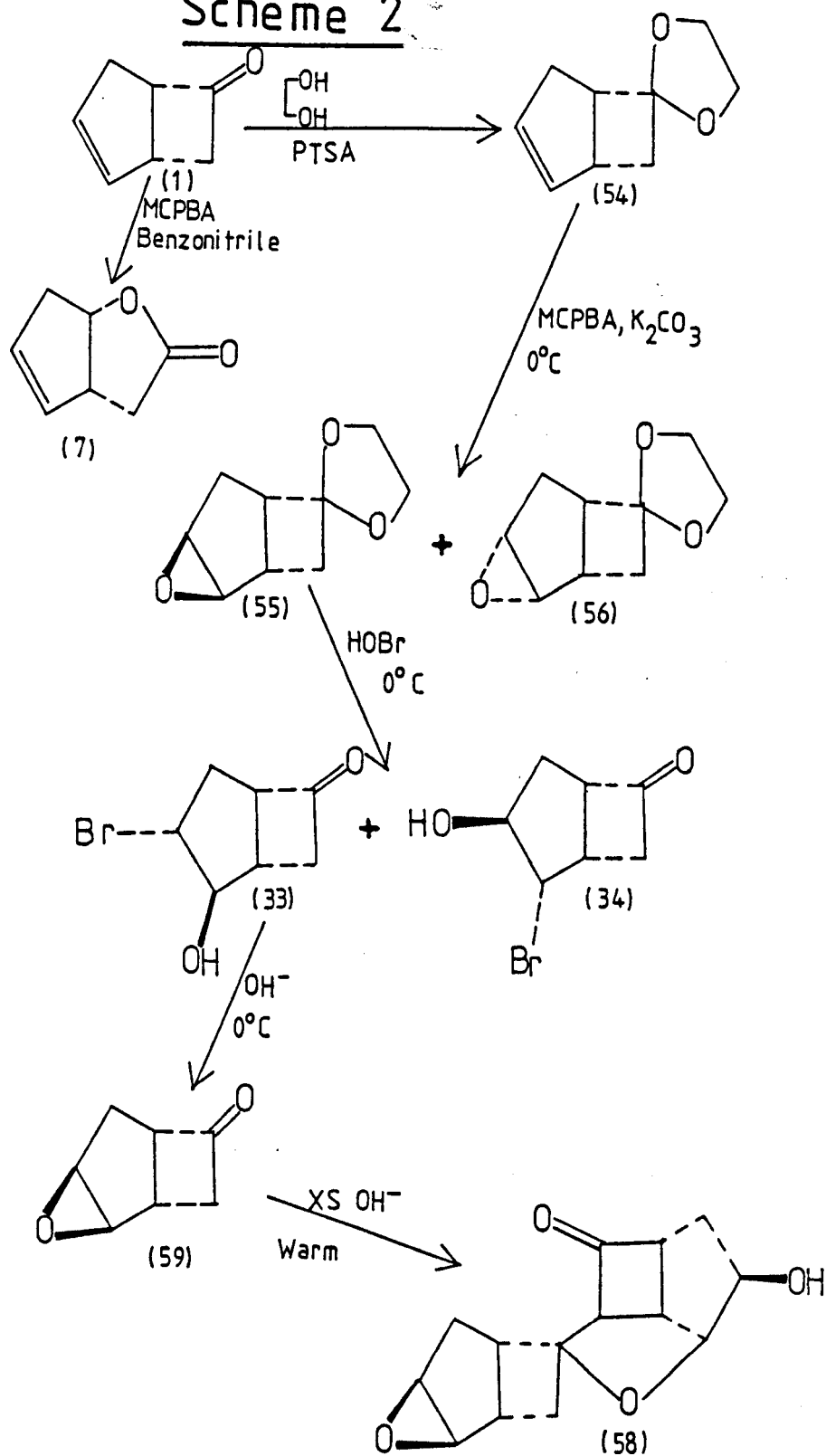


The epoxide (6) was formed from the bromohydrin (2) on treatment with sodium hydroxide in methanol (79% yield)⁵.

Scheme 2

Bicyclo[3.2.0]hept-2-ene-6-one (1) was refluxed with ethylene glycol in benzene with the addition of toluene-4-sulphonic acid as catalyst to give the ketal (54) in 92% yield.

Scheme 2



Scheme 2.2

Synthetic scheme leading to the exo-epoxide (59).

Oxidation with m-chloro-peroxybenzoic acid buffered with potassium carbonate gave a mixture of the epoxy-ketals (55) and (56) (combined yield 91%) in the ratio of 91:9 (exo (55):endo (56)) by g.l.c. Separation of the components by flash column chromatography (F.C.)²⁵ gave products in the ratio of 92:8 (exo (55):endo (56)). The isolated exo-epoxyketal (55) was treated with hydrobromic acid in an acetonitrile/water mixture giving the bromohydrins (33) and (34) (combined yield of 83%) obtained in the ratio of 95:5 (2-exo-3-endo (33):2-endo-3-exo (34)) by g.l.c. and separation of components by F.C. gave the bromohydrins (33) (2-exo-3-endo) and (34) (2-endo-3-exo) in the ratio of 91:9 ((33):(34)). The isolated bromohydrin (33) in methanol, on addition of an equivalent amount of sodium hydroxide in methanol gave the exo-epoxyketone (59) with a yield of 93%. It was important to avoid the addition of excess sodium hydroxide as under these conditions the aldol condensation product (58) is also formed.

Deprotection of the ketal (55) to give the ketone (59) using aqueous sulphuric acid was unsuccessful as this reaction resulted in a mixture with no useful yield of the desired product.

Direct epoxidation of (1) using hydrogen peroxide in benzonitrile²⁶ resulted in the Bayer-Villiger product (7).

2.5 The Reactions of Synthetic Intermediates and Products

The following abbreviations have been used:

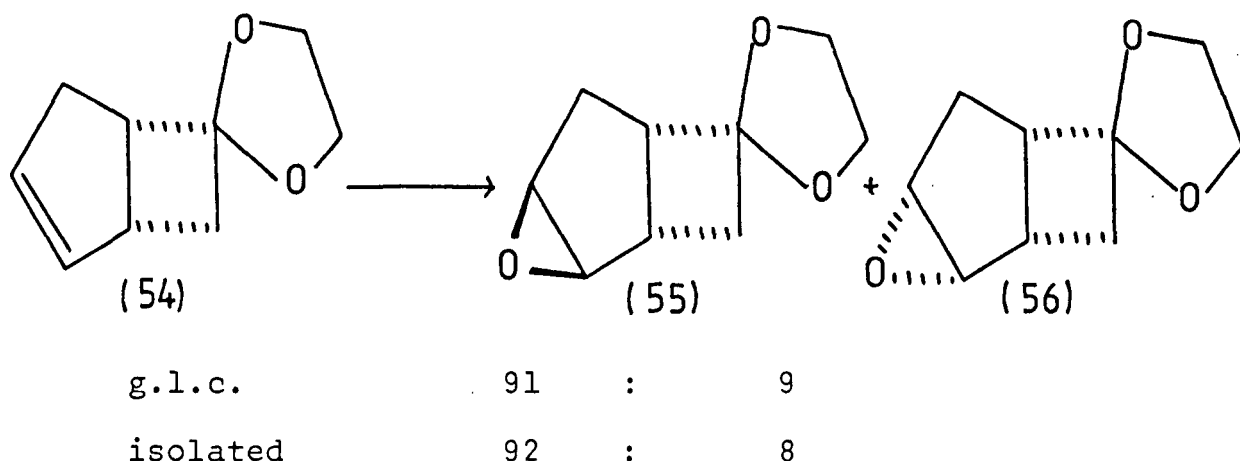
'isolated' refers to the mass of a single component in a mixture expressed as a percentage of the total mass of all the components isolated from a mixture.

'g.l.c.' refers to the ratio of isomers in a mixture expressed

as a percentage of the total of isomers detected by gas-liquid chromatography.

The epoxidation of (54) was carried out at 25°C with *m*-chloroperoxybenzoic acid²⁷ in dichloromethane (buffered with potassium carbonate to remove benzoic acid produced during the course of the reaction) to give the epoxy ketals (55) and (56) in the ratios shown in Table 2.1.

TABLE 2.1 Isomer ratio on treatment of (54) with *m*-chloroperoxybenzoic acid at 25°C



Treatment of the epoxy-ketals (55) and (56) with hydrobromic acid in an acetonitrile/water mixture afforded the bromohydrins (2), (32), (33), (34), in the ratios shown in Table 2.2.

TABLE 2.2 Isomer ratios on treatment of the epoxy-ketals (55) and (56) with hydrobromic acid at 25°C

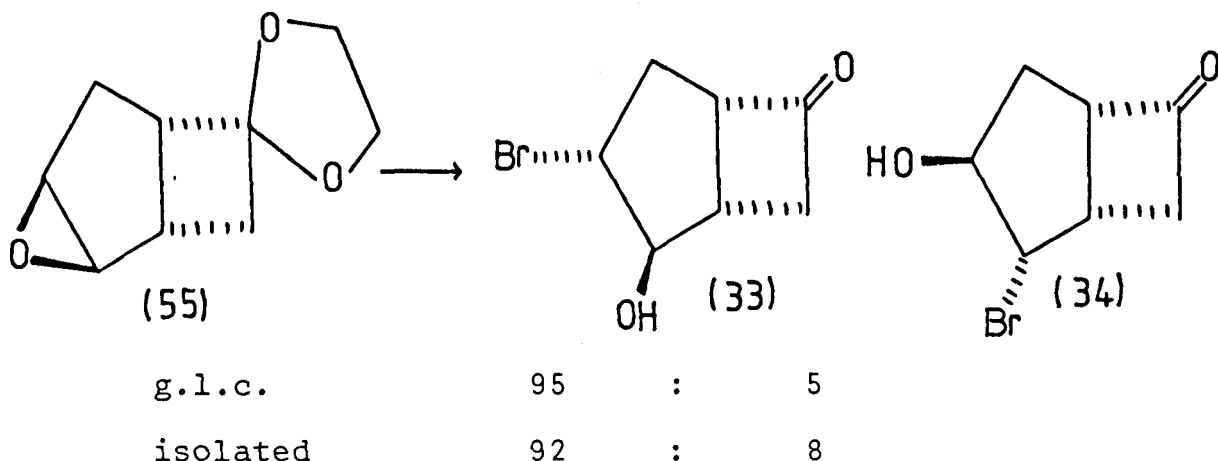
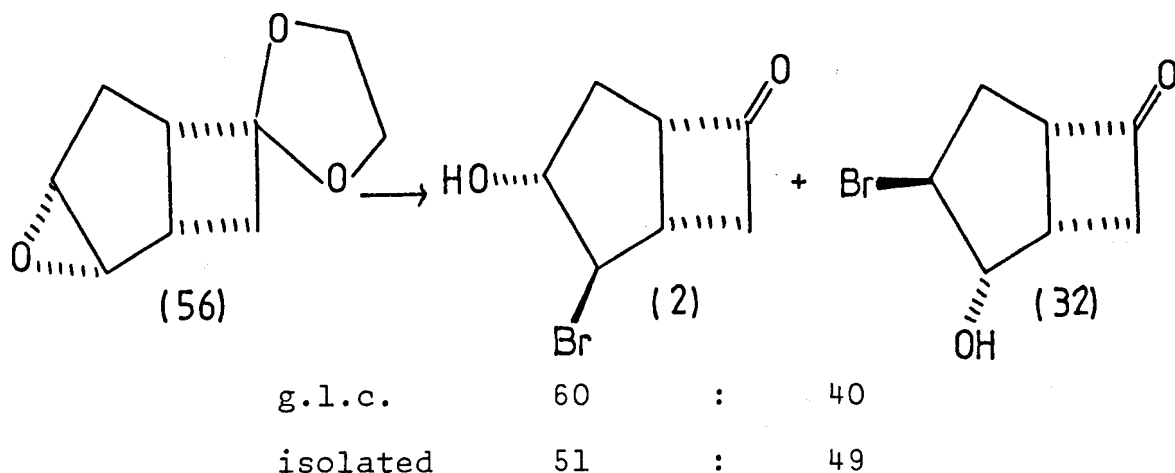


Table 2.2 (continued)



The endo- and exo-epoxy-ketones (6) and (59) were treated with hydrobromic acid at 0°C and 25°C in a series of solvents of varying polarity.

The endo-epoxy ketone (6) afforded the bromohydrins (2) and (32) in the ratios shown in Table 2.3.

The reaction of (6) in carbon tetrachloride at 25°C was carried out by addition of a dry saturated solution of hydrogen bromide in carbon tetrachloride.

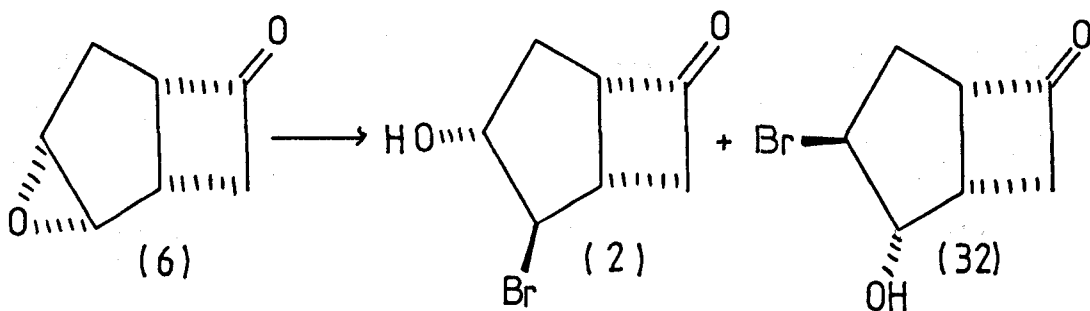
The exo-epoxy-ketone (59) afforded the bromohydrins (33) and (34) in the ratios shown in Table 2.4.

On treating the endo-epoxide (6) with hydrobromic acid in tetra-hydrofuran (T.H.F.), one isomer appears as the T.H.F. derivative (57), Table 2.5.

The treatment of the bicycloheptenone (1) with 1,3-dibromo-5,5-dimethylhydantoin in acetone at 0°C and 25°C gave rise to 4 bromohydrin isomers (2), (32), (33) and (34) in the ratios given in Table 2.6. Two of the isomers, (32) and (34) have identical R_f values on silica and were isolated as a mixture.

TABLE 2.3 Isomer ratios on treatment of 2,3-endo-epoxy-
bicyclo[3.2.0]heptan-6-one with hydrobromic
acid at 0°C and 25°C

T = 0°C



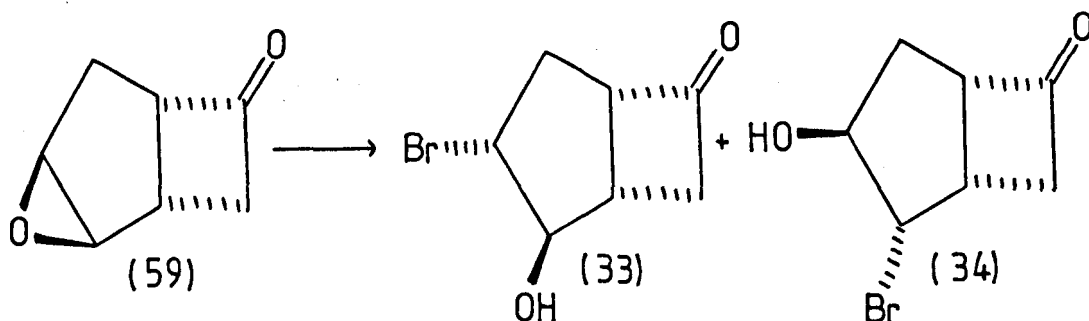
	Solvent		
g.l.c.	CCl ₄	74	: 26
g.l.c.	CH ₂ Cl ₂	83	: 17
g.l.c.	Acetonitrile	84	: 16
g.l.c.	D.M.F. (dimethylformamide)	85	: 15
isolated components	CH ₂ Cl ₂	76	: 24

T = 25°C

g.l.c.	CCl ₄ (dry)	84	: 16
g.l.c.	CH ₂ Cl ₂	83	: 17
g.l.c.	Acetonitrile	77	: 23
g.l.c.	D.M.F.	82	: 18

TABLE 2.4 Isomer ratios on treatment of 2,3-exo-epoxy-
bicyclo[3.2.0]heptan-6-one with hydrobromic
acid at 0°C and 25°C

T = 0°C



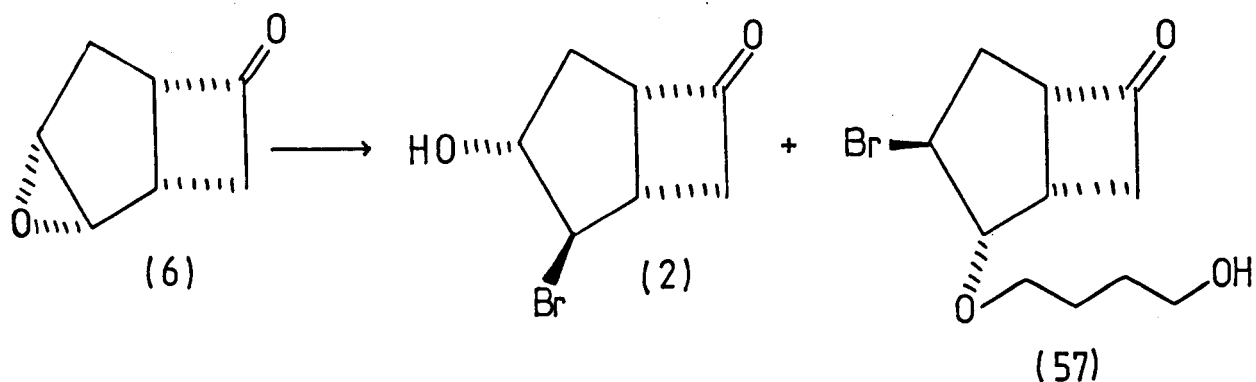
Solvent

g.l.c.	CCl ₄	98	:	2
g.l.c.	CH ₂ Cl ₂	98	:	2
g.l.c.	Acetonitrile	98	:	2
g.l.c.	D.M.F. (dimethylforma- mide)	98	:	2
isolated components	CH ₂ Cl ₂	99	:	1

T = 25°C

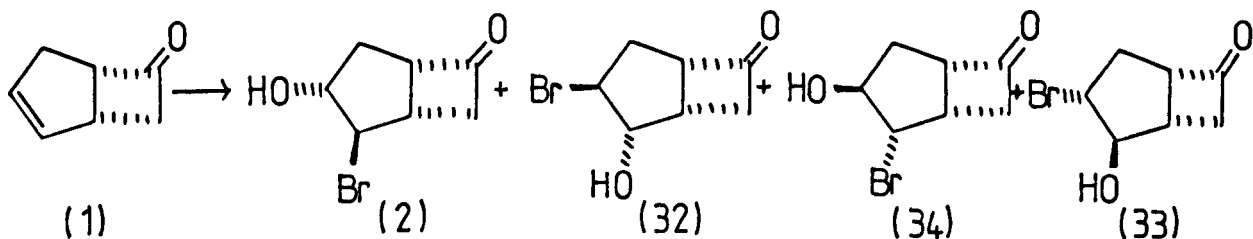
g.l.c.	CCl ₄	98	:	2
g.l.c.	CH ₂ Cl ₂	98	:	2
g.l.c.	Acetonitrile	97	:	3
g.l.c.	D.M.F.	97	:	3

TABLE 2.5 Isomer ratio on treatment of (6) with hydrobromic acid in THF at 25°C



g.l.c.	81	:	19
isolated	85	:	15

TABLE 2.6 Isomer ratios on addition of the elements HOBr to (1)



T = 0°C

g.l.c.	90	1	4	5
isolated	87	— 8 —		5

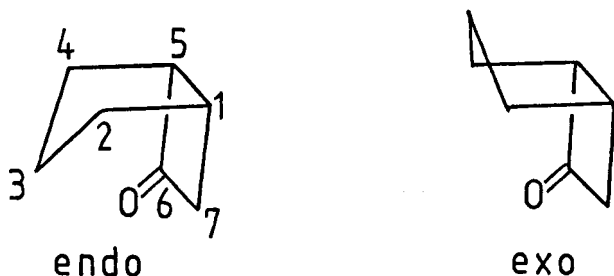
T = 25°C

g.l.c.	90	1	4	5
isolated	91	— 5 —		4

2.6 Conformational Analysis of Bicyclo[3.2.0]heptan-6-one derivatives by n.m.r.

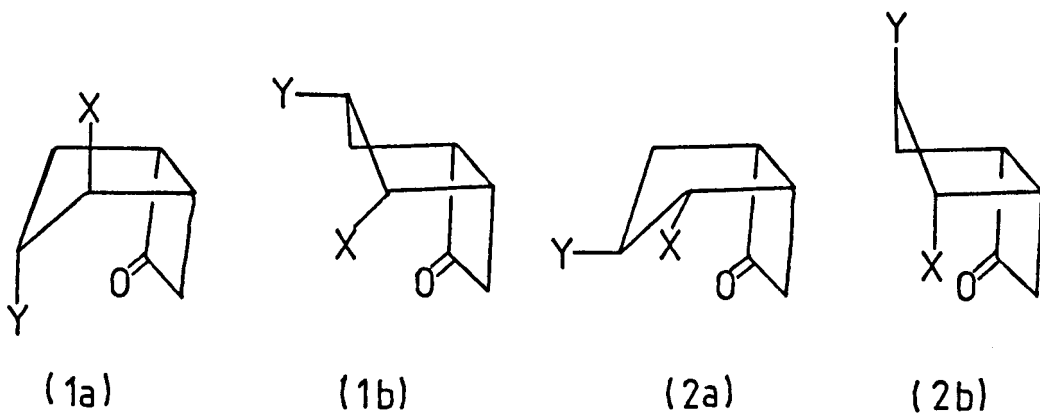
A number of derivatives of the bicyclo[3.2.0]heptan-6-one system in CCl_4 solution have been analysed by ^1H nuclear magnetic resonance spectroscopy (n.m.r.) to determine the approximate preferred conformations of these compounds in solution.

This bicyclic system can essentially take up two conformations between the limiting exo- and endo-envelopes.



The products of anti-periplanar addition (to C(2) and C(3)) can take up 4 limiting conformations:

- 1(a) with X and Y pseudoaxial
- 1(b) with X and Y pseudoequatorial
- 2(a) with X and Y pseudoequatorial
- 2(b) with X and Y pseudoaxial



The magnitudes of the coupling constants depend principally, in this case, on the dihedral angle between coupled protons. The measurement of these couplings can lead, via the Karplus relationships (1) and (2)³², to an estimate of the dihedral angle between coupled protons.

$$(1) \quad J_{ab} = J_0 \cos^2\theta \quad (0-90^\circ)$$

$$(2) \quad J_{ab} = J_{180} \cos^2\theta \quad (90-180^\circ)$$

The angle θ° is the dihedral angle between two vicinal protons and J_0 and J_{180} are constants chosen by comparison with similar compounds of known stereochemistry. The values assumed here are $J_0 = 9\text{Hz}$ and $J_{180} = 12\text{Hz}$.

The protons HC-X and HC-Y produce splittings dependent on the conformation of the system. The dihedral angles for the four limiting conformations have been measured from Dreiding models and are given in Table 2.7.

TABLE 2.7 Dihedral angles measured from Dreiding models ($^\circ$)

Dihedral angle	1a	1b	2a	2b
$\theta_{1.2}$	105	130	20	0
$\theta_{2.3}$	95	135	150	110
$\theta_{3.4}$ <u>exo</u>	40	10	160	100
$\theta_{3.4}$ <u>endo</u>	90	135	30	20

The predicted coupling constants are given in Table 2.8.

TABLE 2.8 Coupling constants from the Karplus equation (Hz)³⁷

Conformation	H2	H3
1a	0,0	5,0,0
1b	4.5,4.5	8.5,4.5,4.5
2a	8,9	10,9,6.5
2b	9,0	8,0,0

These coupling constants can only be regarded as approximate as factors other than dihedral angle can influence the values obtained³³. These factors include:

(1) the electronegativities of the substituents.

J vicinal (Hz) decreases with increasing electronegativity of the substituents (such groups are present here)

(2) the orientation of the substituents; the conformations considered here are limiting ones only

(3) the values of J₀ and J₁₈₀ are arbitrarily chosen.

However, the difference between the limiting exo- and endo-envelopes is sufficiently large to permit a reasonably accurate deduction of the preferred conformation to be made.

The compounds studied are given in Table 2.9.

From the results, it is evident that the endo-envelope is preferred in solution.

Table 2,9 n.m.r. coupling constants (Hz)

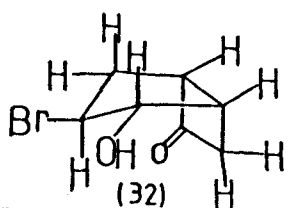
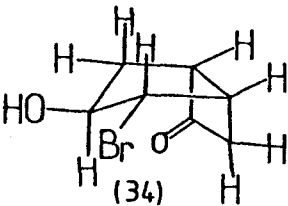
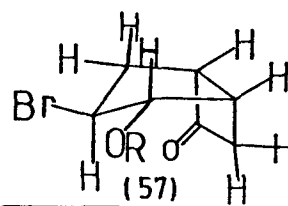
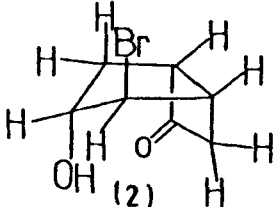
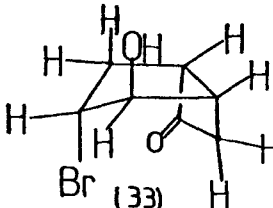
	$J_{1,2ex}$	$J_{2ex,3en}$	$J_{3en,4ex}$	$J_{3en,4en}$	$J_{4ex,5}$	$J_{4en,5}$	$J_{4ex,4en}$	Conf.
 <p>(32)</p>		9	11	6.5	9	1.5		endo
 <p>(34)</p>	6	9	9	6	9	1	12.5	endo
 <p>(57)</p>	7.5	9	9	6	9	1	13.5	endo

Table 2,9 (cont'd)

	$J_{1,2en}$	$J_{2en,3ex}$	$J_{3ex,4ex}$	$J_{3ex,4en}$	$J_{4ex,5}$	$J_{4en,5}$	$J_{4ex,4en}$	Conf.
	1	1	3	1	9	1	14.5	endo
	1	1	1	1	8	3		endo

2.7 Summary of Results

The isomer ratios determined by g.l.c. in the reactions described in sections 2.4 and 2.5 correlate well with the ratios obtained by isolation and characterisation of the products. This strongly suggests that the g.l.c. results refer to the correct compounds in the correct ratios.

The role of solvent polarity and temperature in the determination of regio- and stereo-specificity appear to be minimal. Since these factors do not appear to affect the isomer ratios in a significant or consistent manner, the results at different temperatures in different solvents have been averaged. These results are summarised in Figure 2.1.

The epoxidation of (54) proceeds in a highly stereo-selective manner favouring exo-epoxidation.

The opening of the exo-epoxy-ketal (55) is highly regio-specific favouring the 2-exo-3-endo product.

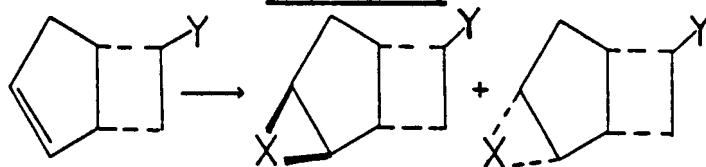
Similarly, opening of the endo-epoxy-ketal (56) again favours the 2-exo-3-endo product. However, in this case the reaction is not as regio-specific.

Opening of the endo-epoxy-ketone (6) proceeds regio-selectively favouring the 2-exo-3-endo product.

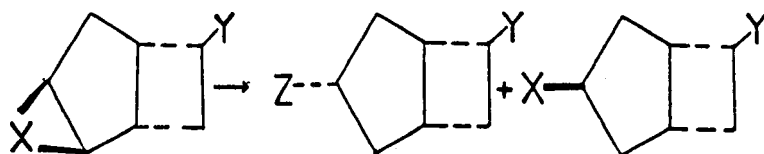
Opening of the exo-epoxy-ketone (59) proceeds with very high regio-specificity giving almost exclusively the 2-exo-3-endo product.

The addition of the elements HOBr to (1) results in formation of the exo- (10) and endo- (9) bromonium ions in the ratio 91:9 (90 + 1:5 + 4). The exo-bromonium ion (10) opens almost exclusively to give the 2-exo-3-endo product. The endo-bromonium ion (9) is opened less selectively though again

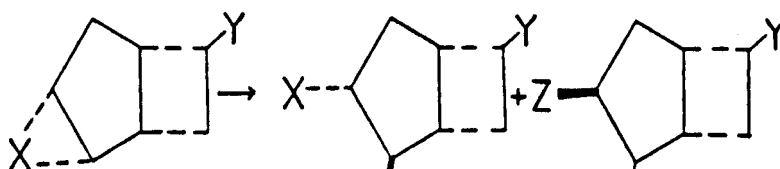
Fig 2,1



Y				X	Y	
	(54)	91 : 9		o		e
=0	(1)	91 : 9		Br ⁺	=0	b



X	Y			X	Y	Z
Br ⁺	=0	(10)	99 : 1	Br	=0	OH b
o<	=0	(59)	98 : 2	OH	=0	Br e
o<		(55)	95 : 5	OH	=0	Br e



X	Y			X	Y	Z
Br ⁺	=0	(9)	56 : 44	Br	=0	OH b
o<	=0	(6)	82 : 18	OH	=0	Br e
o<		(56)	60 : 40	OH	=0	Br e

Figure 2.1

The ratios of products observed on bromonium ion formation and epoxidation and the isomer ratios obtained upon opening these compounds are summarised here. The ratios quoted are the average of the product ratios observed in different solvents and at different temperatures as determined by g.l.c. Those results designated 'b' refer to reactions involving bromonium ions. Those designated 'e' refer to reactions involving epoxide.

favouring the 2-exo-3-endo product.

The stereo-selectivity of epoxidation (for (54)) and bromonium ion formation (for (1)) are identical. This suggests that similar factors (probably steric) control the approach of the reacting species. This appears to rule out intra-molecular hydrogen-bonding between the transition state during epoxidation and the endo-ketal oxygen (or transannular nucleophilic attack (BDS, Chapter 4)).

The opening of the exo-epoxide (59) and the corresponding exo-bromonium ion (10) give almost identical isomer ratios. This suggests that the factors controlling regio-selectivity are identical in both these systems.

Opening of the endo-epoxide (6) and the analogous endo-bromonium ion (9) both favour the same substitution pattern (2-exo-3-endo). However, in this case the epoxide displays higher selectivity.

These results are discussed in detail in combination with X-ray structural data and force-field calculations in Chapters 4 and 5.

2.8 Experimental

Melting points were determined by the capillary tube method and are uncorrected. The Büchi-Kugelrohr (bulb to bulb) system was used for distillation and the boiling points reported are oven temperatures at distillation.

Thin layer chromatography (t.l.c.) was carried out on Camlab 'Polygram' pre-coated silica-gel plates which were developed by 2,4-dinitrophenylhydrazine unless otherwise stated. Where necessary, solvents were distilled in the recommended manner.

Petroleum ether refers to the fraction of boiling range 60°-80°C.

¹H nuclear magnetic resonance spectra (n.m.r.) were recorded on a Varian E.M.390 (90 MHz) spectrometer by the Analytical Department of Glaxo Group Research, Ware, Hertfordshire (unless otherwise stated). Protons were identified by double irradiation techniques where appropriate. Tetramethylsilane was employed as an internal standard and all spectral values are quoted in parts per million (δ). Additional coupling constants (Hz) are given where applicable in Chapter 2.6. Infra-red spectra (i.r.) were recorded on a Perkin-Elmer 402 instrument.

Mass spectra were determined on a Jeol JMS D100 mass spectrometer combined with a Jeol JCS 20K gas chromatograph and using an Instem Data Mass Maxi data processing system.

Micro analysis and gas liquid chromatography (g.l.c.) were carried out at the Analytical Laboratories of Glaxo Group Research, Ware, Hertfordshire. G.l.c. was performed on a Hewlett-Packard 5880. The carrier gas was helium, with a typical inlet pressure of 1.5 ml/m. The detector was a flame ionisation detector (F.I.D.).

Flash column chromatography (F.C.) refers to the technique described in reference 25. The stationary phase was Kieselgel 60, Merck 9385. Column size was varied from 2 cm diameter to 10 cm diameter depending on the sample loading.

Spiro{bicyclo[3.2.0]hept-2-ene-6,2'(1.3)dioxolan} (54)

A stirred solution of bicyclo[3.2.0]hept-2-ene-6-one (1) (24g, 0.22 mol), benzene (200 ml), 1,2-ethanediol (250 ml) and p-toluene sulphonic acid (50 mg) was heated under reflux and water was removed using a Dean-Stark trap. After 72 hours, the cooled

solution was washed with 8% potassium carbonate solution and the washings back extracted with cyclohexane (2 x 80 ml). The combined organic layers were dried (Na_2SO_4) and evaporated to give spiro{bicyclo[3.2.0]hept-2-ene-6,2'-(1,3)dioxolan} (54) (31g, 92%) as a colourless oil.

n.m.r.: $\delta(\text{CDCl}_3)$ 5.7-5.8 (2H,m,H-2,H-3), 3.7-4.0(4H,m,H-2'),
3.1(1H,m,H-5), 1.9-2.8(5H,m,H-1,2xH-4,2xH-7).

Found: (M^+), 152.0883. $\text{C}_9\text{H}_{12}\text{O}_2$ requires 152.0837.

2,3-endo-epoxybicyclo[3.2.0]heptan-6-one (6).

2-exo-bromo-3-endo-hydroxybicyclo[3.2.0]heptan-6-one (2) (18.15g, 0.089 mol) in methanol (100 ml) was added to a stirred solution of sodium hydroxide (8.5g, 0.021 mol) in methanol (180 ml). After 3 hours at ambient temperature the mixture was neutralised with acetic acid (7.44g), diluted with water (100 ml), and extracted with dichloromethane (3 x 75 ml). Evaporation of the dried (MgSO_4) extracts and flash column chromatography of the residue, eluting with ethyl acetate-light petroleum (1:1) gave an oil which was further purified by Kügelrohr distillation (at 115°C and 2 mmHg) to give 2,3-endo-epoxybicyclo[3.2.0]heptan-6-one (6) as a colourless oil which solidified in the refrigerator.

t.l.c. single spot at $R_f = 0.15$ (ethyl acetate:petroleum ether;
3:7)

i.r. ν_{max} (film) 1773,1035,833 cm^{-1}

n.m.r. $\delta(\text{CDCl}_3)$ 3.4-3.8(3H,m,H-3,H-2,H-5),2.7-3.2(3H,m,H-7 exo,
H-7 endo,H-1), 2.48(1H,m,H-4 endo), 1.9(1H,m,H-4 exo).

The ^1H n.m.r. and i.r. spectra were identical with an authentic specimen.

Spiro{2,3-exo-epoxybicyclo[3.2.0]heptane-6,2'(1,3)-dioxolan} (55)

A solution of m-chloroperoxybenzoic acid (85%, 57g) in dichloromethane (150 ml) was added dropwise (over 15 minutes) with stirring to an ice cooled mixture of spiro{bicyclo[3.2.0]-hept-2-ene-6,2'-(1,3)dioxolan} (54) (43.8g, 0.288 mol) and potassium carbonate (3.0g) in dichloromethane (160 ml).

After 3 hours aqueous sodium sulphite solution was added until a starch-iodide test was negative. The mixture was washed with 8% aqueous sodium bicarbonate, brine and water. The organic layer was dried ($MgSO_4$) and evaporated to give a mixture of the exo- (55) and endo- (56) epoxy-ketals (44.05g, 91%) in the ratio 91:9 by g.l.c. (2m OV275 column, 120-150°C, F.I.D.). The individual isomers were isolated by subjecting a portion (12.0g) of this mixture to flash column chromatography eluting with ethyl acetate-light petroleum (1:1).

The major isomer was

spiro{2,3-exo-epoxybicyclo[3.2.0]heptane-6,2'(1,3)dioxolan} (55) isolated as an oil (10.23g, 77%).

t.l.c. single spot at R_f 0.55 (ethyl acetate:petroleum; 1:1)

i.r. ν_{max} (film) 1035, 833 cm^{-1}

n.m.r. δ ($CDCl_3$) 3.7-4.0 (4H, m, H-2'), 3.3-3.6 (2H, m, H-3, H-2), 1.8-2.9 (6H, m, H-4, H-5, H-1, 2xH-7).

Found (M^+), 168.0773. $C_9H_{12}O_3$ requires 168.0786.

The minor isomer was spiro{2,3-endo-epoxy-bicyclo[3.2.0]-heptane-6,2'-(1,3)dioxolan} (56) obtained as an oil (0.87g, 6.6%).

t.l.c. single spot at R_f = 0.33 (ethyl acetate:petroleum; 1:1)

i.r. ν_{max} (film) 1030, 850 cm^{-1}

n.m.r. δ ($CDCl_3$) 3.7-4.1 (4H, m, H-2'), 3.65 (1H, t, H-2, H-3), 3.53- (1H, t, H-2, H-3), 3.15 (1H, m, H-5), 2.4-2.7 (3H, m, 2xH-7, H-1), 2.27 (1H, m, H-4 endo), 1.12 (1H, m, H-4 exo).

The reaction of spiro{2,3-exo-epoxy-bicyclo[3.2.0]heptane-6,2'-1(1,3)dioxolan} (55) with hydrobromic acid.

A solution of 85% aqueous hydrobromic acid (20g) and water (20 ml) was added dropwise with stirring to a solution of spiro{2,3-exo-epoxybicyclo[3.2.0]heptane-6,2'-(1,3)dioxolan}(55) (10.0g, 0.06 mol) in acetonitrile (150 ml). After 24 hours, water (50 ml) was added and the mixture extracted with dichloromethane (3 x 150 ml). The combined extracts were washed with water, dried ($MgSO_4$) and evaporated to give a mixture (10.0g, 83%) of two bromohydrin isomers in the ratio of 95:5 by g.l.c. (trimethylsilyl ether derivatives, 2m 1.5% QF-1 column, $140^\circ C$), separation by flash column chromatography eluting with ethyl acetate:cyclohexane (2:1) afforded 2-endo-bromo-3-exo-hydroxybicyclo[3.2.0]heptan-6-one (34) (higher R_f) as a colourless oil (0.83g, 7%).

t.l.c. single spot at $R_f = 0.33$ (ethyl acetate:n-hexane; 1:1)

i.r. ν_{max} (film) 3440, 1780 cm^{-1}

n.m.r. δ ($CDCl_3$) 4.3 (2H, m, H-3, H-2), 3.57 (1H, m, H-5),
3.0-3.4 (3H, m, H-1, H-7 endo, H-7 exo), 2.7 (1H, s, H-OH),
2.27 (1H, m, H-4 endo), 1.77 (1H, m, H-4 exo).

Found (M^+), 203.9793 and 205.9777. $C_7H_9O_2Br$ requires
203.9787 and 205.9767.

The major isomer (lower R_f) was 3-endo-bromo-2-exo-hydroxy-bicyclo[3.2.0]heptan-6-one (33) obtained as a white crystalline solid (8.09g, 66%), m.p. $42^\circ C$.

i.r. ν_{max} (0.5% $CHBr_3$) 3585, 1780 cm^{-1}

n.m.r. δ ($CDCl_3$) 4.56 (1H, m, H-2), 4.3 (1H, m, H-3), 3.77 (1H, m, H-5),
2.2-2.5 (2H, qq, H-7 exo, H-7 endo), 2.9 (1H, m, H-1),
2.3-2.8 (2H, m, H-4 exo, H-4 endo), 4.2 (1H, s, H-OH).

Found, C, 39.85; H, 4.4. $C_7H_9O_2Br$ requires C, 41.0; H, 4.4%.

2,3-exo-epoxybicyclo[3.2.0]heptan-6-one (59)

A solution of sodium hydroxide (2.28g, 0.057 mol) in methanol (55 ml) was added dropwise (over 30 minutes) to a stirred solution of 3-endo-bromo-2-exo-hydroxybicyclo[3.2.0]heptan-6-one (33) in methanol (200 ml). During the addition the temperature was maintained at 20°C, and by frequent checking with universal indicator paper the pH was maintained at pH6-7. Water (250 ml) was added and the product extracted into dichloromethane (1 x 200, 1 x 50 ml). Evaporation of the dried (MgSO₄) organic extracts afforded 2,3-exo-epoxybicyclo[3.2.0]heptan-6-one (59) (5.44g, 93%) as a colourless oil, homogeneous by t.l.c., which solidified after refrigeration, m.p. 32°C.

i.r. ν_{\max} (0.5% CHBr₃) 1773, 845 cm⁻¹

n.m.r. δ (CDCl₃) 3.45-3.58(3H,m,H-2,H-3,H-5), 2.6-3.4(3H,m,H-1, H-7 exo,H-7 endo), 1.9-2.4(2H,m,H-4 exo,H-4 endo).

Found (M⁺), 124.0523; calculated for C₇H₈O₂ 124.0524.

If this preparation is carried out at elevated temperature with an excess of sodium hydroxide, then an additional product is obtained;

spiro{5-exo-hydroxy-3-oxatricyclo[5.1.1.0^{4,9}]nonan-8-one-2-1'(4',5'-exo-epoxybicyclo[3.2.0]heptane)} (58)

i.r. ν_{\max} (0.5% CHBr₃) 3595, 1770 cm⁻¹

n.m.r. δ (CDCl₃) 4.46-4.49(2H,dd,H-4,H-5), 3.5-3.75(4H,m,H-1, H-4',H-9,H-3), 3.42(1H,d,H-5'), 3.06(1H,txt,H-2'), 2.59(1H,q, J=7.4 Hz,H-6'), 2.27(1H,ddd,J=2,38,15 Hz,H-3' endo), 2.06(1H,dd, J=9.5,15Hz,H-3' exo), 2.21(1H,dxt,J=4.5,14.5Hz,H-6 endo), 1.85(1H,dd,J=10,14Hz,H-6 exo), 2.04(1H,ddd,J=3,8.5,12.5Hz,H-7' exo), 1.85(1H,dd,J=7.5,12.5Hz,H-7' endo), 1.60(1H,bs,H-OH). The

assignments were proven by decoupling experiments at 200 and 250MHz.

The reaction of spiro{2,3-endo-epoxybicyclo[3.2.0]heptane-6,2'-(1,3)dioxolan} (56) with hydrobromic acid

A solution of 85% aqueous hydrobromic acid (3.9g) in acetonitrile (20 ml) was added dropwise with stirring to spiro{2,3-endo-epoxybicyclo[3.2.0]heptane-6,2'-(1,3)dioxolan} (56) (1.72g, 0.01 mol) in acetonitrile (100 ml) and water (20 ml). After 24 hours 8% potassium bicarbonate solution (50 ml) was added and the solution extracted with dichloromethane (2 x 100 ml). The combined extracts were washed with water, dried ($MgSO_4$) and evaporated to give a white solid (2.1g). 3 components were present in the mixture in the ratio 51:35:14. 2 components (5.3, 5.9 mins) had almost identical retention times. The peaks at 4.2 and 5.3 mins appeared to correspond to the expected bromohydrins (trimethylsilyl ether derivatives, 2m 1.5% QF1 column, $T=140^{\circ}C$, F.I.D.). Separation was accomplished by flash column chromatography eluting with ethyl acetate-cyclohexane (2:1).

The isomer with higher R_f was 2-exo-bromo-3-endo-hydroxybicyclo-[3.2.0]heptan-6-one (2) obtained as a white crystalline solid (1.0g, 48%), m.p. $88^{\circ}C$ (lit. $87-89^{\circ}C$).

i.r. ν_{max} (Nujol mull) $3580, 1772\text{ cm}^{-1}$

n.m.r. $\delta(CDCl_3)$ 4.75(1H, m, H-3), 4.35(1H, m, H-2), 3.82(1H, m, H-5), 3.6-3.1(3H, m, H-1, H-7 exo, H-7 endo), 3.2(1H, s, OH), 7.2-8.0(2H, m, H-4 exo, H-4 endo) (identical with an authentic specimen).

Found, C, 40.75; H, 4.3. $C_7H_9O_2Br$ requires C, 41.0; H, 4.4%.

The isomer of lower Rf was

3-exo-bromo-2-endo-hydroxybicyclo[3.2.0]heptan-6-one (32)

obtained as a white crystalline solid (0.96g, 46%), m.p. 52°C.

i.r. ν_{\max} (Nujol mull) 3550, 1075 cm^{-1}

n.m.r. δ (CDCl₃) 4.48(1H, m, H-2), 4.05(1H, m, H-3), 3.6(1H, m, H-5),
3.5-2.9(3H, m), 2.78(1H, s, H-OH), 2.53(1H, m, H-4 endo),
2.14(1H, m, H-4 exo).

Found, C, 41.17; H, 4.44. C₇H₉O₂Br requires C, 41.0; H, 4.4%.

The reaction of 2,3-endo-epoxybicyclo[3.2.0]heptan-6-one (6)
with hydrobromic acid

Hydrobromic acid (48%, 18.0g) was added to a solution of 2,3-endo-epoxybicyclo[3.2.0]heptan-6-one (6) (4.03g, 0.033 mol) in dichloromethane (5 ml) at 0°C. After 2 hours, the mixture was extracted with dichloromethane (3 x 10 ml). The extracts were washed with water, dried (MgSO₄) and evaporated to give a white solid (6.8g, 100%) which was a mixture of two bromohydrin isomers in the ratio of 83:17 by g.l.c. (trimethylsilyl ether derivatives, 3% OV210 column, T = 130°C, F.I.D.). Flash column chromatography of the mixture, eluting with ethyl acetate-cyclohexane (1:1) afforded 2-exo-bromo-3-endo-hydroxybicyclo[3.2.0]heptan-6-one (2) (4.5g, 67%) as a white crystalline solid, m.p. 88°C.

t.l.c. single spot at Rf = 0.48 (ethyl acetate:cyclohexane; 1:1).

i.r. ν_{\max} (Nujol mull) 3580, 1772 cm^{-1}

n.m.r. δ (CDCl₃) 4.75(1H, m, H-3), 4.35(1H, m, H-2), 3.82(1H, m, H-5),
3.1-3.6(3H, m, H-1, 2xH-7), 2.88 (1H, s, H-OH), 2.0-2.8
(2H, m, H-4 endo, H-4 exo).

The minor component was 3-exo-bromo-2-endo-hydroxybicyclo[3.2.0]heptan-6-one (32) (1.43g, 21%) as a white crystalline solid, m.p. 52°C.

t.l.c. single spot at $R_f = 0.33$ (ethyl acetate:cyclohexane; 1:1).

i.r. ν_{\max} (0.5%CHBr₃) 3550, 1075 cm^{-1}

n.m.r. δ (CDCl₃) 4.48(1H,m,H-2), 4.05(1H,m,H-3), 3.6(1H,m,H-5)
2.9-3.5(3H,m,H-1,H-7 exo,H-7 endo), 2.78(1H,s,H-OH),
2.53(1H,m,H-4 endo), 2.14(1H,m,H-4 exo).

The reaction of 2,3-exo-epoxybicyclo[3.2.0]heptan-6-one (59) with hydrobromic acid.

Hydrobromic acid (85%, 4.5g) was added dropwise to a stirred solution of 2,3-exo-epoxybicyclo[3.2.0]heptan-6-one (59) (1.46g, 0.012 mol) in dichloromethane (10 ml) at 0°C. After 2 hours the mixture was neutralised by addition of 8% sodium bicarbonate solution and extracted with dichloromethane (3 x 10 ml). The organic extracts were washed with water and the aqueous washings back extracted with dichloromethane (2 x 10 ml). The combined organic fractions were dried (MgSO₄) and evaporated to give an oil (2.4g, 100%) which was a mixture of the two bromohydrin isomers in the ratio of 98:2 by g.l.c. (trimethylsilyl ether derivatives, 3% OV210 column, T = 120°C, F.I.D.). Flash column chromatography eluting with ethyl acetate-petroleum ether (2:1) gave 3-endo-bromo-2-exo-hydroxybicyclo[3.2.0]heptan-6-one (33) (2.15g, 89%) as a white crystalline solid, m.p. 42°C. N.m.r. and i.r. spectra were identical with a previously authenticated sample. The other isomer 2-endo-bromo-3-exo-hydroxybicyclo[3.2.0]heptan-6-one (34) (30 mg., 1%) was obtained as a colourless oil.

t.l.c. a single spot at $R_f = 0.33$ (ethyl acetate:petroleum ether; 1:1)

g.l.c. indicated the sample was 79% pure by area (trimethylsilyl ether derivative, column 3% OV210, $T = 120^\circ\text{C}$, F.I.D.)

i.r. ν_{max} (film) 3440, 1780 cm^{-1}

n.m.r. $\delta(\text{CDCl}_3)$ 4.3(2H,m,H-3,H-2), 3.6(1H,m,H-5),
3.0-3.4(3H,m,H-1,H-7 exo,H-7 endo), 2.5(1H,s,H-OH),
2.27(1H,m,H-4 endo), 1.8(1H,m,H-4 exo).

The reactions of 2,3-endo-epoxybicyclo[3.2.0]heptan-6-one (6) and 2,3-exo-epoxybicyclo[3.2.0]heptan-6-one (59) with hydrobromic acid in various solvents at 0°C and 25°C .

The following general procedure was used:-

Hydrobromic acid (85% 0.025g, 2 equivalents) was added to a solution of the epoxide (50 mg/ml) in the appropriate solvent at either 0°C or at 25°C dropwise with stirring. After 2 hours, water was added and the products extracted into ether.

Evaporation of the dried (MgSO_4) extracts gave the crude product mixture.

Different experimental conditions were used at 25°C with carbon tetrachloride as solvent. Here, a saturated solution of hydrogen bromide in carbon tetrachloride was prepared by passing dried (H_2SO_4) hydrogen bromide gas (15g) through carbon tetrachloride (15 ml) giving a solution of 0.33g HBr/100 ml of CCl_4 . This solution (5 ml) was added and the products worked up (as above).

In all cases, isomer ratios were determined by g.l.c. (trimethylsilyl ether derivatives, QF1 column, $T = 130^\circ\text{C}$, F.I.D.) Identification of isomers was by comparison of retention times (g.l.c.)

with authentic samples under the same experimental conditions. The results are tabulated in Tables 2.3 and 2.4.

The attempted conversion of spiro{2,3-exo-epoxybicyclo[3.2.0]-heptane-6,2'-(1,3)dioxolan} (55) to the ketone (59) using sulphuric acid.

A mixture of spiro{2,3-exo-epoxybicyclo[3.2.0]heptane-6,2'-(1,3)-dioxolan} (55) (0.2g, 0.01 mol), acetonitrile (3 ml), water (2 ml) and 2N sulphuric acid (0.5 ml) was stirred for 4 hours. 8% sodium bicarbonate was added (10 ml) and the products extracted into ethyl acetate (3 x 10 ml), dried (MgSO_4) and solvent evaporated to give an oil (0.12g).

t.l.c. showed a diffuse spot at $R_f = 0.12$ (ethyl acetate: petroleum; 1:1)

I.r. and n.m.r. indicated a mixture of diols and starting material.

The reaction of 2,3-endo-epoxybicyclo[3.2.0]heptan-6-one (6) with hydrobromic acid in tetrahydrofuran.

To a stirred solution of 2,3-endo-epoxybicyclo[3.2.0]heptan-6-one (6) in tetrahydrofuran (10 ml) at -10°C was added hydrobromic acid (47%, 10.3g) dropwise over 10 minutes. After 2 hours, excess hydrobromic acid was neutralised (NaHCO_3), water was added (10 ml) and the products extracted into dichloromethane (3x15 ml), dried (MgSO_4) and the solvent evaporated. T.l.c. showed 2 spots at $R_f = 0.48$ and $R_f = 0.32$ (cyclohexane-ethyl acetate; 1:1).

The components were separated by flash column chromatography (ethyl acetate-cyclohexane; 1:1) to give 2-exo-bromo-3-endo-hydroxybicyclo[3.2.0]heptan-6-one (2) as a white crystalline solid (1.26g, 77%) m.p. 88°C . I.r. and n.m.r. were identical

with an authentic sample.

The component of lower Rf was 3-exo-bromo-2-endo-(1'-oxa-butan-4'-ol)bicyclo[3.2.0]heptan-6-one (57) as an oil (0.3g, 13%).

t.l.c. showed a single spot at Rf = 0.32 (cyclohexane:ethyl acetate; 1:1)

i.r. ν_{\max} (film) 3420, 1770 cm^{-1}

n.m.r. δ (CDCl_3) 4.48(1H, dd, J=9, 7.5 Hz, H-2), 4.08(1H, ddd, J=9, 6.7, 11.3 Hz, H-3), 3.44-3.7(4H, m, 2xH-4', 2xH-1'), 2.8-3.7(3H, m, H-5, H-1, H-7 exo, H-7 endo), 2.48(1H, ddd, H-4 endo), 2.1(1H, s, H-3'), 2.0-2.1(1H, ddd, J=11.2, 1.5, 13.2, H-4 exo), 1.5-2.1(4H, m, 2xH-2', 2xH-3'), 2.2(1H, s, H-OH).

Analysis of the reaction mixture by g.l.c. (trimethylsilyl ether derivative, 3% OV210 column, T = 120°C, F.I.D.) showed 2 components in the ratio 78:18 (96% purity). The major isomer was 2-exo-bromo-3-endo-hydroxybicyclo[3.2.0]heptan-6-one (2) (g.l.c. Rf identical with an authentic sample) and the minor component was 3-exo-bromo-2-endo-(1'-oxabutan-4'-ol)bicyclo[3.2.0]heptan-6-one (57) (g.l.c. Rf identical with isolated component).

The attempted ketal exchange of spiro{2,3-exo-epoxybicyclo[3.2.0]heptane-6,2'-(1,3)dioxolan} (55) with acetone

A mixture of spiro{2,3-exo-epoxybicyclo[3.2.0]heptane-6,2'1(1,3)dioxolan} (55) (1.74g, 0.01 mol), acetone (50 ml) and toluene-4-sulphonic acid (50 mg) was left to stand for 64 hours, then diluted with water (50 ml) and extracted into petroleum ether (3 x 50 ml), dried (Na_2SO_4) and solvent evaporated to give an oil (1.08g).

An i.r. spectrum of the product showed no evidence for the cyclobutane carbonyl group (ca. 1780 cm^{-1}) and the spectrum was consistent with starting material.

The reaction of bicyclo[3.2.0]hept-2-ene-6-one (1) with 1,3-dibromo-5,5-dimethylhydantoin at 0°C and 25°C.

1,3-dibromo-5,5-dimethylhydantoin (3g, 0.01 mol) was added to a stirred solution of bicyclo[3.2.0]hept-2-ene-6-one (1) (2.0g, 0.02 mol) in acetone (100 ml) and water (50 ml) at 0°C. After 4 hours at 0°C (in the refrigerator) the solvent was evaporated under reduced pressure. The residue was treated with water (50 ml) and extracted into dichloromethane (3 x 75 ml). Evaporation of the dried (MgSO₄) extracts afforded the crude product, a mixture of bromohydrin isomers (3.59g, 88%).

A sample was derivatised and analysed by g.l.c. (trimethylsilyl ether derivatives, SP200 capillary column, T = 120°C, F.I.D.) and showed the presence of four bromohydrin isomers in the ratio of 90:1:4:5. These had g.l.c. retention times (g.l.c. Rf) identical with those of authentic specimens (Table 2.6). The crude product was subject to flash column chromatography utilising multiple eluting with ethyl acetate-petroleum (1:1) and the following components were isolated and identified by spectroscopic comparison (i.r. and n.m.r.) and chromatographic comparison (t.l.c.) with authentic samples. The above procedure was repeated at 25°C.

- (1) 2-exo-bromo-3-endo-hydroxybicyclo[3.2.0]heptan-6-one (2) (2.22g at 0°C, 54%; 2.58g at 25°C, 63%), (g.l.c. Rf = 3.3 minutes). T.l.c. showed a single spot at Rf = 0.48 (ethyl acetate-hexane; 1:1).
- (2) A mixture of 3-exo-bromo-2-endo-hydroxybicyclo[3.2.0]-heptan-6-one (32) (g.l.c. Rf = 3.8 minutes) and 2-endo-bromo-3-exo-hydroxybicyclo[3.2.0]heptan-6-one (34) (g.l.c. Rf = 4.0 minutes). These isomers were inseparable

by chromatography on silica (combined yields were 0.20g at 0°C, 5%; 0.14g at 25°C, 3%). T.l.c. showed a single spot at $R_f = 0.33$ (ethyl acetate-hexane; 1:1).

- (3) 3-endo-bromo-2-exo-hydroxybicyclo[3.2.0]heptan-6-one (33) (0.13g at 0°C, 3%; 0.11g at 25°C, 5%), (g.l.c. $R_f = 4.4$ minutes). T.l.c. showed a single spot at $R_f = 0.23$ (ethyl acetate-hexane; 1:1).

The total isolated yields of bromohydrins after chromatography were 62% at 25°C and 71% at 25°C.

The results are displayed in Table 2.6.

2.9

REFERENCES

1. Newton, R.F., Roberts, S.M., Tetrahedron Report No. 90, 1980.
2. Ali Mubaric, S., Crossland, N.M., Lee, T.V., Roberts, S.M., Newton, R.F., J.Chem.Soc.Perkin I, 1979, p.122.
3. Grieco, P.A., J.Org.Chem., 1972, 37, p.2363.
4. Dimsdale, M.J., Newton, R.F., Rainey, D.K., Webb, C.F., Lee, T.V., Roberts, S.M., J.Chem.Soc.Chem.Comm., 1977, p.716.
5. Newton, R.F., Howard, C.C., Reynolds, D.P., Wadsworth, A.H., Crossland, N.M., Roberts, S.M., J.Chem.Soc.Chem.Comm., 1978, p.662.
6. Caton, M.P., Tetrahedron, 1979, Vol.35, p.2705.
7. Newton, R.F., Paton, J., Reynolds, D.P., Young, S., Roberts, S.M., J.Chem.Soc.Chem.Comm., 1979, p.908.
8. Reynolds, D.P., Newton, R.F., Roberts, S.M., J.Chem.Soc.Chem.Comm., 1979, p.1150.
9. Crossland, N.M., Roberts, S.M., Newton, R.F., J.Chem.Soc.Perkin I, 1979, p.2397.
10. Chapleo, C.B., Finch, M.A.W., Lee, T.V., Roberts, S.M., Newton, R.F., J.Chem.Soc.Chem.Comm., 1979, p.676.
11. Finch, M.A.W., Lee, T.V., Roberts, S.M., Newton, R.F., J.Chem.Soc.Chem.Comm., 1979, p.677.
12. Ali Mubaric, S., Finch, M.A.W., Roberts, S.M., Newton, R.F., J.Chem.Soc.Chem.Comm., 1979, p.679.
13. Chapleo, C.B., Roberts, S.M., Newton, R.F., J.Chem.Soc.Chem.Comm., 1979, p.680.

14. Grudzinski, Z., Roberts, S.M., J.Chem.Soc.Perkin I, 1975, p.1767.
15. Roberts, I., Kimba, G.E., J.Amer.Chem.Soc., 1937, 59, p.947.
16. Barton, D., Ollis, W.D., 'Comprehensive Organic Chemistry', Pergamon Press, 1979.
17. Ingold, C.K., 'Structure and Mechanism in Organic Chemistry', Cornell University Press, Ithaca, New York, 1953.
18. Olah, G.A., Bollinger, J.M., J.Am.Chem.Soc., 1967, 89, p.4744; *ibid.*, 1968, 90, p.947.
19. Jones, R.A.Y., 'Physical and Mechanistic Organic Chemistry'. Cambridge University Press, 1979, p.171.
20. Dewar, M.J.S., Ann.Rev.Phys.Chem., 1965, 16, p.321.
21. Fahey, R.C., 'Topics in Stereochemistry', edited by E. L. Eliel and N. L. Allinger, Vol.3, p.285.
22. Kwart, H., Takeshita, T., J.Org.Chem., 1963, 28, p.670.
23. Parker, R.E., Isaacs, N.S., Chem.Rev., 1959, 59, p.737.
24. Addy, J.K., Parker, R.E., J.Chem.Soc., 1963, p.915.
25. Still, C.W., Kahn, M., Mitra, A., J.Org.Chem., 1978, Vol.43, No. 14, p.2923.
26. Payne, G.B., Tetrahedron, 1962, Vol.18, p.763.
27. Fieser, L.F., Fieser, M., 'Reagents for Organic Synthesis', Vol.1, p.136, John Wiley and Sons, Inc.
28. Toromanoff, E., Tetrahedron Report No. 96, Tetrahedron, 1980, Vol.36, p.2809.
29. Bucourt, R., 'The torsion angle concept in conformational analysis'. Topics in Stereochemistry, (ed. Eliel, E.L., Allinger, N.L. (1974)), Vol.8, p.159, Interscience, New York.
30. Henbest, H.B., McCullough, J.J., Proc.Chem.Soc., 1962, p.74.
31. Watson et al., J.Am.Chem.Soc., 1981, Vol.103, No. 8, p.2023.

32. Karplus, M., J.Chem.Phys., 1959, 30, p.11.
33. Jackman, L.M., Sternhell, S., 'Applications of Nuclear Magnetic Resonance Spectroscopy in Organic Chemistry', 2nd ed., Pergamon Press (Germany), p.281.
34. Burkert, U., Angewandte Chemie, Int.Ed.Engl. 1981, 20, No. 6/7, p.572.
35. Newton, R.F., Reynolds, D.P., Kay, P.B., Roberts, S.M., Glen, R.C., Murray-Rust, P., J.Chem.Soc.Chem.Comm., 1981, submitted.
36. Glen, R.C., Murray-Rust, P., Reynolds, D.P., Newton, R.F., J.Chem.Soc.Chem.Comm., 1981, submitted.
37. Klinkert, G., personal communication.

CHAPTER 3Contents

- 3.1 Introduction
- 3.2 The geometry and conformation of compounds studied by X-ray diffraction
- 3.2.1 2-(S)-exo-bromo-3-(S)-endo-hydroxybicyclo[3.2.0]heptan-6-one (3)
- 3.2.2 7,8-endo-epoxy-2-oxatricyclo[3.3.0.0.^{4,6}]octan-3-one (60)
- 3.2.3 2,3-endo-epoxybicyclo[3.2.0]heptan-6-one-p-nitrophenylhydrazone (61)
- 3.2.4 3-exo-methoxy-6,7-endo-epoxybicyclo[3.3.0]octane (62)
- 3.2.5 spiro{5-exo-hydroxy-3-oxatricyclo[5.1.1.0^{4,9}]-nonan-8-one-2-1'(4',5'-exo-epoxybicyclo[3.2.0]heptane)} (58)
- 3.2.6 6-endo-methoxy-8-trans-N-methyl-N-p-toluene-sulphonamide-2-oxabicyclo[3.2.1]octan-2-one (63)
- 3.2.7 2-exo-bromo-3-endo-hydroxy-7,7-dichlorobicyclo[3.2.0]heptan-6-one (29)
- 3.3 X-ray crystallography experimental
- 3.3.1 2-(S)-exo-bromo-3-(S)-endo-hydroxybicyclo[3.3.0]heptan-6-one (3)
- 3.3.2 7,8-endo-epoxy-2-oxatricyclo[3.3.0.0.^{4,6}]octan-3-one (60)
- 3.3.3 2,3-endo-epoxybicyclo[3.2.0]heptan-6-one-p-nitrophenylhydrazone (61)
- 3.3.4 3-exo-methoxy-6,7-endo-epoxybicyclo[3.3.0]octane (62)
- 3.3.5 spiro{5-exo-hydroxy-3-oxatricyclo[5.1.1.0^{4,9}]-nonan-8-one-2-1'(4',5'-exo-epoxybicyclo[3.2.0]heptane)} (58)
- 3.3.6 6-endo-methoxy-8-trans-N-methyl-N-p-toluene-sulphonamide-2-oxabicyclo[3.2.1]octan-2-one (63)
- 3.3.7 2-exo-bromo-3-endo-hydroxy-7,7-dichlorobicyclo[3.2.0]heptan-6-one (29)

Chapter 3 Contents (contd.)

3.4 Appendix

(A) Structure solution by the heavy atom method

(B) Direct methods of phase determination

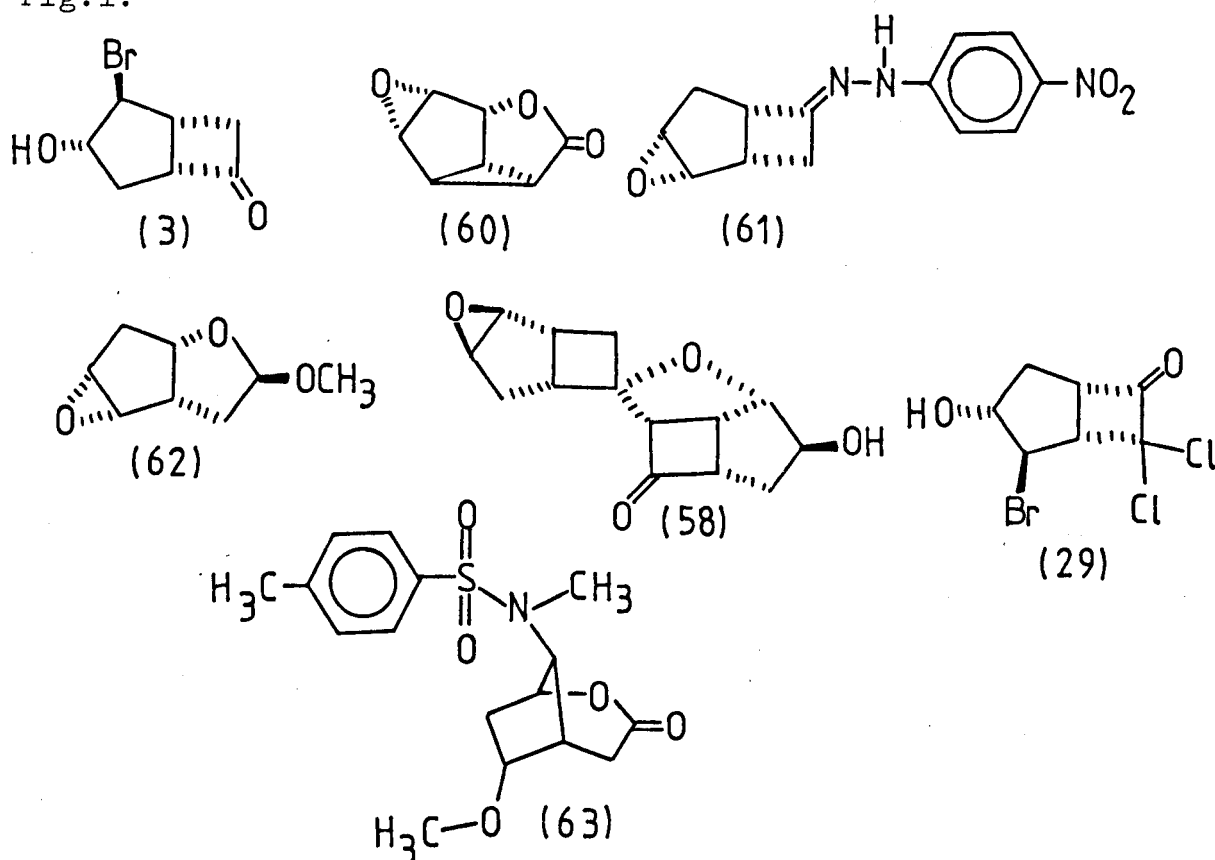
(C) Anomalous dispersion

3.5 References

3.1 Introduction

The structures of 7 compounds (Figure 1) have been determined by X-ray crystallography.

Fig.1.



These compounds were selected (or designed) to elucidate the conformational, electronic and steric factors of importance in promoting regio- and stereo-selectivity in small polycyclic ring systems.

The conformation and geometrical properties of each structure is described in detail (Chapter 3.2) along with some features which may be relevant to regio- and stereo-control.

Of special interest has been the possibility that particular conformations and transition states in compounds of interest, e.g. (2), could be stabilised by transannular interactions between a suitably orientated nucleophile on one

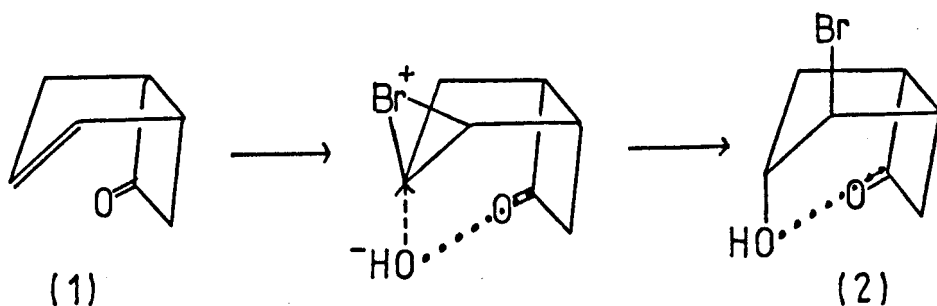
ring and an electrophilic group on another ring². Interactions of this type are indeed observed in some of the crystal structures described here. This aspect is discussed fully in Chapter 4.

The elucidation of the crystal structures is described in an experimental section (Chapter 3.3). X-ray structural data are given in Appendix 1.

3.2 The geometry and conformation of compounds studied by X-ray diffraction

3.2.1 2-(S)-exo-bromo-3(S)-endo-hydroxybicyclo[3.2.0]heptan-6-one (3)^{6,32}

This bromohydrin isomer is the major product on addition of the elements HOBr to bicyclo[3.2.0]hept-2-en-6-one (1) (Chapter 2.5).¹⁵ Knowledge of the ground state geometry is important in assessing the role of steric and conformational factors in the preferential formation of this isomer. Also, from models, it appears that there is the possibility of a transannular interaction of the type described by Bürgi, Dunitz and Shefter² between the hydroxyl and ketone which could conceivably influence the observed bromohydrin isomer ratios by stabilising the transition state leading to (2).



..... BDS interaction

The enantiomer (3) was resolved via a novel method involving yeast enzymes³.

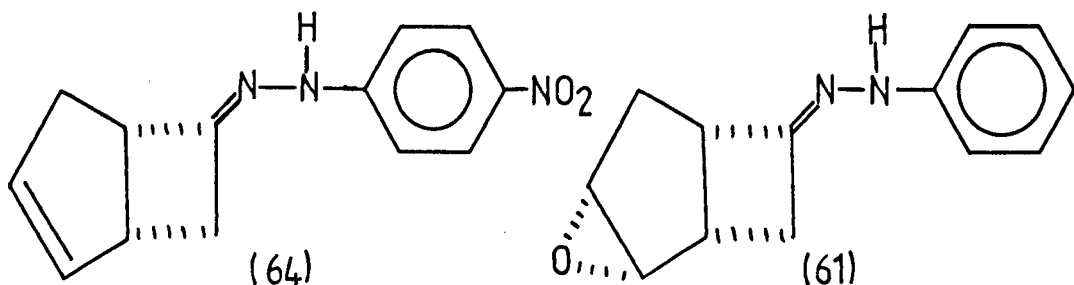
The structure was solved by the classical heavy atom method and the absolute configuration was determined by anomalous dispersion⁴ (Appendix C).

Molecular geometry

The structure consists of molecules hydrogen bonded along the 3_1 axis ($C(3)...O(3)(1-x,x-y,1/3+z) = 2.766(15)\text{\AA}$. (Figure 3.1). Bond lengths, bond angles and torsion angles of interest are given in Figure 3.2.

The molecule (Figure 3.3) adopts a conformation with the cyclopentane ring in the endo-envelope arrangement (approximate mirror plane bisects C(1)-C(5)). The ring substituents are pseudoaxial in an approximate trans arrangement ($|\tau|_{Br(1)-C(2)-C(3)-O(3)} = 158(1)^\circ$). Since the C(1)-C(5) bond is almost eclipsed ($|\tau| = 2.7(1)^\circ$) in the cyclopentane ring, this provides a driving force for the cyclobutane ring to be completely flat ($C(1)-C(5)-C(6)-C(7) = 0(1)^\circ$).

This is in contrast to other structures such as (64)⁵ and (61)⁶ where the different constraints in the 5-membered ring cause noticeable puckering in the 4-membered ring ($|\tau| = 5-11^\circ$).



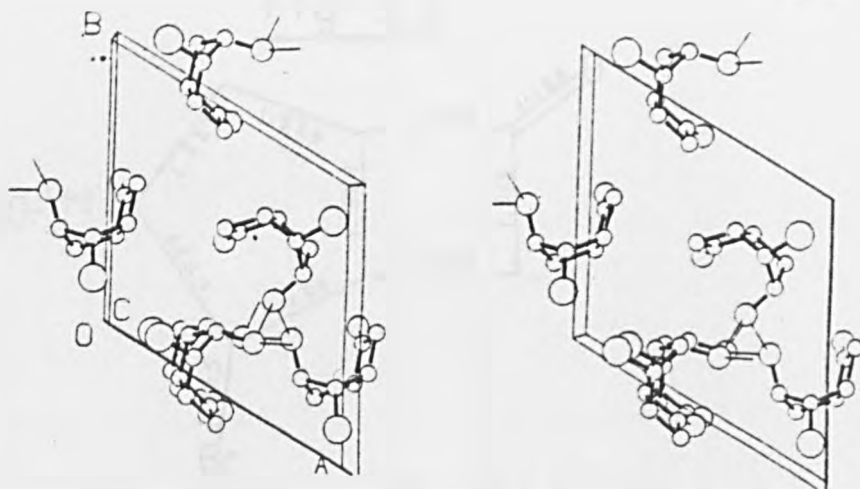


Fig 3,1

Packing diagram of (3). Hydrogen bonds are depicted in the figure by ———

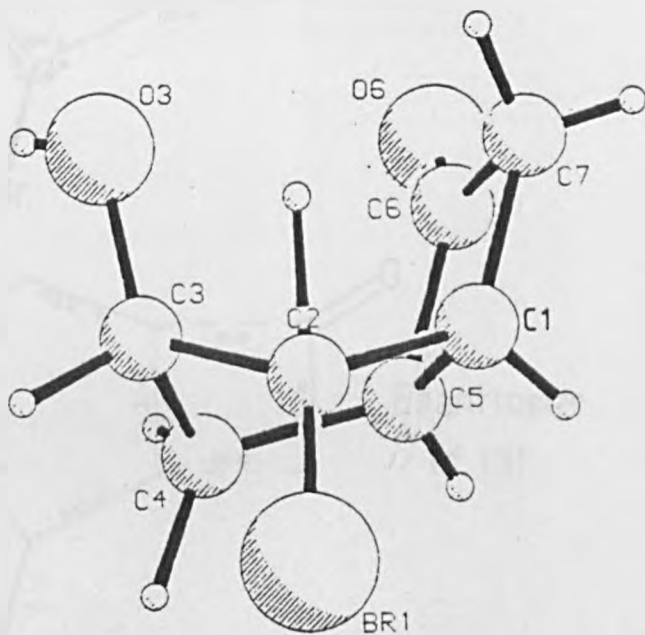


Fig 3,3

The structure of (3).

Fig 3,2

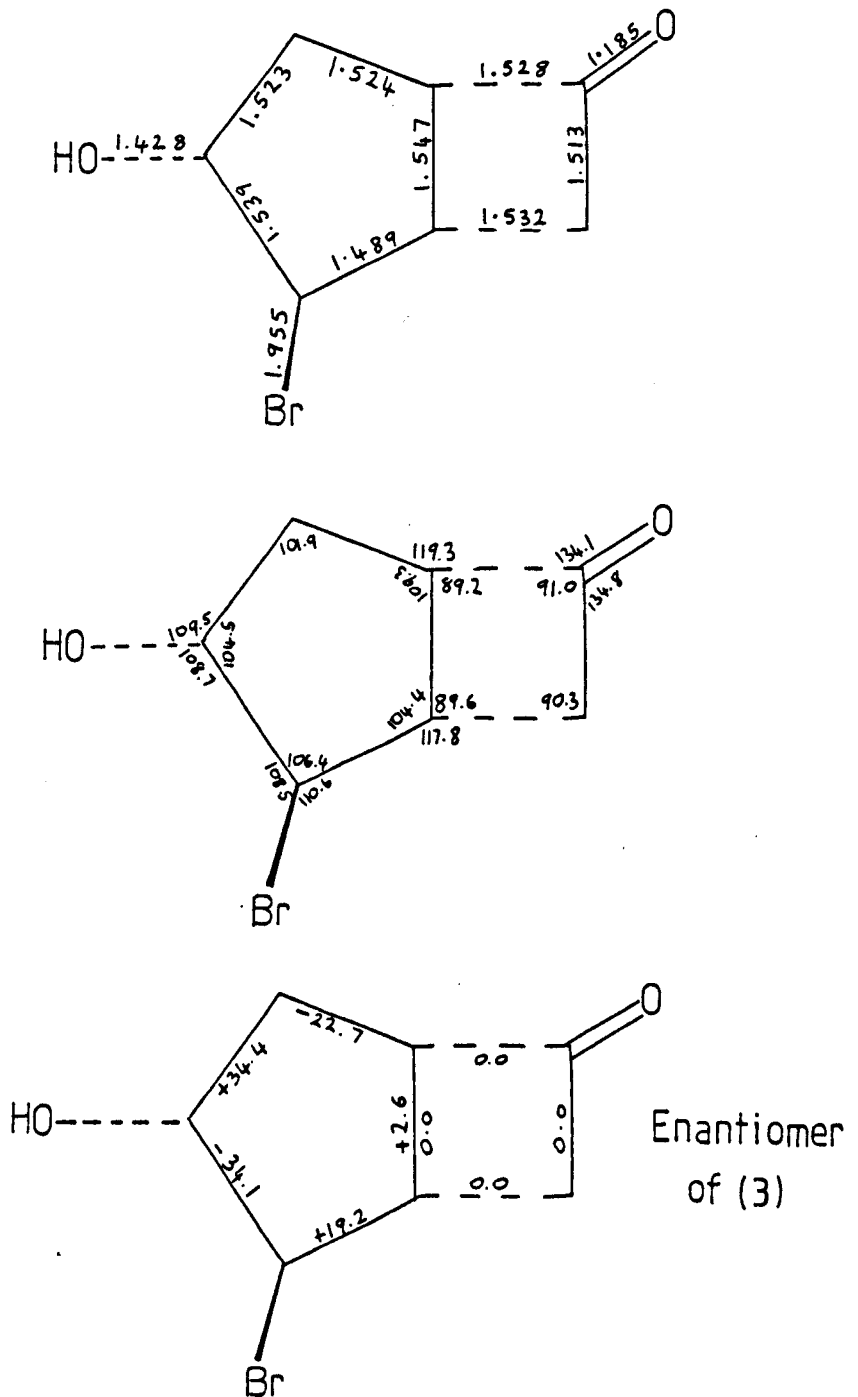


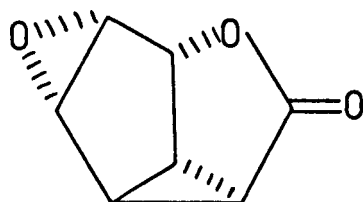
Figure 3.2

Bond lengths (Å), bond angles (°) and torsion angles (°) for (3).

An additional feature is the C(6)...O(3) distance of 2.990(15)Å which may indicate weak incipient nucleophilic attack by O(3) on C(6) of the type proposed by BDS. In keeping with this, C(6) is displaced from the plane C(7),C(5),O(6) by 0.013Å towards O(3). However, although of the expected magnitude, this displacement is of the same order as the standard deviation (0.015Å) and the interaction can only be inferred by comparison with other molecules, e.g. (61).

3.2.2 7,8-endo-epoxy-2-oxatricyclo[3.3.0.0^{4,6}]octan-3-one³¹ (60)

This is a highly strained tricyclic compound (60)⁷ in which the epoxide is constrained to a close approach on the lactone group thus introducing the possibility of a strong transannular interaction between the epoxide and the ketone of the type described by BDS.



(60)

Molecular geometry

Bond lengths, bond angles and torsion angles of interest are given in Figure 3.4. The crystal structure consists of discrete molecules (Figure 3.5) with no unusually short intermolecular contacts (Figure 3.6).

The ring fusions probably govern the conformations of the 5-membered rings.

Fig 3,4

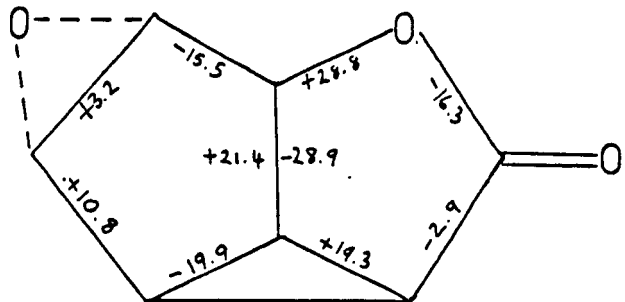
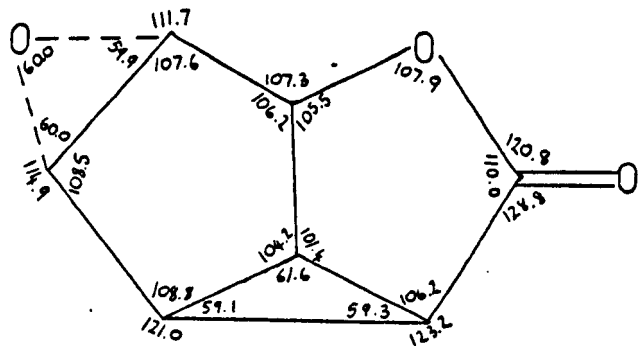
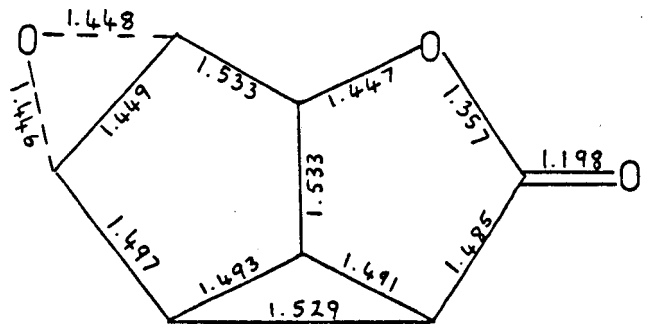


Figure 3.4

Bond lengths (Å), bond angles (°) and torsion angles (°) for (60).

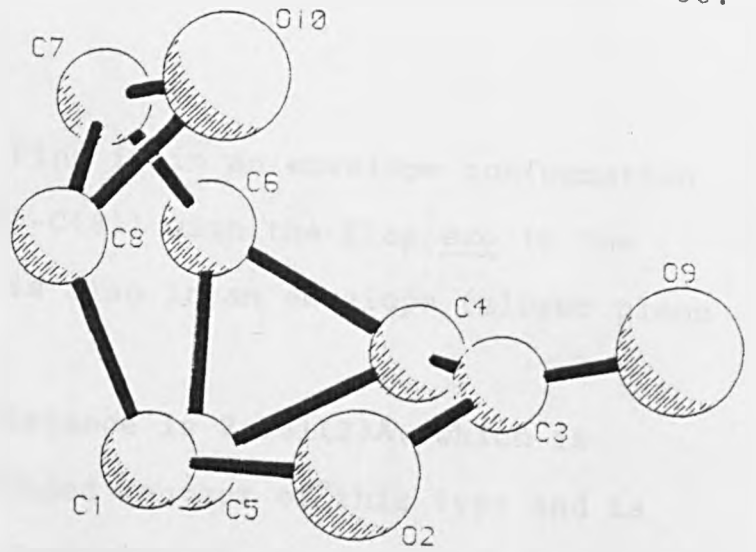


Fig 3,5

The structure of (60)

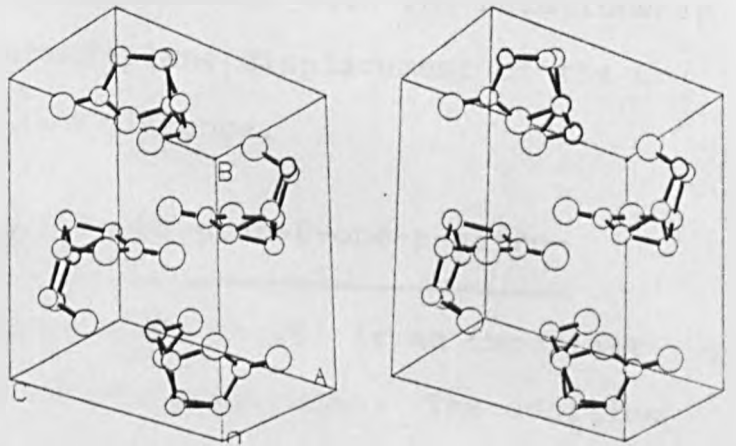


Fig 3,6

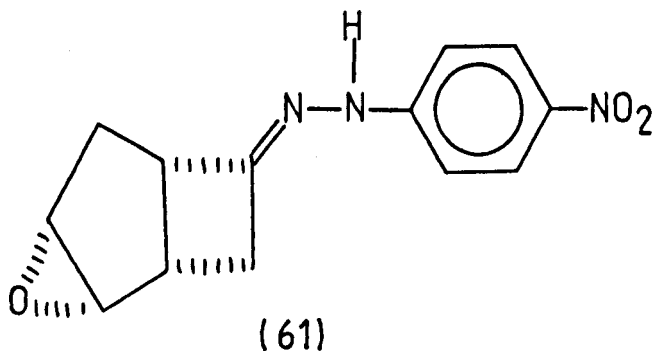
Packing diagram for (60)

The cyclopentane ring is in an envelope conformation (mirror plane bisecting C(7)-C(8)) with the flap exo to the epoxide. The lactone ring is also in an envelope (mirror plane bisecting C(3)-C(4)).

The O(10)...C(3) distance is 2.651(2)Å, which is unusually small for a non-bonded contact of this type and is mainly due to geometrical constraints imposed on the two 5-membered rings by the C(4)-C(6) bond. Incipient nucleophilic attack by the lone pair of O(10) on the carbonyl carbon C(3) of the type described by BDS is observed. In confirmation of this, C(3) is displaced from the plain O(2),C(4),O(9) by 0.052(1)Å towards O(10). This agrees well with the relationship derived by BDS between the out-of-plane displacement of the C atom and the nucleophile O...C=O distance.

3.2.3 2,3-endo-epoxybicyclo[3.2.0]heptan-6-one-p-nitrophenylhydrazone (61)³⁵

The addition of nucleophiles to (6) is an important step in a number of syntheses of prostaglandins. The addition proceeds with high regio- and stereo-selectivity, giving predominantly the 3-endo-hydroxy product (Chapter 2.5). Since (6) is a liquid, the crystal structure of (61) (Figure 3.7), a solid derivative of (6), has been determined.



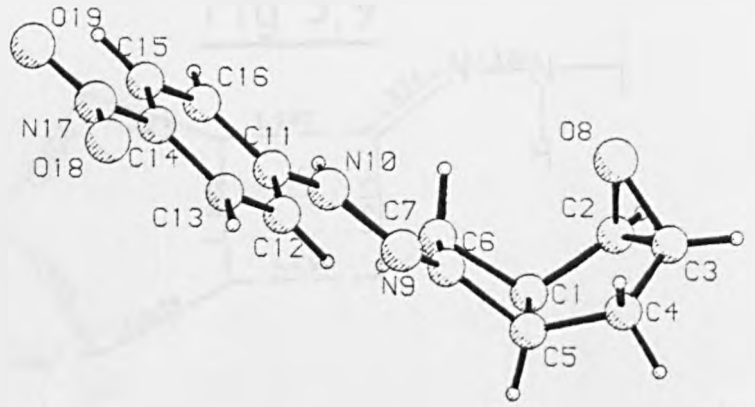


Fig 3,7

The structure of (61)

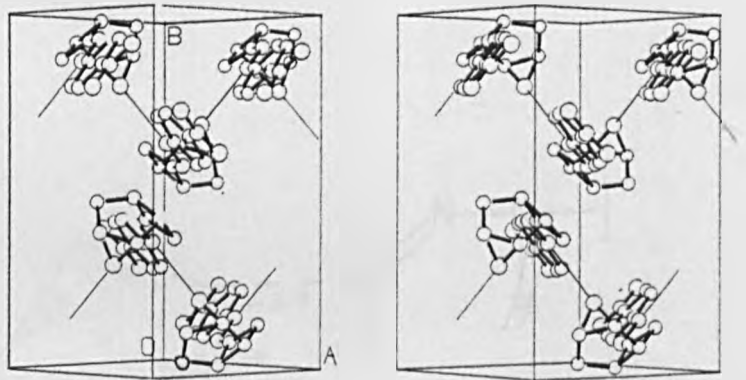


Fig 3,8

Packing diagram for (61). Hydrogen bonding is indicated by _____

Fig 3,9

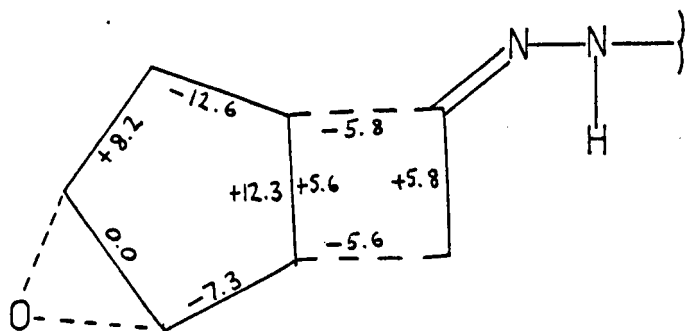
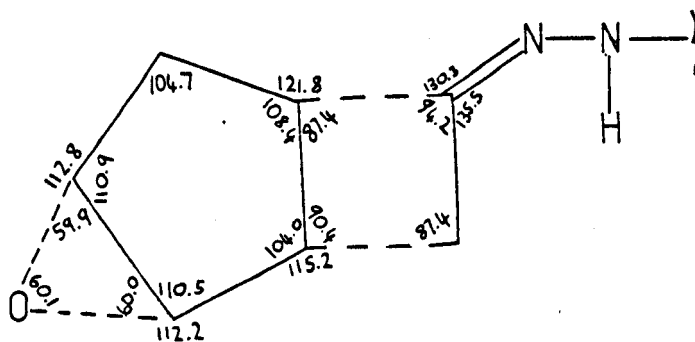
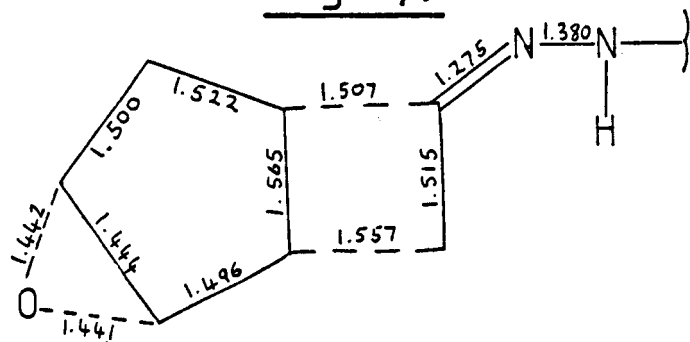


Figure 3.9

Bond lengths (Å), bond angles (°) and torsion angles (°) for (61).

Molecular geometry

The molecules are hydrogen-bonded to form chains $N(10)(x, 0.5-y, z-0.5) \dots O(8) = 2.970(2)\text{\AA}$. (Figure 3.8).

Bond lengths, bond angles and torsion angles of interest are given in Figure 3.9. The 5-membered ring has an envelope conformation with the flap endo to the epoxide (mirror plane bisects C(2)-C(3)).

The 4-membered ring has a twist conformation ($|\tau|C(1)-C(7)-C(6)-C(5) = 5.8^\circ$). The conformation of the 5-membered ring is not completely transmitted across the ring junction ($|\tau|C(2)-C(1)-C(5)-C(4) = 12.3^\circ$, $|\tau|C(6)-C(5)-C(1)-C(7) = 5.6^\circ$) and this introduces torsional strain (6.7°). This effect appears to be a result of the constraint applied to the 5-membered ring by the epoxide.

The $O(8) \dots C(6)$ distance is $2.990(3)\text{\AA}$ which is short enough to be considered as incipient nucleophilic attack of the type described by BDS. In confirmation of this, C(6) is displaced from the plane C(7), C(5), N(9) by $0.008(3)\text{\AA}$ towards O(8).

3.2.4 3-exo-methoxy-6,7-endo-epoxy-2-oxabicyclo-[3.3.0]octane (62)³⁴

The crystal structure of (62) was undertaken to provide data on the effect of an epoxide substituent on the conformation of the bicyclo[3.3.0] system. Also, unlike other bicyclic epoxides studied in this series, there is no possibility of transannular incipient nucleophilic attack by the epoxide (as in (8)⁸).

The structure (62) consists of discrete molecules (Figure 3.10) with no unusually short intermolecular contacts (Figure 3.11).

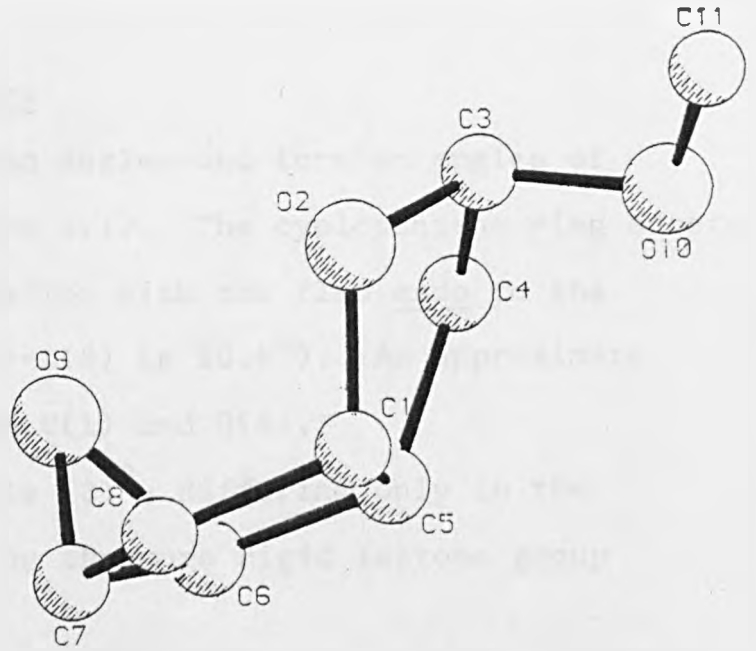


Fig 3,10

The structure of (62)

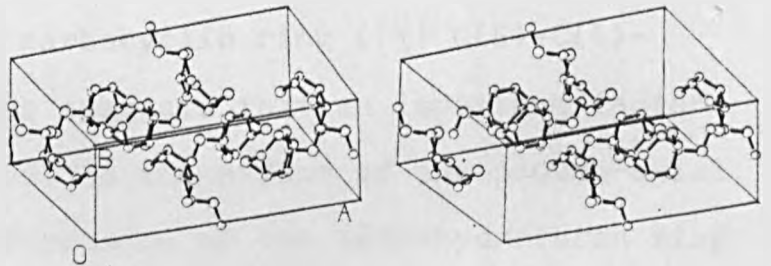


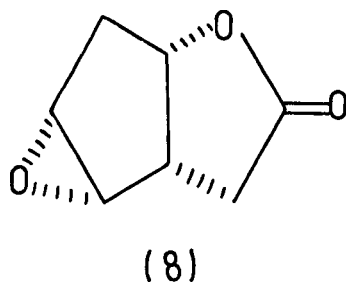
Fig 3,11

Packing diagram for (62)

Molecular geometry

Bond lengths, bond angles and torsion angles of interest are given in Figure 3.12. The cyclopentane ring adopts a shallow envelope conformation with the flap endo to the epoxide ($|\tau|$ C(6)-C(5)-C(1)-C(8) is 10.5°). An approximate mirror plane passes through C(1) and O(9).

A similar molecule (8)⁸, differing only in the replacement of the acetal by the more rigid lactone group



has a much more puckered carbocyclic ring ($|\tau|$ C(6)-C(5)-C(1)-C(8) is 18.5°). This suggests that an important factor in the conformation of (62) is the effect of the pseudo-axial methoxy group on the conformation of the tetrahydrofuran ring which is forced to take up a twist arrangement (diad through C(5)). The torsional strain about O(2)-C(3) is thus much reduced ($|\tau|$ C(1)-O(2)-C(3)-O(10) = 79.5°), but only at the cost of transmitting some strain to the carbocyclic ring. In confirmation of this, the unsubstituted cyclopentene epoxide (67)⁹ is considerably more puckered than either (8) or (62) ($|\tau|$ C(2)-C(3)-C(4)-C(5) in (67) is 27.9°). Relief of torsional strain might also have been possible if the methoxy group had taken up a pseudo-equatorial position, but models suggest that a rather short O(9)...C(3) distance would then be found.

Fig 3,12

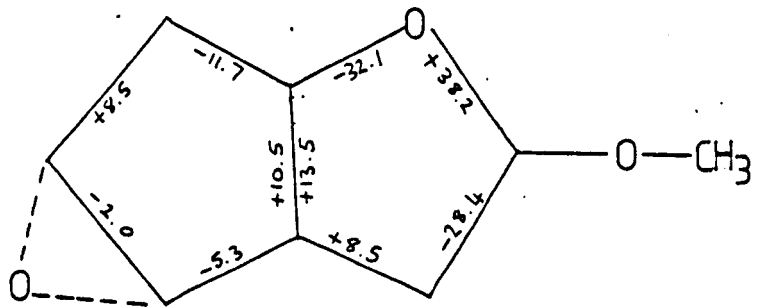
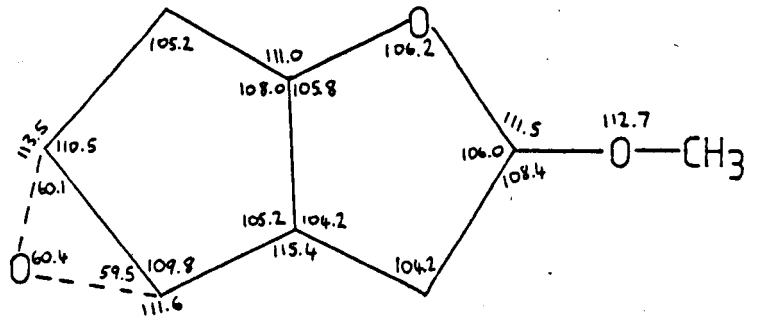
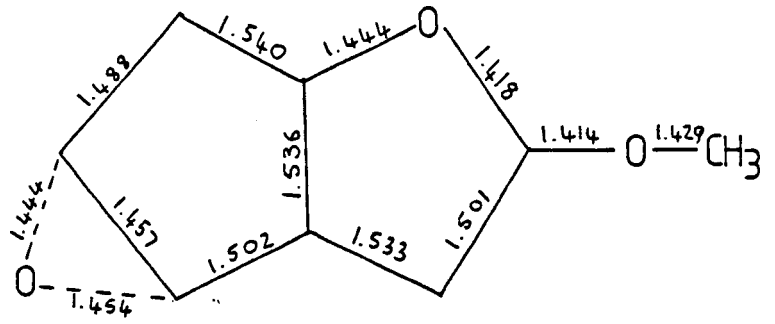
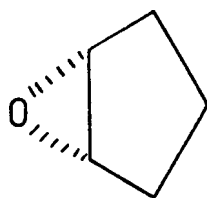


Figure 3.12

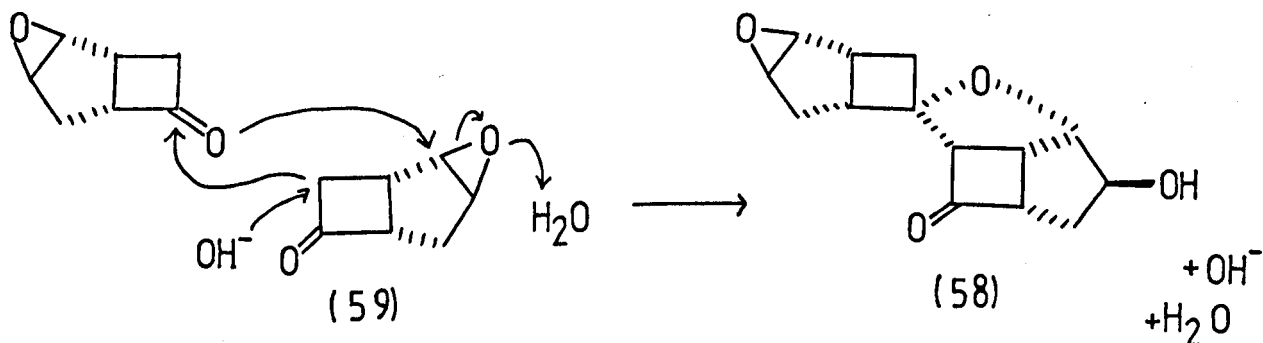
Bond lengths (Å), bond angles (°) and torsion angles (°) for (62).



(67)

3.2.5 5-exo-hydroxy-3-oxatricyclo[5.1.1.0^{4,9}]nonan-8-one, 2,1'-spiro{4',5'-exo-epoxybicyclo[3.2.0]heptane}(58)

This molecule (58) is formed from the exo-epoxide (59) by an aldol condensation at elevated temperature with excess base (Chapter 2.4).



Spectroscopic methods (i.r., n.m.r., mass spectroscopy) failed to positively identify this structure. Thus, an X-ray investigation was undertaken.

This structure offers the opportunity to analyse the effects of the exo-epoxide group on the geometry and conformation of the bicyclo[3.2.0] system. Also this is the first structure in this series with a saturated 4-membered ring.

Molecular geometry

Bond lengths, bond angles and torsion angles of interest are given in Figure 3.13.

Fig 3,13

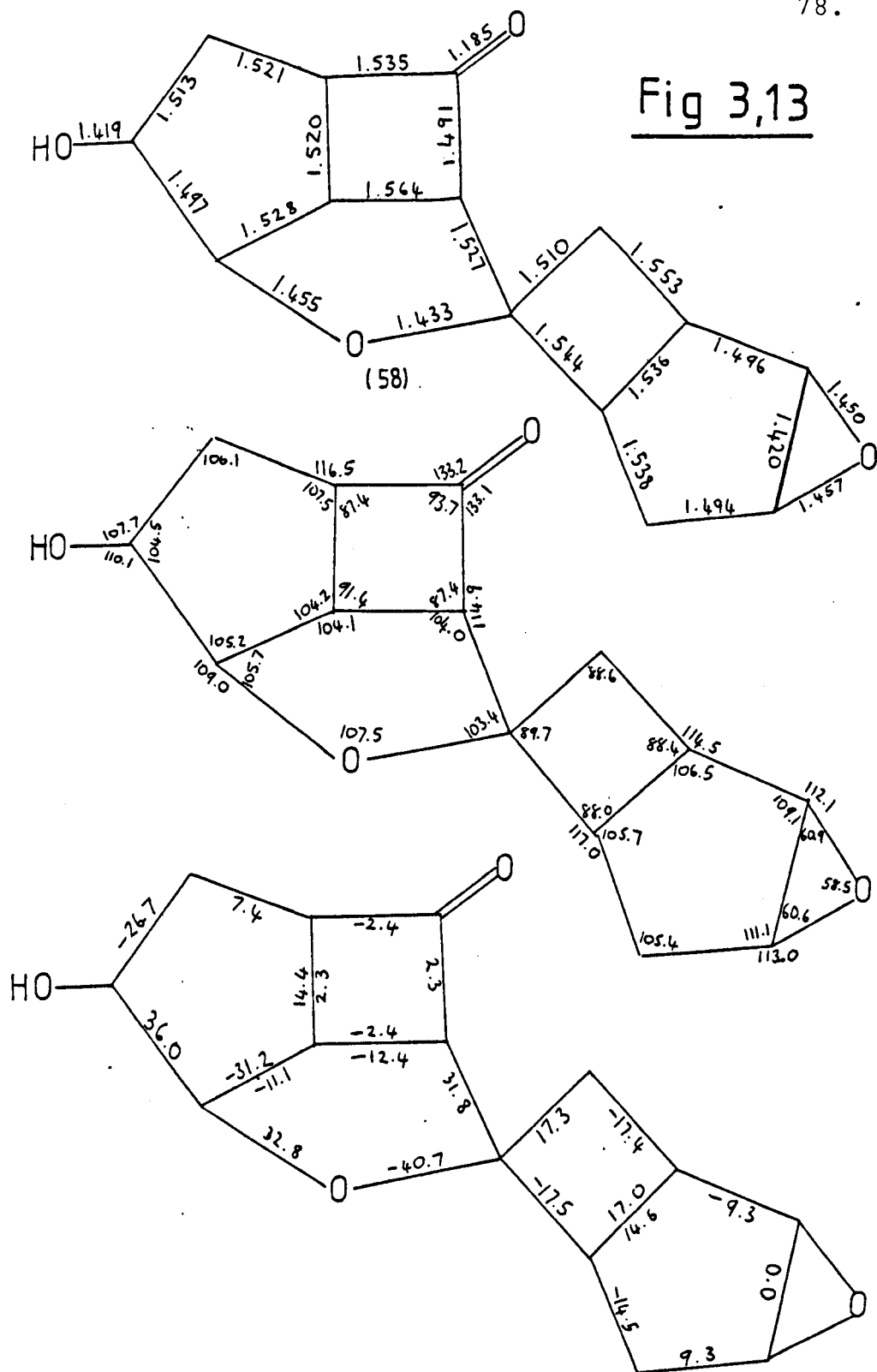


Figure 3.13

Bond lengths (Å), bond angles (°) and torsion angles (°) for (58).

The structure (58) (Figure 3.14) consists of molecules hydrogen-bonded head to tail in chains, $O(15)\dots O(3)(x,y-1,z) = 2.819\text{\AA}$ (Figure 3.15).

The tricyclic fragment adopts a conformation partly constrained by the ether bridge from C(2) to C(8). Here, the cyclopentane ring is in an approximate twist conformation (diad bisecting C(2)-C(3)) with O(3) almost anti-periplanar to O(8) ($|\tau| O(3)-C(3)-C(2)-O(8) = 167.7^\circ$), while the cyclobutanone ring is almost planar ($|\tau| = 2.4^\circ$). This introduces considerable torsional strain across the C(1)-C(5) bond ($|\tau| C(2)-C(1)-C(5)-C(4) = 14.3^\circ$ and $|\tau| C(7)-C(1)-C(5)-C(6) = 2.2^\circ$). The furan fragment is also in a twist conformation (diad through C(1)) with O(8) endo to the cyclobutane ring. The inequality of the bond lengths O(8)-C(2) (1.455(4)\AA) and O(8)-C(8) (1.433(5)\AA) may be due to steric strain. The approach of O(8) towards C(6) (a 1-4 interaction) is a close contact, however, there does not appear to be any evidence for incipient nucleophilic attack by O(8) on C(6). The O(8) lone pair is not suitably orientated towards C(6), and the O(8)...C(6)-O(6) angle is rather oblique at 124° . The carbonyl carbon C(6) is planar to within experimental error with 0.004(6)\AA deviation from the plane of C(5),C(7),O(6).

In the bicyclic fragment, the cyclopentane ring has an envelope conformation (mirror plane bisecting C(9)-C(10)). The degree of hybridisation of C(8) has been reduced from sp^2 to sp^3 with the result that the cyclobutane ring is more puckered ($|\tau| = 17^\circ$) than in the keto form and therefore transannular strain about C(9)-C(13) is much reduced ($|\tau| C(10)-C(9)-C(13)-C(12) = 14.6^\circ$).

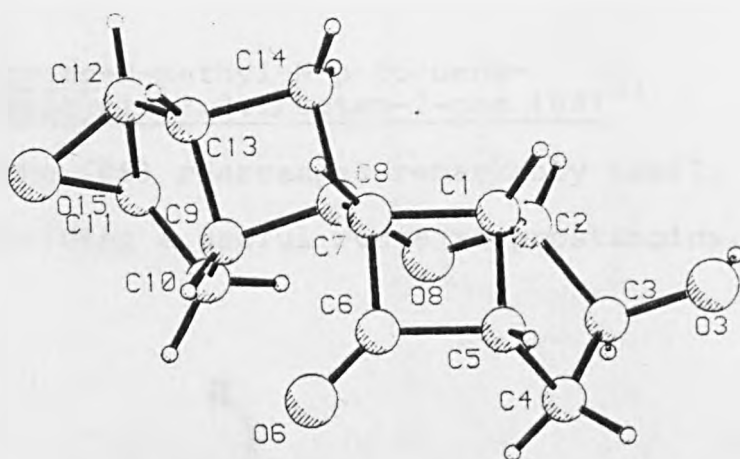


Fig 3,14

The structure of (58)

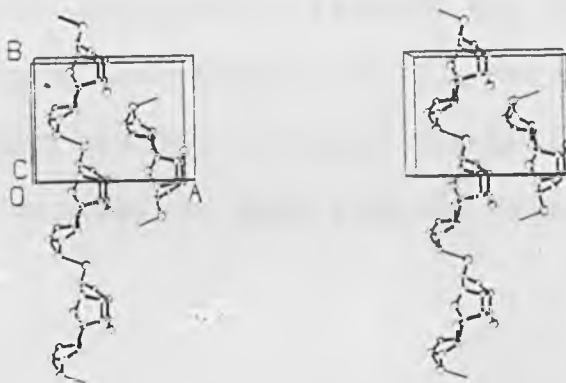
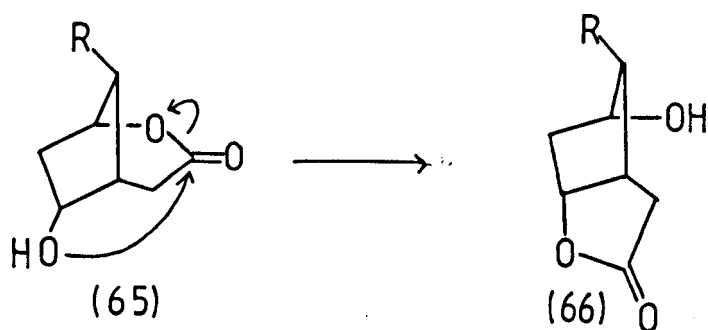


Fig 3,15

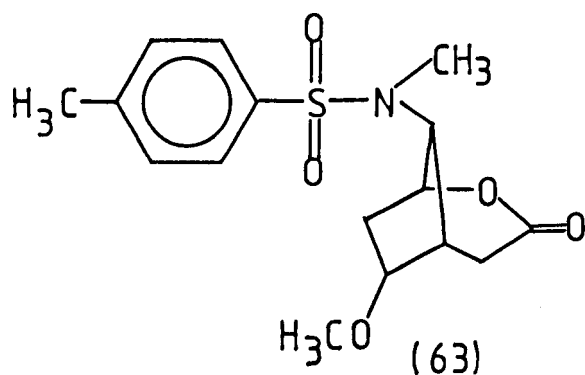
Packing diagram for (58). The hydrogen bonds are indicated by ———

3.2.6 6-endo-methoxy-8-trans-N-methyl-N-p-toluene-sulphonamide-2-oxabicyclo[3.2.1]octan-2-one (63)³³

The hydroxylactone (65) rearranges remarkably easily to the γ -lactone (66)¹ providing a useful route to prostanoids.

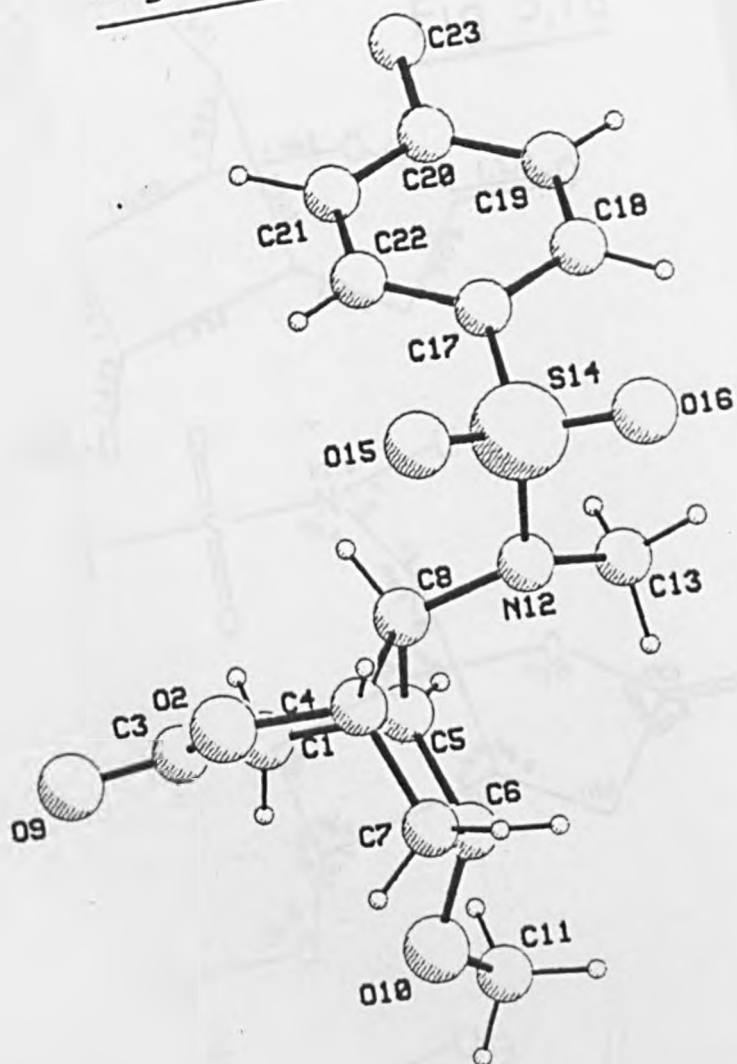
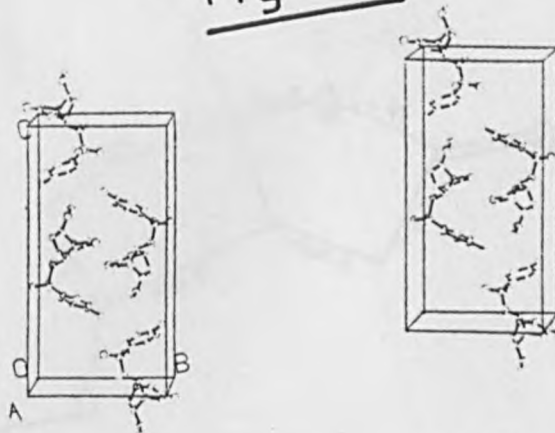


This reaction seems to be promoted by the steric properties of the molecule and in particular by the possibility of a transannular intramolecular interaction between the hydroxy and the lactone group of the type described by BDS². Accordingly, the model compound (63) has been studied in which the assistance of a transannular interaction similar to that seen in related molecules seemed probable.



Molecular geometry

The crystal structure of (63) consists of discrete molecules (Figure 3.16) with no unusually short intermolecular contacts (Figure 3.17).

Fig 3,16Fig 317Figure 3.16 The structure of (63)Figure 3.17 Packing diagram for (63).

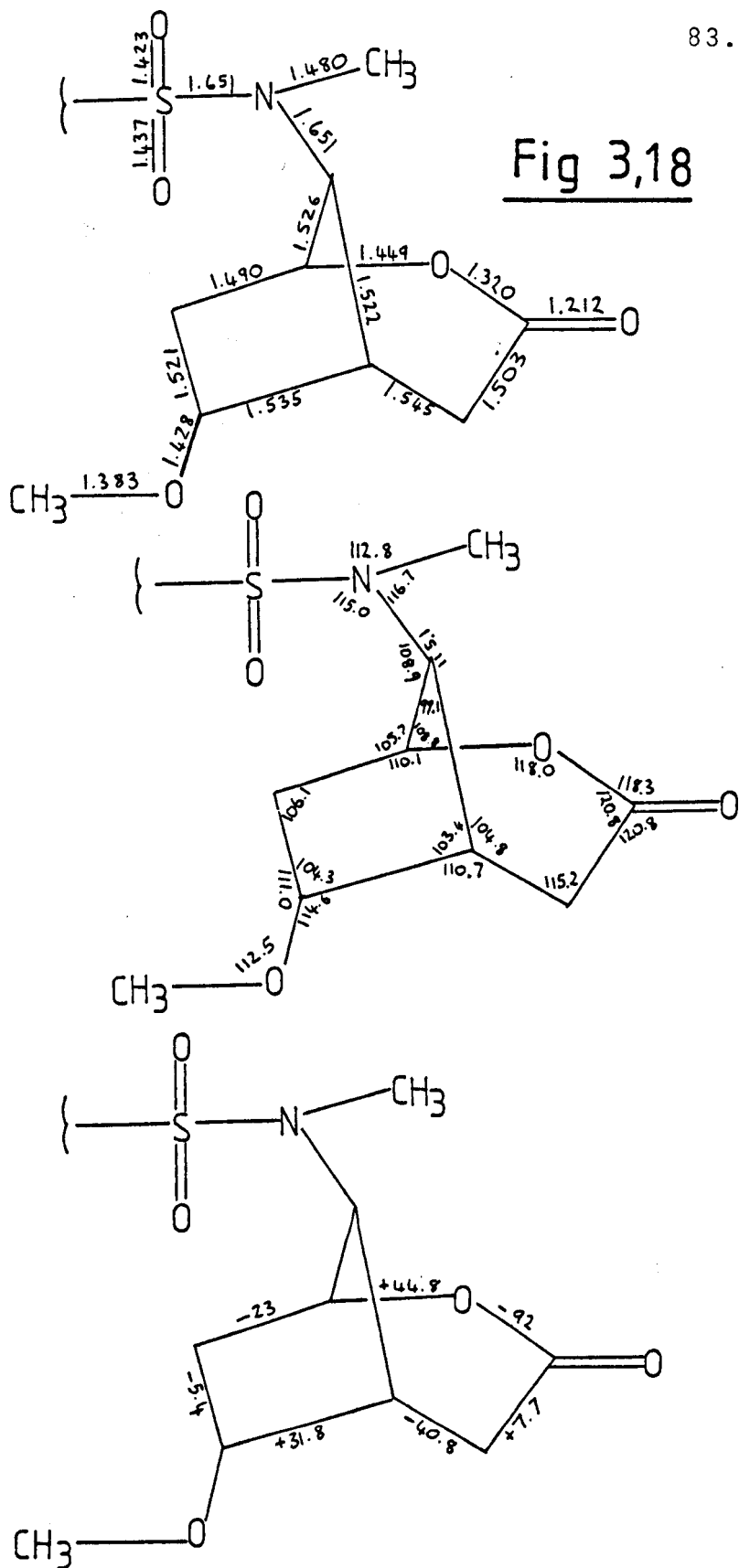


Figure 3.18

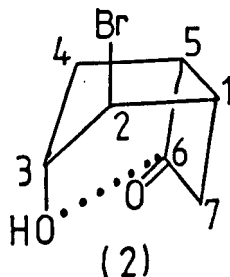
Bond lengths (Å), bond angles (°) and torsion angles (°) for (63).

Bond lengths, bond angles and torsion angles of interest are given in Figure 3.18.

The carbocyclic 5-membered ring has a strongly puckered envelope conformation with an approximate mirror plane through C(8). The lactone ring has a sofa conformation with C(1), O(2), C(3), C(4), C(5) almost coplanar. The methoxy substituent is thus directed away from the ring system and the observed C(3)...O(10) distance (3.492(6)Å) is much larger than that (3.1Å) for the weakest interaction found by BDS. There are no structural data for the bicyclic system or analogous molecules, but the geometry is essentially that which would be predicted for the unsubstituted ring system. It is clear, therefore, that any energy gained by incipient nucleophilic attack of O(10) on C(3) is insufficient to distort the relatively rigid bicyclic nucleus (see Chapter 4).

3.2.7 2-exo-bromo-3-endo-hydroxy-7,7-dichlorobicyclo-[3.2.0]heptan-6-one (29)³⁰

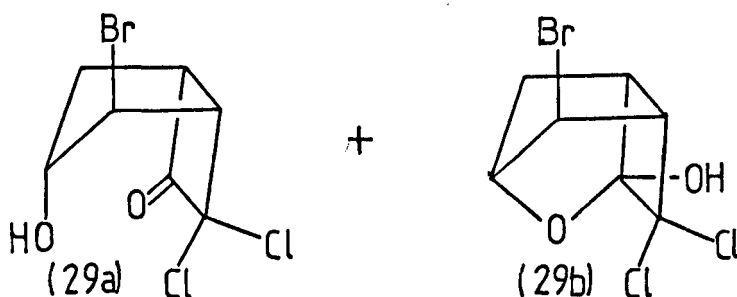
The bromohydrin (2) displays a weak transannular interaction between the hydroxy group on C(3) and the ketone carbon, C(6).(.....)



The interaction displayed by (2) could be interpreted as a 'frozen-out' intermediate on the reaction pathway of nucleophilic addition to a carbonyl. Unfortunately the interaction seen here was so weak that it could only be inferred from comparison with similar compounds. However there was the possi-

bility that activation of the ketone group by electron withdrawing substituents would give a structure further along the reaction pathway. Compound (29), in which the carbonyl is activated by the presence of two adjacent chlorines, was reported (on ^1H n.m.r. evidence)¹² to exist in CCl_4 solution as an equimolar mixture of (29a) and (29b). The ketone and ketal form thus represent the reactant and product of nucleophilic attack by the hydroxyl on the ketone.

X-ray structure analysis of the solid which crystallises from CCl_4 revealed that, remarkably, the two independent molecules in the asymmetric unit correspond to (29a) and (29b).



Their molecular geometries show little distortion along the reaction pathway (29a)...(29b); the $\text{O}\cdots\text{C}=\text{O}$ length is $2.83(2)\text{\AA}$ in (29a) and $1.43(1)\text{\AA}$ in (29b). The expected out-of-plane displacement of the carbonyl in (29a) is masked by experimental error.

It appears, therefore, that crystal packing forces, whilst not strong enough to trap an intermediate, have isolated both partners in a chemical equilibrium.

Though frequently seen in conformational processes, this is unusual for chemical reactions involving bond formation and is normally limited to proton exchange¹⁴ (e.g. in anthranilic acid where both the neutral molecule and zwitterion coexist in the crystal)¹³.

This is the first example of ring-chain tautomers being isolated as partners in a crystal lattice.

For (29), it seems the crystal structure of (29a)+(29b) is more stable than either (29a) or (29b), provided that (29a) and (29b) are equilibrating in solution and that crystallisation gives the thermodynamically controlled product. Although the last point cannot easily be formally verified, differential scanning calorimetry of the crystals showed no phase transitions in the range 173K to 352K (M.Pt.).

The ^{13}C n.m.r. spectrum of crystals of (29) in CHCl_3 solution at 298K shows 14 resonances (Table 3.2).

*TABLE 3.2 ^{13}C N.m.r. spectrum of (29) at 298K

<u>ppm</u>	<u>atom assignment</u>	<u>integral</u>
195.4(s)	(6a)	
104.2(s)	(6b)	
89.1(s)	(7b)	0.9
87.4(s)	(7a)	1.0
82.5(d)	(3a)	16.5
80.6(d)	(3b)	17.3
60.4(d)	(2b)	
59.5(d)	(2a)	
54.5(d)		
52.5(d)		
47.2(d)	(1a),(5a),(1b),(5b)	
47.0(d)		
36.2(t)	(4a)	20.4
33.0(t)	(4b)	18.1

At 298K the ^{13}C n.m.r. may be interpreted as a mixture of (29a)+(29b) in the ratio of 1.0:1.1.

The spectrum appears independent of temperature (compare Tables 3.2 and 3.3) suggesting that the inter-conversion of (29a) \rightleftharpoons (29b) is very slow and that the 1:1 composition in the

solid is determined by the stoichiometry of the crystal.

*TABLE 3.3 ^{13}C N.m.r. spectrum of (29) at 304K

<u>ppm</u>	<u>atom</u>	<u>integral</u>
88.9	(7b)	19.4
87.2	(7a)	21.7
82.4	(3a)	58.5
80.3	(3b)	56.2
36.1	(2a)	32.3
32.9	(2b)	40.8

Addition of a trace of acid catalyst ($p\text{-CH}_3\text{C}_6\text{H}_4\text{SO}_3\text{H}$) markedly alters the spectrum, giving a non-integral ratio which is temperature dependent.

*TABLE 3.4 Temperature dependence of integrated intensities of the ^{13}C n.m.r. of (29) in CHCl_4 solution with a trace of acid catalyst

<u>ppm</u>	<u>atom</u>	<u>238K</u>	<u>243K</u>	<u>304K</u>
195.4	(6a)			
104.2	(6b)			
89.1	(7b)	49.4	42.3	15.4
87.4	(7a)	20.5	20.0	14.1
82.5	(3a)	52.8	47.6	43.8
80.6	(3b)	10.6	14.9	39.6
60.4	(2b)			
59.5	(2a)			
54.5				
52.5				
47.2				
47.0				
36.2	(2a)	9.8	10.6	29.0
33.0	(2b)	42.0	30.4	32.1

From the integrated intensities of the resonances at 33.0, 36.2, 80.6, 82.5, 87.4, 89.1 ppm, an estimate was made of the ratio of (29a):(29b) (Table 3.5).

TABLE 3.5*

<u>T(K)</u>	<u>ratio (29a):(29b)</u>
238	4:1
243	3:1
304	1:1

*
The above n.m.r. spectra were obtained on a Bruker WP80 at 20.13 MHz in inverse gated decoupling mode.

Increasing the concentration of the acid or raising the temperatures led, as expected, to coalescence of peaks with (29a) \rightleftharpoons (29b) becoming rapid on the n.m.r. time scale.

Recrystallisation of (29) from a number of solvents: MeOH, MeNO₂, CHCl₃, CCl₄ with or without acid catalysis, always led to the same solid. This was verified by infra-red spectroscopy since the spectrum of (29a)+(29b) in a KBr disc is very characteristic with a double peak in the OH region (3380 and 3480 cm⁻¹) (Figure 3.19). The crystal morphology and melting points were also used as checks. This is evidence that despite the composition of the solution, packing forces appear to control the crystal structure and stoichiometry of the solid.

Molecular geometry

Bond lengths, bond angles and torsion angles of interest are given in Figure 3.20.

The structure is hydrogen-bonded O(1a)...O(2b) = 2.979Å (x,-y,Z-0.5); O(2b)...O(2a) = 2.836Å (0.5-x,0.5-y,-z) in chains along the c-glide (Figure 3.21). The ketone of (29a) is H-bonded to the hydroxyl of (29b). The hydroxyl of (29b) is

Fig 3,19

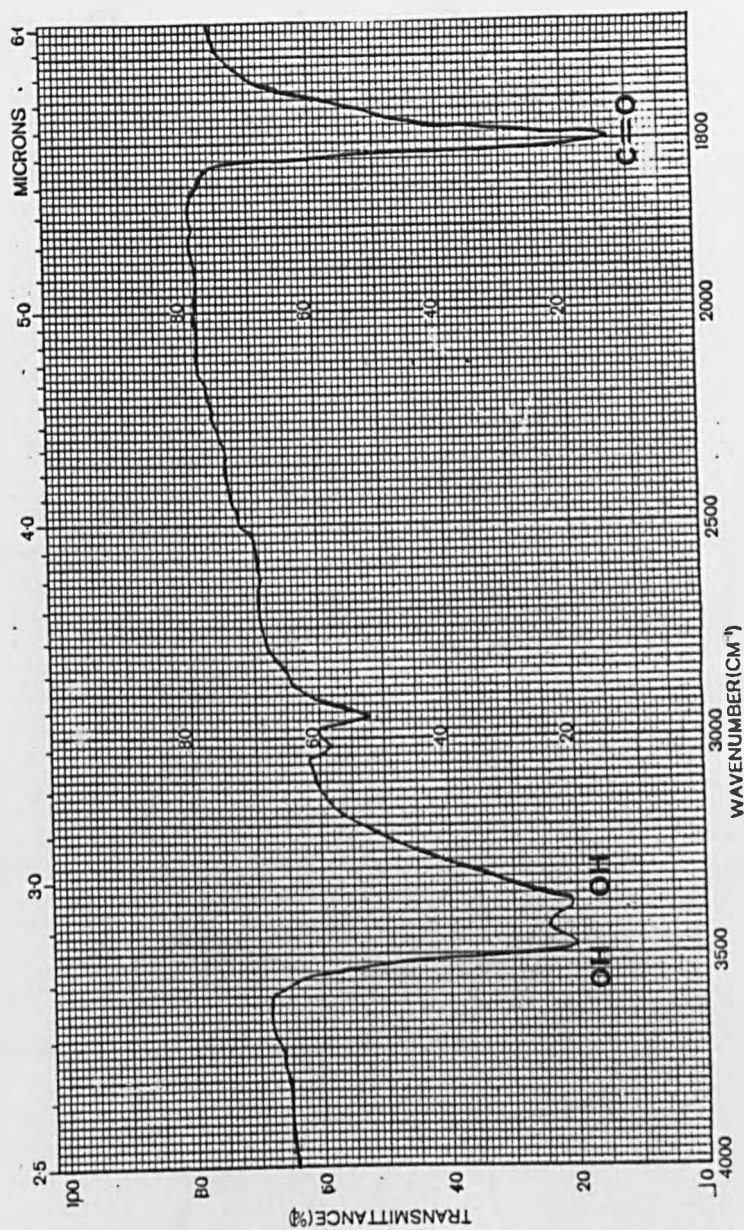


Figure 3.19

I.r. spectra of (29) displaying a double OH peak at 3350 and 3450 cm^{-1} , corresponding to the 2 isomers (29a) and (29b).

Fig 3,20a

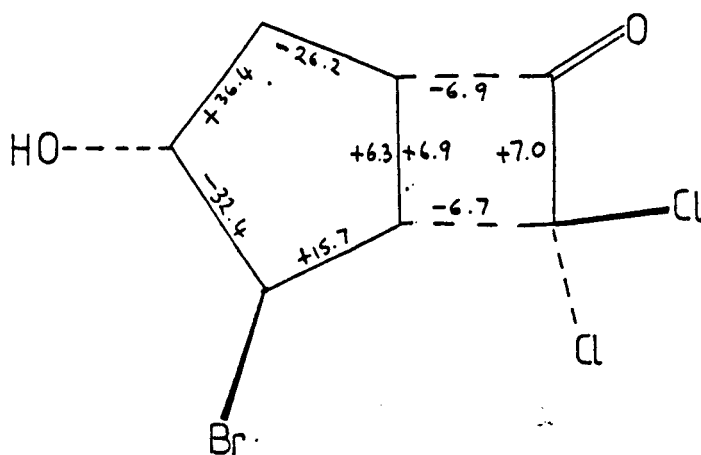
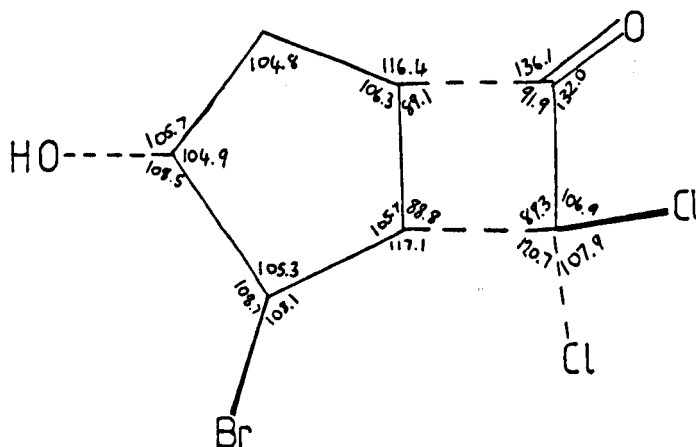
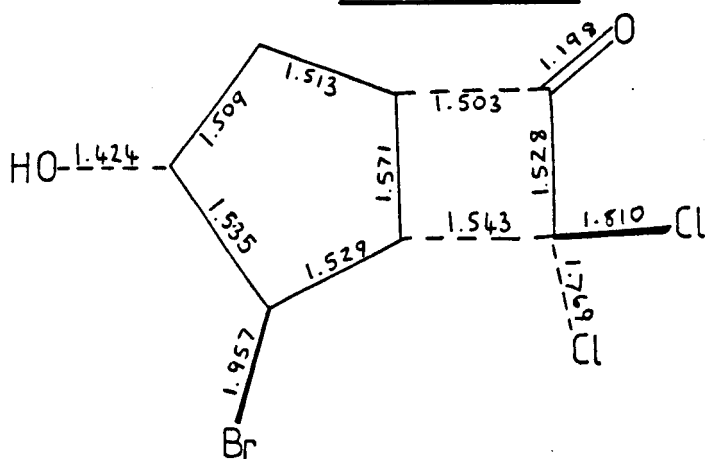


Figure 3.20a

Bond lengths (Å), bond angles (°) and torsion angles (°) for (29a) (the bicyclic partner).

Fig 3, 20b

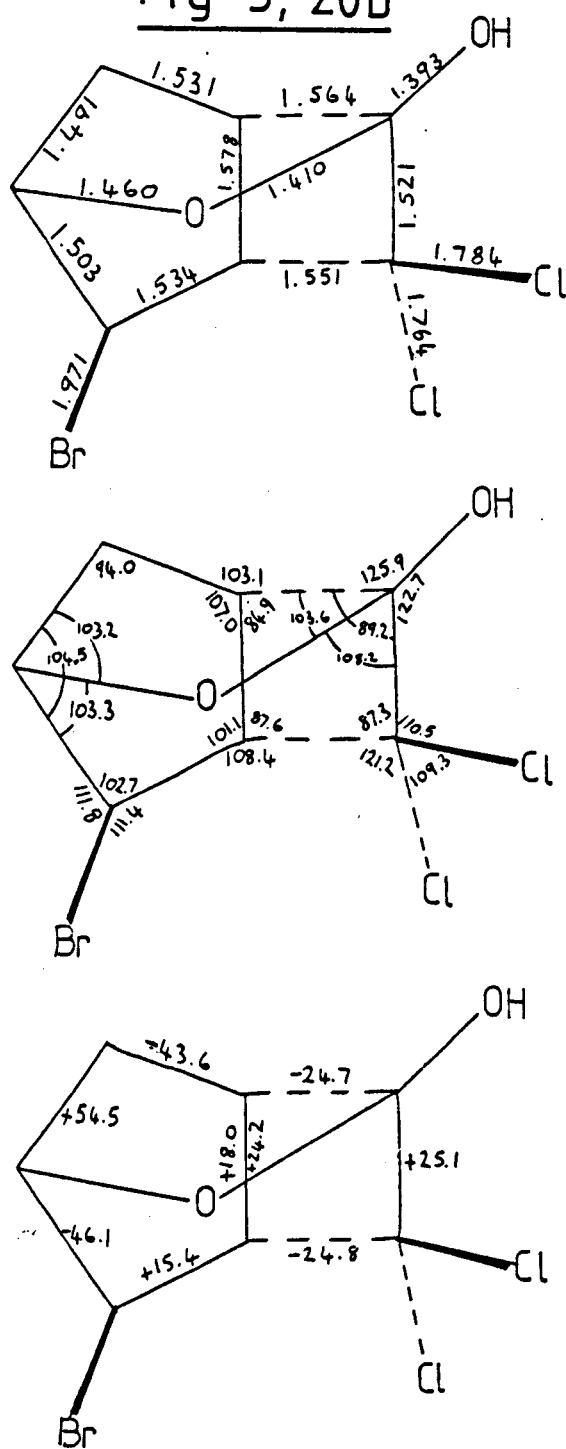


Figure 3.20b

Bond lengths (Å), bond angles ($^{\circ}$) and torsion angles ($^{\circ}$) for (29b) (the tricyclic partner).

also H-bonded to the hydroxyl of (29a) (i.e. the next molecule in the chain). The ketone of this molecule of (29a) is H-bonded to the hydroxyl of (29b) (etc.). The structure has 2 molecules in the asymmetric unit (Figure 3.22).

The bicyclic molecule (29a), has the 5-membered ring in an endo-envelope conformation with an approximate mirror plane bisecting C(1a)-C(5a). The 4-membered ring has a twist conformation ($|\tau|C(7a)-C(1a)-C(5a)-C(6a) = 6.9^\circ$). There is a relatively strong transannular interaction of the type described by BDS; $O(1a)\dots C(6a) = 2.808(10)\text{\AA}$ with an out-of-plane displacement of C(6a) from the plane C(5a),C(7a),O(2a) towards O(1a) of $0.016(12)\text{\AA}$.

The tricyclic molecule (29b) is considerably different conformationally from the bicyclic molecule (29a). Here, the 5-membered ring is an approximate twist conformation (diad bisecting C(3b)-C(4b)). The reduction of the carbonyl (which appears to encourage a planar geometry of the 4-membered ring) to a hemiketal results in the 4-membered ring displaying a conformation which is considerably twisted ($|\tau|C(7b)-C(1b)-C(5b)-C(6b) = 24.2^\circ$). Also, there is the additional constraint of the ether linkage O(1b). The close proximity of C(7b)endo to O(1b) ($3.163(10)\text{\AA}$ in (29a) and $3.016\text{\AA}(10)$ in (29b)) results in steric repulsion which further assists twisting of the 4-membered ring. The formation of the transannular ether linkage is accomplished (conformationally) by an increase in the pucker of the 5-membered ring; the angle between the mean planes C(4),C(5),C(1),C(2) and C(2),C(3),C(4) is 145° in (29a) and 128° in (29b). Also, the angle between the 4- and 5-membered rings is reduced i.e. the angle between the mean planes

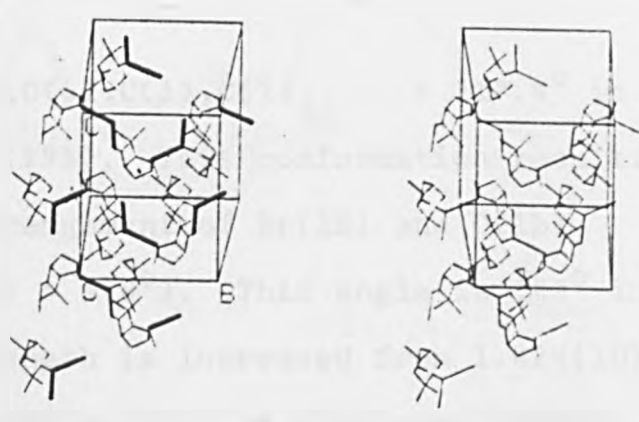


Fig 3, 21

Packing diagram for (29). This is a section through the unit cell showing chains of hydrogen-bonded molecules (H-bonding is depicted as —).

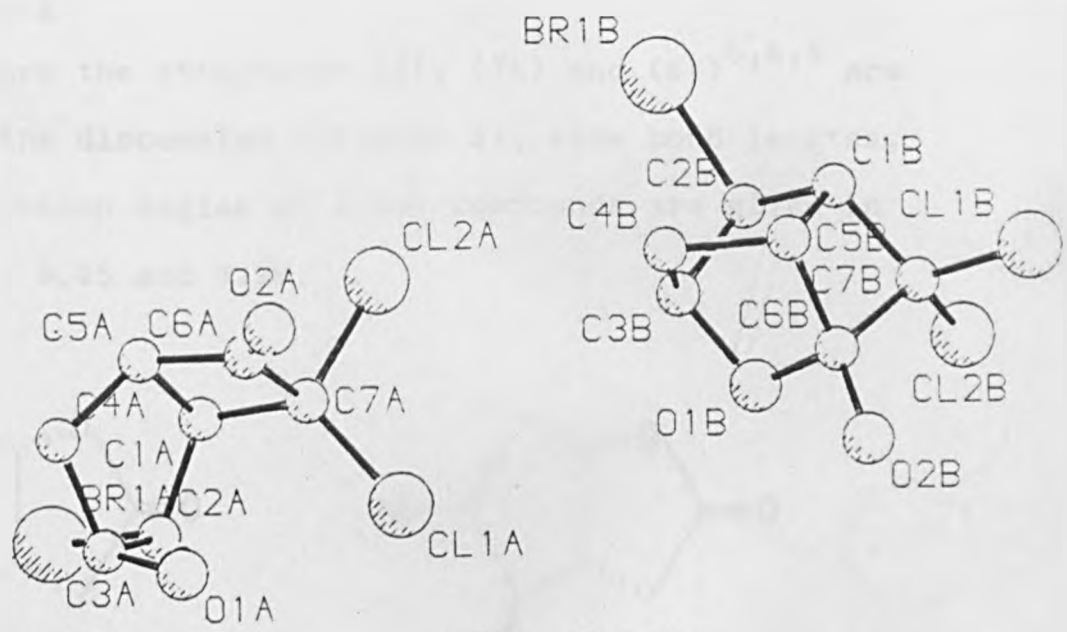


Fig 3, 22

The structure of (29). Remarkably, the crystal structure consists of both the open chain (29a) and ring forms (29b) in a single crystal.

C(4),C(5),C(1),C(2) and C(6),C(5),C(1),C(7) = 117.4° in (29a) is reduced to 102° in (29b). This conformation results in an almost anti-periplanar arrangement of Br(1b) and O(1b) ($|\tau|$ O(1b)-C(3b)-C(2b)-Br(1b) = 178°). This angle is 163° in (29a). The O(1)-C(3) bond length is increased from $1.424(10)\text{\AA}$ in (29a) to $1.460(12)\text{\AA}$ in (29b) as O(1) is displaced towards C(6). The O(1a)...C(6a) distance of $2.808(10)\text{\AA}$ is reduced to $1.410(10)$ on forming a bond with C(6). Also, the carbonyl bond (C(6a)-O(2a) = $1.198(10)\text{\AA}$) increases in length, as expected, on formation of the hemiketal (C(6b)-O(2b) = $1.393(13)\text{\AA}$).

Stereo diagrams of the structures are displayed in Figure 3.23 a-g.

Since the structures (8), (74) and (64)^{5,6,8} are included in the discussion (Chapter 5), some bond lengths, angles and torsion angles of these compounds are given in Figures 3.24, 3.25 and 3.26.

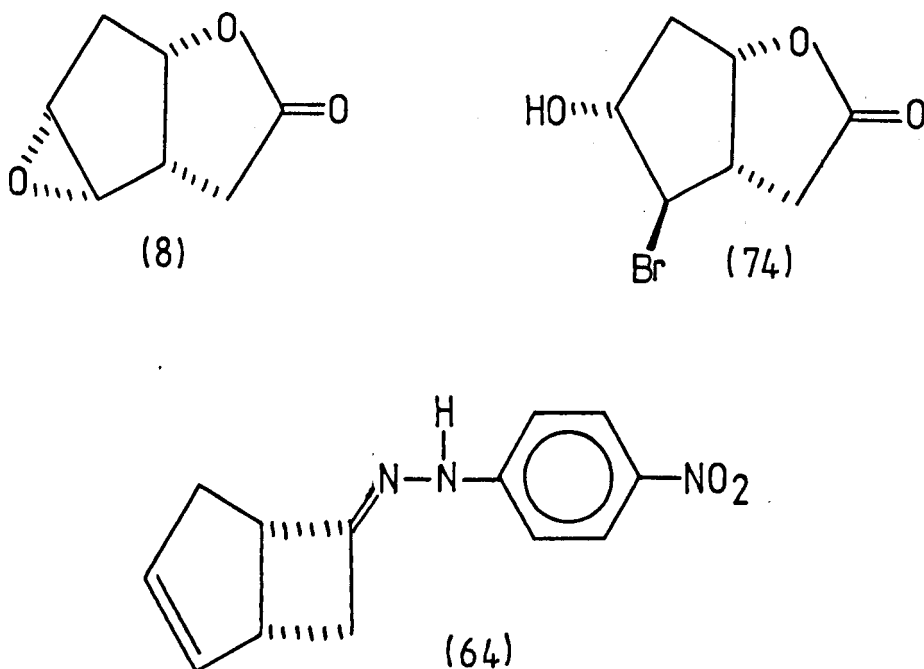


Fig 3, 23

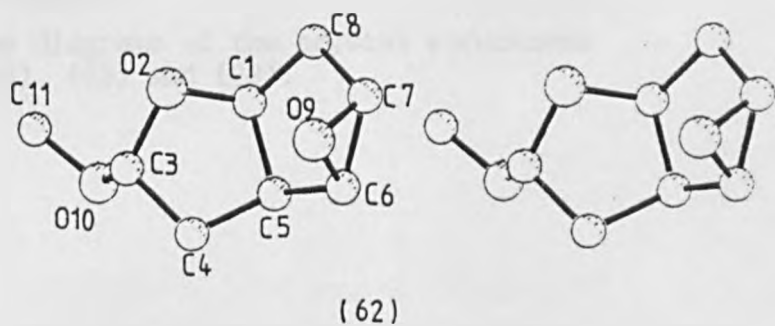
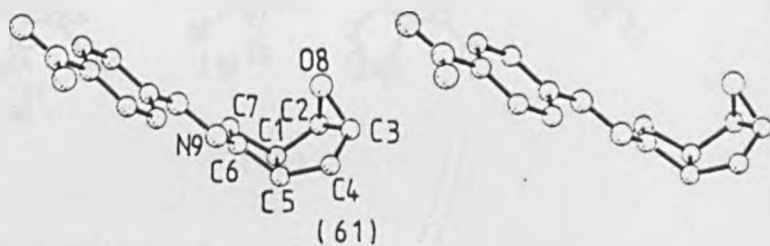
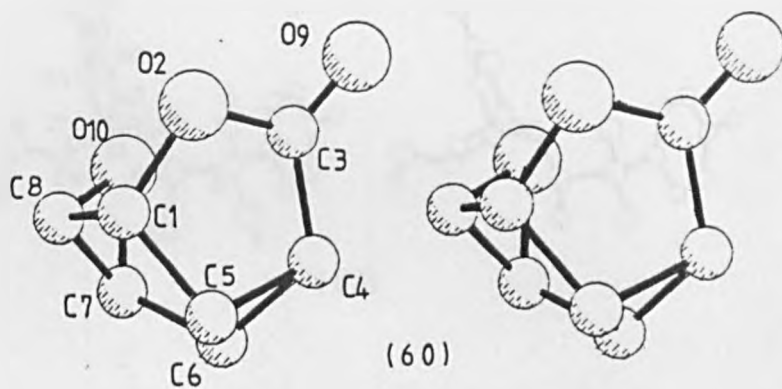
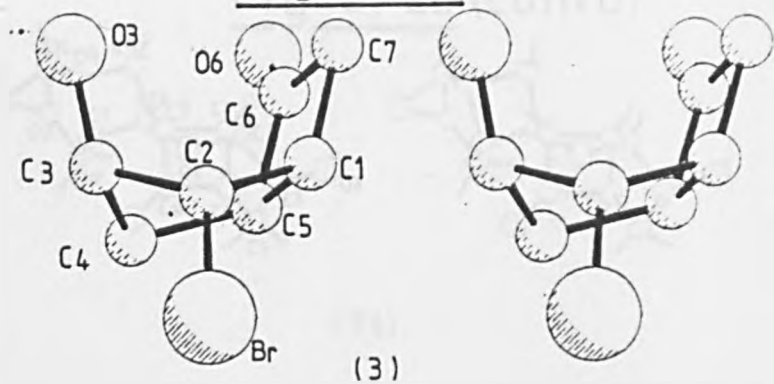


Figure 3.23

Stereo diagrams of the crystal structures of (3), (60), (61) and (62).

Fig 3, 23 (cont'd)

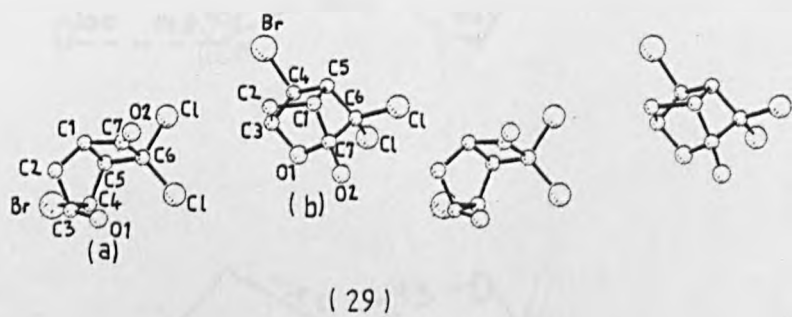
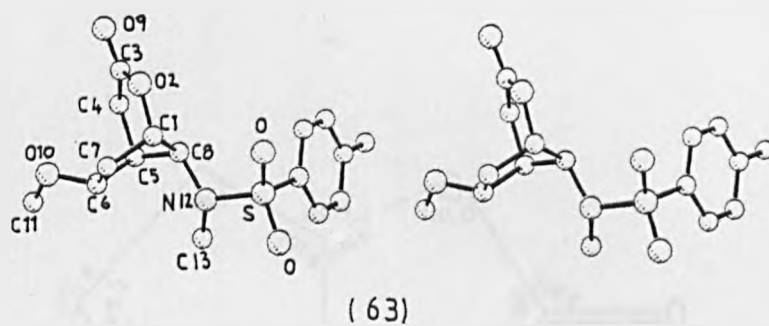
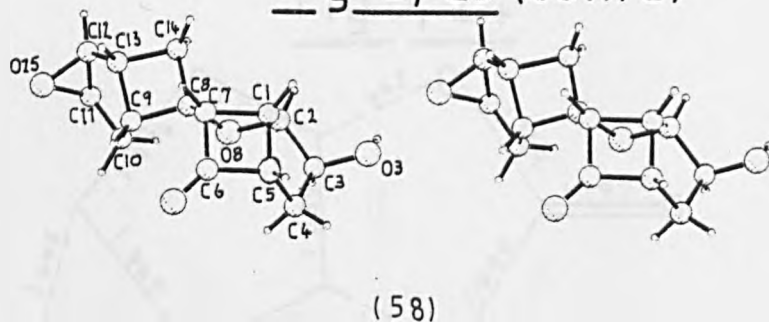


Figure 3.23 (contd.)

Stereo diagrams of the crystal structures of (58), (63) and (29).

Fig 3, 24

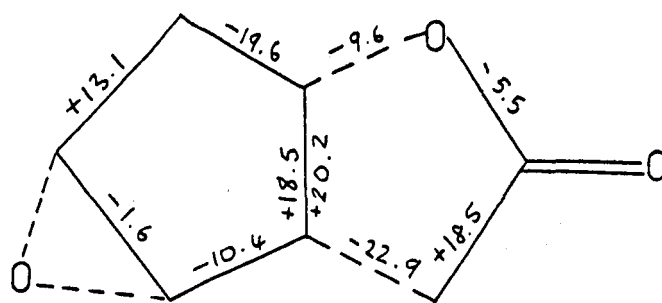
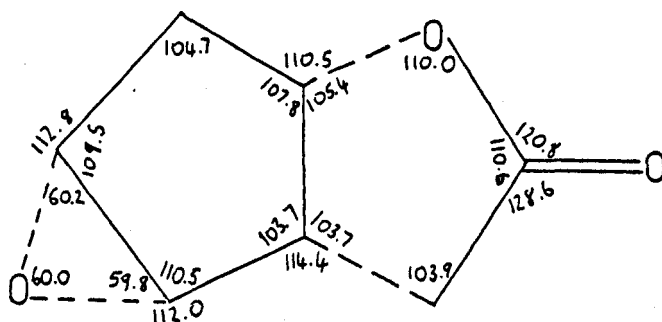
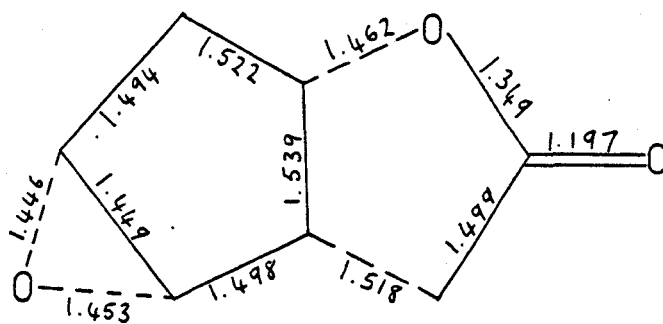
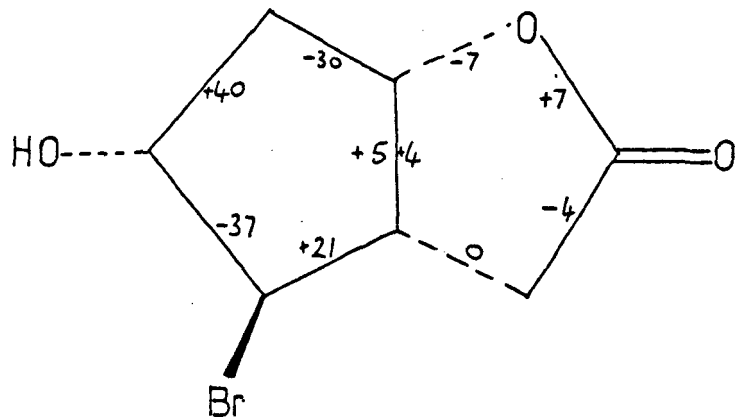
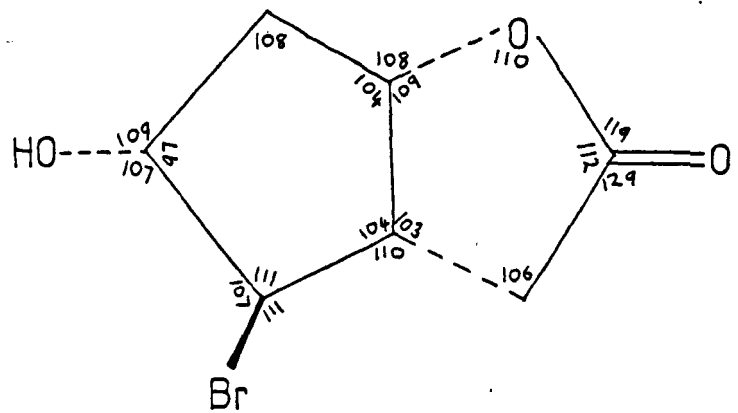
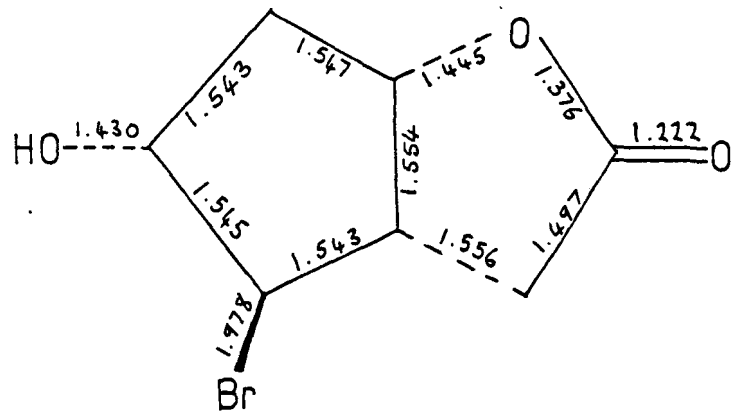


Figure 3.24

Bond lengths (Å), bond angles (°) and torsion angles (°) for (8).

Fig 3, 25aFigure 3.25a

Bond lengths (Å), bond angles (°) and torsion angles (°) for (15a). There are two independent molecules in the asymmetric unit.

Fig 3, 25b

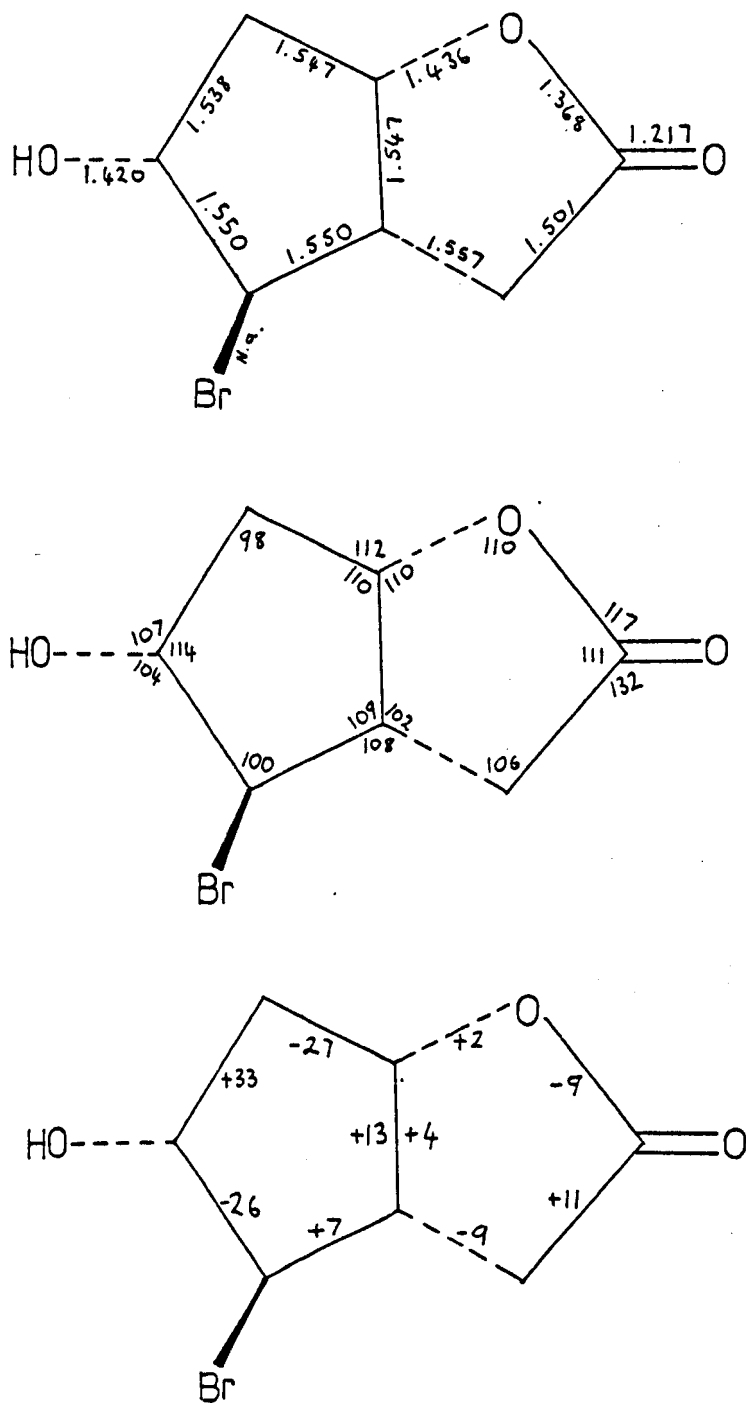


Figure 3.25b

Bond lengths (Å), bond angles (°) and torsion angles (°) for (15b). There are two independent molecules in the asymmetric unit.

Fig 3,26a

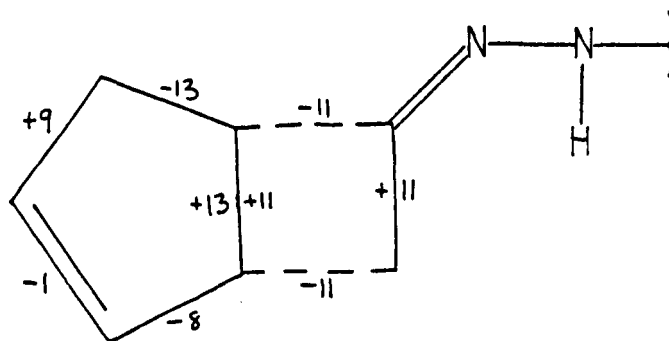
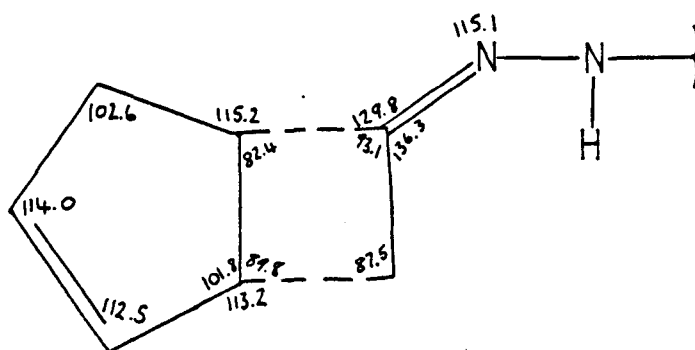
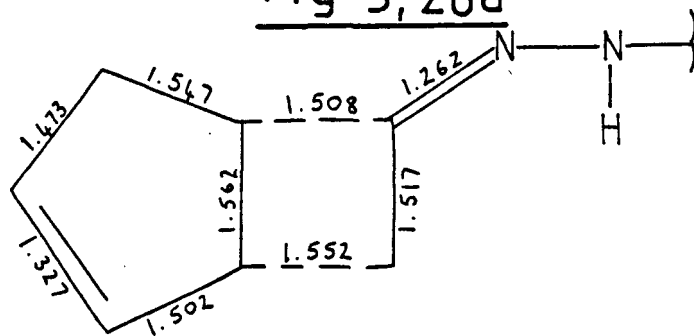


Figure 3.26a

Bond lengths (Å), bond angles (°) and torsion angles (°) for (64a). There are two independent molecules in the asymmetric unit.

Fig 3, 26b

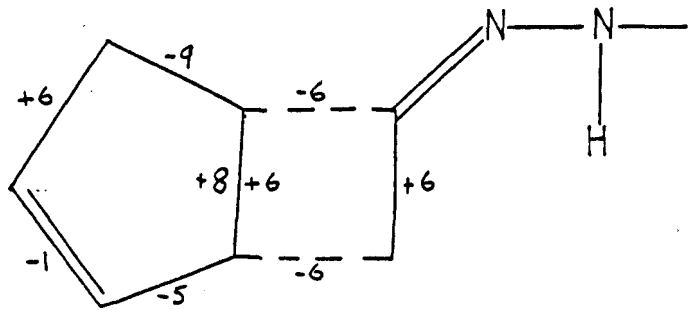
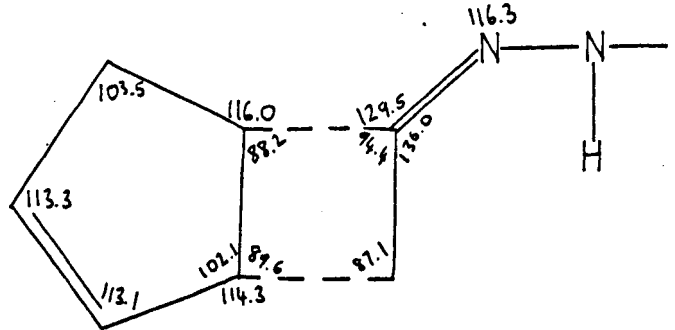
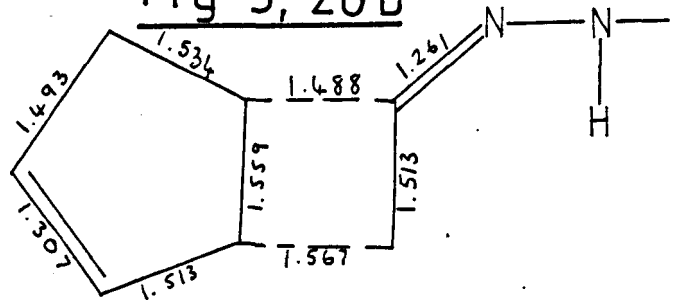


Figure 3.26b

Bond lengths (Å), bond angles (°) and torsion angles (°) for (64b). There are two independent molecules in the asymmetric unit.

3.3 X-ray Experimental Method (all compounds)

Exploratory photographic data were collected on a Stoe Weissenberg camera using nickel filtered $\text{CuK}\alpha$ radiation and a Supper precession camera using zirconium filtered $\text{MoK}\alpha$ radiation.

Intensity data were collected on a Stadi-2 2-circle diffractometer using graphite monochromated $\text{MoK}\alpha$ radiation.

Integrated intensities were typically collected in 1 second steps by an ω° -scan of $80 \times \Delta\omega^\circ$ about the reflection peak over a variable range of $\Delta\omega^\circ = A + B \sin \mu / \tan\theta^\circ$ where $A = B = 1.2$.

Background intensities were collected for 20 steps of 1 second before and after the reflection (in ω°).

Corrections were made for Lorentz and polarisation effects (but not for extinction or absorption) and the data scaled by a Wilson plot (SHELX76¹⁷).

SHELX76 and MULTAN77¹⁸ computer packages were used for structure solution where indicated. All refinement calculations were carried out with SHELX76.

Complex neutral atomic scattering factors were taken from International Tables for X-ray Crystallography (1974)¹⁶.

The structures were refined by full matrix least squares minimisation. The functions minimised were $R = \sum ||F_o| - |F_c|| / |F_o|$ and $R_w = \sum (||F_o| - |F_c|| \omega^{1/2}) / |F_o| \omega^{1/2}$.

The refinement was assumed to have converged when the shifts in the atomic parameters were less than their standard deviations.

Hydrogen atoms were initially assigned calculated positions and included in the refinement (unless otherwise stated).

Densities were measured by the flotation method.

3.3.1 2-(S)-exo-bromo-3(S)-endo-hydroxybicyclo-[3.2.0]heptan-6-one (3).

The crystals were transparent, needle shaped and extinguished under crossed polars parallel to the needle axis. In cross section they appeared to have a C_3 axis.

A crystal of approximate dimensions 0.3 x 0.3 x 0.5mm was selected and mounted parallel to the needle axis.

Space group determination

A zero layer Weissenberg ($h0l$) photograph displayed rhombohedral or hexagonal symmetry ($\beta = 120^\circ$), however the spot intensities indicated a C_6 axis. An upper layer Weissenberg photograph ($h1l$) showed a C_3 axis from spot intensities. A precession photograph ($0kl$) indicated systematic absences; $000l:l=3n$. Precession and oscillation photographs gave cell dimensions consistent with trigonal symmetry ($a=b=10.13\text{\AA}$, $c=6.66\text{\AA}$, $\alpha=\gamma=90^\circ$, $\beta=120^\circ$). The experimental density was measured as 1.72 MgM^{-3} , which indicated 3 molecules per unit cell. The space group was assumed to be either $P3_1$ or $P3_2$ with inversion of axes.

Intensity data collection

Data were collected for $hki0-6l$ with $\theta_{\text{max}}=25^\circ$. This gave 752 data of which 563 reflections (including 52 Friedel pairs of the form $hki0$ with $I>3\sigma(I)$) were used in subsequent calculations.

The crystal blackened on prolonged exposure to X-rays.

Structure solution

The structure was solved by the heavy atom method⁴ with SHELX76.

The equivalent positions for space group $P3_1$ are (1) x,y,z ; (2) $-y,x-y,1/3+z$; (3) $y-x,-x,2/3+z$. A single heavy atom gives rise to the vectors in Table 3.6.

TABLE 3.6

<u>combination</u>	<u>vector</u>	
1,2	$x+y, 2y-x, -1/3$	a
1,3	$2x-y, y+x, -2/3$	b
2,3	$-2y+x, 2x-y, -1/3$	c
2,1	$-y-x, x-2y, 1/3$	-a
3,1	$y-2x, -x-y, 2/3$	-b
3,2	$2y-x, -2x+y, 1/3$	-c

The bromine atom coordinates were found as follows: Vectors a, b and c are related by the 3-fold axis and $a+c=b$. A Patterson map gave the atom-atom vectors; those of highest intensity (apart from the base peaks) are due to Br-Br vectors. The coordinates of peak 3 on the Patterson map (0.0656, 0.312, 0.6677, peak height = 292) when substituted in equation (-b) gives

$$y-2x = 0.0656$$

$$-x-y = 0.3120.$$

These equations solve to give the coordinates of one bromine position $-.1259, -.1861, z$.

The bromine phased Fourier map contained many spurious peaks and could not be interpreted. From a difference map could be deduced a 5-membered ring and a carbonyl (at this stage $R=0.20$).

Structure refinement

All the non-hydrogen atoms were identified from difference maps giving $R = 0.074$. The inclusion of a weighting scheme, anisotropic thermal parameters for the non-hydrogen atoms and hydrogen atoms which were refined from calculated positions (except the H of OH) gave $R = 0.069$.

The hydroxyl-hydrogen was identified from a difference map and the refinement converged at $R = 0.0416$.

Determination of chirality

The absolute configuration of the molecule was determined using the anomalous dispersion effect of the bromine atoms.

Weighted full matrix least squares refinement converged at $R = 0.0416$ in $P3_1$ and $R = 0.0450$ in the enantiomeric structure in $P3_2$. (In most space groups, a simple inversion of the axes will produce coordinates for the enantiomeric structure. However, in this space group, which possesses a 3-fold screw axis, the handedness of the screw axis must also be changed, in this case from a 3_1 screw axis to a 3_2 screw axis.)

The correct enantiomorph may be deduced using Hamiltons R-factor ratio²⁰.

There were 563 reflections and 97 parameters in the refinement, therefore $n-m=466$.

The ratio of the R-factors i.e. $RP3_2/RP3_1$ was $= 1.0817$. The hypothesis that the structure in $P3_2$ is the correct structure is a one dimensional hypothesis (the dimensionality of this hypothesis has been subject to debate recently¹⁹). Since $R_{1,466,0.005} = 1.0079$, we may reject the configuration in $P3_2$ at lower than the 0.005 level.

This result was subsequently confirmed by examination of 41 Bijvoet pairs. 34 pairs had $F_o(A)/F_o(B)$ and $F_c(A)/F_c(B)$ both >1 or <1 where (A) and (B) refer to refinement in $P3_1$ and in $P3_2$ with inversion of coordinates.

Crystal data are given in Table 3.7.

TABLE 3.7

Molecular formula $C_7H_9O_2Br$. $M_r=204.9$

Approximate crystal dimensions 0.3 x 0.3 x 0.5mm.

Trigonal, $P3_1$, from structure solution and refinement

$a=b=10.13(2)$, $c=6.66(1)$ Å from diffractometer measurements (MoK α radiation)

$V = 592$ Å³, $Z=3$

$D_m = 1.72$ MgM⁻³, $D_c = 1.73$ MgM⁻³

$F(000)=306$, $\mu=5.22$ mm⁻¹

$[\alpha]_D^{20.0} = -60^\circ$

In $P3_1$, $R=0.0416$, $R_w=0.0287$ ($w=3.0286/(\sigma^2(F_o)+0.000036(F_o)^2)$)

In $P3_2$, $R=0.045$, $R_w=0.0361$ ($w=1/\sigma^2(F_o)+0.000123(F_o)^2$).

3.3.2 7,8-endo-epoxy-2-oxatricyclo[3.3.0.0^{4,6}]-octan-3-one (60)

Preliminary oscillation photographs of 4 crystals showed them to be unsuitable due to multiple reflections. The fifth crystal selected had approximately monoclinic morphology and exhibited extinctions under crossed polars parallel to the needle axis.

Space group determination

An oscillation photograph exhibited mirror symmetry. From Weissenberg ($h0l, h1l$) and precession photographs ($hk0, 0k0$) systematic absences; $h0l:l$ odd; $0k0:k$ odd were observed.

Approximate cell dimensions from photographs were consistent with monoclinic symmetry. The measured density was 1.59MgM^{-3} , which implied 4 molecules per unit cell. The space group was assumed to be $P2_1/c$.

Intensity data collection

Data were collected for $h0-10\lambda$ with $\theta_{\text{max}}=25^\circ$. This gave 1481 data of which 1124 unique reflections with $I > 3\sigma(I)$ were used in subsequent calculations.

Crystal quality deteriorated by ca. 5% in (I) (standard reflection $(2,2,0)$) during the course of the experiment and therefore an empirical correction was applied.

Structure solution

The structure was solved by direct methods with SHELX76.

A convergence map gave 2631 unique phase relations. The automatic centrosymmetric structure solution routine gave 2 E-maps. All the non-hydrogen atom positions could be deduced from E-map 1.

Structure refinement

The inclusion of a weighting scheme and anisotropic temperature factors gave $R=0.074$. Hydrogen atom positions were deduced from a difference synthesis giving $R=0.045$. Omission of the $(0,1,3)$ reflection (probably affected by the backstop) gave $R=0.041$.

Crystal data are given in Table 3.8.

TABLE 3.8 Molecular formula $C_7H_6O_3$. $M_r=138.1$

Approximate crystal dimensions 0.6 x 0.3 x 0.1mm.

Monoclinic $P2_1/c$. $a=6.36(1), b=9.58(2), c=9.71(1)\text{\AA}$, $\beta=75.13(2)^\circ$,
from diffractometer measurements (MoK α radiation).

$V=572\text{\AA}^3$, $Z=4$,

$D_m=1.59\text{MgM}^{-3}$, $D_c=1.60\text{MgM}^{-3}$.

$F(000)=288$, $\mu=0.08\text{mm}^{-1}$.

$R=0.041$, $R_w=0.045$ ($w=3.1037/(\sigma^2(F_o)+0.000368(F_o)^2)$).

3.3.3 2,3-endo-epoxybicyclo[3.2.0]heptan-6-one-
p-nitrophenylhydrazone (61)

The crystal selected was orange and extinguished under crossed polars parallel to an approximate needle axis. The approximate crystal dimensions were 0.6 x 0.5 x 0.15mm. The crystal was mounted parallel to the direction of extinction.

Space group determination

Oscillation, Weissenberg ($h0l, hll$) and precession ($hk0, 0kl$) photographs indicated monoclinic symmetry ($2/m$) with systematic absences; $h0l:l$ odd; $0k0:k$ odd. Approximate cell dimensions measured from photographs were consistent with monoclinic symmetry. The density was measured as 1.37MgM^{-3} , which indicated 4 molecules per unit cell.

The space group was assumed to be $P2_1/c$.

Intensity data collection

Data were collected for $h0-6l$ and $0-3kl$ with $\theta_{\max}=25^\circ$. 2164 unique data were recorded for the b axis and 832 data for the a axis (the crystal was remounted). The data were merged without layer scales after structure solution to give 2351 unique data of which 1538 reflections with $I > 3\sigma(I)$ were used in subsequent calculations.

Structure solution

The structure was solved by direct methods with SHELX76 using the intensity data from axis b. The non-hydrogen atoms could be deduced from E-map 2.

Structure refinement

The inclusion of all the non-hydrogen atoms gave $R=0.144$. The addition of hydrogen atoms at calculated positions and a weighting scheme gave $R=0.127$. The temperature factors of the non-hydrogen atoms were made anisotropic giving $R=0.045$. At this stage data from axis a was merged (merging R-factor = 0.0498 (mean $\text{abs}(E \times E - 1) = (\text{approx.}) 0.97$ in effective N range)). The refinement converged at $R=0.048$.

Crystal data are given in Table 3.9.

TABLE 3.9

Molecular formula $C_{13}H_{13}N_3O_3$. $M_r = 259.14$

monoclinic, $P2_1/c$. $a=9.50(2)$, $b=13.73(2)$, $c=9.70(2)\text{\AA}$, $\beta=83.19(2)^\circ$,
from diffractometer measurements (MoK α radiation).

$V=1257\text{\AA}^3$, $Z=4$

$D_m=1.37\text{MgM}^{-3}$, $D_c=1.36\text{MgM}^{-3}$.

$F(000)2545$, $\mu=0.061\text{mm}^{-1}$

$R=0.0479$, $R_w=0.0459$ ($w=4.4729/(\sigma^2(F_o)+0.000169(F_o)^2)$).

3.3.4 3-exo-methoxy-6,7-endo-epoxy-2-oxabicyclo-
[3.3.0]octane (62)

The crystals selected were white with no obvious crystal faces. Preliminary oscillation photographs indicated they decomposed or sublimed in air, therefore a suitable crystal was enclosed in a sealed glass tube to prevent deterioration. This crystal extinguished under crossed polars parallel (and perpendicular) to an approximate needle axis.

Space group determination

Weissenberg photographs ($h0l, h1l, h2l$) displayed monoclinic symmetry ($2/m$) with systematic absences, $hkl:h+k=2n$; $h0l:l=2n$; $0k0:k=2n$. Cell dimensions were measured from Weissenberg and oscillation photographs and were consistent with monoclinic symmetry. The approximate density (the crystals dissolved slowly in a number of solvents tried) was 1.2MgM^{-3} , which implied 8 molecules per unit cell. The space group was assumed to be $C2/c$.

Intensity data collection

Data were collected for $h0-7l$ with $\theta_{\text{max}}=25^\circ$. This gave 1698 data of which 905 unique reflections with $I > 3 \sigma(I)$ were used in subsequent calculations.

Structure solution

The SHELX76 automatic centrosymmetric structure solution routine gave 4 E-maps. All the non-hydrogen positions could be deduced from E-map 1.

Structure refinement

The temperature factors of the non-hydrogen atoms were made anisotropic giving $R=0.136$. The addition of a weighting scheme and hydrogen atoms at calculated positions gave $R=0.068$. Omission of the 402 reflection (which had a low observed I , probably due to the backstop) gave $R=0.0483$, at which point the refinement had converged.

Crystal data are included in Table 3.10.

TABLE 3.10

Molecular formula $C_8H_{12}O_3$. $M_r=156.18$

approximate crystal dimensions 0.5x0.3x0.2mm.

Monoclinic, C2/c. $a=17.15(2)$, $b=6.15(2)$, $c=14.99(2)\text{\AA}$,

$\beta=82.47(3)^\circ$ from diffractometer measurements (MoK α radiation).

$V=1568\text{\AA}^3$, $Z=8$,

$D_c=1.32\text{MgM}^{-3}$, $D_m=1.2\text{MgM}^{-3}$,

$F(000)=672$, $\mu=0.061\text{mm}^{-1}$.

$R=0.0483$, $R_w=0.0510$ ($w=3.16/\sigma^2(F_o)+0.001(F_o)^2$).

3.3.5 spiro{5-*exo*-hydroxy-3-oxatricyclo[5.1.1.0^{4,9}]-nonan-8-one-2-1'(4',5'-*exo*-epoxybicyclo[3.2.0]-heptane)} (58)

Recrystallisation from an ethanol/methanol mixture gave clear needle like crystals which extinguished parallel and perpendicular to the needle axis. A fragment of approximate size 0.5x0.2x0.1mm was mounted parallel to the needle axis.

Space group determination

An oscillation photograph displayed mirror symmetry. Weissenberg ($h0l$) and precession ($h0l,0kl$) photographs showed systematic absences; $0k\bar{l}:\bar{l}=2n$, $h0l:h=2n$ and cell dimensions consistent with the orthorhombic space groups $Pca2_1$ or $Pcam$.

The density was measured to be 1.45MgM^{-3} which implied 4 molecules per unit cell. The space group was assumed to be $Pca2_1$.

Intensity data collection

Data were collected for $hk0-9l$ with $\theta_{\max}=25^\circ$. This gave 1401 data of which 987 unique reflections with $I > 3\sigma(I)$ were used in subsequent calculations.

Structure solution

A convergence map gave 2449 unique phase relations.

3 origin defining reflections were chosen

(6,0,1; 16,1,0; 5,1,0) and assigned phases of 0° . An enantiomorph defining reflection (12,6,5) was assigned phases of 45° and 135° and one multiresolution reflection (3,12,1) was assigned the possible phases of $45^\circ, 135^\circ, 225^\circ, 315^\circ$. From this starting set, 8 E-maps were computed.

From E-map 1, all the non-hydrogen atom positions could be deduced.

Structure refinement

The inclusion of a weighting scheme and anisotropic temperature factors gave $R=0.08$. The addition of hydrogen atoms at calculated positions followed by least squares refinement gave $R=0.046$, at which point the refinement had converged.

Crystal data are given in Table 3.11.

TABLE 3.11

Molecular formula $C_{14}H_{16}O_4$, $M_r=248.28$

approximate crystal dimensions 0.5x0.2x0.1mm.

orthorhombic, $Pca2_1$, $a=11.78$ (2), $b=9.04$ (2), $c=11.09$ (3)Å

from diffractometer measurements (MoK α radiation).

$V=1182.13\text{\AA}^3$, $Z=4$

$D_m=1.36\text{MgM}^{-3}$, $D_c=1.39\text{MgM}^{-3}$.

$F(000)=528$, $\mu=0.06\text{mm}^{-1}$

$R=0.046$, $R_w=0.0495$ ($w=1/\sigma^2(F_o)+0.0014(F_o)^2$).

3.3.6 6-endo-methoxy-8-trans-N-methyl-N-p-toluenesulphonamide-2-oxabicyclo[3.2.0]octan-2-one (63)

Preliminary oscillation photographs of two crystals showed them to be unsuitable due to 'tails' on the reflections

(these would present difficulty in background intensity measurement).

The third crystal was monoclinic in shape and extinguished along the needle axis under crossed polars. The approximate crystal dimensions were 0.6x0.2x0.6mm. It was mounted parallel to the needle axis.

Space group determination

Weissenberg ($0k\ell, \ell k\ell$) and precession ($h0\ell, hk0$) photographs indicated $2/m$ symmetry with systematic absences; $hQ\ell: \ell$ odd, $0k0:k$ odd. Approximate cell dimensions measured from photographs were consistent with monoclinic symmetry. The density was measured as 1.35MgM^{-3} , which implied 4 molecules per unit cell.

The space group was assumed to be monoclinic, $P2_1/c$.

Intensity data collection

Data were collected for $0\text{-}6k\ell$ with $\theta_{\text{max}}=25^\circ$. This gave 3253 data of which 1655 unique reflections with $(I) > 3\sigma(I)$ were used in subsequent calculations.

Structure solution

The SHELX76 programs were used for all calculations.

A convergence map gave 2631 unique phase relations.

The structure was solved by manual symbolic addition²¹.

A Σ_2 listing gave 475 reflections with $|E| > 1.30$.

From the Σ_2 listing, 3 origin defining reflections of high E were chosen; 5,3,3; -5,6,7; -1,2,9 and assigned a phase of 0° . A further 4 reflections were assigned the symbolic phases a,b,c,d.

In the space group $P2_1/c$ the following relationships may be derived ($s=\text{sign}$):

$$s(hk\ell)=s(-h-k-\ell)=s(h-k\ell)=s(-hk-\ell) \text{ for } h+\ell=2n$$

$$s(hk\ell)=s(-h-k-\ell)=-s(h-k\ell)=-s(-hk-\ell) \text{ for } k+\ell=2n+1.$$

These relationships were utilised to assign phases to a further 21 reflections. From the solution $a=b=0$ and $c=d=\pi$ an electron density map was computed using the signed E values as coefficients. From this map, the non-hydrogen atom positions could be deduced.

Structure refinement

The addition of a weighting scheme gave $R=0.118$. Hydrogen atoms were attached in calculated positions and the temperature factors of the non-hydrogen atoms made anisotropic giving $R=0.063$.

The high temperature factors of the hydrogens attached to C(23) indicated disorder. These were refined as 2 methyl groups with occupancies summed to unity, giving $R=0.056$. At this stage, the refinement had converged. A difference map showed no unusual features.

Crystal data are given in Table 3.12.

TABLE 3.12

Molecular formula $C_{16}H_{21}NO_5S$. $M_r=339.4$

approximate crystal dimensions $0.6 \times 0.2 \times 0.6$ mm.

monoclinic, $P2_1/c$. $a=6.46(2)$, $b=11.77(1)$, $c=22.62(1)$ Å,

$\beta=101.97(1)^\circ$ from diffractometer measurements (MoK α radiation).

$V=1683$ Å³, $Z=4$

$D_m=1.35$ MgM⁻³, $D_c=1.34$ MgM⁻³.

$F(000)=720$, $\mu=0.172$ mm⁻¹.

$R=0.057$, $R_w=0.041$ ($w=(3.76/(\sigma^2(F_o)+0.000022(F_o)^2))$).

3.3.7 2-exo-bromo-3-endo-hydroxy-7,7-dichlorobicyclo-
[3.2.0]heptan-6-one (29)³⁰

Recrystallisation from CCl_4 solution gave clear colourless crystals of approximately monoclinic shape which extinguished parallel to the needle axis. The crystals selected were mounted about the needle axis.

Space group determination

Preliminary oscillation photographs of 4 crystals displayed unfavourable characteristics due to absorption (crystal too big) or multiple reflection (tails on reflections). The 5th crystal of dimensions 0.5x0.7x0.7mm was of suitable quality.

An oscillation photograph displayed mirror symmetry. Weissenberg photographs ($hk0, 0k\ell$) gave approximate cell dimensions consistent with monoclinic symmetry with systematic absences; $hk\ell:h+k=2n$, $h0\ell:\ell=2n$; $0k0:k=2n$. The measured density was 1.7MgM^{-3} . This implied 8 molecules per unit cell.

The space group was assumed to be monoclinic, $C2/c$.

Intensity data collection

2 data sets were collected. The first (using the above crystal) was used for structure solution.

Data set 1:

Data were collected for $h0-9k\ell$ with $\theta_{\text{max}}=25^\circ$. This gave 3139 data of which 1361 unique reflections with $I>3\sigma(I)$ were used for subsequent calculations.

Data set 2:

Data were collected on a new crystal, mounted about axis c , of dimensions 0.8x0.8x0.5mm for $hk0-9\ell$ with $\theta_{\text{max}}=25^\circ$. This gave 2871 data of which 1596 with $I>3\sigma(I)$ were used in subsequent calculations. An empirical correction

was applied as the standard reflection (2,-2,0) decreased in intensity by ca. 6% during the experiment.

Structure solution

Data set 1 was used for structure elucidation. SHELX76 direct methods failed due to severe pseudo symmetry of the bromine atoms, which appeared to be near a pseudo mirror plane. This was evident from the data as odd layers were of low intensity. Similarly the Patterson (vector) map was not easy to interpret. Intensity data was input into MULTAN78. The data was scaled by a Wilson plot and 188 of the largest E-values (with the 6 smallest E values, used to calculate psi zero figure of merit) were used to prepare a convergence map. Two origin defining reflections (0,4,1 and 17,3,-4) and 3 other reflections (0,4,4; 2,6,8; 12,2,-4) were chosen as a starting set. Tangent formula expansion followed by a Fourier synthesis gave 8 E-maps. E-map 2 appeared to give the positions of 2 bromine and 4 chlorine atoms.

Structure refinement

The structure was refined on SHELX76.

The non-hydrogen atom positions of a bicyclo[3.2.0] fragment were deduced from a difference map which included the atom coordinates determined by MULTAN78, giving $R=0.26$.

A further difference map revealed another polycyclic fragment.

Inclusion of a weighting scheme and anisotropic thermal parameters gave $R=0.0758$. Hydrogen atom positions were determined from difference maps. The refinement for data set 1 converged at $R=0.0641$.

The second data set refined to $R=0.0537$ and this was

used for subsequent calculations. A final difference map revealed no additional features.

Crystal data are given in Table 3.13.

TABLE 3.13

Molecular formula $C_7H_7BrClO_2$, $M_r=273.9$, $Z=16$.
 approximate crystal dimensions $0.8 \times 0.6 \times 0.4$ mm.
 monoclinic, $C2/c$. $a=22.98(1)$, $b=12.05(1)$, $c=14.41(1)$ Å,
 $\beta=72.22(1)^\circ$ from diffractometer measurements (MoK α radiation).
 $V=3801 \text{ \AA}^3$, $F(000)=2144$,
 $\mu=4.71 \text{ mm}^{-1}$,
 $D_m=1.7 \text{ MgM}^{-3}$, $D_c=1.8 \text{ MgM}^{-3}$.
 $R=0.0537$, $R_w=0.0507$ ($w=3.2568/(\sigma^2(F_o)+0.000398(F_o)^2)$).

3.4

APPENDIX A: Structure solution by heavy atom methods^{4,22,26}

The electron density of an averaged unit cell can be reconstructed by summing the Fourier series

$$\rho(x,y,z) = \frac{1}{V} \sum_{\mathbf{H}} |F_{\mathbf{H}}| \cos[2\pi(\mathbf{H} \cdot \mathbf{r}) - \phi(\mathbf{H})]$$

Unfortunately, only the intensities are observable from an X-ray diffraction experiment, the phases ϕ are unknown.

Patterson²⁷ derived a new Fourier series which could be calculated directly from experimental data. This considered not the atomic positions but the interatomic vectors. The Patterson function²² is usually written in 3 dimensions as:

$$P(u,v,w) = \frac{2}{V_c} \sum_h \sum_k \sum_l |F_{\mathbf{H}}|^2 \cos 2\pi(hu+kv+lw)$$

The Patterson function can be handled in a similar fashion to the corresponding electron density function, however, the peaks of maximum intensity now correspond to interatomic vectors between atom pairs. There are as many Patterson peaks as there are i, j pairs of atoms, i.e. N^2 . The N peaks corresponding to i, j pairs appear at the origin of the Patterson function and the remaining $N(N-1)$ peaks are centrosymmetrically distributed about the origin. It is thus only really necessary to consider half the Patterson unit cell. Although the crystal structure may be any one of the 240 space groups, the Patterson function introduces a centre of symmetry, thus only the primitive and centred Laue groups are seen.

The geometry of the peak locations in a Patterson function is due to the sets of interatomic vectors, each set using one atom as an origin, repeated for each atom and

weighted according to the electron density of the atom at the origin.

The height of a Patterson peak is proportional to the atomic numbers of the 2 atoms forming the vector.

In very favourable cases, if the Patterson peaks do not overlap it is possible to deduce atomic positions from vector triplets⁴. However, this is seldom the case due to the large number of peaks present in even relatively small structures.

If there are heavy atoms present in the structure e.g. bromine in an organic molecule containing only carbon, hydrogen and oxygen, since the Patterson peak intensities are proportional to the atomic numbers of the atoms involved, those peaks corresponding to vectors between the light atoms are of relatively low intensity, those corresponding to light and heavy atoms are of greater intensity and those of highest intensity correspond to interatomic vectors between the heavy atoms. This means that peaks may be assigned to particular atom pairs, i.e. those involving the heavy atoms.

From the symmetry elements of the space group, the possible interatomic vectors between symmetry related atoms are evident. Since the Patterson peaks correspond to these interatomic vectors, the coordinates of the heavy atoms may be deduced from a series of simultaneous equations.

The clarity of the Patterson map may be increased by using a sharpened Patterson function. In this case, the atomic scattering factors are modified to behave as point atoms where their scattering power is not a function of $\sin\theta/\lambda$ but of their atomic number Z . A common approximation is²⁶

$$|F_{\tilde{H}}|_{\text{mod}}^2 = \frac{|F_{\tilde{H}}|_{\text{obs}}^2}{\exp[-2B(\sin^2\theta)/\lambda^2] \left(\sum_{i=1}^N f_i^2 \right)}$$

Once $|F \text{ point}|$'s are obtained from the measured $|F \text{ real}|$, they can be squared and used in a sharpened Patterson function. This technique shows up more peaks.

Also, the origin peak can be a problem, swamping the close-in peaks and causing problems of scale. This may be removed by using modified coefficients of the form²⁶ (with F 's placed on an absolute scale)

$$I_{\tilde{H}} = |F_{\tilde{H}}|^2 - \sum_{i=1}^N f_i^2$$

APPENDIX B: Direct methods of phase determination^{4,22}

Direct methods are analytical approaches to phase determination which are independent of trial structures (or nearly so). They are designed to find the phase information hidden in the intensities of the observed reflections by the use of approximate mathematical relationships and statistical methods.

The major source of information on the crystal structure is contained in the very strong and very weak reflections, where strong and weak refer to the intensities of the reflections corrected for scattering angle i.e. the structure factors are converted to normalised structure factors, $E_{\tilde{H}}$.

$$E_{\tilde{H}} = \frac{F_{\tilde{H}}}{(\epsilon \sum_i f_i^2)^{\frac{1}{2}}}$$

Thus, $E_{\tilde{H}}$ is the ratio of $F_{\tilde{H}}$ to its root mean square expectation value and the quantity ϵ is introduced to allow for space group symmetry, which affects the intensities of some reflections e.g. in the space group $P2_1/c$ where systematic absences are present, some reflections are missing while others are increased in intensity. The average intensities of $(h0\ell)$ reflections for which $\ell = 2n$ is twice as large as for $hk\ell$ reflections.

The experimental data are usually on an arbitrary scale, however the proportionality factor and the overall temperature factor can be derived.

If k is the unknown scale factor to convert relative F values to the absolute values then

$$k(F_{\tilde{H}})_{\text{rel}} = F_{\tilde{H}}$$

$$k^2 \langle F_{\tilde{H}}^2 \rangle_{\text{rel}} = \sum_i f_i^2 = \sum_i (f_i^0)^2 \exp(-2B \sin^2 \theta / \lambda^2)$$

thus,

$$\ln \left\{ \frac{\langle F_{\tilde{H}}^2 \rangle_{\text{rel}}}{\sum_i (f_i^0)^2} \right\} = -2(\ln k + B \sin^2 \theta / \lambda^2)$$

So, by calculating $\langle F_{\tilde{H}}^2 \rangle$ and $\sum_i (f_i^0)^2$ in various $\sin \theta / \lambda$ ranges and plotting the l.h.s. of the above equation against $\sin^2 \theta / \lambda^2$ the straight line fitted to these points has a slope corresponding to the temperature factor coefficient B and from the intercept at $\sin \theta / \lambda = 0$, the scale factor k may be obtained.

Most modern direct methods use normalised structure factors or E values. In recent years, a number of inequality and equality relationships have been derived which attempt to predict the signs (or phases if non-centrosymmetric) of particular reflections. Sayre's equation is the basis of many such relationships. If one of the products is large, it will tend to dominate the sum. For a centrosymmetric structure, for $F_{hkl}, F_{h'k'l'}, F_{h-h', k-k', l-l'}$ all large, it follows that

$$s(hkl)s(h'k'l')s(h-h', k-k', l-l') \approx +1$$

where $s = \text{sign}$.

The symbol \approx means 'probably equals'.

The vectors associated with these reflections $d^*(hkl), d^*(h'k'l')$ and $d^*(h-h', k-k', l-l')$ form a closed triangle or vector triplet. The physical significance of these triplets is that if they are drawn in real space, their points of intersection correspond to atomic positions. The probability is particularly strong if they have high E values.

This may be written in a more general form²³.

$$s[E(hk\ell)] \approx s \left[\sum_{h',k',\ell'} E(h'k'\ell') E(h-h',k-k',\ell-\ell') \right]$$

The summation is over all vector pairs with known signs which form a triplet $(hk\ell)$. The probability P is given by

$$P_+(hk\ell) = \frac{1}{2} + \frac{1}{2} \tanh[(\sigma_3/\sigma_2^{3/2})\alpha']$$

where α' is given by

$$\alpha' = |E(hk\ell)| \sum_{hk\ell} E(h'k'\ell') E(h-h',k-k',\ell-\ell')$$

and σ_n by

$$\sigma_n = \sum_i Z_i^n \quad Z_i = \text{atomic number of the } i\text{th atom.}$$

In practice, a list of strong triples and their associated triple products is produced. This is helped in many cases by the space group symmetry. When glide planes or screw axes are present, additional relationships hold e.g. in $P2_1/c$,

$$k+\ell=2n: \quad s(hk\ell)=s(-h,-k,-\ell)=s(h,-k,\ell)=s(-h,k,-\ell)$$

$$k+\ell=2n+1: \quad s(hk\ell)=s(-h,-k,-\ell)=-s(h,-k,\ell)=-s(-h,k,-\ell).$$

A listing of triple sign relationships is developed (Σ_2) by considering each value of $E_{hk\ell}$ greater than a preset limit e.g. 1.4, in order of decreasing magnitude as a basic $hk\ell$ vector and searching the data for all interactions with $h'k'\ell'$ and $h-h',k-k',\ell-\ell'$.

One possible continuation of this approach is to assign phases symbolically²⁴.

The first step is to fix the origin (of the x,y,z , coordinates of the structure) using a few phases guessed either uniquely or symbolically. In centrosymmetric crystals the selection of phases is relatively easy (compared to the non-centrosymmetric case) due to Friedel's law as the imaginary part

of the structure factor disappears

$$A'(hkl) = \sum_{i=1}^{n/2} g_i [\cos 2\pi(hx_i + ky_i + lz_i) + \cos 2\pi(-hx_i - ky_i - lz_i)]$$

$$B'(hkl) = \sum_{i=1}^{n/2} g_i [\sin 2\pi(hx_i + ky_i + lz_i) + \sin 2\pi(-hx_i - ky_i - lz_i)]$$

Since for any angle ϕ , $\cos(-\phi) = \cos \phi$ and $\sin(-\phi) = -\sin \phi$

$$A'(hkl) = 2 \sum_{i=1}^{n/2} g_i \cos 2\pi(hx_i + ky_i + lz_i)$$

$$B'(hkl) = 0$$

Thus $\phi_{\tilde{H}} = 0$ if $A'(hkl)$ is positive and $\phi_{\tilde{H}} = \pi$ if $A'(hkl)$ is negative. (g_i is the temperature corrected atomic scattering factor).

Three origin defining reflections are required to uniquely define one of the 8 centres of symmetry in the centrosymmetric cell. These are specially selected such that the parity groups of the reflections are not linearly related. (The sum of the parities of $h+h'+h''$, $k+k'+k''$, $l+l'+l'' \neq ggg$). Reflections belonging to this group are termed structure invariant and their signs depend on the structure. In the case of non-centrosymmetric space groups, a further reflection is usually required to define the enantiomorph.

Those reflections which cannot immediately be assigned a phase are given symbolic signs, usually designated a, b, c, etc. Certain reflections will be involved in several strong triples leading to multiple sign indications which can be used to eliminate symbolic phases. As these are introduced, several contradictions are likely to be encountered and phases must be selected to keep these to a minimum.

An E-map can now be computed using the Fourier synthesis where the coefficients are experimental E-values associated with the derived signs. Generally several such maps are needed using different sign expansion pathways or varying the choice of signs for the symbolic phases.

For non-centrosymmetric structures the problem is much greater since the phase allocated to a reflection is at best only approximately right. However, it was realised that the phase determining procedure could be repeated in an iterative manner using the tangent formula, derived from the Sayre equation²⁵:

$$\tan \phi_{\tilde{H}} \approx \frac{\sum_{\tilde{K}} |E_{\tilde{K}}^{obs}| \sin(\phi_{\tilde{K}} + \phi_{\tilde{H}-\tilde{K}})}{\sum_{\tilde{K}} |E_{\tilde{K}}^{obs}| \cos(\phi_{\tilde{K}} + \phi_{\tilde{H}-\tilde{K}})}$$

(where the sums are taken over all available terms).

With a set of assumed or derived phases for a relatively small number of reflections the tangent formula can be used iteratively to refine the starting set and provide additional phased reflections.

Correct phases are recognised by statistical formula, one of the most generally used criterion being:

$$R = \frac{\sum_{\tilde{H}} (|E_{\tilde{H}}^{obs}| - |E_{\tilde{H}}^{calc}|)}{\sum |E_{\tilde{H}}^{obs}|}$$

where R is minimised.

At this stage in structure solution a number of chemical fragments are probably evident and the structure can be refined using a non-linear least squares procedure.

In symbolic addition a new phase may be indicated several times by the same combinations of symbols, then the individual implications reinforce one another. However, the combination of indications involving entirely different symbols can introduce problems²⁹ e.g. if 2 separate sign indications for the phase of ϕ are $(a+b)$ and $(c+d)$ and $a = \pi/4$, $b = 3\pi/4$, $c = -\pi/4$, $d = -3\pi/4$, then the combinations of $(a+b)$ and $(c+d)$ equal π . However, symbolic combination of $1/2(a+b+c+d) = 0$, the incorrect solution.

The multisolution approach avoids these problems by assigning numeric rather than symbolic phases at an early stage. It is then possible to combine individual phase indications by the tangent formula.

The phase determining procedure is based on a starting set of phases:

- (a) origin and enantiomorph definition, requiring up to 4 phase assignments
- (b) phases derived from a Σ_1 formula or another method
- (c) further phases required to initiate a continuous phase determining process by tangent formula expansion.

The Σ_1 relationship is derived from the Σ_2 relationship:

$$\Sigma_2 s_{\tilde{H}} \approx s\left(\sum_{\tilde{K}_r} s_{\tilde{K}} s_{\tilde{H}-\tilde{K}}\right)$$

when only a single triplet is considered,

$$s_{\tilde{H}} \cdot s_{\tilde{K}} s_{\tilde{H}-\tilde{K}} \approx 1$$

known as a triple product sign relationship. For the special case of $\tilde{H} = -\tilde{K}$ (\tilde{H} and \tilde{K} are vectors hkl and $h'k'\ell'$) in

space group $P\bar{1}$; for example

$$\phi_{\tilde{H}} \approx \phi_{-\tilde{H}} + \phi_{2\tilde{H}} \approx \frac{1}{2}\phi_{2\tilde{H}}$$

similarly, in $P\bar{1}$ since $\phi_{\tilde{H}} = 0, \pi$ it follows that $s_{\tilde{H}} = s_{-\tilde{H}} = \pm 1$ hence

$$s(2\tilde{H}) \approx 1$$

The above two equations are referred to as Σ_1 relationships²⁹. The program MULTAN utilises the multisolution approach.

The initial starting phases are given numerical values according to space group symmetry. General non-centrosymmetric phases are assigned the values $+\pi/4, +3\pi/4$ and for enantiomorph $-\pi/4$. A total of p variable phases including enantiomorph selection will now give $2 \times 4^{p-1}$. This method gives an initial maximum error in the starting phases of 45° . A weighted tangent formula is used to expand the initial starting set of phases

$$\tan \phi_{\tilde{H}} = \frac{\sum_{\tilde{K}} Q_{\tilde{H}, \tilde{K}} \sin(\phi_{\tilde{K}} + \phi_{\tilde{H}-\tilde{K}})}{\sum_{\tilde{K}} Q_{\tilde{H}, \tilde{K}} \cos(\phi_{\tilde{K}} + \phi_{\tilde{H}-\tilde{K}})} = \frac{T_{\tilde{H}}}{B_{\tilde{H}}}$$

where $Q_{\tilde{H}, \tilde{K}} = w_{\tilde{K}} w_{\tilde{H}-\tilde{K}} |E_{\tilde{K}}||E_{\tilde{H}-\tilde{K}}| / (|U_{\tilde{H}}|^2)$

with

$$w_{\tilde{H}} = \tan[\sigma_3 \sigma_2^{-3/2} E_{\tilde{H}}(T_{\tilde{H}}^2, B_{\tilde{H}}^2)^{1/2}]$$

and

$$|U_{\tilde{H}}| = |F_{\tilde{H}}| / \sum_{j=1}^N f_j$$

the unitary structure factor.

$\sigma_3 \sigma_2^{-3/2}$ is a correction for different types and numbers of atoms in the unit cell.

The weighting scheme is designed to give poorly assigned phases a low weight while still incorporating them in the sign expansion.

Phase sets are assessed by three figures of merit ABS FOM, PSI ZERO and RESID²⁹ prior to calculation of E maps.

ABS FOM(Z) (a measure of the internal consistency among the two relationships)

$$Z = \frac{\sum_{\tilde{H}} (\alpha_{\tilde{H}} - \alpha_{R_{\tilde{H}}})^2}{\sum_{\tilde{H}} (\alpha_{E_{\tilde{H}}} - \alpha_{R_{\tilde{H}}})^2}$$

$\alpha_{R_{\tilde{H}}}$ is the value expected for random phases and $\alpha_{E_{\tilde{H}}}$ is an estimate of calculated during the convergence procedure.

PSI ZERO

$$\psi_0 = \sum_{\tilde{H}} \sum_{\tilde{K}} |E_{\tilde{K}} \parallel E_{\tilde{H}-\tilde{K}}|$$

the $|E|$ values in this summation are very small. For small $|E_{\tilde{H}}|$, ψ_0 should have a small value for the correct phase set. RESID corresponds to

$$R_K = \frac{\sum_{\tilde{H}} \sum_{\tilde{K}} |E_{\tilde{K}} \parallel E_{\tilde{H}-\tilde{K}}| - |E_{\tilde{H}}|_{\text{calc}}}{\sum_{\tilde{H}} |E_{\tilde{H}}|}$$

where $|E_{\tilde{H}}|_{\text{calc}} = K \langle |E_{\tilde{K}} \parallel E_{\tilde{H}-\tilde{K}}| \rangle_{\tilde{H}}$

and K is a scale factor

$$K = \frac{\sum_{\tilde{H}} |E_{\tilde{H}}|^2}{\sum_{\tilde{H}} \langle |E_{\tilde{K}} \parallel E_{\tilde{H}-\tilde{K}} \rangle^2}$$

The correct set of phases should have the smallest RESID.

APPENDIX C: Anomalous dispersion

In 1951, Bijvoet et al.²⁸ showed that the absolute configuration of an optically active molecule could be determined by measurement of the effects of anomalous dispersion. The method is based on the breakdown of Friedel's law under special conditions.

Friedel's law; $I(hk\ell) = I(-h, -k, -\ell)$ is not an exact relationship and tends to become less so as the atomic numbers of constituent atoms in a crystal increase. The law breaks down severely if the X-rays used have a wavelength just less than that of an absorption edge of an atom in the crystal e.g. with molybdenum radiation and bromine atoms in the crystal structure. Anomalous scattering introduces a phase change into the atomic scattering factor which becomes complex:

$$F = F_0 + \Delta F' + i\Delta F''$$

$\Delta F'$ is a real correction and $\Delta F''$ is an imaginary component which is rotated through 90° in the complex plane with respect to F_0 and $\Delta F'$. The result is best displayed with an Argand diagram. In Figure 3.26 three atoms a, b and c have the structure factors f_a , f_b and f_c . In this case, there is no anomalous dispersion.

Figure 3.27 shows the case with anomalous dispersion. Atoms a and b have no anomalous dispersion. However, atom c, as well as having a real correction to the structure factor f_c' also has an imaginary correction f_c'' .

This result can be applied by comparing the observed and calculated F's. These are tabulated as $F_0(hk\ell)/F_0(-h, -k, -\ell)$ and $F_c(hk\ell)/F_c(-h, -k, -\ell)$ and each pair is compared. If the ratio of the observed reflections is consistently greater than 1

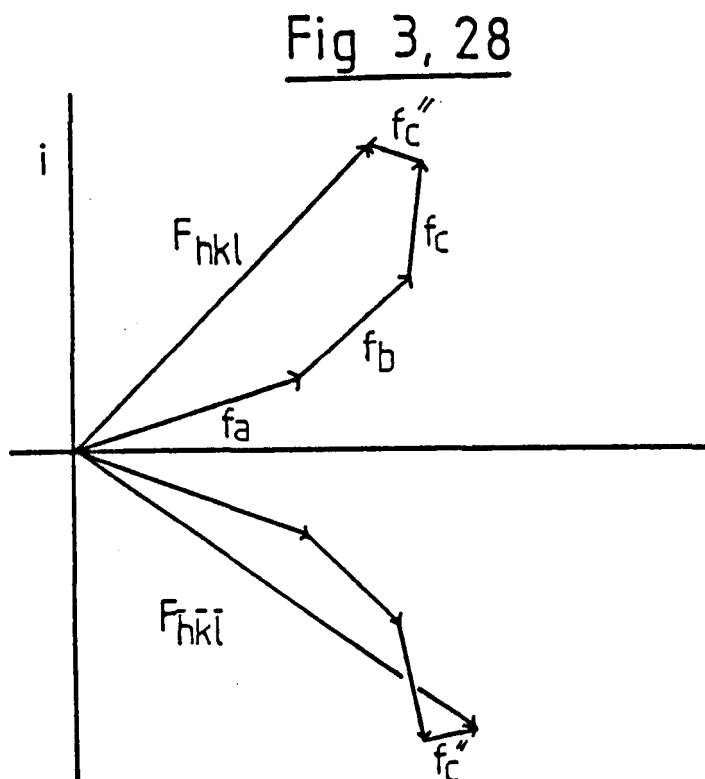
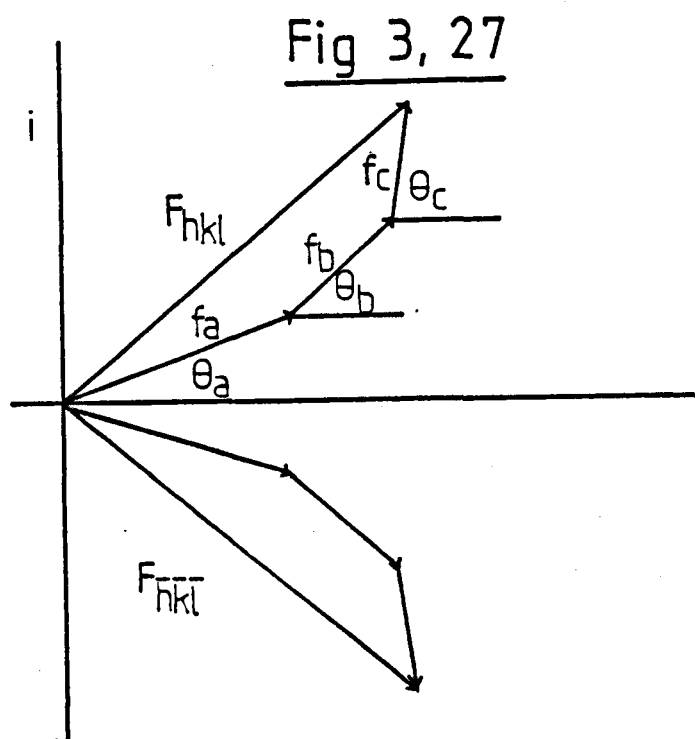


Figure 3.27 Argand diagram for 3 atoms a, b and c with structure factor amplitudes f_a, f_b, f_c and phases $\theta_a, \theta_b, \theta_c$ showing the contribution these atoms make to the observed structure factor $F(hkl)$. In this case, there is no anomalous dispersion and $F(hkl) = F(-h, -k, -l)$.

Figure 3.28 Argand diagram for 3 atoms a, b and c with structure factor amplitudes f_a, f_b, f_c and phases $\theta_a, \theta_b, \theta_c$ showing the atoms contribution to the observed structure factor $F(hkl)$. In this case, there is anomalous dispersion. Hence, $F(hkl) \neq F(-h, -k, -l)$.

when the ratio of the calculated reflections is less than 1, the wrong configuration has been chosen²⁶.

For low symmetry space groups the enantiomorph is obtained by changing the sign of the coordinates; x to $-x$, y to $-y$, z to $-z$. For space groups which occur in enantiomorphic pairs (e.g. P_{3_1} / P_{3_2}) in which compound (3) (Chapter 3) crystallises) the enantiomorph is obtained by change of space group and simultaneous inversion of the signs of all coordinates, e.g. (x,y,z) in P_{3_1} and $(-x,-y,-z)$ in P_{3_2} are enantiomorphs.

3.5

REFERENCES

1. Crossland, N.M., Roberts, S.M., Newton, R.F., Webb, C.F., J.Chem.Soc.Chem.Comm., 1978, p.660.
2. Burgi, H.B., Dunitz, J.D., Shefter, E., Acta Cryst., 1974, B30, p.1517.
3. Newton, R.F., Paton, J., Reynolds, D.P., Young, S., Roberts, S.M., J.Chem.Soc.Chem.Comm., 1979, p.908.
4. Dunitz, J.D., 'X-Ray Analysis and The Structure of Organic Molecules', Cornell Univ.Press, Ithaca, U.S.A., 1979, p.117.
5. Murray-Rust, P., Murray-Rust, J., Brown, A., Acta Cryst., 1979, B35, p.1915.
6. Brown, A., Glen, R., Murray-Rust, P., Murray-Rust, J., Newton, R.F., J.Chem.Soc.Chem.Comm., 1980, p.1178.
7. Ali, S.M., Chapleo, C.B., Roberts, S.M., Wooley, G.T., Newton, R.F., J.Chem.Soc.Perkin I, 1981, (Paper 9/1259) in press.
8. Murray-Rust, P., Murray-Rust, J., Newton, R.F., Acta Cryst., 1979, B35, p.1918.
9. Hilderbrandt, R.L., Wieser, J.D., J.Molecular Structure, 1974, 22, p.247.
10. Allinger, N.L., Advances in Physical Organic Chemistry, 1976, 13, p.1.
11. Allinger, N.L., J.Am.Chem.Soc., 1977, Vol.99, No.25, p.8127.
12. Grudzinski, Z., Roberts, S.M., J.Chem.Soc.Perkin I, 1975, p.1769.
13. Brown, C.J., Proc.Roy.Soc.London A302, 1968, p.185.

14. Kaftory, M., Dunitz, J.D., *Acta Cryst.*, 1976, B32, p.1.
15. Newton, R.F., Reynolds, D.P., Webb, C.F., Young, S.N., Grudzinski, Z., Roberts, S.M., *J.Chem.Soc.Chem.Commun.*, 1979, p.909.
16. 'International Tables for X-Ray Crystallography', 1974, Vol.4, p.99. Birmingham: Kynoch Press.
17. Sheldrick, G.M., (1976). SHELX76 program for crystal structure determination. University of Cambridge, England.
18. Main, P., Hull, S.E., Lessinger, L., Germain, G., Declercq, J., Woolfson, M.M. MULTAN78. A system of computer programs for the automatic solution of crystal structures from diffraction data. University of York, England and Louvain, Belgium.
19. Rogers, D., *Acta Cryst.*, 1981, A37, p.734.
20. Hamilton, W.C., *Acta Cryst.*, 1965, 18, p.502.
21. Ladd, M.F.C., Palmer, R.A., 'Structure Determination by X-Ray Crystallography', Plenum Press, 1977.
22. *Ibid.*, p.281.
23. Hauptman, H., Karle, J., 'Solution of the Phase Problem, 1. The Centrosymmetric Crystal', American Crystallographic Association Monograph No. 3, 1953.
24. Karle, J., Karle, I.L., *Acta Cryst.*, 1966, 21, p.849.
25. Karle, J., Hauptman, H., *Acta Cryst.*, 1956, 9, p.635.
26. Stout, G.H., Jensen, L.H., 'X-Ray Structure Determination', The Macmillan Company, 1968.
27. Patterson, A.L., *Z.Krist.*, 1935, A90, p.517.
28. Bijvoet, J.M., Peerdman, A.F., Van Bommel, A.J., *Nature*, 1951, 168, p.271.

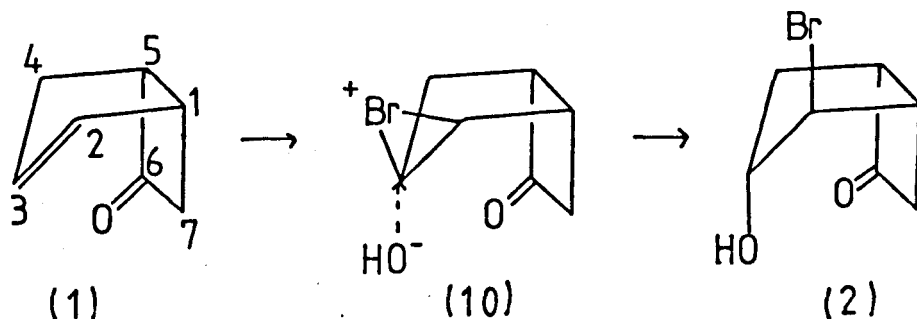
29. Ladd, M.F.C., Palmer, R.A., editors, 'Theory and Practice of Direct Methods in Crystallography', Plenum Press, 1980.
30. Glen, R.C., Murray-Rust, P., Kay, P., Newton, R.F., Riddell, F.G., J.Chem.Soc.Chem.Comm., 1981, No. 1009, in press.
31. Murray-Rust, P., Glen, R.C., Newton, R.F., Ali, S.M., Acta Cryst., 1981, WH2765, in press.
32. Murray-Rust, P., Glen, R.C., Newton, R.F., Acta Cryst., 1981, WH2763, in press.
33. Murray-Rust, P., Glen, R.C., Newton, R.F., Acta Cryst., 1981, WH2761, in press.
34. Murray-Rust, P., Glen, R.C., Newton, R.F., Acta Cryst., 1981, WH2764, in press.
35. Murray-Rust, P., Glen, R.C., Newton, R.F., Acta Cryst., 1981, WH2762, in press.
36. Newton, R.F., Reynolds, D.P., Kay, P.B., Roberts, S.M., Glen, R.C., Murray-Rust, P., J.Chem.Soc.Chem.Comm., 1981, submitted.
37. Glen, R.C., Murray-Rust, P., Reynolds, D.P., Newton, R.F., J.Chem.Soc.Chem.Comm., 1981, submitted.

CHAPTER 4An investigation of regio- and stereo-chemical control by transannular O...C=O interactionsCONTENTS

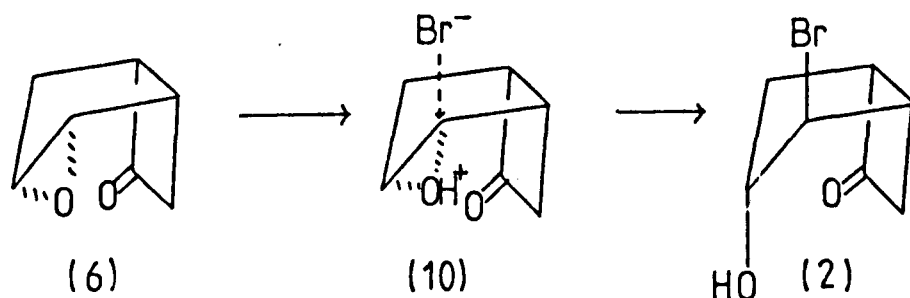
- 4.1 Introduction
- 4.2 Review
- 4.3 Survey of O...C=O interactions involving 4-, 5- and 6-membered rings
- 4.4 Discussion
- 4.5 References

4.1 Introduction

The addition of the elements HOX to (1) (X=Cl,Br,I) gives the bromohydrin (2) in high yield via stereo-specific formation of the exo-bromonium ion (10) followed by regio-specific attack by nucleophile predominately at C(3). (Chapter 2).

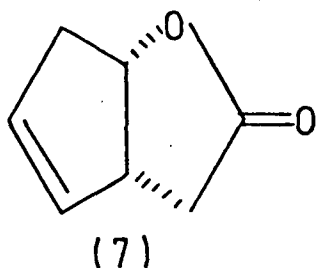


Similarly, nucleophilic attack on the corresponding protonated epoxide of (6) proceeds in an analogous fashion with regio-specific attack by nucleophile at C(2).

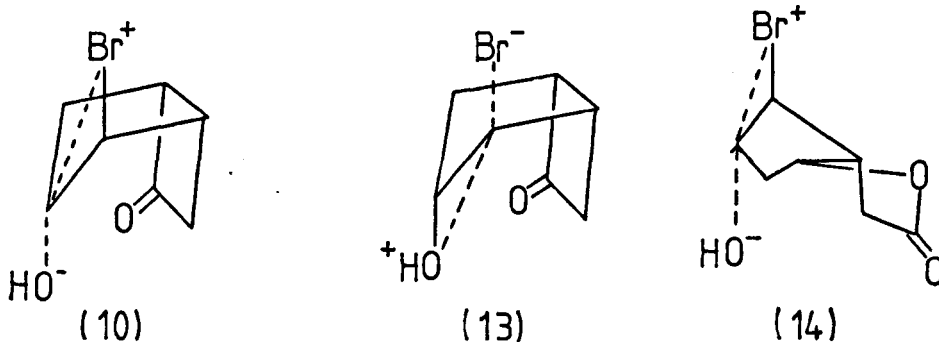


In contrast, the oxabicyclo[3.3.0]octenone (7) forms both exo- (14) and endo- (16), (18) bromonium ions in equal proportions. However, the exo-bromonium ion is again attacked regio-specifically by nucleophile to give only the bromohydrin (15)⁹.

Nucleophilic attack on the bromonium ions (10), (14) and the protonated epoxide of (6) presumably proceeds via a transition state where the carbocyclic 5-membered ring adopts



an endo-envelope conformation with the halogen and hydroxy functions trans diaxial.

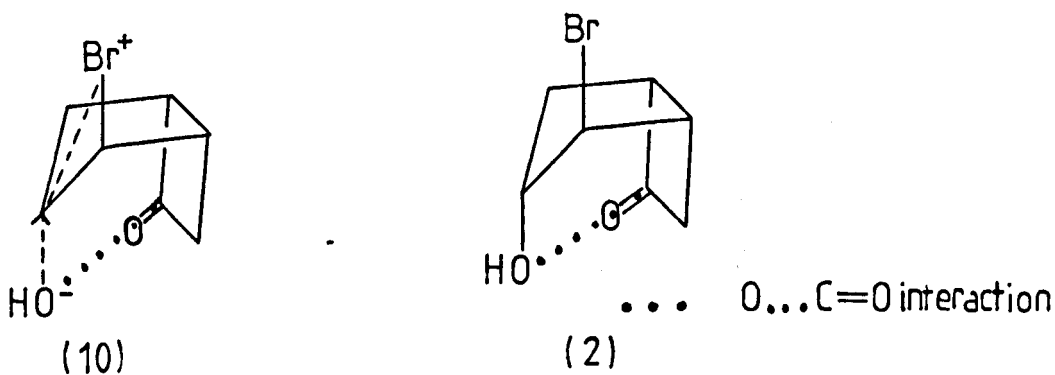


Attack at the alternative site would require the carbocyclic ring to take up an exo-envelope conformation (assuming an anti-periplanar transition state). N.m.r. evidence suggests that in solution bicyclo[3.2.0]heptan-6-one derivatives (Chapter 2) exist predominately in the endo-envelope conformation with the substituents pseudoaxial. The preference of the bicyclo[3.2.0]-heptane system for the endo-envelope conformation has also been confirmed by force-field calculations (Chapter 5) and X-ray studies (Chapter 3).

There is however another factor which could stabilise the endo-conformation and direct the course of nucleophilic attack.

Substituted bicycloheptanones and 2-oxabicycloöctanones (of the type described above) and other polycyclic compounds (e.g. (65)) have the possibility of transannular intra-molecular interactions analogous to those described by Bürgi, Dunitz and Shefter (BDS)³ if one of the rings has as a substituent a nucleophile (e.g. OH) and the other ring, an electrophile (e.g. C=O) in a suitable orientation to each other. In the cases described above (1) to (14), the cis ring fusion accompanied by an endo-envelope conformation results in the

molecules having a folded appearance with the nucleophile presented to the electrophile in a very favourable geometry for transannular attack. Inspection of models appears to indicate that the orientation of the hydroxyl and ketone is such that other conformations (e.g. an exo-envelope) or substitution patterns (e.g. 2-endo-hydroxy-3-exo-bromo-) do not achieve the optimum geometry for a strong O...C=O interaction. Thus approach of an attacking nucleophile could be directed and the transition state stabilised by this type of interaction e.g. nucleophilic attack on the bromonium ion (10).



It seems therefore, that the presence of this interaction could possibly be the controlling factor in the observed regio-chemical nucleophilic attack. This view was encouraged when an investigation of the epoxy-lactone (8)¹² by X-ray analysis indicated an interaction with an O...C=O distance of 2.992(2)Å.

However, the degree to which the transannular O...C=O interaction exerts control of the conformation and energy of (8) and similar small polycyclic molecules required further data on similar molecular systems.

To achieve this aim, nucleophilic attack of the type

described by BDS¹⁰ is reviewed (Chapter 4.2) and the role of this interaction on the ground state geometry and conformation of small polycyclic molecules has been investigated utilising the Cambridge Crystallographic Data Files (CCDC), X-ray analysis and force-field calculations (Chapter 4.2 and Chapter 4.4).

4.2 Review

Dunitz et al. have found striking geometric correlations between nucleophilic groups and electrophilic centres which appear to map out the minimum energy pathway (reaction coordinate) of a series of chemical interactions³ very similar in nature to those observed in some of the compounds studied in Chapter 3.

From this work came the principle of structural correlation i.e. if a correlation can be found between 2 or more independent parameters describing the structure of a given structural fragment in a variety of environments, then the correlation function maps a minimum energy pathway in the corresponding parameter space⁴.

To apply this hypothesis, correlations between selected parameters describing the geometry of a subsystem frozen in a number of molecular or crystal environments are extracted from X-ray structural data. Molecular interactions of interest may perturb the subsystem, which will modify its geometry so as to minimise the energy of the crystal as a whole. The subsystem may now be considered to be constrained at some point along the reaction coordinate. If a sufficient number of structures are available covering the range of the interaction of interest, then comparison can be made between dynamic chemical reactions and the corresponding static crystal structures. The

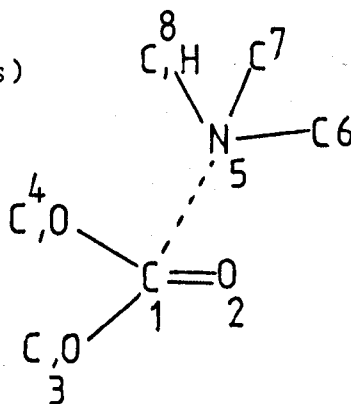
transition state is energetically at the apex of the reaction coordinate and hence is difficult to observe. However, the approach of the nucleophile towards the electrophilic centre (and the departure of the leaving group) may be observed 'frozen' by inter- and intra-molecular forces in the crystalline environment.

Using this approach the N...C=O interaction has been investigated by Dunitz et al. in some detail. In this investigation the data on the N...C=O interaction were obtained by a careful (if tedious) survey of the literature. To test the sensitivity of automatic search methods (using CCDC⁸) and in the hope of retrieving a larger set of structures displaying N...C=O interactions, this search has been repeated for intra-molecular N...C=O interactions.

A connectivity search using the criteria of Table 4.1, retrieved 721 structures.

TABLE 4.1: Connectivity search (CONN SER and RETRIEVE)

Q intra N...C=O
 C retrieves ketones, esters etc.
 At1 C 3 0 E
 At2 O 1 0 E
 At3 C,O
 At4 C,O
 C retrieves tertiary amines (amides)
 At5 N 3 E
 At6 C
 At7 C
 At8 C,H
 BO 1 2 2
 BO 1 3
 BO 1 4
 BO 5 6 1
 BO 5 7 1
 BO 5 8 1
 ENDQ



The data were screened, removing data sets without published coordinates and structures containing disordered atoms, reducing the number of compounds to 540.

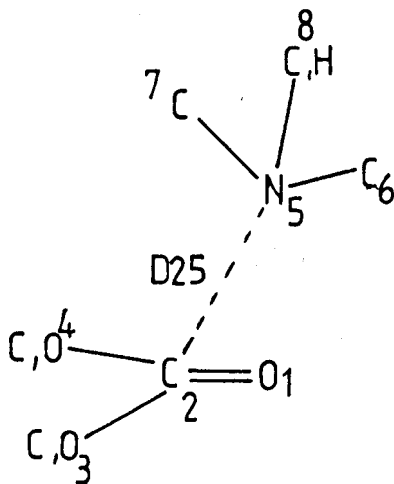
The geometries of the chemical fragments of interest were calculated (Table 4.2).

TABLE 4.2: Geometry screen (GEOM)

```

CALC INTRA N 2.4
FRAC INTRA N...C=O
AT1 O
AT2 C
AT3 C,O
AT4 C,O
AT5 N
AT6 C
AT7 C
AT8 C,H
C only compounds with N...C=O are processed
BO 1 2 1.1,1.35
BO 2 3 1.15,1.6
BO 2 4 1.15,1.6
BO 2 5 1.49,3.3
BO 5 6 1.1,1.6
BO 5 7 1.1,1.6
BO 5 8 .8,1.7
C angle screen
TEST ANG 5 2 1 85,125
ENDF
DEF *RFACT
DEF *AS
C plane of carbonyl is P1
SETUP P1 1 3 4
DEF D12 1 2
DEF D25 2 5
DEF A521 521
DEF DELTC P1 2
DEF DELTN P1 5
ENDQ

```



Only 29 structures contained the required fragments. The remaining structures were screened by hand. Those structures with an R-Factor greater than 0.12, 1-4 N...C=O interactions or with P1..AT2 less than 1.4Å were removed. 17 structures remained. (The compounds are identified by their CCDC codes, Table 4.3).

TABLE 4.3: N...C=O interactions

Code	R-Factor	C=O(Å)	C..N(Å)	NCO(°)	deltc(Å)
AEPCNQ10	.069	1.221	2.908	100.7	.010 *
CLIVOR10	.039	1.258	1.993	110.2	.213
CPSAIA	.043	1.211	2.879	112.1	.002 *
CRYPTP	.042	1.209	2.581	102.2	.102
DMUVIC	.060	1.165	2.988	117.7	.009 *
IKIDBB10	.113	1.153	3.170	93.3	.049 *
MAZUNO	.045	1.217	2.457	111.1	.097
METHAD	.040	1.215	2.911	105.1	.064
METHAD01	.038	1.207	2.912	105.0	.057
MMANCX	.038	1.336	2.995	94.3	.062
NMZNON	.086	1.211	2.759	112.5	.023
NMZNON	.081	1.216	2.690	114.4	.055
NANMEK	.047	1.218	2.559	104.2	.088
NANPCX	.056	1.215	2.602	102.2	.063
OTOSEN10	.061	1.259	2.180	107.7	.133 *
PROTPN	.043	1.218	2.555	101.6	.115
SENKIR10	.045	1.213	2.292	109.4	.116

The relationship between out-of-plane displacement (Δ) and N...C=O distance (d2) is displayed in Figure 4.2.

The automatic structure retrieval process retrieved all the fragments in the original survey by BDS¹⁰. Surprisingly, only a few additional compounds were retrieved (indicated by *).

The approach of a nucleophilic group (in this case a tertiary amine group) to a carbonyl is accompanied by an out-of-plane displacement (Δ) of the carbonyl carbon from the plane of R1,R2,O and an extension of the C=O bond length (Figure 4.1, after BDS⁵). These results are consonant with re-hybridisation of the carbonyl carbon from sp² to sp³ with associated change in geometry from trigonal to tetrahedral.

Table 4.3 also shows that the preferred angle of attack by the nucleophilic nitrogen on the carbonyl is ca. 100-112°¹⁰.

The search procedure used for the N...C=O interaction proved very successful and has been modified to search for intramolecular interactions between oxygen nucleophiles and carbonyls on 4, 5 and 6-membered rings (of the type observed in Chapter 2).

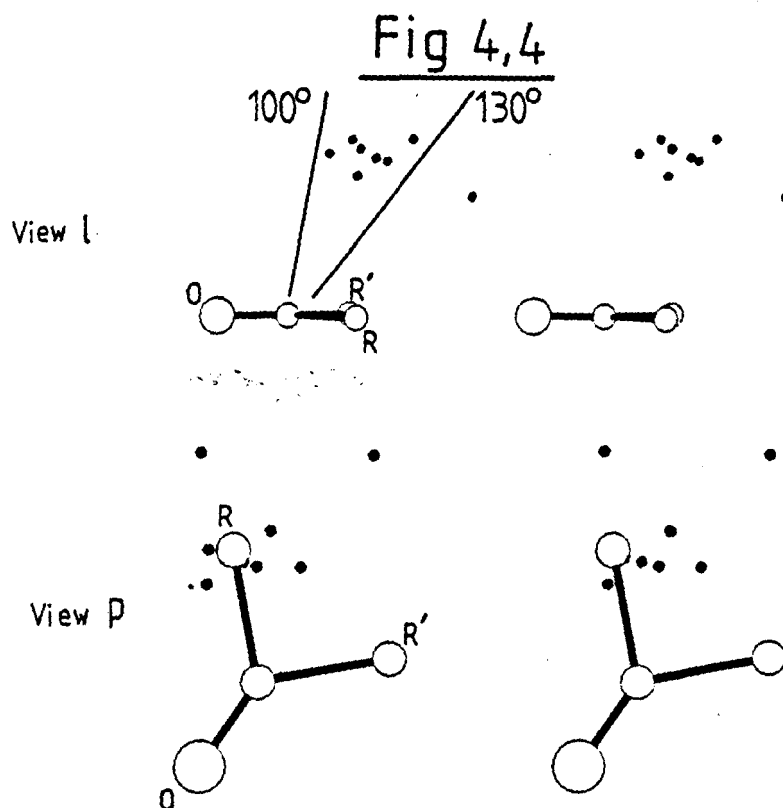
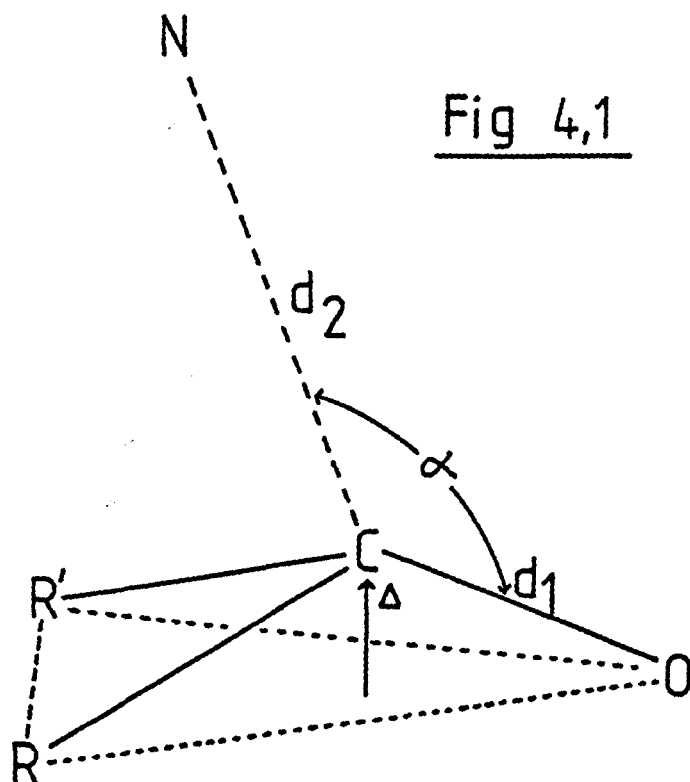


Figure 4.1 Nucleophilic attack on a carbonyl ($=O, R, R'$) by a nucleophile N at a distance d_2 occurs at an angle α and results in an out-of-plane displacement (Δ) of the carbonyl carbon from the plane R, R', O and a lengthening of the $C=O$ bond length d_1 . (After BDS).

Figure 4.4 Stereo diagrams of transannular nucleophilic attack (of the type described by BDS) observed in the crystal structures (3), (60), (61), (8), (29), (14), (62), (63) (p =view perpendicular to $R, R', =O$, l =view line through $R-R'$).

Figure 4.2

In N...C=O interactions retrieved from the Cambridge Crystallographic Data files, as the N...C=O distance (d_2) decreases from 3.2Å to 2.0Å, the out-of-plane displacement (Δ) of the carbonyl increases.

Δ (Å)

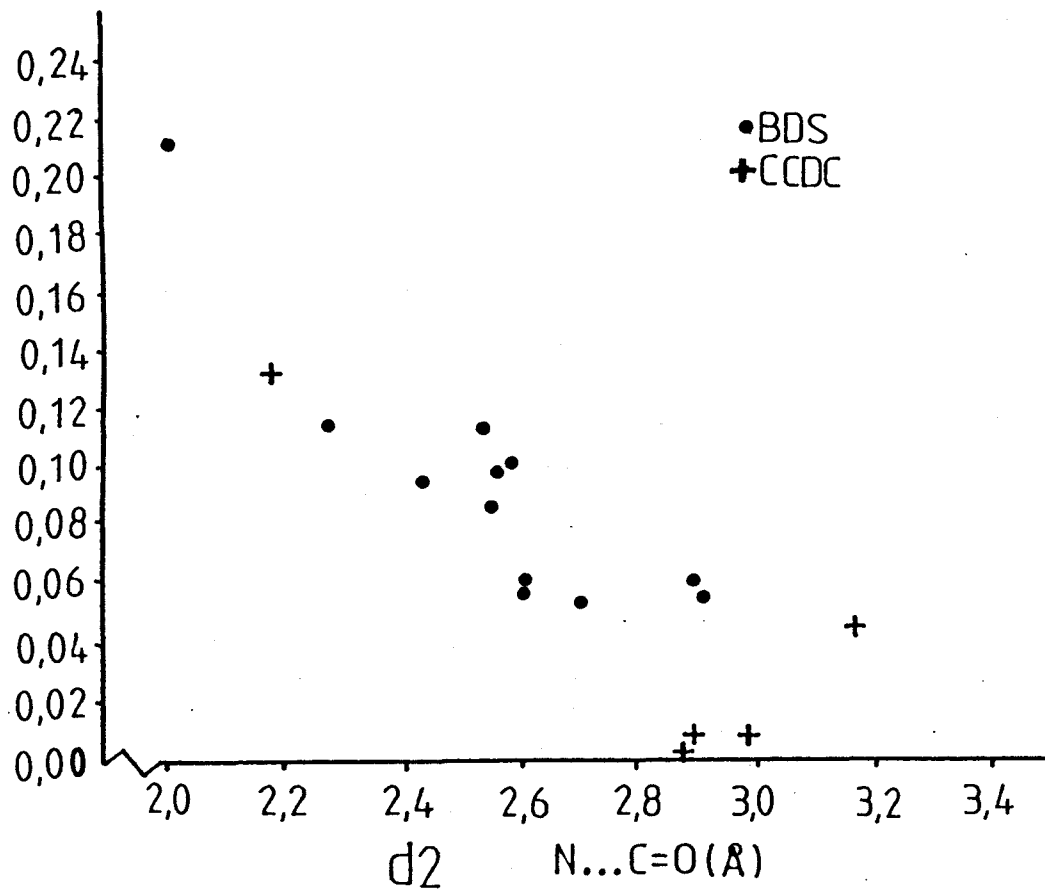


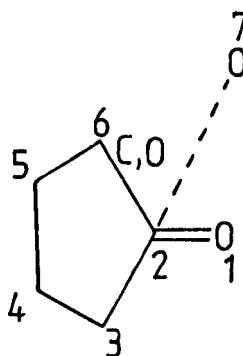
Fig 4,2

4.3 Survey of O...C=O interactions involving 4-, 5- and 6-membered rings

Intramolecular interactions between a carbonyl on a 5-membered ring and suitably orientated oxygen are considered first (Table 4.4).

TABLE 4.4: Connectivity search (CONNSEER and RETRIEVE)

```
Q INTRA O...C=O
C 5-membered ring with carbonyl
AT1 O 1 0 E
AT2 C 3 0 E
AT3 C 2
AT4 C 2
AT5 C 2
C includes lactones
AT6 C,O 2
AT7 O
BO 1 2
BO 2 3 C
BO 3 4 C
BO 5 6 C
BO 6 2 C
ENDQ
```



945 structures were retrieved. The geometries of the chemical fragments of interest were calculated (Table 4.5).

TABLE 4.5: Geometry screen (GEOM)

```
FRAG INTRA O...C=O
AT1 O
AT2 C
AT3 C
AT4 C
AT5 C
AT6 C,O
AT7 O
BO 1 2 1.15,1.3
BO 2 3 1.3,1.6
BO 3 4 1.3,1.6
BO 4 5 1.3,1.6
BO 5 6 1.3,1.6
BO 2 6 1.2,1.6
BO 2 7 2.4,3.1
C angle screen
TEST ANG 7 2 1 85,125
ENDF
DEF *RFACT
DEF *AS
CALC INTRA O 2.2
C plane of carbonyl
SETUP P1 1 3 6
(continued)
```

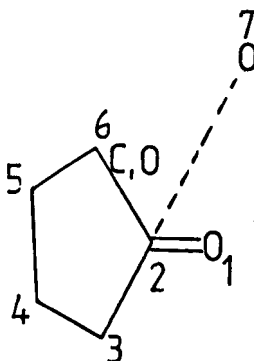


Table 4.5 (continued)

```

DEF D12 1 2
DEF D27 2 7
DEF A721 7 2 1
DEF DELTC P1 2
DEF DELTO P1 7
END

```

There were 110 structures with a possible interaction (disordered structures and those without published coordinates were removed). These were screened by hand. Those structures were removed: with an R-Factor greater than 0.12; where the O...C=O interaction was a 1-4 interaction; where DELTO was less than 0.5Å; containing transition metals; where D27 is less than 2.3Å. 32 structures remained (these are identified by their CCDC code, Table 4.6).

TABLE 4.6 O...C=O (5-membered ring) (CCDC nomenclature)

Code	R-Factor	C=O(Å)	C..O(Å)	OCO(°)	delto(Å)
ANONAL10	.056	1.233	2.649	100.6	.032
APTSPN	.060	1.214	2.886	111.2	.026
BHELIN10	.058	1.200	2.812	99.7	.031
CPACHO	.090	1.237	3.100	118.7	.009
CXAEZT	.076	1.201	2.622	96.2	.017
DANETN	.049	1.214	3.055	119.9	.009
DCLACM10	.041	1.210	2.436	99.9	.001
EMCZTO	.083	1.186	2.871	87.2	.015
ENXBCO	.036	1.197	2.992	118.9	.010
EREMTB10	.061	1.215	2.683	120.1	.038
EREOLA10	.056	1.188	2.650	115.0	.011
GLULAD	.040	1.215	2.902	104.7	.000
HELENI	.052	1.221	2.620	112.6	.015
ICASIN	.039	1.204	2.734	96.5	.007
ITHANE	.061	1.197	3.012	120.7	.010
KISCIT10	.046	1.195	3.069	122.3	.010
LYCPER	.059	1.207	2.902	116.9	.008
MCLPHD10	.090	1.236	2.843	99.4	.001
MEGAMI	.048	1.199	2.826	113.9	.021
MOLOLD	.067	1.196	2.882	95.2	.024
MXTHPO	.071	1.208	2.878	109.2	.022
NTMCPO	.049	1.201	2.901	95.8	-.002
NTRYQV	.054	1.196	2.469	101.7	.055
OTUBST10	.074	1.208	2.690	111.3	.019

(continued)

Table 4.6 (continued)

Code	R-Factor	C=O(Å)	C..O(Å)	OCO(°)	delta(Å)
PEUNCN	.038	1.199	3.064	122.1	.015
PLENOL10	.041	1.186	2.843	91.7	-.019
PODOLB	.048	1.177	3.013	88.4	.022
PROPTO	.047	1.202	3.089	86.6	.013
PSCHDA	.054	1.195	2.653	117.6	-.030
ROSIGN	.053	1.210	2.692	110.2	-.016
THPDEC10	.065	1.220	2.902	95.6	.034
TMHPFE	.065	1.170	2.720	90.6	.028

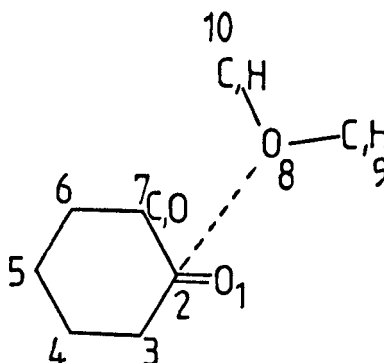
A similar search was carried out on 6-membered rings (Table 4.7).

TABLE 4.7: Connectivity search (CONNSER and RETRIEVE)

```

Q INTRA O...C=O
C 6-membered ring with carbonyl
AT1 O 1 E
AT2 C 3 E
AT3 C
AT4 C
AT5 C
AT6 C
C includes lactones
AT7 C,O
AT8 O
AT9 C,H
AT10 C,H
BO 1,2
BO 2 3 C
BO 3 4 C
BO 4 5 C
BO 5 6 C
BO 6 7 C
BO 7 2 C
BO 8 9
BO 8 10
ENDQ

```



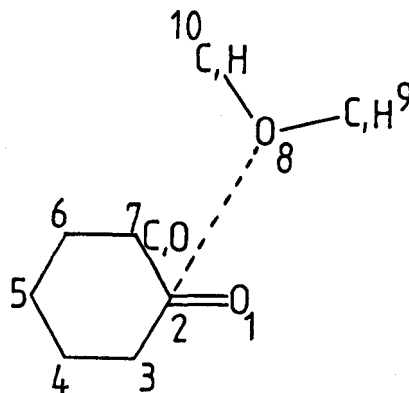
929 structures were retrieved. Those structures containing transition metals or having 1-4 interactions were removed leaving 885 structures. Those structures not having published coordinates or containing disordered atoms were removed leaving 648 structures. The geometry of the fragments of interest was calculated (Table 4.8).

TABLE 4.8: Geometry calculation (GEOM)

```

FRAG INTRA 0...C=O
AT1 O
AT2 C
AT3 C
AT4 C
AT5 C
AT6 C
AT7 C,O
AT8 O
AT9 C,H
AT10 C,H
BO 1 2 1.15,1.4
BO 2 3 1.3,1.6
BO 3 4 1.3,1.6
BO 4 5 1.3,1.6
BO 5 6 1.3,1.6
BO 6 7 1.3,1.6
BO 7 2 1.3,1.6
BO 2 8 2.4,3.2
BO 8 9 .8,1.6
BO 8 10 .8,1.6
C angle screen
TEST ANG 8 2 1 85,125
ENDF
DEF *RFACT
DEF *AS
CALC INTRA 0 2.2
C plane of carbonyl P1
SETUP P1 1 3 7
DEF D12 1 2
DEF A821 8 2 1
DEF DELTC P1 2
DEF DELTO P1 8
END

```



22 structures remained. These were screened by hand (as with the 5-membered ring structures), to give 18 remaining structures (these are identified by their CCDC codes, Table 4.9).

TABLE 4.9

Code	R-Factor	C=O(A)	C..O(A)	OCO(^o)	delta(A)
AOTETC	.076	1.228	2.560	103.3	-.003
AXIPBT	.052	1.209	2.956	99.6	.010
BANEOV	.091	1.164	2.784	104.5	.056
CHASIN	.043	1.212	2.763	118.7	-.004
CYHPOC	.062	1.197	2.673	98.7	.032
DCHCBN	.079	1.218	3.042	85.1	-.003
FOMANN	.072	1.229	3.050	87.19	.030
GILMAN	.057	1.221	2.801	97.6	.003
ICOLID10	.096	1.195	2.937	94.7	.022
LOBSTE	.065	1.217	2.783	100.5	.016
MCPLNE	.054	1.217	2.858	91.7	.012
MFSUDT	.041	1.207	3.129	97.4	-.005
MXPCD010	.039	1.210	3.055	91.5	-.024
MXRCDC	.045	1.215	2.773	104.0	.037
NEPETA	.042	1.210	2.724	109.0	.041
NONFRA	.055	1.202	3.063	95.9	.024
PAFLEB	.107	1.229	2.556	104.2	.040
TBDMXT01	.047	1.245	2.724	97.4	.006

A search for oxygen interactions with 4-membered rings containing a carbonyl (as before) retrieved no additional structures (1-4 interactions and those with an R-factor greater than .012 were omitted).

The variation of out-of-plane displacement of the carbonyl carbon (delta) with O...C=O distance (d2) is displayed in Figure 4.3.

Although there is an abundance of X-ray structural data on the O...C=O interaction, it is more difficult to determine precise correlations than in the case of the N...C=O interaction. Figure 4.3 shows that the O...C=O interaction displays a much smaller out-of-plane displacement than its N...C=O counterpart for a given X...C=O distance. Also, the scatter of points in Figure 4.3 (O...C=O) is much greater than in Figure 4.2 (N...C=O). These results imply the O...C=O interaction is much weaker and is very susceptible to perturbations in its environment⁷. There is a distinct gap in the available data between O...C=O

Figure 4.3

The relationship between out-of-plane displacement of the carbonyl carbon (Δ) and O...C=O distance (d_2).

Δ (Å)

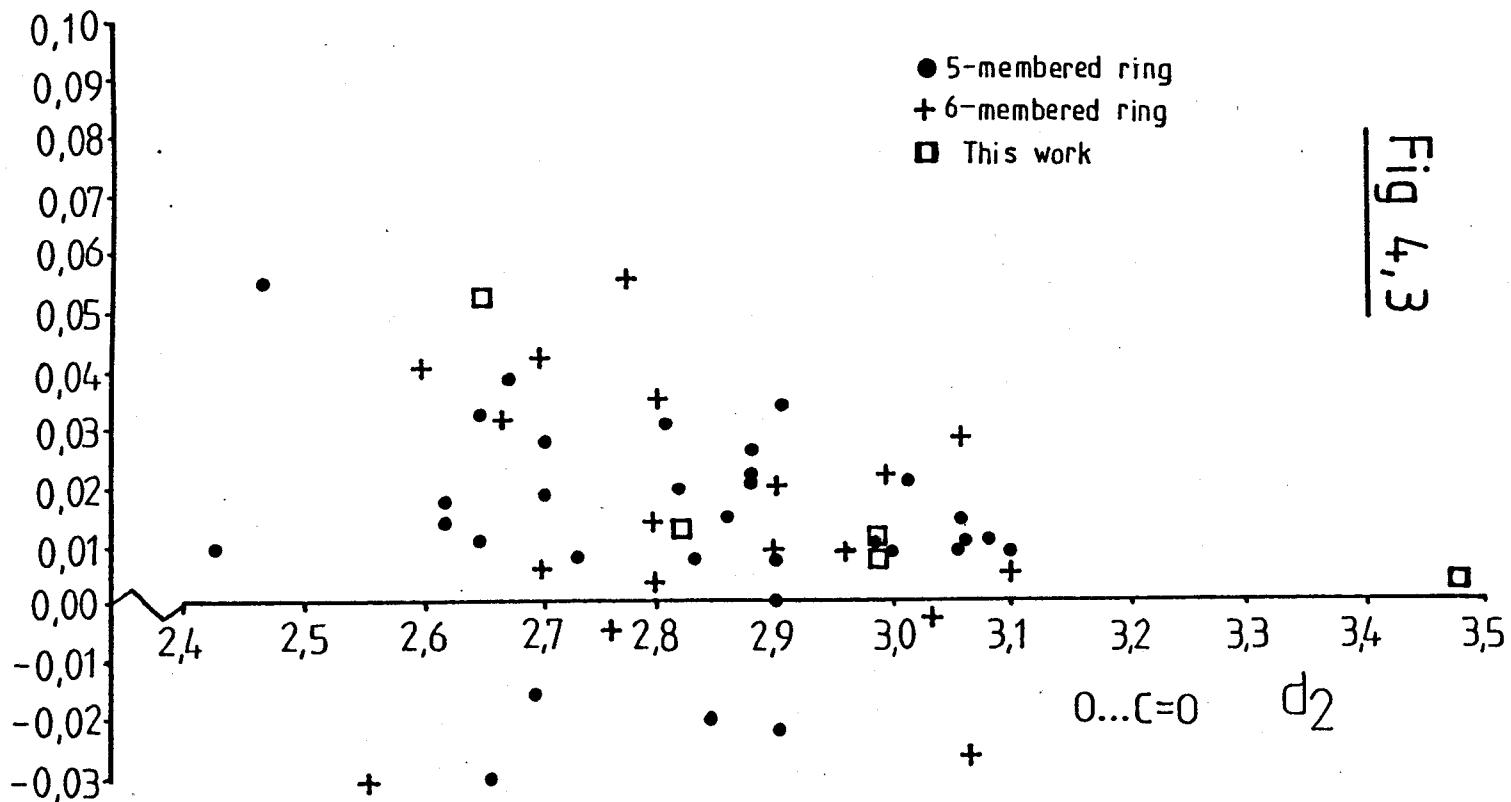
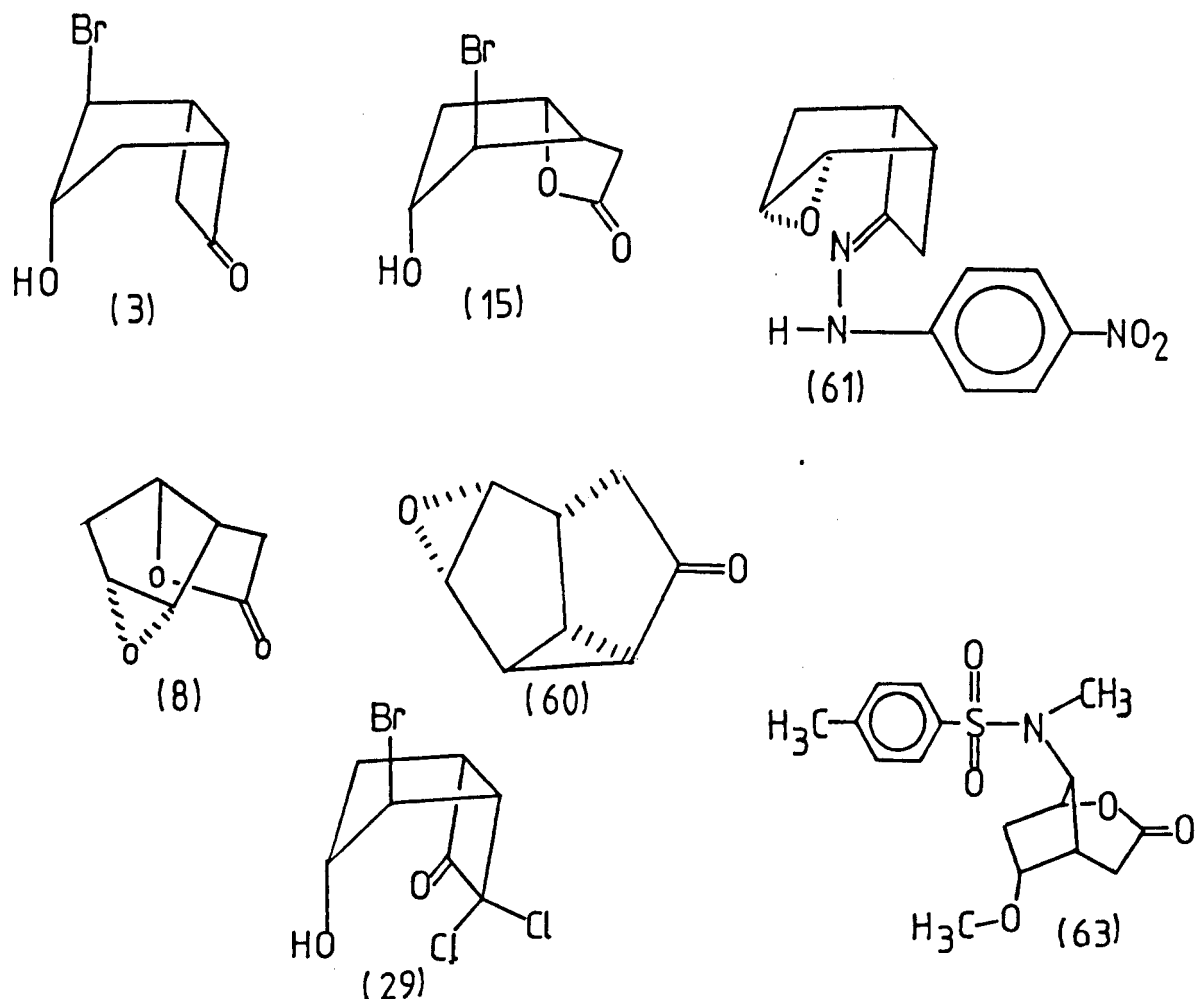


Fig 4,3

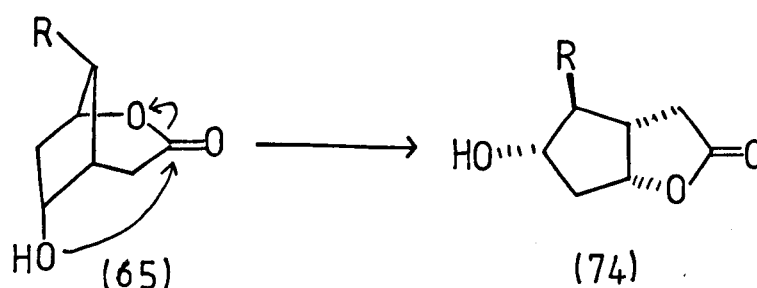
distances of 1.5-2.4Å and this is probably due to the unstable nature of this weak interaction near the intermediate transition state⁷. The out-of-plane displacement of the carbonyl carbon is only about 1/3 that observed for nitrogen nucleophiles (Figure 4.3 (O...C=O interactions) and Figure 4.2 (N...C=O interactions)). This suggests the energy of the O...C=O interaction is only about 1/10 that of the N...C=O interaction¹⁰. The preferred angle of approach tends to be more dependent on the crystal and molecular environment than in the N...C=O case and lies in the range 85-120° (Tables 4.6 and 4.9) (see also reference 7).

4.4 Discussion

A number of polycyclic compounds having the possibility of a transannular O...C=X (X=O,N) interaction have been investigated by X-ray diffraction (Chapter 2).



Of these compounds, (3)¹¹ and (15)¹¹ are the products of regio-selective reactions favouring the 2-exo-3-endo product. (6) (the p-nitro phenylhydrazone derivative (61) was analysed) and (8)¹² are attacked regio-selectively by nucleophile giving predominately the 2-exo-3-endo product. (65) undergoes a facile rearrangement which takes place spontaneously under the reaction conditions¹³ and involves transannular nucleophilic attack.



(The model compound (63) was analysed by X-ray diffraction).

The steric course of these reactions could conceivably be influenced by a transannular O...C=O interaction (as detailed above)¹⁰. Similarly, the facile rearrangement of (65) suggests the presence of an O...C=O interaction in the ground state.

In addition, the model compounds (60) and (29) were specifically designed to display strong O...C=O interactions. In (60) the ring fusions constrain the epoxide to a close approach on the carbonyl while in (29), the electrophilicity of the carbonyl is increased by the presence of 2 vicinal chlorines.

The geometries of the interactions observed are described in Table 4.10.

TABLE 4.10: O...C=X (X=O,N) interactions

Compound	R-Factor	C=O(Å)	C...O(Å)	A521(°)	deltac(Å)
(63)	.057	1.320(6)	3.492(6)	125(1)	.004(6)
(8)	.036	1.197(2)	2.992(2)	119(1)	.010(2)
(3)	.042	1.185(13)	2.99(2)	111(1)	-.013(15)
(61)	.048	1.275(3)	2.990(3)	124(1)	.008(3)
(60)	.041	1.198(2)	2.651(2)	116(1)	.052(2)
(29a)	.068	1.198(7)	2.826(7)	104(1)	.015(12)
(29b)	.068	1.393(7)	1.410(7)	105(1)	.397(12)
(15a)	.11	1.22(5)	3.02(5)	111(2)	-.06(8)
(15b)	.11	1.22(5)	3.01(5)	115(2)	.02(8)

The nucleophile:carbonyl positions derived from Table 4.10 are displayed graphically in a stereo-plot (Figure 4.4). Compounds which cannot display an intramolecular O...C=O interaction (e.g. (64)²² and (55)) display planar carbonyl geometry (to within experimental error).

Inspection of Table 4.10 indicates that the O...C=O interaction appears to range from 3.1Å (weak, planar C=O) to 2.65Å (strong, Δ = ca. .05Å) (Figure 4.3). Dunitz¹⁰ has estimated the energy required for pyramidalisation of the carbonyl from the out-of-plane bending force constant to be approximately 0.5Kcal/mol for Δ = 0.05Å (which is about the maximum deformation observed in Table 4.10).

The X-ray studies of the bromohydrins (3) and (74) indicate weak O...C=O interactions which can only be inferred (the out-of-plane displacement of the carbonyl carbon is less than the estimated standard deviation) by comparison with Figure 4.3.

Similarly, the epoxides (8) and (61) also display weak interactions at the limit of observability.

(63) (a derivative of (65)), which was expected to display an O...C=O interaction, displays no interaction at all. The O...C=O distance of 3.320(6)Å is well outside the range where an interaction could be observed.

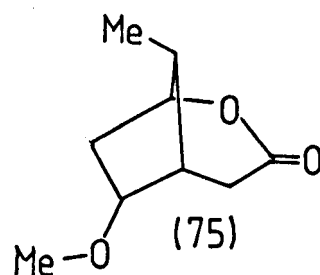
To explain this apparently surprising result force-field calculations have been performed on the system (75), a model for (63) using the force-field of Allinger et al. (MM2, 1980 version) (Chapter 5, Appendix A).

This model can give an indication of the energies involved on constraining the methoxy oxygen to closer approach on the carbonyl (Table 4.11). An attractive O...C=O interaction can be simulated by introducing opposite charges on the hydroxyl and carbonyl carbon.

TABLE 4.11:

O...C=O(Å)	charge*		ΔE.(Kcal/mol)
	OH(i)	C=O(j)	
3.51	0.0	0.0	0.0 (minimised)
3.18	-0.3	0.3	1.2
2.87	-0.4	0.4	2.5
2.59	-0.5	0.5	4.3

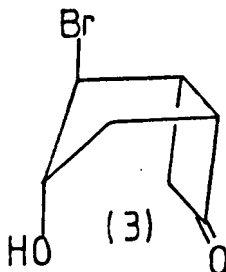
$$* E_{\text{electrostatic}} = k \frac{e_i e_j}{r_{ij}}$$



In this calculation the methoxy oxygen and the carbonyl carbon were assigned equal and opposite charges (dipole/dipole interaction suppressed) chosen to reduce the O...C=O distance while the geometry of the rest of the molecule is subjected to energy minimisation.

When the molecule is constrained to a conformation where a detectable O...C=O interaction would be expected to occur, i.e. ca. 2.9Å, an additional amount of strain in the region of 2.5Kcal/mol is imparted to the molecule. This appears to imply that the strain is sufficient to overcome any weak (certainly less than 2.5Kcal/mol) attractive O...C=O interaction, if indeed the interaction is attractive in the range studied here.

A similar set of calculations were performed on the bromohydrin (3) (using the force-field MM2).



The minimised geometry indicated an O...C=O distance of 3.03Å in the ground state. (X-ray structure determination of (3) gave an O...C=O distance of 2.99(2)Å). As before, charges were placed on the hydroxyl group and the carbonyl to simulate an attractive O...C=O interaction (Table 4.12).

TABLE 4.12:

O...C=O(Å)	charge*		ΔE.(Kcal/mol)
	OH(i)	C=O(j)	
3.03	0.0	0.0	0.0
2.89	-.4	.4	2.9
2.79	-.4	.6	5.2

$$* E_{\text{electrostatic}} = \frac{e_i e_j}{r_{ij}}$$

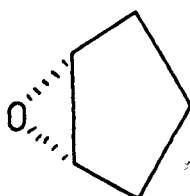
Again, the force-field suggests that an attractive O...C=O interaction of only ca. 2.5Kcal/mol is required to reduce the O...C=O distance significantly (although the force-

field is less reliable in this case due to the presence of bromine).

It appears therefore that there is no evidence the net O...C=O interaction is attractive at any $r(O...C=O)$.

Even in these cases where a strong interaction is observed, the net interaction appears to be repulsive.

Evidence for this is seen in the tricyclic system (60) where the epoxide is constrained by the ring fusions to a close approach on the carbonyl. A small O...C=O distance and a large out-of-plane displacement of the carbonyl carbon is seen in agreement with the general trend observed in Figure 4.3. However, careful examination of the epoxide geometry shows that the angle between the plane of the epoxide (C(7),C(8),O(10)) and the plane of the substituent carbon atoms (C(6),C(7),C(8),C(1)) (planar to within 0.018Å) is $107.0(2)^\circ$, which is significantly larger than in less hindered cyclopentene epoxides. In cyclopentene epoxide itself (67) gas phase electron diffraction gives an interplanar angle of $104.7(1)^\circ$ ¹⁴ and in three other structures containing the cyclopentene epoxide fragment (61), (62) and (8)¹² this angle is in the range $104.8(3)^\circ$ to $105.0(2)^\circ$. To obtain more information on the cyclopentene epoxide geometry, the CCDC files⁸ were searched for molecules containing the fragment (76).



(76)

The connectivity search retrieved 50 structures. 32 fragments having the specified geometry were retrieved. Those structures having disordered atoms, no published coordinates, a trans ring fusion, or an R-factor greater than 0.06 were rejected leaving 3 fragments^{14,15,16}. The relationship between the close approach of another atom or group (X) to the epoxide oxygen and the effect on the cyclopentene epoxide geometry is given in Table 4.13.

TABLE 4.13: The effect of non-bonded interactions on epoxide geometry

In substituted cyclopentene epoxides, θ° is the angle between the plane of the epoxide (P1) and the least-squares plane of the substituent atoms (P2). X is an atom of group forming a close non-bonded contact (d) to the epoxide oxygen (O), where $r(O)$ and $r(X)$ are their Van der Waals radii (Å) (Pauling (1960)²; C=1.6, O=1.4, N=1.5, CH₂=2.0) and $D=d(O...X)-r(O)-r(X)$ (Figure 4.5).

Structure	X	d(Å)	D(Å)	θ°
(67)	-	-	-	104.7
(61)	O	2.99	0	104.7
(62)	O	3.15	>0	104.9
(8)	O	2.93	>0	104.9
(60)	O	2.62	-0.18	106.9
XZCVIN (68)	N	2.68	- .22	107.9
MEXOFE (69)	CH ₂	2.55	- .85	109.7
ENDRIN (70)	CH ₂	2.53	- .87	110.5

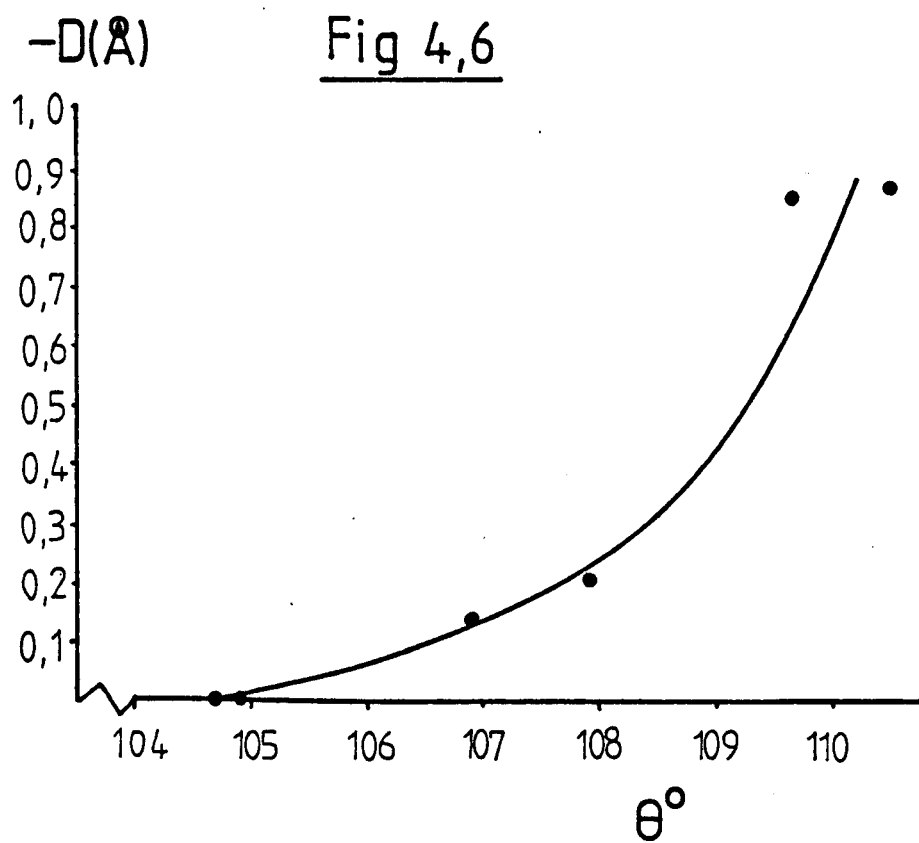
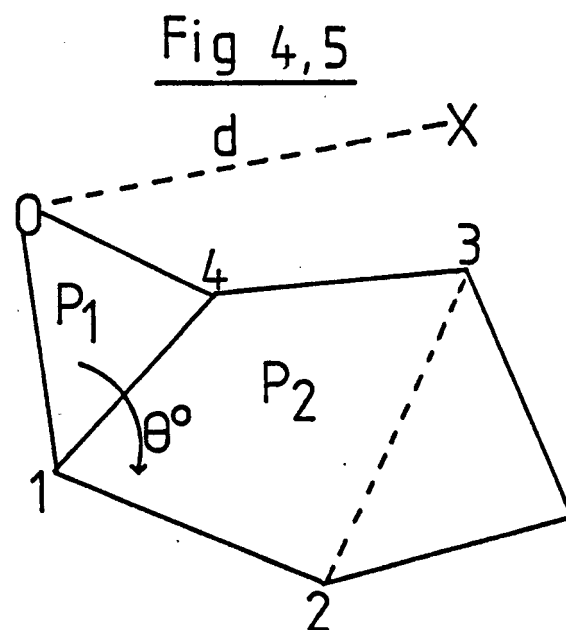
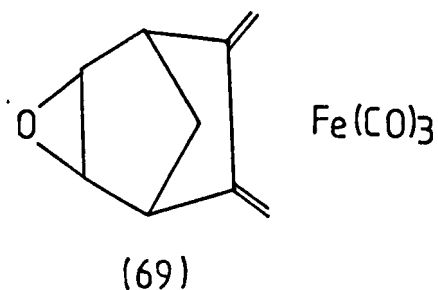
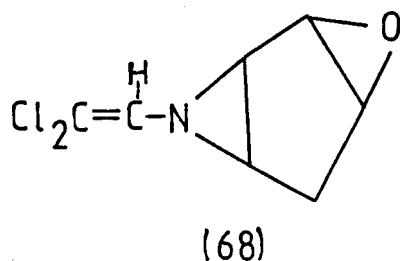
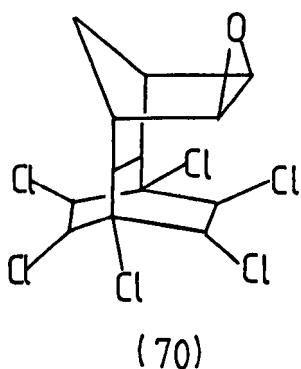


Figure 4.5 Effect on the cyclopentene epoxide geometry on approach of another atom or group (X) to the epoxide oxygen (O). As X approaches O, the interplanar angle θ (the angle between the planes O, C1, C4 and C2, C1, C4, C3) is seen to increase (Figure 4.6).

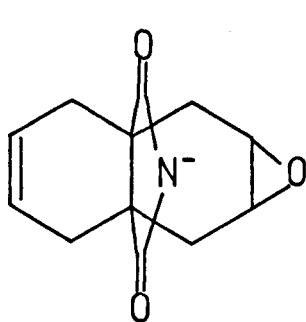
Fe(CO)₃

When another atom or group is constrained to a distance from the epoxide oxygen of less than the sum of their Van der Waals radii², the angle θ increases as expected, primarily due to steric repulsion. In the case of (60), the highly strained tricyclic epoxide, this effect does not appear to be moderated by the BDS interaction (Figure 4.6); therefore at this distance the net $O \dots C=O$ interaction is repulsive. This is in keeping with the structural results on (3) and (74) where the $O \dots C=O$ interaction is at the limits of detection.

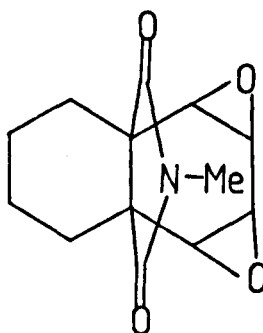
The $O \dots C=O$ interaction can be assisted by placing electron withdrawing substituents next to the carbonyl carbon. (29) is a molecule near the transition state which displays an enhanced interaction. In CCl_4 solution, it exists as a 1:1.1 mixture of (29a) + (29b) while in the crystalline state it exists as a remarkable 1:1 mixture of (29a) + (29b). Both forms (29a) and (29b) in the crystal show very small movement along the nucleophilic addition pathway (Chapter 3)²³. The movement observed is primarily due to the presence of the two

vicinal chlorines which greatly increase the electrophilic nature of the carbonyl carbon and effectively reduce the barrier to nucleophilic attack.

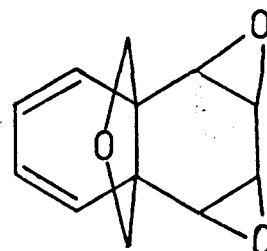
Recent work on propellanes (Kaftory et al.^{17,18,19,20}) which contained suitably orientated O...C=O fragments investigated the possibility that significant departures from mirror symmetry in (71) and (72) were due primarily to attractive O...C=O interactions. Although O...C=O interactions were seen (using the



(71)



(72)



(73)

criteria defined above) and at first appeared to account for the conformational changes observed, replacement of the carbonyls by CH₂ groups resulted in a structure which displayed similar departures from mirror symmetry (73). The observed O...C=O interactions appeared therefore to be present due to geometrical constraints and did not play a significant role in modifying the molecular conformation²¹. Subsequent force-field calculations showed that the deformation could be explained by conformation-stability arguments rather than due to the attractive interaction of the O lone pair electrons²¹.

It appears from the results discussed above that the energy gained by O...C=O interactions is sufficient to

distort relatively flexible acyclic angles e.g. 1,8-disubstituted naphthalene derivatives³ (probably introducing about 0.5Kcal/mol of strain) but is not of sufficient energy to distort to any significant degree more rigid cyclic systems of the type described above (e.g. (63)) which require ca. 2.5Kcal/mol for any significant distortion. When constrained, small distortions may occur to minimise the overall energy of the molecule, however, the overall conformation is not controlled by the interaction. Although therefore the O...C=O interaction is frequently seen (defined by the criteria of $d(O...C=O)$ less than ca. 3.0Å, a related non-planarity of the carbonyl group and O...C=O angles of $110(20)^\circ$) it would seem to be a consequence of constraints (by steric factors and possibly crystal packing) rather than a constraint in itself.

Therefore, the weight of evidence implies that the O...C=O interaction does not influence the regio-selectivity of nucleophilic attack in the molecules investigated here. Other evidence suggests that steric and conformational factors are more important (Chapter 5).

4.5

REFERENCES

1. Birnbaum, K.B., *Acta Cryst.*, 1972, B28, p.2825.
2. Pauling, L. (1960). 'The Nature of The Chemical Bond', 3rd ed., Cornell Univ.Press, Ithaca, New York.
3. Dunitz, J.D., *Phil.Trans.R.Soc.London.* 1975, B272, p.99.
4. Murray-Rust, P., Burgi, H.B., Dunitz, J.D., *J.Am.Chem.Soc.*, 1975, 97, p.921.
5. Bürgi, H.B., Dunitz, J.D., Shefter, E., *J.Am.Chem.Soc.*, 1973, 95, p.5065.
6. Bürgi, H.B., Lehn, J.M., Wipff, G., *J.Am.Chem.Soc.*, 1974, 96, p.1956.
7. Bürgi, H.B., Dunitz, J.D., Shefter, E., *Acta Cryst.*, 1974, B30, p.1517.
8. Allen, F.H., Bellard, S., Brice, M.D., Cartwright, B.A., Doubleday, A., Higgs, H., Hummelink, T., Hummelink-Peters, B.G., Kennard, O., Motherwell, W.D.S., Rogers, J.R., Watson, D.G., *Acta Cryst.*, 1979, B35, p.2331.
9. Ali, S.M., Crossland, N.M., Lee, T.V., Roberts, S.M., *J.Chem.Soc.Perkin I*, 1979, p.122.
10. Dunitz, J.D., 'X-Ray Analysis and the Structure of Organic Molecules', Cornell University Press, 1979.
11. Brown, A., Glen, R., Murray-Rust, P., Murray-Rust, J., Newton, R.F., *J.Chem.Soc.Chem.Comm.*, 1979, p.1178.
12. Murray-Rust, P., Murray-Rust, J., *Acta Cryst.*, 1979, B35, p.1918.
13. Crossland, N.M., Roberts, S.M., Newton, R.F., Webb, C.F., *J.Chem.Soc.Chem.Comm.*, 1978, p.660.

14. van Meerssche, M., Germain, G., Declercq, J.P.,
Bodart-Gilmont, J., Viehe, H.G., Merenyi, R.,
Francotte, E., *Acta Cryst.*, 1977, B33, p.3553.
15. Delacy, T.P., Kennard, C.H.L., *J.Chem.Soc.Perkin II*,
1972, p.2153.
16. Wenger, J., Thuy, N.H., Boschi, T., Roulet, R.,
Chollet, A., Vogel, P., Pinkerton, A.A., Schwarzenbach, D.,
J.Organomet.Chem., 1979, 174, p.89.
17. Kaftory, M., Dunitz, J.D., *Acta Cryst.*, 1976, B32, p.617.
18. Kaftory, M., Dunitz, J.D., Mills, O.S., *Acta Cryst.*,
1976, B32, p.619.
19. Kaftory, M., *Acta Cryst.*, 1978, B34, p.952.
20. Kaftory, M., *Acta Cryst.*, 1979, B35, p.1637.
21. Kaftory, M., *Acta Cryst.*, 1980, B36, p.2668.
22. Murray-Rust, P., Murray-Rust, J., Brown, A.,
Acta Cryst., 1979, B35, p.1915.
23. Glen, R.C., Kay, P., Murray-Rust, P., Newton, R.F.,
Riddell, F.G., *J.Chem.Soc.Chem.Comm.*, 1981, No. 1009,
in press.

CHAPTER 5

5.1 INTRODUCTION

The reactions of the bicyclo[3.2.0]heptane system can display a high degree of regio- and stereoselectivity. Although the factors controlling the observed regio- and stereochemistry (e.g. the addition of the elements HOBr to (1)) are complex, they may be simplified by treating the overall reaction as a 2-step process. The first step is the formation of a 3-membered ring.

In the reactions studied in Chapter 2, the 3-membered ring may be either a bromonium ion or an epoxide. This is a highly stereoselective process strongly favouring exo-attack.

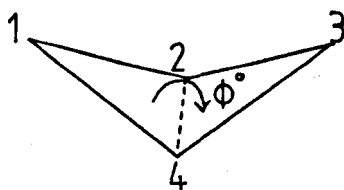
The second step is the opening of the 3-membered ring, generally in a regioselective fashion. In this case, the degree of regioselectivity appears to depend on the conformational properties of the molecule.

These processes are considered separately in Chapters 5.3 and 5.4. First, however, an understanding of the observed regio- and stereoselectivity requires a knowledge of the conformational properties of the bicyclo[3.2.0] system. This aspect is investigated in Chapter 5.2.

5.2 The Conformation of Bicyclo[3.2.0]heptanes

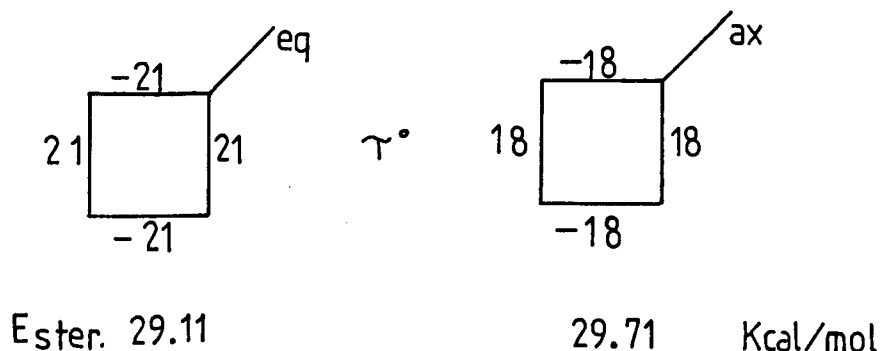
The bicyclo[3.2.0]heptane system is a combination of a 4- and a 5-membered ring. In the molecules studied here, these rings are cis-fused. The properties of bicyclo[3.2.0]-heptanes are to some extent determined by the conformational and steric properties of the constituent rings.

Stereochemical understanding of the cyclobutane ring (81) is at a considerably less well developed stage than, for example, cyclohexane. Recent studies show it to prefer a non-planar conformation with $|\tau|$ C(1)-C(2)-C(3)-C(4)= 22° (the torsion angles around the cyclobutane ring are equal in magnitude and alternate in sign). The pucker angle ϕ (the angle between the planes C(1),C(2),C(4) and C(2),C(3),C(4)) is ca. $25-35^\circ$.^{21,30} The pucker angle $\phi \approx 1.4 \times |\tau|$ ²².

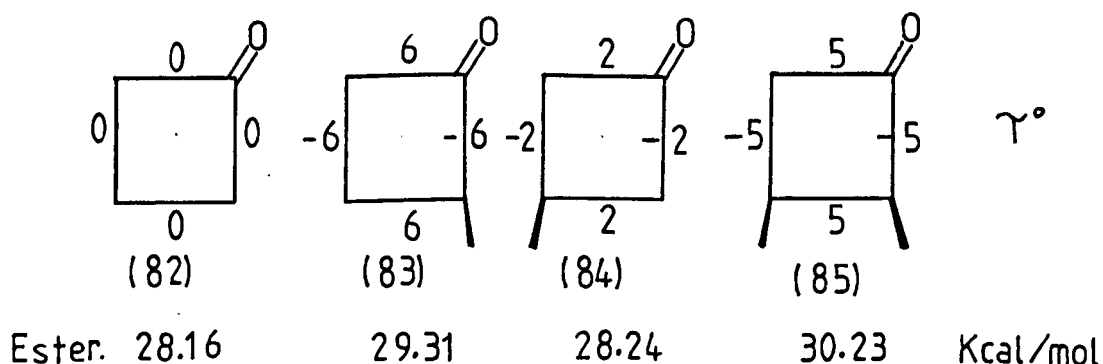


(81)

The reasons for the deviation from non-planarity are not completely understood, although calculations by Wiberg and Lampman²⁴ imply that the major factor is minimisation of the C-C-C-C torsional energy at the expense of angle strain. The barrier to inversion via the planar conformation appears to be ca. 1.4 Kcal/mol from infra-red studies²⁵. The geometry calculated by molecular mechanics (Appendix A; all calculations are by MM2⁴⁴) suggests $|\tau| = 20^\circ$ ²⁸ with a barrier to inversion via the planar conformation of 0.9 Kcal/mol. A number of substituted cyclobutane rings analysed by electron diffraction³⁴ indicate that $|\tau| = 23(5)^\circ$ is the most common arrangement. The difference in energy between substituents in an axial or equatorial position is ca. 0.6 Kcal/mol²³, e.g. substitution by a methyl group (MM2).



In contrast to the puckered conformation observed in cyclobutane, force-field calculations indicate that cyclobutanone (82) takes up a planar conformation and experimental data from microwave²⁷ and infra-red studies²⁶ confirm this result. Small deviations from planarity result in an appreciable increase of strain energy e.g. substitution of the cyclobutanone ring (83), (84), (85) results in conformations which are still relatively planar (in comparison with cyclobutane).

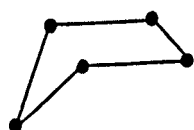


It appears that an increase in $|\tau|$ from 0° to 7° requires ca. 1.5 Kcal/mol.

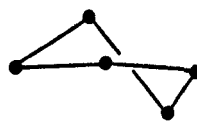
To determine the preferred conformation of the cyclobutanone system in the crystalline state, the Cambridge Crystallographic Data File (CCDC)⁴³ was searched for the cyclobutanone fragment (82). 67 structures were retrieved. Structures without published coordinates or having disordered atoms were removed leaving 59 structures. Those remaining were screened to remove fragments where the carbonyl was involved in

conjugation, spiro ring fusions or ring fusions introducing a large amount of strain (e.g. trans ring fusion). The cyclobutanone fragments in the remaining 38 structures displayed almost planar geometry ($|\tau| \text{ C(1)-C(2)-C(3)-C(4)} = 0.7^\circ$) with the exception of two fragments with gem-dichloro substituents for which $|\tau| = 17(1)^\circ$.

The cyclopentane-ring has been studied intensively^{29,30}. Unsubstituted cyclopentane exhibits nearly free pseudorotation²⁹. The pseudorotation pathway varies between an 'envelope' form (86a) with C_s symmetry and a 'twist' form (86b) with C_2 symmetry. The energy barrier between these has been calculated as 0.005 Kcal/mol³².



(86a)

 C_s 

(86b)

 C_2

The molecule can invert from the C_2 to the C_s form easily, avoiding the planar conformation which is of high energy, the barrier to planarity being ca. 5.5 Kcal/mol³¹.

Mono substituted cyclopentanes were initially taken to exist in the envelope conformer with the substituent equatorial on the flap of the envelope. However, a number of substituents, particularly halogens appear to prefer a pseudoaxial orientation. This also seems to be the case for trans-1,2-di-substitution by halogens. However, as the size of the substituent increases the equatorial form may become favoured²⁹.

Considering the cyclopentane ring as existing in

distinct and well-defined conformations e.g. envelope (C_5) and twist (C_2) forms may be misleading. It is probably better to consider the system as a series of intermediate conformations with those conformers of lowest energy having the highest population²⁹. The smaller the substituents the larger the range of 'pseudolibration'²⁹.

The introduction of a double bond into the cyclopentane ring has the effect of severely restricting pseudorotation resulting in an envelope form with a flap inversion barrier of < 1 Kcal/mol²⁹ and a pucker angle of $29(2.5)^\circ$ (electron diffraction study³³).

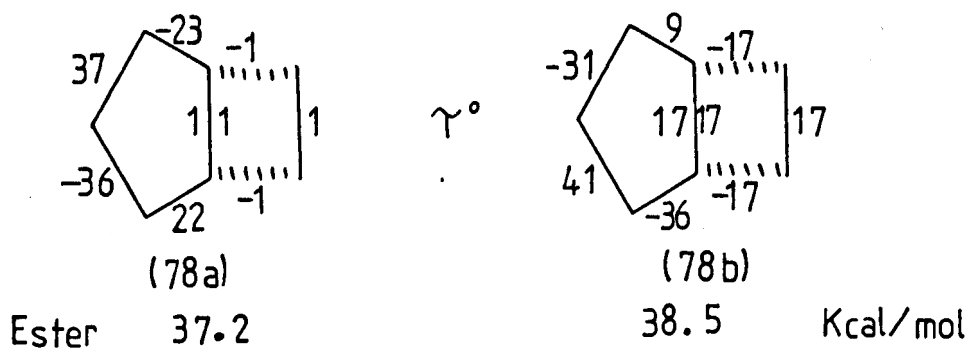
Similarly, substitution of the ring by a 3-membered ring²⁹ results in a boat conformation which, from microwave data, appears to be the only conformer present. The flap of the 5-membered ring takes up an endo conformation with respect to the substituent. The exclusive preference for this conformer appears to be due to the tendency of the cis (1,2) and (4,5) hydrogens (or substituents) to avoid eclipsing strain present in the chair form.

If the 4- and 5-membered rings are compared, it appears that the 4-membered ring has a range of conformations which are relatively stable: non-planar for the unsubstituted saturated species and planar for the cyclobutanones. This is in contrast to the relative flexibility of cyclopentane moieties which (in the saturated cases) are relatively free to pseudorotate. The combination of these conformational aspects leads to interesting stereochemical consequences via conformational transmission between the rings.

In the bicyclo[3.2.0]heptane system the conformations

available to the cyclobutane ring are still accessible ($|\tau| = 0 \pm 25^\circ$) but the pseudorotation of the cyclopentane ring is limited by the cis ring fusion. If (as seems to be the case) the C(1)-C(5) torsion angles are restricted to lie in the range $\tau = -20^\circ$ to $+20^\circ$ then by utilising the relationship between torsion angle and phase angle coordinate (due to Dunitz⁴²) it appears that only two distinct regions each allowing 72° pseudorotation, are available i.e. about the limiting exo- and endo-envelope conformations.

Force-field calculations on bicyclo[3.2.0]heptane and derivatives indicate that this system has two conformational potential minima. These correspond to an endo-envelope form (78a) with C(3) endo to the 4-membered ring and an exo-twist form (78b) with C(3) exo to the 4-membered ring.



For (78), the endo conformer ($E_{\text{ster}} = 37.2$ Kcal/mol) and the exo-twist conformer ($E_{\text{ster}} = 38.5$ Kcal/mol) have an energy difference of 1.3 Kcal/mol which suggests that (neglecting entropy) these conformers are in the ratio of 90:10 (endo:exo-twist) at 298K. The 4-membered ring is considerably puckered in the exo-twist conformer (τ C(1)-C(5)-C(6)-C(7) = 17°) in which the cyclopentane takes up a conformation intermediate between an envelope (flap at C(3)) and twist, (diad through C(2)-C(3)),

conformations. This is in contrast to the endo-conformation in which the cyclobutane ring is flat.

By driving the torsion angle C(3)-C(2)-C(1)-C(7) from -70° to -135° an estimate of the barrier to inversion may be obtained. However, this method requires care as it does not always follow the minimum energy pathway³⁵. Nevertheless, a barrier of ca. 3 Kcal/mol is indicated in going from the endo- to the exo-twist conformer. The force-field calculation indicates that the major contributors to the barrier height are bending strain and Van der Waals (1,4) interactions. The increases in bending and Van der Waals strain are somewhat offset by the decrease in torsional strain (Figure 5.1).

The bicyclo[3.2.0]heptan-6-one system (77) has been investigated in a similar fashion. The energy difference between the endo- (steric energy = 36.2 Kcal/mol) and exo-twist (steric energy = 37.8 Kcal/mol) conformations is 1.6 Kcal/mol which indicates that the ratio of endo:exo-twist is ca. 94:6. In contrast to the puckered cyclobutane ring, the cyclobutanone ring is relatively planar τ C(1)-C(5)-C(6)-C(7) = 2° (endo) and -4° (exo-twist). X-ray analysis of (3), (61), (64), and (29a) (all of these have the cyclobutanone ring) show $|\tau|$ (1)-C(5)-C(6)-C(7) is in the range 0° to 11° . However, in (58), where the cyclobutane ring is saturated, τ (1)-C(5)-C(6)-C(7) = 17° . Driving from the endo- to the exo-twist conformation indicates a barrier height of ca. 3.5 Kcal/mol (Figure 5.2). The preference for the endo-envelope conformation (in the absence of strong steric factors) is confirmed by X-ray analysis (Chapter 3) and n.m.r. data (Chapter 2).

The preferred conformation is however influenced by substituents. If the C(2)-C(3) bond is sp^2 or substituted by an

Fig 5,1

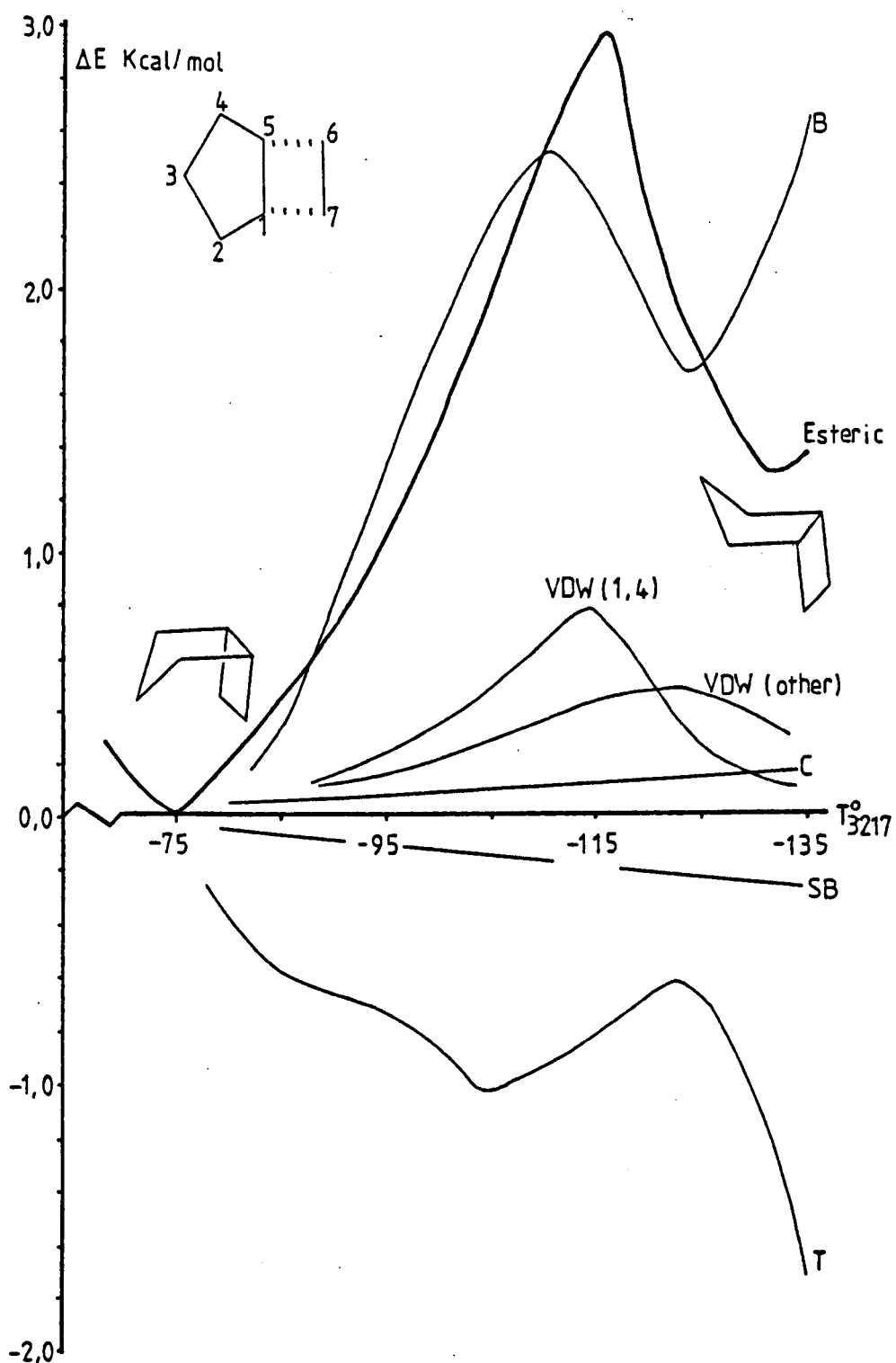


Figure 5.1

The variation in strain energies observed upon driving τ_{3217} from -70° to -135° (endo- to exo-conformation).

Esteric = total strain energy

B=angle strain

SB=stretch-bend strain

VDW(1,4)=(1,4)Van der Waals interaction strain

VDW(other)=other Van der Waals interaction energy

C=bond strain

τ =torsional strain

The energies at -75° are (kcal/mol)

C=0.92

B=15.03

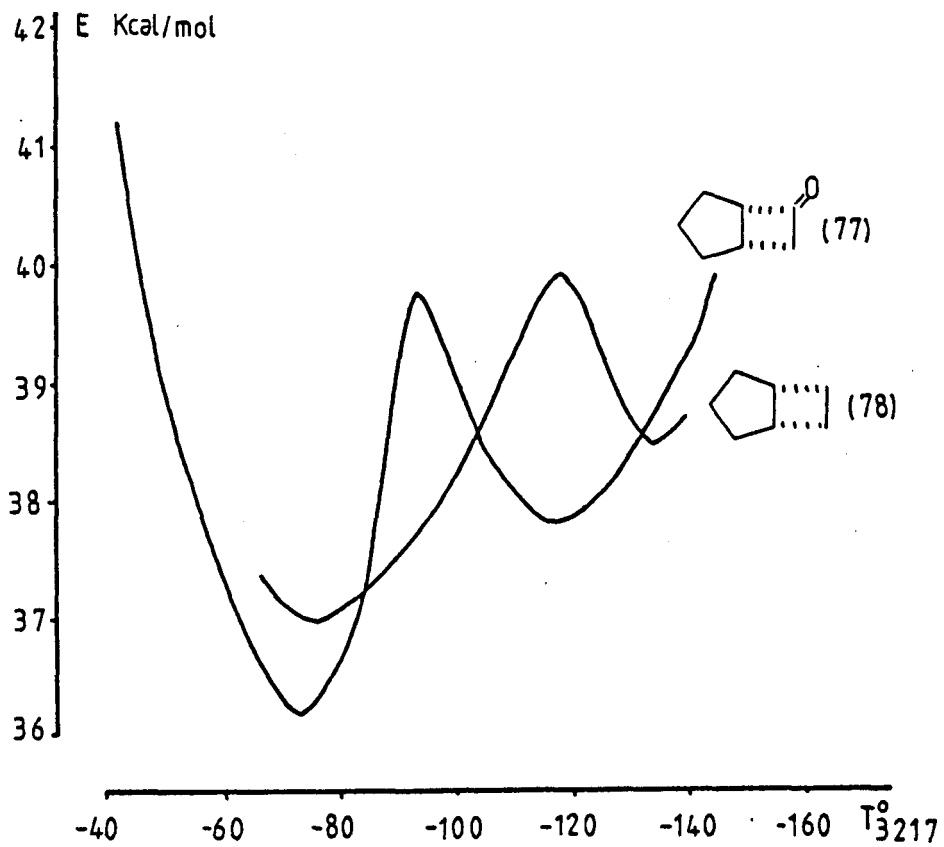
SB=0.88

VW(1.4)=3.44

VW(other)=-1.12

Et=19.8

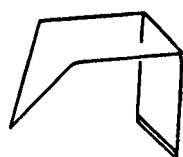
Ester=37.2

Fig 5,2Figure 5.2

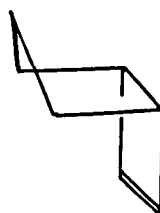
The variation in steric energy for (77) and (78) upon driving τ_{3217} from -40° to -160° (endo- to exo-conformation).

epoxide the cyclopentane ring is flattened (crystal structures (26) and (61)) and $|\tau|$ C(1)-C(2)-C(3)-C(4) is in the range 0° to 1° . In this substitution pattern the cyclopentane ring is in an envelope conformation with the flap at C(4). Trans substitution at C(2) and C(3) to form the bromohydrin (3) results in a more puckered envelope conformer (Br favours a near axial position) as the cyclopentane ring is no longer constrained by a double-bond or epoxide e.g. the crystal structures (3) and (29a).

The presence of a double bond at C(6)-C(7) in the cyclobutane ring has the effect of restricting the ring to a flat conformation. Thus the cyclopentane ring can take up two limiting envelope conformations:-

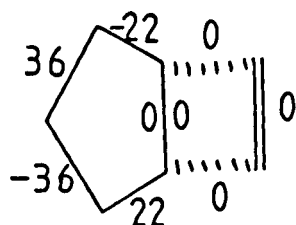


(87a)



(87b)

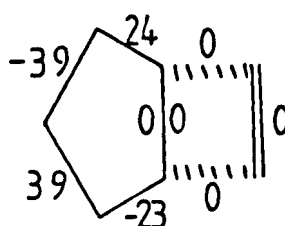
An electron diffraction study³⁶ on bicyclo[3.2.0]-hept-6-ene (87) implied that this molecule takes up an exo-envelope conformation in the gas phase. This is contradictory to what would be expected given the X-ray data of Chapter 3 and the calculations outlined above. Indeed, molecular mechanics calculations on (87) imply that the endo conformer is of lower energy by ca. 2.7 Kcal/mol.



Ester.

39.57

(87a)



42.32

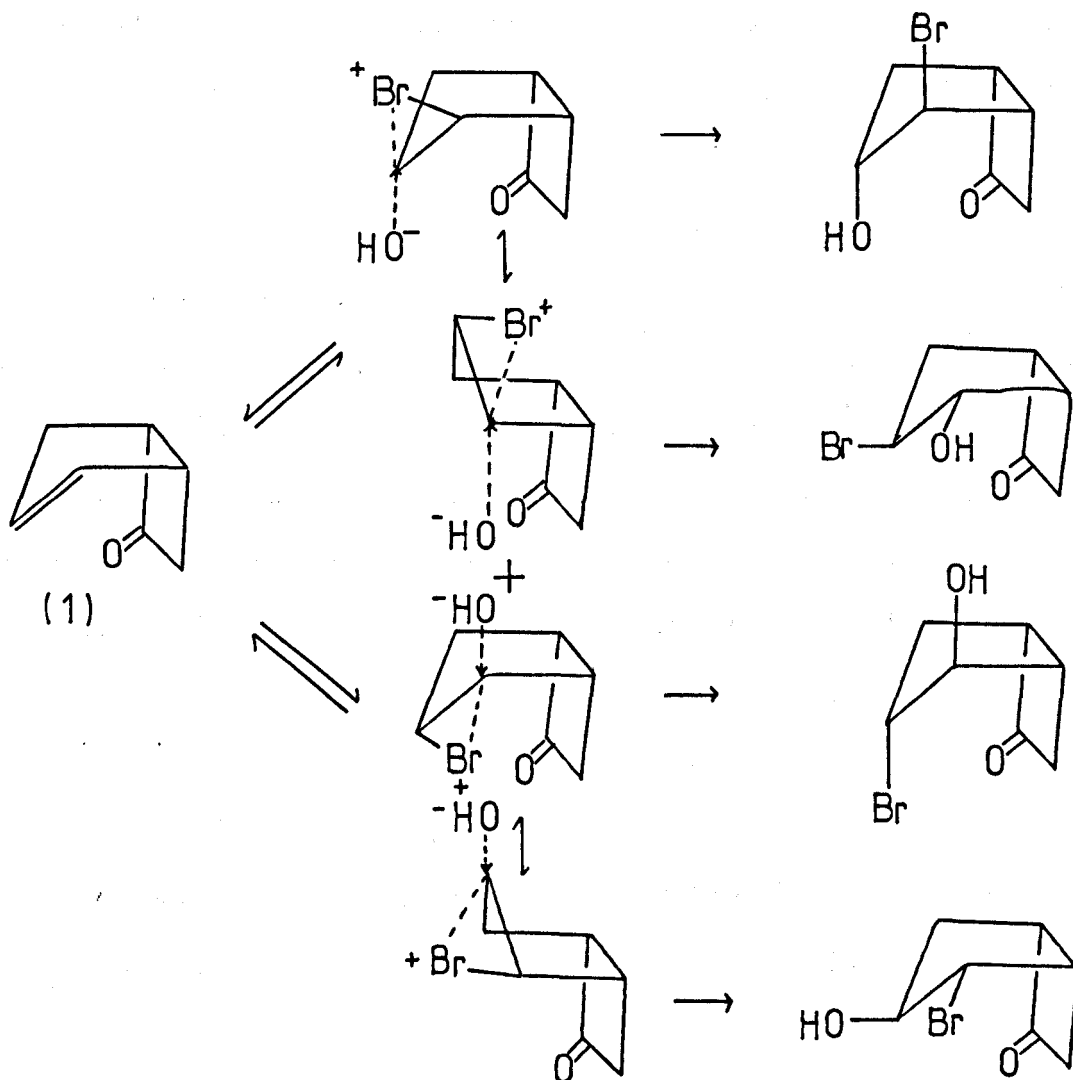
Kcal/mol

(87b)

The published structure appears to have a calculated strain (MM2) of ca. 75 Kcal/mol. We believe that the electron diffraction data has been refined to the incorrect structure.

5.3 Stereoselectivity

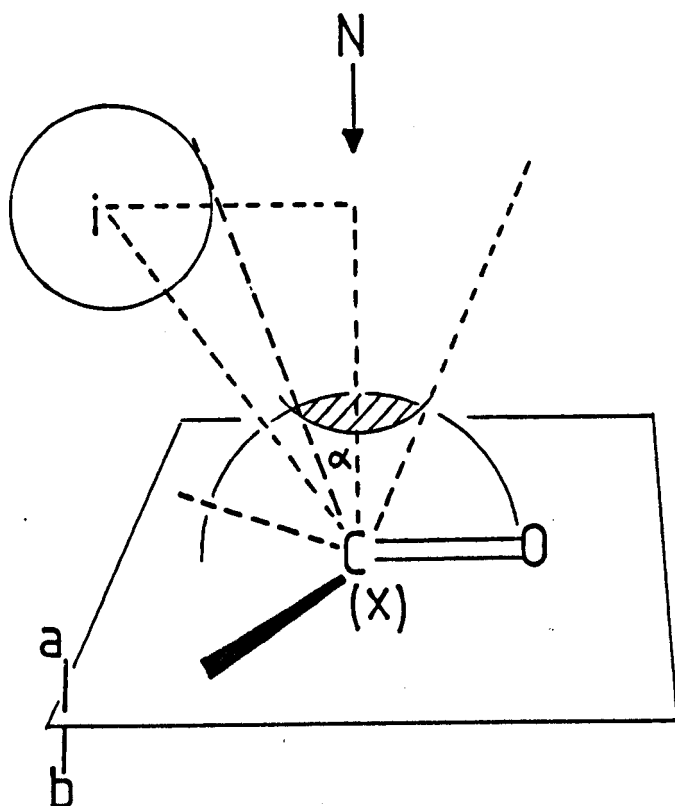
Bromohydrin of (1) is assumed to take place via reversible bromonium ion formation, both exo- and endo-bromonium ions being formed. Each ion can then be attacked by OH^- at either the 2- or 3-position, giving two pairs of isomers.



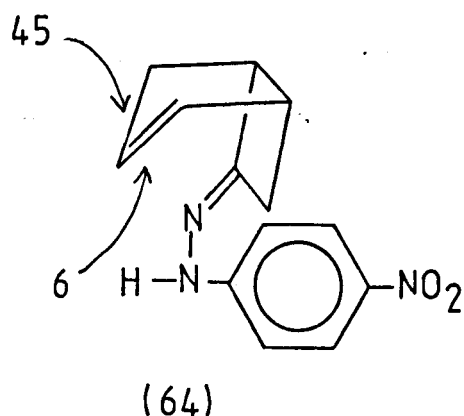
All four bromohydrin isomers have been isolated and characterised (Chapter 2). From the product ratios one can estimate the ratio of exo- to endo-bromonium ion if it is assumed that OH^- attack is equally rapid on either ion. This is supported by the exo:endo ratio in a very similar reaction, the epoxidation of spiro{bicyclo[3.2.0]hept-2-ene-6,2' (1,3) dioxolan} (54) by meta-chloroperoxybenzoic acid where the epoxide formed is a model for the bromonium ion and where the same steric factors might be expected to hold.

The steric congestion about the double bond in (1) can be estimated by Wipke's algorithm^{37,38}. In this calculation (Fig. 5.3, after Wipke et al.³⁸), the accessibility of atom x on side a with respect to electrophilic attack by atom N is determined by each hindering atom i. The cone of preferred approach for each atom is calculated and intersection of this cone with a sphere of unit radius defines a spherical cross section of preferred approach. The solid angle α is equated with the accessibility on side a. A corrective term is included in the calculation to take into account non-bonded repulsion³⁸. The results are summed for all the atoms on one side of the double bond. The reciprocal of the accessibility is the congestion. This is repeated for the other side of the double bond and the results for each side may be compared to predict the favoured side for electrophilic approach.

In this calculation, the coordinates for the crystal structure (64) were used as a model for (1)³⁹ and electrophilic attack was simulated on the mid-point of the C(2)-C(3) bond.

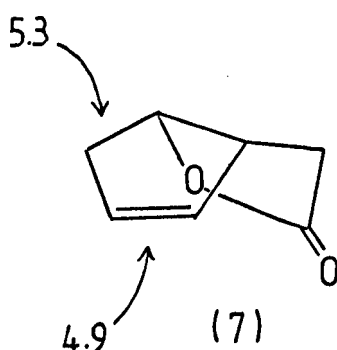
Fig 5,3Figure 5.3

The cone of preferred approach for each atom is calculated (after Wipke et al.¹⁷) and intersection of this cone with a sphere of unit radius defines a spherical cross section of preferred approach. The solid angle α is equated with the accessibility on side a. A corrective term is included in the calculation to take into account non-bonded repulsion¹⁷. The results are summed for all the atoms on one side of the double bond ('a' in this case). The reciprocal of the accessibility is the congestion.



The ratio of the congestion for exo- and endo- attack is 45:6 (exo:endo). This agrees well with the experimental ratios observed on bromonium ion formation (91:9) and epoxide formation (91:9). It appears that steric crowding is of paramount importance in controlling the stereoselectivity.

The reason for the difference in stereoselectivity in (1), which displays high stereoselectivity on bromonium ion formation (91:9, exo:endo) compared to (7),



which displays no stereoselectivity on bromonium ion formation⁴⁰ (1:1, exo:endo) can be explained on purely steric congestion. For (7) the calculated congestion, using the minimised structure predicted by molecular-mechanics, is 4.9 : 5.3 (endo:exo). This agrees well with the experimental results.

The possibility that a bent double bond (Chapter 1)

could enhance the stereoselectivity observed in (1) appeared possible. The crystal structure (64) appears to show a deformation of the double bond of ca. 4° (from improper torsion angles about the double bond). Unfortunately, the experimental error in the hydrogen positions makes any conclusion here unreliable.

5.4 Regioselectivity

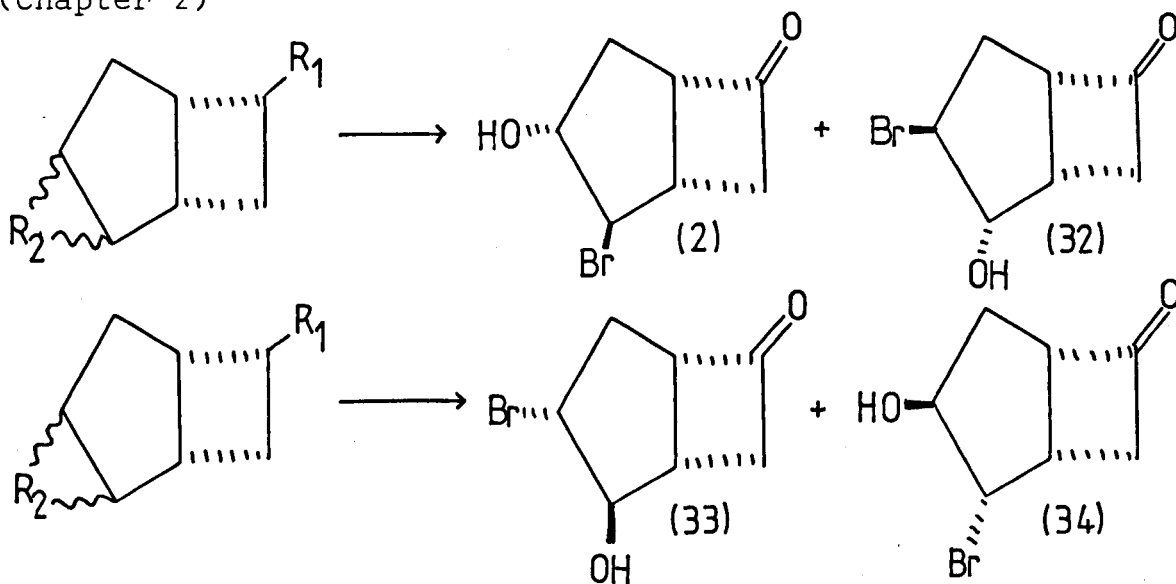
The regiochemical reactions of bicyclo[3.2.0]heptane derivatives can be explained if the geometry of the transition state is fairly similar to that of the major product. Using this approach, the results from X-ray analysis and force-field calculations of reactant and product like molecules can indicate the preferred conformation of the transition state, assuming least conformational change during the course of the reaction⁴⁷.

The protonated endo-epoxide and endo-bromonium ion can be attacked by nucleophile at C(2) or C(3). Attack at C(2) requires that the molecule take up the endo-envelope conformation while attack at C(3) requires the exo-twist conformation. This rationale assumes that attack by nucleophile occurs in a trans fashion with an approximate antiperiplanar geometry for the reactants. Force-field calculations on a number of substituted bicyclo[3.2.0]heptane derivatives indicate that the endo-envelope

Table 5.1

Product ratios of the ring opening of bicyclo[3.2.0]-
heptane-2,3-epoxides and the analogous bromonium ions.

(Chapter 2)



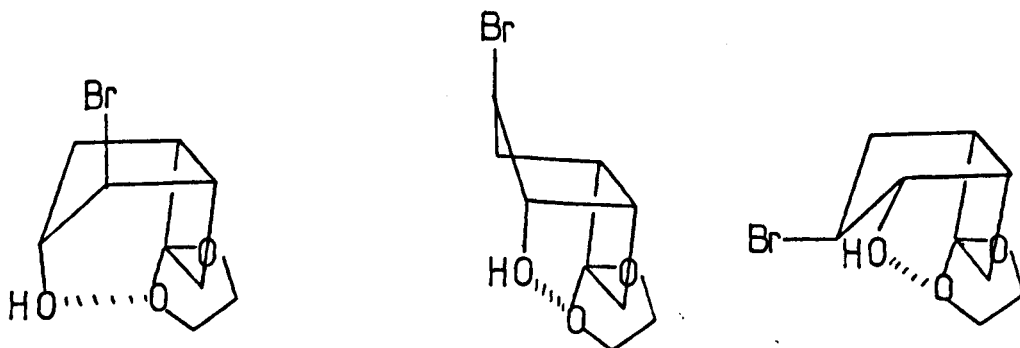
R ₁	Reagent	R ₂	Ratio
<u>Endo</u> epoxides			(2) : (32)
(a) =0	HBr	0	82 : 18
(b) OCH ₂ CH ₂ O	HBr	0	60 : 40
<u>Endo</u> bromonium ion			
(c) =0	HBr	Br ⁺	56 : 44
<u>Exo</u> epoxides			(33) : (34)
(d) =0	HBr	0	98 : 2
(e) OCH ₂ CH ₂ O	HBr	0	95 : 5
<u>Exo</u> bromonium ion			
(f) =0	HBr	Br ⁺	99 : 1

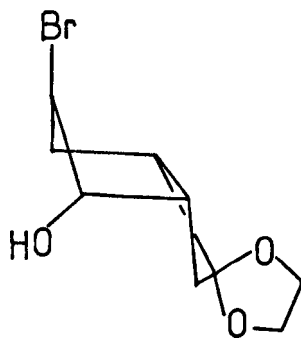
conformation is preferred. Also, the bromohydrin (3), the major product of addition of the elements HBr to (1), has an endo-envelope conformation.

From the results of opening bicyclo[3.2.0]heptane epoxides and bromonium ions by HBr (Chapter 2) (Table 5.1), the regioselectivity varies, particularly between the opening of the exo- and endo 3-membered rings.

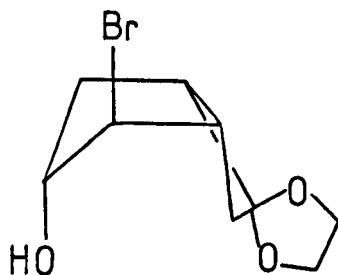
The ketones (a) and (d) display very constant product ratios on opening the epoxide with HBr despite variations of solvent and temperature (Chapter 2). The endo-bromonium ion opening is approximate due to the very small amount of material isolated. The reaction is more complex in the case of the ketals since the acid also opens the ketal ring. The final product ratio is based on the ketones. It appears, by monitoring the reaction by t.l.c., i.r. and n.m.r. spectroscopy that the epoxide ring opens first, but results from ketals must be only approximate.

The opening of the endo-epoxy ketals could be influenced by hydrogen-bonding (Chapter 1). There is the possibility of hydrogen-bonding between a 3-endo-hydroxyl group and the endo-ketal oxygen provided that the cyclopentane-ring is in an endo-envelope conformation. Also, a 2-endo-hydroxy group and the endo-ketal oxygen can form a hydrogen-bond if the cyclopentane ring is the exo-twist or endo conformations.



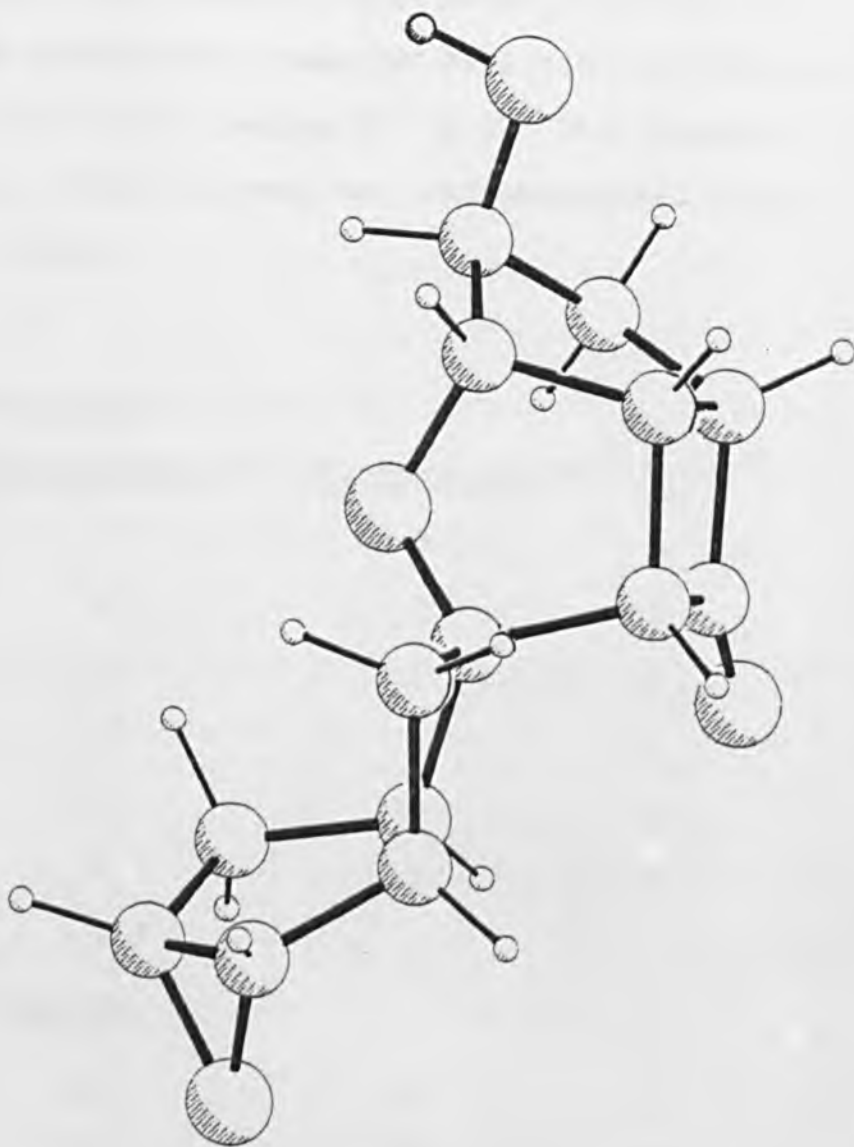


Both these cases require that the 4-membered ring is not in the twist-conformation with the ketal group directed exo.



However, force-field calculations suggest that the 4-membered ring is twisted, τ C(7)-C(1)-C(5)-C(6) = -10° and that the ketal group takes up a pseudo-equatorial position. If the cyclobutane ring is twisted in the opposite sense, orienting the ketal in a pseudo-axial conformation, τ C(7)-C(1)-C(5)-C(6) = 9° , requires ca. 0.7 Kcal/mol (MM2).

With the ketal in a pseudo-equatorial conformation hydrogen-bonding is not possible. In confirmation of a pseudo-equatorial conformation, (58), which is a model for the exo-epoxy ketal clearly shows that the cyclobutane ring is twisted ($|\tau| = 17^\circ$) and that the model ketal takes up a pseudo-equatorial position (Figure 5.4). The energy gained by hydrogen-bonding may be sufficient to overcome the tendency of the ketal to take up a pseudo-equatorial position and this could be important in promotion of the 2-exo-3-endo product in the transition state.

Fig 5,4Figure 5.4

The structure of (58), a model for the *exo*-epoxyketal showing the twist in the cyclobutane ring ($|\tau| = 17^\circ$) and the pseudo-equatorial position of the model ketal.

From five crystal structures of reactant-like and product-like molecules, the torsion angle about C(1)-C(5) in the cyclopentane and cyclobutane rings is very similar (Table 5.2). Over a range of torsion angles 0° to 17° the standard deviation is 2° , i.e. there is excellent conformational transmission between the rings.

TABLE 5.2

Bicyclo[3.2.0]heptane system

<u>Structure</u>	<u>Cyclopentane ($^\circ$)</u>	<u>Cyclobutane ($^\circ$)</u>	<u>Δ ($^\circ$)</u>
(3)	3	0	3
(29a)	6	7	1
(58)	16	17	2
(61)	12	6	6
(64a)	13	11	2
(64b)	8	6	2

$$\sigma_{n-1} = 1.7$$

Bicyclo[3.3.0]octane system

(8)	18	20	2
(60)	21	29	8
(62)	11	14	3
(74a)	5	4	1
(74b)	13	4	9

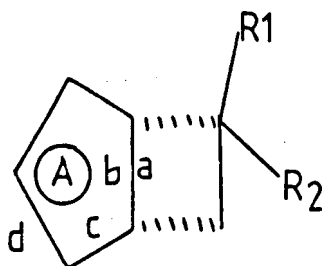
$$\sigma_{n-1} = 3.6.$$

Interestingly, the X-ray structures of bicyclo[3.3.0]-octane derivatives (Table 5.2) indicate lower conformational transmission with a standard deviation of 3.6° between the rings. Bicyclo[3.3.0]octane derivatives also display lower regioselectivity.

Force-field calculations on the ketal (56) and the ketone (77) indicate that the ketone should display greater regioselectivity as indicated by the difference in energy between the endo- and exo-twist conformations. Also, there appears to be a greater energy barrier between the two conformations (endo-envelope and exo-twist) of the ketone (77) than the unsubstituted compound (78). This may be due to the constraints applied to the cyclopentane ring by the cyclobutane ring (which is constrained to be flat) by the ketone. The differences between the exo- and endo-envelope conformers is shown in Table 5.3.

TABLE 5.3

3-exo and 3-endo envelope conformations and energies. Structures (defined by torsion angles ($^{\circ}$)). The last column ($E(\text{endo-exo})$) estimates the difference in steric energy between the 3-endo and 3-exo envelope conformations for each substitution pattern.



R1	R2	Ring A	a	b	c	d	Steric E Kcal/mol	Δ
=O		3- <u>endo</u>	2	1	22	-36	36.20	
=O		3- <u>exo</u>	4	3	-27	41	37.81	1.6
OCH ₂ CH ₂ O		3- <u>endo</u>	-2	0	23	-36	47.49	
OCH ₂ CH ₂ O		3- <u>exo</u>	-17	-16	-10	32	48.00	0.5

Low selectivity thus depends on the ability of the cyclopentane ring to adopt a 3-exo envelope. This conformation is not so easily accessible to 6-ketones in which (as the crystal structures show) the cyclobutane ring is constrained to be nearly flat.

The opening of the exo-bromonium ions and protonated epoxides is even more selective than in the case of the endo-analogues.

The major product on opening the exo-epoxide and exo-bromonium ions probably involves a product-like transition state with a 3-endo-envelope conformation and 2-exo-3-endo-substituents. The minor product requires 2-endo-3-exo-substitution of the less favoured (energetically) 3-exo-envelope.

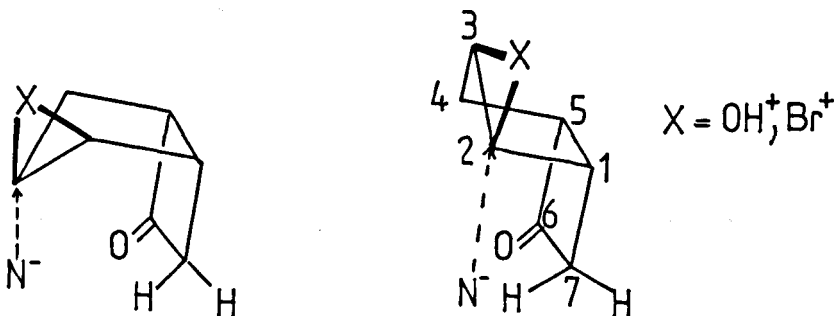
The exo-epoxide fragment is found in the model compound (58) (formed when the exo-epoxyketone (59) undergoes aldol condensation and transannular epoxide opening). The structure of this, determined by X-ray crystallography, is an excellent model for the ketal of (55) (Figure 5.4).

As in cyclopentene epoxide⁴⁶ the cyclopentane ring is in an envelope conformation with the flap (C(5)) endo to the epoxide so that τ C(2)-C(1)-C(5)-C(4) = -15° . In the endo-epoxy derivative of bicyclo[3.2.0]heptene (61) the flap is still endo to the epoxide, i.e. τ C(2)-C(1)-C(5)-C(4) = $+12^\circ$. Force-field calculations suggest that in the 3-endo-envelope conformation of the major product (and transition state) this torsion angle is about -2° (ketone) to -4° (unsubstituted 6-position).

Thus for the exo-epoxides and bromonium ions the starting geometry is closer to the transition state (for the major product) than for the endo-epoxide and bromonium ions hence favouring the 2-exo-3-endo product.

As well as product development control, steric control is present. In the exo-twist conformation, H(7)endo obstructs attack at C(2) and there is also an unfavourable torsional interaction between the attacking moiety and the

C(1)-C(7) bond.



This relative favouring of the 2-exo-3-endo pathway in the exo-epoxide/bromonium ion system leads to the greater regioselectivity observed.

APPENDIX A: Molecular mechanics^{1,2,3}

There are a large number of experimental methods available today for the elucidation of molecular structure. These include X-ray crystallography, electron diffraction, microwave, vibrational and n.m.r. spectroscopy. Of these methods, X-ray crystallography is undoubtedly the most useful in determining geometry and conformation. However, crystals of the compound of interest may be impossible to obtain and the structure elucidated relates to the molecule(s) in the crystalline state and not in solution or the gas phase which are the states of most interest when considering chemical reactivity.

A number of calculational procedures have been developed to provide knowledge of molecular states not directly observable by experiment. The most accurate of these methods are those based on quantum mechanics. However, even approximate solutions of the Schrödinger equation are voracious users of computer time.

The quantum approach essentially involves assuming or fixing the positions of the nuclei and establishing the electronic configuration (using the Born-Oppenheimer approximation). The force-field method (or molecular mechanics or Westheimer method) considers the nuclear positions but does not consider the electronic configurations explicitly (but attempts to take them into account).

The fundamental idea behind the force-field is to use the large mass of data available on small molecules to

predict the structure and energy of more complex molecules. This presupposes that sufficient data on the class of compound of interest are currently available.

In the molecular mechanics model a molecule is described as a collection of masses held together by simple harmonic or elastic forces. Deformation of the molecule will result in strains being set up. These strains may be calculated if the necessary force laws and constants are known.

Using the available data on the class of molecule of interest, the force laws may be chosen intuitively and the force constants tailored to reproduce the basis set of molecules as accurately as possible in terms of the thermodynamic and structural properties of the molecules (sometimes spectroscopic data are also utilised).

Most force-field programs consists of three major parts:

- (a) a set of equations from which the strain energy of the molecule may be calculated
- (b) a set of force constants (for substitution in (a)) relating to each type of atom in the molecule which configure the force-field for a particular class of compound
- (c) a procedure to vary the geometry of the molecule such that the minimum energy geometry(s) may be found.

In (a), a suitable model based on classical equations which essentially treats the molecule as a set of masses joined by springs is set up.

Bonds and bond angles appear to have particular 'natural' values. If the bond or angle is stretched or bent

from these relaxed values, a certain amount of strain energy is imposed on the molecule. Bond deformation is easily calculated by Hooke's law. Bond angle deformation energy may be calculated in a similar fashion.

$$E_s = \sum \frac{k_s}{2} (\ell - \ell_0)^2$$

$$E_\theta = \sum \frac{k_\theta}{2} (\theta - \theta_0)^2$$

ℓ_0 is the natural bond length

θ_0 is the natural angle

k_s , k_θ are constants.

The bond and angle strain is summed over all the bonds and angles in the molecule. Hooke's law is reasonably accurate only for small deformations, larger deformations require additional anharmonic (usually cubic) terms to be added to the equations. However, the model should be as simple as possible so as the interpretation of the results is not obscured. The constants (k) should be chosen such that they are transferable from one molecule to another.

In addition to stretching and bending, the atoms of the molecule are subject to repulsive and attractive forces from other atoms in the molecule i.e. van der Waals forces. The van der Waals energy is generally calculated as the sum of an attractive (dispersion) and repulsive (kinetic energy) term. This interaction is particularly difficult to emulate¹⁴ (Allinger's early force-field MM1⁴ had a particularly steep potential for hydrogen ('hard' hydrogens). This gave problems with compounds like cyclodecane⁵.)

The potentials used are usually similar to the Hill equation

$$E_{\text{vdw}} = \epsilon \left[-c_1 \left(\frac{r^*}{r} \right)^6 + c_2 \exp(-c_3 r/r^*) \right]$$

The c 's are universal constants, r is the interatomic distance and the energy minimum is at r^* (the sum of the van der Waals radii of the two interacting atoms), ϵ is an energy parameter; or the Lennard-Jones 6-12 potential

$$u(r) = 4\epsilon \left\{ \left(\frac{\sigma}{r} \right)^{12} - \left(\frac{\sigma}{r} \right)^6 \right\}$$

The interactions are summed over all the other atoms in the molecule not directly joined to the atom considered (in some force-fields, 1-3 interactions are not considered). Any intervening electron density is not considered to affect the interaction.

A further contributor to the energy of the molecule is a torsional term, which has a form similar to that for ethane

$$E_{\omega} = \frac{V_0}{2} (1 - \cos 3\omega)$$

V_0 is a force constant and ω is the H-C-C-H dihedral angle. This potential is usually expanded as a Fourier series and summed over all non-terminal bonds

$$E_{\omega} = \Sigma \left[\frac{V_1}{2} (1 + \cos \omega) + \frac{V_2}{2} (1 - \cos 2\omega) + \frac{V_3}{2} (1 + \cos 3\omega) + \dots \right]$$

This type of simple force-field gives an energy for the molecule that is a sum of the various types of interaction

$$E = E_S + E_{\theta} + E_{\text{vdw}} + E_{\omega}$$

Various refinements can be added to improve the accuracy of the force-field. Allinger has added a stretch-bend term⁴

$$E_{s\theta} = k_{s\theta} (l - l_0)(\theta - \theta_0)$$

to take into account the long bonds in cyclobutane.

Onefold and twofold rotational barriers for the torsional energy have been used by Allinger⁶ to resolve the problem of obtaining a sufficiently large gauche-butane interaction while keeping the hydrogens sufficiently small (soft) for good structural predictions.

$$E_{\omega} = \frac{V_1}{2}(1 + \cos\omega) + \frac{V_2}{2}(1 - \cos 2\omega) + \frac{V_3}{2}(1 + \cos 3\omega)$$

The inclusion of charge/charge interactions and dipole/dipole interactions⁷, molecular vibrations¹³ etc. increases the accuracy of the model for some types of compound.

The geometry and energy calculated from the above force-field model for a given set of atomic coordinates would represent a point on the energy hypersurface which would not correspond to a real physical situation (unless one were very lucky). A scheme to minimise the energy of the molecule by varying the geometry (as in (b)) is required since the structure of the molecule will correspond to that geometry where the energy is at a minimum.

If the total energy of the molecule is written

$$E = E_{\text{electronic}} + E_s + E_{\theta} + E_{\text{vdw}} + \text{cross terms, etc.}$$

then the first derivative with respect to each degree of freedom should be equal to zero at each energy minimum. A number of methods of evaluating the energy minimum have been developed.

The steepest descent method⁸ involves calculating an initial trial geometry and then moving each atom in the x, y, and z directions by a test increment where the energy is recalculated. This process is repeated for all the atoms. The atoms are then moved simultaneously in directions which result in a lowering of energy. The amount each atom is moved depends on the reduction in energy obtained by the test increment. This procedure is repeated until there is no appreciable change in energy.

An improvement on the steepest descent method is pattern minimisation². This is similar to the previous method, but information on the direction of motion of the atoms is saved from one iteration to the next. The correction terms calculated from the previous iteration and the latest iteration are summed with the result that the minimisation procedure is accelerated.

If the minimum energy conformation of the molecule is sought, one point worth emphasising is that the starting point on the energy hypersurface must be within the energy well which has as its base the global minimum as neither of the above methods are capable of climbing out of a false minimum.

A more sophisticated procedure for minimisation of molecular geometry is the Newton-Raphson method.

The energy function (with respect to each coordinate) is differentiated. An energy minimum will be found when

$$f'(x^*) = 0$$

if $x + dx$ is a close approximation to a minimum x^* , then

$$f'(x + \delta x) = 0 \text{ and } f'(x + \delta x) = f'(x) + f''(x)\delta x + \dots$$

and using Taylor's expansion and truncating the series after the linear term

$$f'(x) + f''(x)\delta x = 0$$

or
$$\delta x = -f''(x)^{-1}f'(x)$$

this can be written in a more general form

$$\delta x = -\lambda f''(x)^{-1}f'(x)$$

where λ is a scalar called the step length. If x is not a good approximation to the minimum geometry there is the danger that the equation becomes oscillatory or divergent. This may be overcome by setting $0 < \lambda < 1$ in the early part of the minimisation³.

In practice, a combination of second derivative methods, quasi-Newton methods (the Newton iteration with numerical and analytical derivatives) and discrete quasi-Newton methods (setting f'' equal to the diagonal matrix d^2V_s/dx_i^2 ¹⁰, or setting f'' equal to the block diagonal matrix $d^2V_s/dx_j, dx_i; i, j, \geq 3$ for each atom¹⁰) offers the best hope of achieving global minimisation³.

The parameterisation of the force-field (selection of appropriate constants) can proceed in two ways. The constants can be fitted to the available spectroscopic and thermodynamic data by a least squares procedure¹¹. However, this method is not generally used as the surplus of observations over parameters is not large. Trial and error adjustment of the force constants is the most generally used procedure¹².

In recent years, force fields have been developed for many classes of compound. Hydrocarbons (alkanes and alkenes)

have been investigated extensively^{6,2,15} and the approach has been extended to include hetero-atoms (this is rather difficult, especially the torsional interactions between different atom types)^{1,16,2}, conjugated systems¹⁷ (this also is not particularly successful) and intermolecular interactions^{18,19}.

5.5

REFERENCES

1. Allinger, N.L., *Adv.Phys.Org.Chem.*, 1976, 13, p.1.
2. Engler, E.M., Andose, J.D., Schleyer, P. von R.,
J.Am.Chem.Soc., 1973, 95, p.8005.
3. White, D.N.J., *Computers & Chemistry*, 1977, Vol.1, p.225.
4. Wertz, D.H., Allinger, N.L., *Tetrahedron*, 1974, Vol.30,
p.1579.
5. White, D.N.J., Bovill, M.J., *J.Mol.Struct.*, 1976, 33, p.273.
6. Allinger, N.L., *J.Am.Chem.Soc.*, 1977, Vol.99, Number 25,
p.8127.
7. Allinger, N.L., Dosen-Micovic, L., *Tetrahedron*, 1978, 34,
3385.
8. Wiberg, K.B., *J.Am.Chem.Soc.*, 1965, 87, p.1070.
9. Bixon, M., Liffson, S., *Tetrahedron*, 1967, 23, p.769.
10. White, D.N.J., Sim, G.A., *Tetrahedron*, 1973, 29, p.3933.
11. Lifson, S., Warshel, A., *J.Chem.Phys.*, 1968, 49, p.5116.
12. Allinger, N.L., Hirsch, J., Miller, M.A., Tyminski, I.J.,
Van-Catledge, F.A., *J.Am.Chem.Soc.*, 1968, 90, p.1199.
13. Wertz, D.H., Allinger, N.L., *Tetrahedron*, 1979, Vol.35, p.3.
14. Wiberg, K.B., *Computers and Chemistry*, 1977, Vol.1, p.221.
15. White, D.N.J., Boville, M.J., *J.Chem.Soc., Perkin 2*,
1977, p.1610.
16. Bovill, M.J., Chadwick, D.J., Sutherland, I.O.,
J.Chem.Soc., Perkin 2, 1980, p.1529.
17. Allinger, N.L., Sprague, J.T., *J.Am.Chem.Soc.*, 1973, 95,
p.3893.
18. Lifson, S., Hagler, A.T., Dauber, P., *J.Am.Chem.Soc.*,
1979, Vol.101, No. 18, p.5111.

19. *ibid.*, p.5122.
20. Ali, S.M., Lee, T.V., Roberts, S.M., *Synthesis*, 1977, p.155.
21. 'Topics in Stereochemistry', Moriarty, R.M., 1974, Vol.8, p.271. Editors E. L. Eliel, N. L. Allinger, John Wiley & Sons.
22. *Ibid.*, p.286.
23. *Ibid.*, p.291.
24. Wiberg, K.B., *J.Amer.Chem.Soc.*, 1965, 87, p.1070.
25. Miller, F.A., Capwell, R.J., *Spectrochim.Acta.*, 1971, 27a, p.947.
26. Durig, J.R., Lord, R.C., *J.Chem.Phys.*, 1966, 45, p.61.
27. Scharpen, L.H., Laurie, V.W., *J.Chem.Phys.*, 1968, 49, p.221.
28. Allinger, N.L., *J.Am.Chem.Soc.*, 1977, Vol.99, No. 25, p.8127.
29. 'Topics in Stereochemistry', Fuchs, B., 1978, Vol.10, p.1. Editors E. L. Eliel, N. L. Allinger, John Wiley & Sons.
30. *Molecular Structure by Diffraction Methods*, Bohn, R.K., 1977, Vol.5, p.23.
31. Ikeda, T., Lord, R.C., Malloy, T.B., Ueda, T., *J.Chem.Phys.*, 1972, 56, p.1434.
32. Lifson, S., Warshel, A., *J.Chem.Phys.*, 1968, 49, p.5116.
33. Davis, M.I., Mueke, T.W., *J.Phys.Chem.*, 1970, 74, p.1104.
34. Rankin, D.W.H., 'Molecular Structure by Diffraction Methods', 1977, Vol.5, Chapter 1, p.23.
35. Muller, K., *Angew.Chem.Int.Ed.Eng.* 1980, 19, p.1.
36. Chiang, J.F., Bauer, S.H., *J.Am.Chem.Soc.*, 1966, 88:3, p.420.
37. Wipke, W.T., Gund, P., *J.Am.Chem.Soc.*, 1974, Vol.96:1, p.299.
38. Wipke, T.D., Gund, P., *J.Am.Chem.Soc.*, 1976, 98:25, p.8107.
39. Congest calculations performed on 'Video Vector Dynamics Chemical Graphics System', Morrow, C., Chemistry Dept., University of Glasgow.

40. Ali, Mubarcic S., Crossland, N.M., Lee, T.V., Newton, R.F.,
J.Chem.Soc.Perkin 1, 1979, p.122.
41. Dunitz, J.D., 'X-Ray Analysis and the Structure of Organic
Molecules', 1979, Cornell University Press.
42. Ibid., p.431.
43. Allen, F.H., Bellard, S., Brice, M.D., Cartwright, B.A.,
Doubleday, A., Higgs, H., Hummelink, T., Hummelink-Peters,
B.G., Kennard, O., Motherwell, W.D.S., Rogers, J.R.,
Watson, D.G., Acta Cryst., 1979, B35, p.2331.
44. Allinger, N.L., 1980, QCPE program no. 395.
45. Newton, R.F., Howard, C.C., Reynolds, D.P., Wadsworth, A.H.,
J.Chem.Soc.Chem.Comm., 1978, p.662.
46. R. L. Hilderbrandt and J. D. Wieser, J.Mol.Structure,
1974, 22, 247.
47. Toromanoff, E., Tetrahedron, 1980, Vol.36, p.2809.

APPENDIX 12-(S)-exo-bromo-3-(S)-endo-hydroxybicyclo[3.2.0]heptan-6-one(3).

Atomic coordinates

Bond lengths

Bond angles

Torsion angles

Isotropic temperature factors

Anisotropic temperature factors

Structure factors

FRACTIONAL ATOMIC COORDINATES X10000 WITH E.S.D.S. IN BRACKETS

	X/A	Y/B	Z/C	OCCUPANCY
C(1)	10760(14)	3942(13)	4044(20)	
C(2)	9359(10)	2926(10)	5226(13)	
C(3)	8022(12)	2229(12)	3701(16)	
C(4)	8694(13)	1882(16)	1866(19)	
C(5)	10350(17)	5203(14)	1685(21)	
C(6)	10665(12)	4773(13)	1168(21)	
C(7)	11095(17)	5405(15)	3276(22)	
O(3)	7614(11)	3348(10)	3194(15)	
O(6)	10575(13)	5273(10)	-0402(15)	
BR(1)	-1253(1)	-1891(1)	00000	
H(1A)	11520(129)	3715(115)	4067(173)	
H(2A)	9082(74)	3665(81)	6468(123)	
H(3A)	7056(84)	1186(84)	4271(122)	
H(3B)	7004(122)	3073(140)	2760(179)	
H(4A)	4372(84)	1965(78)	0585(136)	
H(4B)	3347(92)	0660(107)	2523(155)	
H(5A)	10851(87)	2915(91)	1542(131)	
H(7A)	11953(118)	6133(106)	3424(150)	
H(7B)	10612(116)	5889(109)	3874(162)	

BOND DISTANCES (Å) WITH E.S.D.S IN BRACKETS

C(1)	- C(2)	1.489(14)
C(1)	- C(5)	1.547(16)
C(1)	- C(7)	1.532(16)
C(2)	- C(3)	1.539(12)
C(3)	- C(4)	1.523(13)
C(3)	- O(3)	1.429(12)
C(4)	- C(5)	1.524(19)
C(5)	- C(6)	1.528(15)
C(6)	- C(7)	1.513(18)
C(6)	- O(6)	1.185(13)
Br(1)	- C(2)	1.955(10)

BOND ANGLES (DEGREES) WITH E.S.D.S IN BRACKETS

C(5)	- C(1)	- C(2)	104.4(10)
C(7)	- C(1)	- C(2)	117.8(11)
C(7)	- C(1)	- C(5)	89.6(4)
C(3)	- C(2)	- C(1)	106.4(10)
C(4)	- C(3)	- C(2)	104.5(8)
O(3)	- C(3)	- C(2)	108.7(8)
O(3)	- C(3)	- C(4)	109.5(9)
C(5)	- C(4)	- C(3)	101.9(10)
C(4)	- C(5)	- C(1)	109.3(11)
C(6)	- C(5)	- C(1)	89.2(10)
C(6)	- C(5)	- C(4)	119.3(11)
C(7)	- C(6)	- C(5)	91.0(10)
O(6)	- C(6)	- C(5)	134.1(12)
O(6)	- C(6)	- C(7)	134.8(11)
C(6)	- C(7)	- C(1)	90.3(10)
Br(1)	- C(2)	- C(1)	111.9(10)
Br(1)	- C(2)	- C(3)	108.0(10)

TORSION ANGLES (DEGREES)

E.s.d's ca. 1.5°

C5 C1 C2 C3	-19.2
C5 C1 C2 BR1	97.9
C7 C1 C2 C3	78.0
C7 C1 C2 BR1	-164.7
C2 C1 C5 C4	-2.6
C2 C1 C5 C6	116.9
C7 C1 C5 C4	-119.8
C7 C1 C5 C6	0.0
C2 C1 C7 C6	-106.5
C5 C1 C7 C6	0.0
C1 C2 C3 C4	34.1
C1 C2 C3 O3	-82.7
BR1 C2 C3 C4	-84.4
BR1 C2 C3 O3	158.5
C2 C3 C4 C5	-34.4
O3 C3 C4 C5	83.6
C3 C4 C5 C1	22.7
C3 C4 C5 C6	-76.9
C1 C5 C6 C7	0.0
C1 C5 C6 O6	-177.9
C4 C5 C6 C7	111.7
C4 C5 C6 O6	-66.3
C5 C6 C7 C1	0.0
O6 C6 C7 C1	177.9

ISOTROPIC PARAMETERS X10000 WITH E.S.O.S IN BRACKETS
 THE EXPRESSION FOR THE TEMPERATURE FACTOR IS
 $\text{EXP}(-2*\text{PI}*\text{PI}*U11*\text{SIN}^2\text{THETA}/\text{LAMBDA}^2)$

H(1A) 0028(402)
 H(2A) 0124(221)
 H(3A) 0167(211)
 H(30) 0335(556)
 H(4A) 0001(231)
 H(4B) 0583(251)
 H(5A) 0019(257)
 H(7A) 0269(328)
 H(7B) 0420(407)

ANISOTROPIC THERMAL PARAMETERS X10000 WITH E.S.O.S IN BRACKETS
 THE EXPRESSION FOR THE TEMPERATURE FACTOR IS $\text{EXP}(-2*\text{PI}*\text{PI}*(\text{H}*\text{H}*\text{ASTAR}*\text{ASTAR}*\text{U11} +$
 $+2*\text{K}*\text{L}*\text{BSIAR}*\text{CSTAR}*\text{U25}))$

	U11	U22	U33	U23	U13	U12
C(1)	0315(71)	0411(68)	0547(88)	-0021(62)	-0095(65)	0190(56)
C(2)	0547(61)	0262(59)	0387(69)	-0024(55)	0015(59)	0095(52)
C(3)	0547(63)	0353(62)	0379(71)	0001(56)	-0056(55)	0215(57)
C(4)	0270(71)	0590(97)	0255(74)	-0068(63)	0022(53)	0177(54)
C(5)	0489(85)	0460(79)	0519(105)	0158(68)	0191(76)	0327(69)
C(6)	0525(71)	0513(96)	0626(106)	0081(75)	-0032(65)	0213(65)
C(7)	0355(82)	0290(73)	0662(115)	0041(77)	-0039(77)	-0004(69)
C(8)	0341(50)	0552(59)	0297(53)	-0134(40)	-0133(46)	0264(44)
C(6)	1275(95)	0675(71)	0528(70)	0118(55)	-0261(63)	0535(69)
BR(1)	0471(8)	0424(7)	0595(5)	-0032(8)	-0091(8)	0153(8)

7,8-endo-epoxy-2-oxatricyclo[3.3.0.0^{4,6}]octan-3-one (60).³¹

Atomic coordinates

Bond lengths

Bond angles

Torsion angles

Isotropic temperature factors

Anisotropic temperature factors

Structure factors

Atom	x	y	z
O1	0.0000	0.0000	0.0000
O2	0.0000	0.0000	0.0000
O3	0.0000	0.0000	0.0000
O4	0.0000	0.0000	0.0000
O5	0.0000	0.0000	0.0000
O6	0.0000	0.0000	0.0000
O7	0.0000	0.0000	0.0000
O8	0.0000	0.0000	0.0000
O9	0.0000	0.0000	0.0000
O10	0.0000	0.0000	0.0000
O11	0.0000	0.0000	0.0000
O12	0.0000	0.0000	0.0000
O13	0.0000	0.0000	0.0000
O14	0.0000	0.0000	0.0000
O15	0.0000	0.0000	0.0000
O16	0.0000	0.0000	0.0000
O17	0.0000	0.0000	0.0000
O18	0.0000	0.0000	0.0000
O19	0.0000	0.0000	0.0000
O20	0.0000	0.0000	0.0000
O21	0.0000	0.0000	0.0000
O22	0.0000	0.0000	0.0000
O23	0.0000	0.0000	0.0000
O24	0.0000	0.0000	0.0000
O25	0.0000	0.0000	0.0000
O26	0.0000	0.0000	0.0000
O27	0.0000	0.0000	0.0000
O28	0.0000	0.0000	0.0000
O29	0.0000	0.0000	0.0000
O30	0.0000	0.0000	0.0000
O31	0.0000	0.0000	0.0000
O32	0.0000	0.0000	0.0000
O33	0.0000	0.0000	0.0000
O34	0.0000	0.0000	0.0000
O35	0.0000	0.0000	0.0000
O36	0.0000	0.0000	0.0000
O37	0.0000	0.0000	0.0000
O38	0.0000	0.0000	0.0000
O39	0.0000	0.0000	0.0000
O40	0.0000	0.0000	0.0000
O41	0.0000	0.0000	0.0000
O42	0.0000	0.0000	0.0000
O43	0.0000	0.0000	0.0000
O44	0.0000	0.0000	0.0000
O45	0.0000	0.0000	0.0000
O46	0.0000	0.0000	0.0000
O47	0.0000	0.0000	0.0000
O48	0.0000	0.0000	0.0000
O49	0.0000	0.0000	0.0000
O50	0.0000	0.0000	0.0000
O51	0.0000	0.0000	0.0000
O52	0.0000	0.0000	0.0000
O53	0.0000	0.0000	0.0000
O54	0.0000	0.0000	0.0000
O55	0.0000	0.0000	0.0000
O56	0.0000	0.0000	0.0000
O57	0.0000	0.0000	0.0000
O58	0.0000	0.0000	0.0000
O59	0.0000	0.0000	0.0000
O60	0.0000	0.0000	0.0000

BOND LENGTHS (Å) WITH U.S.G. V.S. IN BRATRATS

Atom 1	Atom 2	Distance (Å)
O1	O2	1.20(1)
O1	O3	1.20(1)
O1	O4	1.20(1)
O1	O5	1.20(1)
O1	O6	1.20(1)
O1	O7	1.20(1)
O1	O8	1.20(1)
O1	O9	1.20(1)
O1	O10	1.20(1)
O1	O11	1.20(1)
O1	O12	1.20(1)
O1	O13	1.20(1)
O1	O14	1.20(1)
O1	O15	1.20(1)
O1	O16	1.20(1)
O1	O17	1.20(1)
O1	O18	1.20(1)
O1	O19	1.20(1)
O1	O20	1.20(1)
O1	O21	1.20(1)
O1	O22	1.20(1)
O1	O23	1.20(1)
O1	O24	1.20(1)
O1	O25	1.20(1)
O1	O26	1.20(1)
O1	O27	1.20(1)
O1	O28	1.20(1)
O1	O29	1.20(1)
O1	O30	1.20(1)
O1	O31	1.20(1)
O1	O32	1.20(1)
O1	O33	1.20(1)
O1	O34	1.20(1)
O1	O35	1.20(1)
O1	O36	1.20(1)
O1	O37	1.20(1)
O1	O38	1.20(1)
O1	O39	1.20(1)
O1	O40	1.20(1)
O1	O41	1.20(1)
O1	O42	1.20(1)
O1	O43	1.20(1)
O1	O44	1.20(1)
O1	O45	1.20(1)
O1	O46	1.20(1)
O1	O47	1.20(1)
O1	O48	1.20(1)
O1	O49	1.20(1)
O1	O50	1.20(1)
O1	O51	1.20(1)
O1	O52	1.20(1)
O1	O53	1.20(1)
O1	O54	1.20(1)
O1	O55	1.20(1)
O1	O56	1.20(1)
O1	O57	1.20(1)
O1	O58	1.20(1)
O1	O59	1.20(1)
O1	O60	1.20(1)

BOND ANGLES (DEGREES) WITH U.S.G. V.S. IN BRATRATS

Atom 1	Atom 2	Atom 3	Angle (degrees)
O1	O2	O3	120.0
O1	O2	O4	120.0
O1	O2	O5	120.0
O1	O2	O6	120.0
O1	O2	O7	120.0
O1	O2	O8	120.0
O1	O2	O9	120.0
O1	O2	O10	120.0
O1	O2	O11	120.0
O1	O2	O12	120.0
O1	O2	O13	120.0
O1	O2	O14	120.0
O1	O2	O15	120.0
O1	O2	O16	120.0
O1	O2	O17	120.0
O1	O2	O18	120.0
O1	O2	O19	120.0
O1	O2	O20	120.0
O1	O2	O21	120.0
O1	O2	O22	120.0
O1	O2	O23	120.0
O1	O2	O24	120.0
O1	O2	O25	120.0
O1	O2	O26	120.0
O1	O2	O27	120.0
O1	O2	O28	120.0
O1	O2	O29	120.0
O1	O2	O30	120.0
O1	O2	O31	120.0
O1	O2	O32	120.0
O1	O2	O33	120.0
O1	O2	O34	120.0
O1	O2	O35	120.0
O1	O2	O36	120.0
O1	O2	O37	120.0
O1	O2	O38	120.0
O1	O2	O39	120.0
O1	O2	O40	120.0
O1	O2	O41	120.0
O1	O2	O42	120.0
O1	O2	O43	120.0
O1	O2	O44	120.0
O1	O2	O45	120.0
O1	O2	O46	120.0
O1	O2	O47	120.0
O1	O2	O48	120.0
O1	O2	O49	120.0
O1	O2	O50	120.0
O1	O2	O51	120.0
O1	O2	O52	120.0
O1	O2	O53	120.0
O1	O2	O54	120.0
O1	O2	O55	120.0
O1	O2	O56	120.0
O1	O2	O57	120.0
O1	O2	O58	120.0
O1	O2	O59	120.0
O1	O2	O60	120.0

FRACTIONAL ATOMIC COORDINATES X10000 WITH E.S.D.S. IN BRACKET

	X/A	Y/B	Z/C	OCCUPANCY
C(1)	3457(2)	1263(2)	4286(2)	
C(3)	5460(2)	1127(2)	1946(2)	
C(4)	3561(2)	0193(2)	2103(2)	
C(5)	2533(3)	0010(2)	3655(2)	
C(6)	1213(2)	0650(2)	2750(2)	
C(7)	0686(2)	2124(2)	3224(2)	
C(8)	1972(2)	2503(2)	4199(2)	
O(2)	5551(2)	1542(1)	3315(1)	
O(9)	6901(2)	1404(1)	0970(1)	
O(10)	2469(2)	3098(1)	2782(1)	
H(1A)	3747(31)	1094(21)	5217(22)	
H(4A)	3739(31)	-0580(19)	1463(19)	
H(5A)	2239(32)	-0878(22)	4115(21)	
H(6A)	0164(34)	0150(21)	2464(21)	
H(7A)	-0710(34)	2502(22)	3237(19)	
H(8A)	1498(34)	3143(23)	5009(23)	

BOND DISTANCES (Å) WITH E.S.D.S IN BRACKETS

C(1)	-	C(5)	1.533(2)
C(1)	-	C(8)	1.534(2)
C(1)	-	O(2)	1.446(2)
C(3)	-	C(4)	1.486(2)
C(3)	-	O(2)	1.357(2)
C(3)	-	O(9)	1.198(2)
C(4)	-	C(5)	1.492(2)
C(4)	-	C(6)	1.529(2)
C(5)	-	C(6)	1.494(2)
C(6)	-	C(7)	1.496(2)
C(7)	-	C(8)	1.448(2)
C(7)	-	O(10)	1.446(2)
C(8)	-	O(10)	1.448(2)

BOND ANGLES (DEGREES) WITH E.S.D.S IN BRACKETS

C(8)	-	C(1)	-	C(5)	106.2(1)
O(2)	-	C(1)	-	C(5)	105.5(1)
O(2)	-	C(1)	-	C(8)	107.3(1)
O(2)	-	C(3)	-	C(4)	110.0(1)
O(9)	-	C(3)	-	C(4)	128.8(1)
O(9)	-	C(3)	-	O(2)	120.8(1)
C(5)	-	C(4)	-	C(3)	106.2(1)
C(6)	-	C(4)	-	C(3)	123.2(1)
C(6)	-	C(4)	-	C(5)	59.3(1)
C(4)	-	C(5)	-	C(1)	101.4(1)
C(6)	-	C(5)	-	C(1)	104.2(1)
C(6)	-	C(5)	-	C(4)	61.6(1)
C(5)	-	C(6)	-	C(4)	59.1(1)
C(7)	-	C(6)	-	C(4)	121.0(1)
C(7)	-	C(6)	-	C(5)	108.8(1)
C(8)	-	C(7)	-	C(6)	108.5(1)
O(10)	-	C(7)	-	C(6)	114.9(1)
O(10)	-	C(7)	-	C(8)	60.0(1)
C(7)	-	C(8)	-	C(1)	107.6(1)
O(10)	-	C(8)	-	C(1)	111.7(1)
O(10)	-	C(8)	-	C(7)	59.9(1)
C(3)	-	O(2)	-	C(1)	107.9(1)
C(8)	-	O(10)	-	C(7)	60.0(1)

TORSION ANGLES (DEGREES)

E.s.d's ca. 1.5°

C8	C1	C5	C4	84.7
C8	C1	C5	C6	21.4
O2	C1	C5	C4	-28.9
O2	C1	C5	C6	-92.2
C5	C1	C8	C7	-15.5
C5	C1	C8	O10	-79.4
O2	C1	C8	C7	96.9
O2	C1	C8	O10	33.0
C5	C1	O2	C3	28.8
C8	C1	O2	C3	-84.1
O2	C3	C4	C5	-2.9
O2	C3	C4	C6	60.6
O9	C3	C4	C5	169.2
O9	C3	C4	C6	-127.1
C4	C3	O2	C1	-16.3
O9	C3	O2	C1	170.7
C3	C4	C5	C1	19.3
C3	C4	C5	C6	119.3
C6	C4	C5	C1	-100.0
C3	C4	C6	C5	-89.9
C3	C4	C6	C7	4.3
C5	C4	C6	C7	94.5
C1	C5	C6	C4	95.5
C1	C5	C6	C7	-19.9
C4	C5	C6	C7	-115.4
C4	C6	C7	C8	-53.8
C4	C6	C7	O10	10.9
C5	C6	C7	C8	10.8
C5	C6	C7	O10	75.6
C6	C7	C8	C1	3.2
C6	C7	C8	O10	108.6
O10	C7	C8	C1	-105.3
C6	C7	O10	C8	-97.8
C1	C8	O10	C7	98.3

ISOTROPIC PARAMETERS X10000 WITH E.S.D.S IN BRACKETS
 THE EXPRESSION FOR THE TEMPERATURE FACTOR IS
 $\exp(-\delta \cdot \pi \cdot \pi \cdot U_{11} \cdot \sin^2 \theta / \lambda^2)$

H(1A) 0478(52)
 H(4A) 0597(47)
 H(5A) 0506(56)
 H(6A) 0466(50)
 H(7A) 0513(55)
 H(8A) 0564(57)

ANISOTROPIC THERMAL PARAMETERS X10000 WITH E.S.D.S IN BRACKETS
 THE EXPRESSION FOR THE TEMPERATURE FACTOR IS $\exp(-2 \cdot \pi \cdot \pi \cdot (H \cdot H \cdot A^* \cdot A^* \cdot U_{11} +$
 $+ 2 \cdot K \cdot L \cdot B^* \cdot C^* \cdot U_{23}))$

	U11	U22	U33	U23	U13	U12
C(1)	0543(8)	0472(10)	0250(7)	0025(6)	-0075(6)	0060(7)
C(3)	0275(6)	0265(8)	0537(7)	-0004(6)	-0042(5)	0006(6)
C(4)	0518(7)	0250(8)	0554(8)	-0046(6)	-0065(6)	-0015(6)
C(5)	0538(7)	0269(8)	0416(8)	0109(7)	-0020(6)	0011(6)
C(6)	0270(7)	0311(9)	0470(9)	0001(7)	-0112(6)	-0061(6)
C(7)	0245(7)	0317(9)	0470(9)	0037(7)	-0081(6)	0017(6)
C(8)	0572(8)	0354(9)	0524(8)	-0066(7)	-0040(6)	0048(7)
O(2)	0258(5)	0475(7)	0586(6)	-0057(5)	-0117(4)	-0002(4)
O(9)	0598(6)	0504(8)	0453(7)	0001(6)	0082(5)	-0080(6)
O(10)	0565(6)	0267(6)	0429(6)	0042(5)	-0105(5)	-0021(4)

H	K	L	FO	FC	H	K	L	FO	FC	H	K	L	FO	FC	H	K	L	FO	FC	H	K	L	FO	FC
2	5	11	4	3	2	7	11	2	-3	5	1	12	2	2	3	3	12	2	2	3	5	12	3	3
3	5	11	2	-2	-1	0	12	3	4	6	1	12	4	-4	0	4	12	2	-2	2	6	12	6	5
5	5	11	3	3	0	0	12	2	2	-2	2	12	2	2	1	4	12	2	2	0	1	13	3	-3
-1	6	11	2	1	1	0	12	4	-3	0	2	12	5	-5	3	4	12	3	-3	1	1	13	6	5
1	6	11	2	1	3	0	12	2	2	0	3	12	4	-4	4	4	12	4	4	2	1	13	3	-4
2	6	11	3	3	5	0	12	3	3	1	3	12	3	3	4	4	12	3	-2	3	1	13	2	0
3	6	11	4	-4	-2	1	12	4	4	2	3	12	2	1	1	3	12	3	-3	4	1	13	3	3
4	6	11	4	4	-1	1	12	3	3	4	3	12	2	2	3	3	12	3	-3	2	3	13	3	2
5	6	11	3	3	0	1	12	5	-5															

1/2 1/2 1/2 OCCUPANCY

C(1)	2,3-endo-epoxybicyclo[3.2.0]heptan-6-one-p-nitrophenyl-		
C(2)	<u>hydrazone (61).</u>		
C(3)		0005121	-0017121
C(4)		0009121	-0009121
C(5)		0151121	0071121
C(6)	Atomic coordinates	0166121	0039121
C(7)	Bond lengths	0039121	0019121
C(8)	Bond angles	0079121	0066121
C(9)	Torsion angles	0079121	0162121
C(10)	Isotropic temperature factors		0006121
C(11)	Anisotropic temperature factors		0018121
C(12)	Structure factors	0000121	0000121
C(13)		0000121	0000121
C(14)		0000121	-0000121
C(15)		0000121	0000121
C(16)		0000121	0000121
C(17)		0000121	0000121
C(18)		0000121	0000121
C(19)		0000121	0000121
C(20)		0000121	0000121
C(21)		0000121	0000121
C(22)		0000121	0000121
C(23)		0000121	0000121
C(24)		0000121	0000121
C(25)		0000121	0000121
C(26)		0000121	0000121
C(27)		0000121	0000121
C(28)		0000121	0000121
C(29)		0000121	0000121
C(30)		0000121	0000121
C(31)		0000121	0000121
C(32)		0000121	0000121
C(33)		0000121	0000121
C(34)		0000121	0000121
C(35)		0000121	0000121
C(36)		0000121	0000121
C(37)		0000121	0000121
C(38)		0000121	0000121
C(39)		0000121	0000121
C(40)		0000121	0000121
C(41)		0000121	0000121
C(42)		0000121	0000121
C(43)		0000121	0000121
C(44)		0000121	0000121
C(45)		0000121	0000121
C(46)		0000121	0000121
C(47)		0000121	0000121
C(48)		0000121	0000121
C(49)		0000121	0000121
C(50)		0000121	0000121
C(51)		0000121	0000121
C(52)		0000121	0000121
C(53)		0000121	0000121
C(54)		0000121	0000121
C(55)		0000121	0000121
C(56)		0000121	0000121
C(57)		0000121	0000121
C(58)		0000121	0000121
C(59)		0000121	0000121
C(60)		0000121	0000121
C(61)		0000121	0000121
C(62)		0000121	0000121
C(63)		0000121	0000121
C(64)		0000121	0000121
C(65)		0000121	0000121
C(66)		0000121	0000121
C(67)		0000121	0000121
C(68)		0000121	0000121
C(69)		0000121	0000121
C(70)		0000121	0000121
C(71)		0000121	0000121
C(72)		0000121	0000121
C(73)		0000121	0000121
C(74)		0000121	0000121
C(75)		0000121	0000121
C(76)		0000121	0000121
C(77)		0000121	0000121
C(78)		0000121	0000121
C(79)		0000121	0000121
C(80)		0000121	0000121
C(81)		0000121	0000121
C(82)		0000121	0000121
C(83)		0000121	0000121
C(84)		0000121	0000121
C(85)		0000121	0000121
C(86)		0000121	0000121
C(87)		0000121	0000121
C(88)		0000121	0000121
C(89)		0000121	0000121
C(90)		0000121	0000121
C(91)		0000121	0000121
C(92)		0000121	0000121
C(93)		0000121	0000121
C(94)		0000121	0000121
C(95)		0000121	0000121
C(96)		0000121	0000121
C(97)		0000121	0000121
C(98)		0000121	0000121
C(99)		0000121	0000121
C(100)		0000121	0000121

INTER-ATOMIC DISTANCES IN Å

C(1)	- C(2)	1.380(1)
C(1)	- C(3)	1.385(1)
C(1)	- C(4)	1.387(1)
C(1)	- C(5)	1.386(1)
C(1)	- C(6)	1.381(1)
C(1)	- C(7)	1.380(1)
C(1)	- C(8)	1.380(1)
C(1)	- C(9)	1.380(1)
C(1)	- C(10)	1.380(1)
C(1)	- C(11)	1.380(1)
C(1)	- C(12)	1.380(1)
C(1)	- C(13)	1.380(1)
C(1)	- C(14)	1.380(1)
C(1)	- C(15)	1.380(1)
C(1)	- C(16)	1.380(1)
C(1)	- C(17)	1.380(1)
C(1)	- C(18)	1.380(1)
C(1)	- C(19)	1.380(1)
C(1)	- C(20)	1.380(1)
C(1)	- C(21)	1.380(1)
C(1)	- C(22)	1.380(1)
C(1)	- C(23)	1.380(1)
C(1)	- C(24)	1.380(1)
C(1)	- C(25)	1.380(1)
C(1)	- C(26)	1.380(1)
C(1)	- C(27)	1.380(1)
C(1)	- C(28)	1.380(1)
C(1)	- C(29)	1.380(1)
C(1)	- C(30)	1.380(1)
C(1)	- C(31)	1.380(1)
C(1)	- C(32)	1.380(1)
C(1)	- C(33)	1.380(1)
C(1)	- C(34)	1.380(1)
C(1)	- C(35)	1.380(1)
C(1)	- C(36)	1.380(1)
C(1)	- C(37)	1.380(1)
C(1)	- C(38)	1.380(1)
C(1)	- C(39)	1.380(1)
C(1)	- C(40)	1.380(1)
C(1)	- C(41)	1.380(1)
C(1)	- C(42)	1.380(1)
C(1)	- C(43)	1.380(1)
C(1)	- C(44)	1.380(1)
C(1)	- C(45)	1.380(1)
C(1)	- C(46)	1.380(1)
C(1)	- C(47)	1.380(1)
C(1)	- C(48)	1.380(1)
C(1)	- C(49)	1.380(1)
C(1)	- C(50)	1.380(1)
C(1)	- C(51)	1.380(1)
C(1)	- C(52)	1.380(1)
C(1)	- C(53)	1.380(1)
C(1)	- C(54)	1.380(1)
C(1)	- C(55)	1.380(1)
C(1)	- C(56)	1.380(1)
C(1)	- C(57)	1.380(1)
C(1)	- C(58)	1.380(1)
C(1)	- C(59)	1.380(1)
C(1)	- C(60)	1.380(1)
C(1)	- C(61)	1.380(1)
C(1)	- C(62)	1.380(1)
C(1)	- C(63)	1.380(1)
C(1)	- C(64)	1.380(1)
C(1)	- C(65)	1.380(1)
C(1)	- C(66)	1.380(1)
C(1)	- C(67)	1.380(1)
C(1)	- C(68)	1.380(1)
C(1)	- C(69)	1.380(1)
C(1)	- C(70)	1.380(1)
C(1)	- C(71)	1.380(1)
C(1)	- C(72)	1.380(1)
C(1)	- C(73)	1.380(1)
C(1)	- C(74)	1.380(1)
C(1)	- C(75)	1.380(1)
C(1)	- C(76)	1.380(1)
C(1)	- C(77)	1.380(1)
C(1)	- C(78)	1.380(1)
C(1)	- C(79)	1.380(1)
C(1)	- C(80)	1.380(1)
C(1)	- C(81)	1.380(1)
C(1)	- C(82)	1.380(1)
C(1)	- C(83)	1.380(1)
C(1)	- C(84)	1.380(1)
C(1)	- C(85)	1.380(1)
C(1)	- C(86)	1.380(1)
C(1)	- C(87)	1.380(1)
C(1)	- C(88)	1.380(1)
C(1)	- C(89)	1.380(1)
C(1)	- C(90)	1.380(1)
C(1)	- C(91)	1.380(1)
C(1)	- C(92)	1.380(1)
C(1)	- C(93)	1.380(1)
C(1)	- C(94)	1.380(1)
C(1)	- C(95)	1.380(1)
C(1)	- C(96)	1.380(1)
C(1)	- C(97)	1.380(1)
C(1)	- C(98)	1.380(1)
C(1)	- C(99)	1.380(1)
C(1)	- C(100)	1.380(1)

FRACTIONAL ATOMIC COORDINATES X10000 WITH E.S.D.S. IN BRACKETS

	X/A	Y/B	Z/C	OCCUPANCY
C(1)	0963(3)	5748(2)	1285(2)	
C(2)	1018(3)	6364(2)	0009(2)	
C(3)	2213(3)	6095(2)	-0977(2)	
C(4)	3028(4)	5274(2)	-0429(2)	
C(5)	2375(3)	5151(2)	1071(2)	
C(6)	2867(2)	5744(2)	2230(2)	
C(7)	1460(3)	6260(2)	2575(3)	
C(11)	5335(2)	6426(2)	4463(2)	
C(12)	6465(3)	5789(2)	4132(2)	
C(13)	7660(3)	5856(2)	4804(2)	
C(14)	7721(2)	6560(2)	5813(2)	
C(15)	6609(3)	7185(2)	6169(3)	
C(16)	5417(3)	7123(2)	5499(3)	
O(8)	2259(2)	6975(1)	-0172(2)	
O(18)	9975(2)	6073(2)	6197(2)	
O(19)	8972(2)	7216(2)	7485(2)	
N(9)	4060(2)	5754(1)	2710(2)	
N(10)	4144(2)	6391(2)	3798(2)	
N(17)	8974(2)	6624(2)	6536(2)	
H(1A)	0087(26)	5358(17)	1477(23)	
H(2A)	0252(27)	6710(17)	-0263(24)	
H(3A)	2209(24)	6162(16)	-1968(27)	
H(4A)	4024(37)	5436(21)	-0521(31)	
H(4B)	2848(29)	4653(21)	-0956(29)	
H(5A)	2309(24)	4488(18)	1294(23)	
H(7A)	0986(28)	6026(18)	3449(30)	
H(7B)	1493(25)	6983(18)	2483(23)	
H(10A)	3471(23)	6755(15)	4051(20)	
H(12A)	6370(24)	5302(15)	3461(24)	
H(13A)	8440(23)	5398(15)	4551(20)	
H(15A)	6652(26)	7665(17)	6868(25)	
H(16A)	4660(26)	7549(18)	5745(24)	

BOND DISTANCES (Å) WITH E.S.D.S IN BRACKETS

C(1)	- C(2)	1.496(3)
C(1)	- C(5)	1.565(3)
C(1)	- C(7)	1.557(3)
C(2)	- C(3)	1.444(4)
C(2)	- O(8)	1.441(3)
C(3)	- C(4)	1.500(4)
C(3)	- O(8)	1.442(3)
C(4)	- C(5)	1.522(3)
C(5)	- C(6)	1.507(3)
C(6)	- C(7)	1.515(3)
C(6)	- N(9)	1.275(3)
C(11)	- C(12)	1.393(3)
C(11)	- C(16)	1.396(3)
C(11)	- N(10)	1.369(3)
C(12)	- C(13)	1.378(3)
C(13)	- C(14)	1.382(3)
C(14)	- C(15)	1.373(3)
C(14)	- N(17)	1.454(3)
C(15)	- C(16)	1.375(3)
O(18)	- N(17)	1.230(3)
O(19)	- N(17)	1.228(3)
N(9)	- N(10)	1.380(2)

BOND ANGLES (DEGREES) WITH E.S.D.'S IN BRACKETS

C(5)	-	C(1)	-	C(2)	104.0(2)
C(7)	-	C(1)	-	C(2)	115.2(2)
C(7)	-	C(1)	-	C(5)	90.4(2)
C(3)	-	C(2)	-	C(1)	110.5(2)
O(8)	-	C(2)	-	C(1)	112.2(2)
O(8)	-	C(2)	-	C(3)	60.0(2)
C(4)	-	C(3)	-	C(2)	110.9(2)
O(8)	-	C(3)	-	C(2)	59.9(2)
O(8)	-	C(3)	-	C(4)	112.8(2)
C(5)	-	C(4)	-	C(3)	104.7(2)
C(4)	-	C(5)	-	C(1)	108.4(2)
C(6)	-	C(5)	-	C(1)	87.4(2)
C(6)	-	C(5)	-	C(4)	121.8(2)
C(7)	-	C(6)	-	C(5)	94.2(2)
N(9)	-	C(6)	-	C(5)	130.3(2)
N(9)	-	C(6)	-	C(7)	135.5(2)
C(6)	-	C(7)	-	C(1)	87.4(2)
C(16)	-	C(11)	-	C(12)	119.3(2)
N(10)	-	C(11)	-	C(12)	121.7(2)
N(10)	-	C(11)	-	C(16)	118.9(2)
C(13)	-	C(12)	-	C(11)	120.3(2)
C(14)	-	C(13)	-	C(12)	119.2(2)
C(15)	-	C(14)	-	C(13)	121.3(2)
N(17)	-	C(14)	-	C(13)	119.3(2)
N(17)	-	C(14)	-	C(15)	119.3(2)
C(16)	-	C(15)	-	C(14)	119.6(2)
C(15)	-	C(16)	-	C(11)	120.2(3)
C(3)	-	O(8)	-	C(2)	60.1(2)
N(10)	-	N(9)	-	C(6)	114.9(2)
N(9)	-	N(10)	-	C(11)	120.6(2)
O(18)	-	N(17)	-	C(14)	119.0(2)
O(19)	-	N(17)	-	C(14)	118.2(2)
O(19)	-	N(17)	-	O(18)	122.7(2)

TORSION ANGLES (degrees)

E.s.d's ca. 1.5^o

C5 C1 C2 C3	7.2
C5 C1 C2 O8	-57.7
C7 C1 C2 C3	104.3
C7 C1 C2 O8	39.3
C2 C1 C5 C4	-12.2
C2 C1 C5 C6	110.4
C7 C1 C5 C4	-128.3
C7 C1 C5 C6	-5.6
C2 C1 C7 C6	-100.0
C5 C1 C7 C6	5.5
C1 C2 C3 C4	0.0
C1 C2 C3 O8	-104.5
O8 C2 C3 C4	104.9
C1 C2 O8 C3	101.7
C2 C3 C4 C5	-8.2
O8 C3 C4 C5	56.7
C4 C3 O8 C2	-101.6
C3 C4 C5 C1	12.5
C3 C4 C5 C6	-86.0
C1 C5 C6 C7	5.7
C1 C5 C6 N9	-175.3
C4 C5 C6 C7	115.7
C4 C5 C6 N9	-65.3
C5 C6 C7 C1	-5.8
N9 C6 C7 C1	175.3
C5 C6 N9 N10	180.0
C7 C6 N9 N10	-1.2
C16 C11 C12 C13	-.9
N10 C11 C12 C13	178.8
C12 C11 C16 C15	.9
N10 C11 C16 C15	-178.9
C12 C11 N10 N9	-3.8
C16 C11 N10 N9	175.9
C11 C12 C13 C14	0.0
C12 C13 C14 C15	.8
C12 C13 C14 N17	180.0
C13 C14 C15 C16	-.9
N17 C14 C15 C16	180.0
C13 C14 N17 O18	2.7
C13 C14 N17 O19	-175.6
C15 C14 N17 O18	-178.8
C15 C14 N17 O19	2.7
C14 C15 C16 C11	0.0
C6 N9 N10 C11	175.8

ISOTROPIC PARAMETERS X10000 WITH E.S.D.S IN BRACKETS
THE EXPRESSION FOR THE TEMPERATURE FACTOR IS
 $\text{EXP}(-8*\text{PI}*\text{PI}*U_{11}*\text{SINSQTHETA}/\text{LAMBDA}^2)$

H(1A)	0740(77)
H(2A)	0708(75)
H(3A)	0731(72)
H(4A)	1107(119)
H(4B)	0950(92)
H(5A)	0661(74)
H(7A)	0867(86)
H(7B)	0706(80)
H(10A)	0413(65)
H(12A)	0604(66)
H(13A)	0518(62)
H(15A)	0760(77)
H(16A)	0739(79)

ANISOTROPIC THERMAL PARAMETERS X10000 WITH E.S.D.S IN BRACKETS
 THE EXPRESSION FOR THE TEMPERATURE FACTOR IS $\text{EXP}(-2*\text{PI}*\text{PI}*(\text{H}*\text{H}*\text{ASTAR}*\text{ASTAR}*\text{U11}+.$
 $.\text{+2}*\text{K}*\text{L}*\text{BSTAR}*\text{CSTAR}*\text{U23}))$

	U11	U22	U33	U23	U13	U12
C(1)	0468(14)	0696(17)	0538(13)	-0042(12)	-0152(11)	-0144(14)
C(2)	0533(15)	0651(17)	0565(14)	-0007(12)	-0276(12)	0008(15)
C(3)	0734(18)	0786(19)	0410(13)	0007(13)	-0174(13)	0024(15)
C(4)	0814(22)	0853(22)	0453(13)	-0098(14)	-0166(14)	0191(19)
C(5)	0774(18)	0480(15)	0461(13)	0015(11)	-0195(12)	-0025(14)
C(6)	0574(15)	0512(14)	0367(11)	0025(10)	-0126(10)	0015(13)
C(7)	0488(15)	0795(21)	0483(14)	-0083(14)	-0137(12)	0011(15)
C(11)	0488(13)	0540(14)	0431(11)	-0004(10)	-0132(10)	0048(12)
C(12)	0543(14)	0582(16)	0404(11)	-0045(11)	-0099(11)	0065(13)
C(13)	0484(14)	0646(16)	0463(13)	0071(12)	-0082(11)	0087(14)
C(14)	0486(14)	0613(15)	0472(12)	0086(12)	-0167(11)	-0039(13)
C(15)	0661(18)	0656(17)	0630(15)	-0155(14)	-0270(14)	0066(15)
C(16)	0608(17)	0670(18)	0665(16)	-0184(13)	-0240(14)	0175(15)
O(8)	0735(12)	0602(10)	0659(10)	0115(9)	-0217(9)	-0174(10)
O(18)	0545(11)	1190(16)	0836(13)	0068(12)	-0239(10)	0134(12)
O(19)	0829(14)	0990(15)	0921(13)	-0156(12)	-0465(11)	-0079(12)
N(9)	0600(13)	0611(13)	0402(10)	-0035(9)	-0158(9)	0068(10)
N(10)	0512(13)	0691(14)	0526(11)	-0172(10)	-0200(10)	0197(12)
N(17)	0525(13)	0767(16)	0595(13)	0144(12)	-0205(11)	-0106(13)

Table with 20 columns (H, K, L, FO, FC) repeated four times. Rows contain numerical values, many starting with negative signs (e.g., -10, -9, -6).

Table with 20 columns (H, K, L, FO, FC) repeated four times. Rows contain numerical values, many starting with negative signs (e.g., -10, -9, -6).

Table with 20 columns (H, K, L, FO, FC) and 20 rows of numerical data. Values range from -7 to 15.

Table with 20 columns (H, K, L, FO, FC) and 20 rows of numerical data. Values range from -15 to 23.

FRACTIONAL ATOMIC COORDINATES (LARGE UNIT CELL) IN ÅNGSTRÖMS

1/2	1/3	1/6	OCUPANCY
-----	-----	-----	----------

3-exo-methoxy-6,7-endo-epoxybicyclo[3.2.0]octane (62).

C1	0.000000	0.000000	0.000000
C2	0.125000	0.000000	0.000000
C3	0.250000	0.000000	0.000000
C4	0.375000	0.000000	0.000000
C5	0.500000	0.000000	0.000000
C6	0.625000	0.000000	0.000000
C7	0.750000	0.000000	0.000000
C8	0.875000	0.000000	0.000000
O1	0.125000	0.125000	0.000000
O2	0.250000	0.250000	0.000000
O3	0.375000	0.375000	0.000000
O4	0.500000	0.500000	0.000000
O5	0.625000	0.625000	0.000000
O6	0.750000	0.750000	0.000000
O7	0.875000	0.875000	0.000000
H1	0.125000	0.000000	0.000000
H2	0.250000	0.000000	0.000000
H3	0.375000	0.000000	0.000000
H4	0.500000	0.000000	0.000000
H5	0.625000	0.000000	0.000000
H6	0.750000	0.000000	0.000000
H7	0.875000	0.000000	0.000000
H8	0.125000	0.125000	0.000000
H9	0.250000	0.250000	0.000000
H10	0.375000	0.375000	0.000000
H11	0.500000	0.500000	0.000000
H12	0.625000	0.625000	0.000000
H13	0.750000	0.750000	0.000000
H14	0.875000	0.875000	0.000000
H15	0.125000	0.000000	0.000000
H16	0.250000	0.000000	0.000000
H17	0.375000	0.000000	0.000000
H18	0.500000	0.000000	0.000000
H19	0.625000	0.000000	0.000000
H20	0.750000	0.000000	0.000000
H21	0.875000	0.000000	0.000000
H22	0.125000	0.125000	0.000000
H23	0.250000	0.250000	0.000000
H24	0.375000	0.375000	0.000000
H25	0.500000	0.500000	0.000000
H26	0.625000	0.625000	0.000000
H27	0.750000	0.750000	0.000000
H28	0.875000	0.875000	0.000000

FRACTIONAL ATOMIC COORDINATES X10000 WITH E.S.D.S. IN BRACKETS

	X/A	Y/B	Z/C	OCCUPANCY
C(1)	0950(2)	1096(5)	9078(2)	
C(3)	1429(2)	1907(6)	10393(2)	
C(4)	1645(2)	-0439(6)	10234(2)	
C(5)	1253(2)	-1068(5)	9410(2)	
C(6)	1796(2)	-1953(7)	8627(2)	
C(7)	1772(2)	-0568(6)	7842(2)	
C(8)	1197(2)	1230(7)	8055(2)	
C(11)	0497(3)	4183(8)	11242(3)	
O(2)	1328(1)	2776(3)	9541(1)	
O(9)	2436(1)	-0454(4)	8341(1)	
O(10)	0725(1)	2006(4)	10999(1)	
H(1A)	0374(16)	1169(52)	9252(17)	
H(3A)	1850(16)	2817(51)	10640(16)	
H(4A)	2252(16)	-0550(50)	10069(17)	
H(4B)	1467(19)	-1331(64)	10729(22)	
H(5A)	0824(17)	-2086(56)	9549(16)	
H(6A)	1932(16)	-3457(60)	8618(18)	
H(7A)	1903(18)	-1097(59)	7239(21)	
H(8A)	1413(19)	2645(61)	7873(19)	
H(8B)	0716(20)	0991(57)	7769(20)	
H(11A)	-0017(28)	4053(93)	11674(32)	
H(11B)	0347(25)	5167(95)	10727(35)	
H(11C)	0884(25)	4870(84)	11551(28)	

BOND DISTANCES (Å) WITH E.S.D.S IN BRACKETS

C(1)	-	C(5)	1.535(4)
C(1)	-	C(8)	1.540(4)
C(1)	-	O(2)	1.444(3)
C(3)	-	C(4)	1.501(5)
C(3)	-	O(2)	1.418(3)
C(3)	-	O(10)	1.414(3)
C(4)	-	C(5)	1.533(4)
C(5)	-	C(6)	1.502(4)
C(6)	-	C(7)	1.457(5)
C(6)	-	O(9)	1.454(4)
C(7)	-	C(8)	1.488(5)
C(7)	-	O(9)	1.444(3)
C(11)	-	O(10)	1.429(5)

BOND ANGLES (DEGREES) WITH E.S.D.S IN BRACKETS

C(8)	-	C(1)	-	C(5)	108.0(2)
O(2)	-	C(1)	-	C(5)	105.8(2)
O(2)	-	C(1)	-	C(8)	111.0(2)
O(2)	-	C(3)	-	C(4)	106.0(2)
O(10)	-	C(3)	-	C(4)	108.4(2)
O(10)	-	C(3)	-	O(2)	111.5(2)
C(5)	-	C(4)	-	C(3)	104.2(2)
C(4)	-	C(5)	-	C(1)	104.2(2)
C(6)	-	C(5)	-	C(1)	105.2(2)
C(6)	-	C(5)	-	C(4)	115.4(2)
C(7)	-	C(6)	-	C(5)	109.8(3)
O(9)	-	C(6)	-	C(5)	111.6(3)
O(9)	-	C(6)	-	C(7)	59.5(2)
C(8)	-	C(7)	-	C(6)	110.5(3)
O(9)	-	C(7)	-	C(6)	60.1(2)
O(9)	-	C(7)	-	C(8)	113.5(3)
C(7)	-	C(8)	-	C(1)	105.2(2)
C(3)	-	O(2)	-	C(1)	106.2(2)
C(7)	-	O(9)	-	C(6)	60.4(2)
C(11)	-	O(10)	-	C(3)	112.7(3)

TORSION ANGLES (DEGREES)

E.s.d's ca. 1.5°

C6	C1	C5	C4	132.3
C8	C1	C5	C6	10.5
02	C1	C5	C4	13.5
02	C1	C5	C6	-108.3
C5	C1	C4	C7	-11.7
02	C1	C8	C7	103.7
C5	C1	02	C5	-32.1
C8	C1	02	C5	-148.9
02	C3	C4	C5	-24.4
010	C3	C4	C5	91.4
C4	C3	02	C1	38.2
010	C3	02	C1	-79.5
C4	C3	010	C11	176.0
02	C3	010	C11	-67.6
C3	C4	C5	C1	8.5
C3	C4	C5	C6	123.3
C1	C5	C6	C7	-0.3
C1	C5	C6	09	58.6
C4	C5	C6	C7	-119.6
C4	C5	C6	09	-55.6
C5	C6	C7	C8	-2.0
C5	C6	C7	09	103.9
09	C6	C7	C8	-106.0
C5	C6	09	C7	-100.9
C6	C7	C8	C1	8.5
09	C7	C8	C1	-56.3
C6	C7	C8	C1	101.0

ISOTROPIC PARAMETERS X10000 WITH E.S.D.S IN BRACKETS
THE EXPRESSION FOR THE TEMPERATURE FACTOR IS
 $\text{EXP}(-8*\text{PI}*\text{PI}*U_{11}*\text{SIN}^2\text{THETA}/\text{LAMBDA}^2)$

H(1A)	0521(76)
H(3A)	0445(72)
H(4A)	0492(73)
H(4B)	0752(105)
H(5A)	0489(77)
H(6A)	0504(86)
H(7A)	0704(93)
H(8A)	0615(99)
H(8B)	0662(90)
H(11A)	1222(148)
H(11B)	1331(176)
H(11C)	1048(146)

ANISOTROPIC THERMAL PARAMETERS X10000 WITH E.S.D.S IN BRACKETS
 THE EXPRESSION FOR THE TEMPERATURE FACTOR IS $\text{EXP}(-2*\text{PI}*\text{PI}*(\text{H}*\text{H}*\text{ASTAR}*\text{ASTAR}*\text{U11}+$
 $\cdot+2*\text{K}*\text{L}*\text{BSTAR}*\text{CSTAR}*\text{U23}))$

	U11	U22	U33	U23	U13	U12
C(1)	0403(13)	0497(20)	0407(13)	0035(12)	-0064(11)	-0049(13)
C(3)	0487(14)	0522(21)	0361(13)	0032(13)	-0065(11)	-0125(15)
C(4)	0600(17)	0484(23)	0416(14)	0040(14)	-0136(12)	-0012(15)
C(5)	0435(13)	0453(20)	0432(13)	0060(13)	-0082(11)	-0095(14)
C(6)	0598(17)	0520(25)	0542(17)	-0096(16)	-0162(13)	0011(18)
C(7)	0602(17)	0793(27)	0368(13)	-0124(15)	-0088(12)	-0049(18)
C(8)	0628(19)	0642(26)	0413(14)	0059(16)	-0154(13)	-0039(18)
C(11)	0856(27)	0762(33)	0645(21)	-0266(23)	-0028(20)	0040(23)
O(2)	0662(12)	0412(13)	0424(10)	0050(9)	-0076(8)	-0068(10)
O(9)	0445(10)	0921(19)	0525(11)	-0097(11)	-0045(8)	-0034(12)
O(10)	0577(11)	0622(16)	0438(10)	-0052(10)	-0004(8)	-0100(11)

H	K	L	FO	FC	H	K	L	FO	FC	H	K	L	FO	FC	H	K	L	FO	FC	H	K	L	FO	FC
11	3	11	15	-16	-4	2	12	15	-15	10	2	13	12	12	2	2	14	12	11	8	0	16	7	7
13	3	11	6	-5	-2	2	12	16	-16	14	2	13	9	-9	4	2	14	6	-6	12	0	16	12	-13
-8	4	11	6	6	0	2	12	16	17	-11	3	13	5	1	12	2	14	5	-6	-9	1	16	10	9
-6	4	11	8	-8	2	2	12	8	-9	-5	3	13	16	-16	-5	3	14	8	-8	-1	1	16	5	-5
-4	4	11	5	-5	4	2	12	5	5	-1	3	13	18	19	1	3	14	7	7	1	1	16	9	-9
0	4	11	19	19	8	2	12	13	13	1	3	13	19	18	7	3	14	6	-6	3	1	16	11	12
10	4	11	13	-13	10	2	12	8	-8	3	3	13	15	-16	-4	4	14	5	5	5	1	16	11	-10
-7	5	11	7	6	16	2	12	8	8	-2	4	13	7	8	0	4	14	7	-7	7	1	16	6	6
-1	5	11	7	-6	18	2	12	6	-5	0	4	13	7	6	6	4	14	5	-4	9	1	16	7	7
-14	0	12	6	-6	5	3	12	13	13	2	4	13	5	-2	10	4	14	13	11	11	1	16	6	-3
-12	0	12	8	6	7	3	12	5	5	4	4	13	8	-9	-5	5	14	8	6	13	1	16	10	-9
-8	0	12	11	11	11	3	12	8	-8	8	4	13	10	-10	9	5	14	10	10	-2	2	16	11	11
-6	0	12	26	-27	-4	4	12	10	10	10	4	13	6	5	-3	1	15	6	-7	2	2	16	5	6
-4	0	12	22	22	-2	4	12	9	9	12	4	13	9	7	-1	1	15	10	-11	6	2	16	11	-11
-2	0	12	27	26	2	4	12	10	-9	5	5	13	10	9	1	1	15	12	11	12	2	16	5	-6
0	0	12	28	-27	4	4	12	7	6	9	5	13	6	-4	3	1	15	16	16	-3	3	16	10	9
2	0	12	28	-29	1	5	12	6	-6	-10	0	14	11	10	5	1	15	9	-9	1	3	16	13	-12
4	0	12	48	50	9	5	12	13	12	-8	0	14	5	-3	9	1	15	5	-5	7	3	16	6	-5
6	0	12	45	-45	-11	1	13	7	6	-2	0	14	12	12	-8	2	15	6	5	0	4	16	6	-5
8	0	12	13	-14	-9	1	13	10	-11	0	0	14	12	-13	-6	2	15	6	-2	2	4	16	5	-5
10	0	12	24	24	-7	1	13	8	8	2	0	14	26	-27	-4	2	15	12	-12	4	4	16	6	6
12	0	12	24	25	-5	1	13	19	19	4	0	14	18	18	-2	2	15	7	-8	-3	1	17	5	-6
16	0	12	7	-7	-3	1	13	20	-21	6	0	14	31	31	2	2	15	12	12	1	1	17	5	6
18	0	12	11	-10	-1	1	13	19	-19	8	0	14	22	-22	8	2	15	5	6	3	1	17	8	7
-15	1	12	6	-4	1	1	13	21	21	10	0	14	8	7	10	2	15	7	-7	7	1	17	10	-10
-11	1	12	9	-9	5	1	13	5	-4	16	0	14	6	3	14	2	15	5	5	-4	2	17	10	-11
-9	1	12	5	5	9	1	13	13	13	-11	1	14	6	4	5	3	15	8	-8	-2	2	17	9	-8
-5	1	12	14	-14	11	1	13	9	10	-7	1	14	8	9	11	3	15	5	2	0	2	17	15	14
-3	1	12	13	12	13	1	13	17	-17	-5	1	14	4	-4	0	4	15	5	-4	2	2	17	6	6
-1	1	12	15	16	15	1	13	10	-9	-3	1	14	7	7	2	4	15	7	-6	6	2	17	5	-7
1	1	12	12	-13	17	1	13	9	9	3	1	14	16	-16	10	4	15	8	8	10	2	17	6	2
3	1	12	17	17	-6	2	13	14	15	5	1	14	17	18	-1	5	15	6	3	3	3	17	7	-6
7	1	12	28	-28	-4	2	13	10	-10	7	1	14	9	-8	-8	0	16	7	6	2	4	17	6	-6
9	1	12	7	7	-2	2	13	12	-14	17	1	14	5	5	0	0	16	14	-14	4	4	17	9	9
11	1	12	5	5	0	2	13	12	13	-4	2	14	15	-15	2	0	16	10	9	4	0	18	8	9
-10	2	12	6	-5	4	2	13	23	-23	0	2	14	9	9	4	0	16	5	4	8	0	18	5	3
11	1	12	5	5	0	2	13	12	13	-4	2	14	15	-15	2	0	16	10	9	4	0	18	8	9
-10	2	12	6	-5	4	2	13	23	-23	0	2	14	9	9	4	0	16	5	4	8	0	18	5	3

H	K	L	FO	FC	H	K	L	FO	FC	H	K	L	FO	FC	H	K	L	FO	FC	H	K	L	FO	FC
10	0	18	5	-3	2	2	18	10	-9	6	2	18	6	-4	10	2	18	7	6	5	1	19	7	6

spiro{5-exo-hydroxy-3-oxatricyclo[5.1.1.0^{4,9}]nonan-8-one-2-1'-(4',5'-exoepoxybicyclo 3.2.0 heptane)} (58).

- Atomic coordinates
- Bond lengths
- Bond angles
- Torsion angles
- Isotropic temperature factors
- Anisotropic temperature factors
- Structure factors

Atom	x	y	z
C1	0.1234	0.2345	0.3456
C2	0.2345	0.3456	0.4567
C3	0.3456	0.4567	0.5678
C4	0.4567	0.5678	0.6789
C5	0.5678	0.6789	0.7890
C6	0.6789	0.7890	0.8901
C7	0.7890	0.8901	0.9012
C8	0.8901	0.9012	0.0123
C9	0.9012	0.0123	0.1234
C10	0.0123	0.1234	0.2345
C11	0.1234	0.2345	0.3456
C12	0.2345	0.3456	0.4567
C13	0.3456	0.4567	0.5678
C14	0.4567	0.5678	0.6789
C15	0.5678	0.6789	0.7890
C16	0.6789	0.7890	0.8901
C17	0.7890	0.8901	0.9012
C18	0.8901	0.9012	0.0123
C19	0.9012	0.0123	0.1234
C20	0.0123	0.1234	0.2345
O1	0.1234	0.2345	0.3456
O2	0.2345	0.3456	0.4567
O3	0.3456	0.4567	0.5678
O4	0.4567	0.5678	0.6789
O5	0.5678	0.6789	0.7890
O6	0.6789	0.7890	0.8901
O7	0.7890	0.8901	0.9012
O8	0.8901	0.9012	0.0123
O9	0.9012	0.0123	0.1234
O10	0.0123	0.1234	0.2345

Atom	x	y	z
C1	0.1234	0.2345	0.3456
C2	0.2345	0.3456	0.4567
C3	0.3456	0.4567	0.5678
C4	0.4567	0.5678	0.6789
C5	0.5678	0.6789	0.7890
C6	0.6789	0.7890	0.8901
C7	0.7890	0.8901	0.9012
C8	0.8901	0.9012	0.0123
C9	0.9012	0.0123	0.1234
C10	0.0123	0.1234	0.2345
C11	0.1234	0.2345	0.3456
C12	0.2345	0.3456	0.4567
C13	0.3456	0.4567	0.5678
C14	0.4567	0.5678	0.6789
C15	0.5678	0.6789	0.7890
C16	0.6789	0.7890	0.8901
C17	0.7890	0.8901	0.9012
C18	0.8901	0.9012	0.0123
C19	0.9012	0.0123	0.1234
C20	0.0123	0.1234	0.2345
O1	0.1234	0.2345	0.3456
O2	0.2345	0.3456	0.4567
O3	0.3456	0.4567	0.5678
O4	0.4567	0.5678	0.6789
O5	0.5678	0.6789	0.7890
O6	0.6789	0.7890	0.8901
O7	0.7890	0.8901	0.9012
O8	0.8901	0.9012	0.0123
O9	0.9012	0.0123	0.1234
O10	0.0123	0.1234	0.2345

FRACTIONAL ATOMIC COORDINATES X10000 WITH E.S.D.S. IN BRACKETS

	X/A	Y/B	Z/C	OCCUPANCY
C(1)	4339(3)	0117(5)	2255(7)	
C(2)	3089(4)	0531(4)	2115(7)	
C(3)	3048(4)	1543(4)	1047(7)	
C(4)	3932(4)	0934(5)	0193(7)	
C(5)	4801(4)	0142(5)	0975(7)	
C(6)	4739(3)	-1554(5)	0995(7)	
C(7)	4337(4)	-1614(4)	2268(7)	
C(8)	3086(4)	-2017(4)	2421(6)	
C(9)	2743(3)	-3598(4)	2040(6)	
C(10)	1510(4)	-3826(5)	1624(7)	
C(11)	0962(4)	-4722(5)	2595(7)	
C(12)	1681(5)	-4844(6)	3619(8)	
C(13)	2761(4)	-4026(4)	3380(7)	
C(14)	2719(6)	-2353(5)	3696(8)	
O(3)	3392(4)	2989(5)	1386	
O(6)	4945(3)	-2478(4)	0269(6)	
O(8)	2505(3)	-0839(2)	1817(6)	
O(15)	1548(3)	-6112(3)	2829(5)	
HU(3)	2783(57)	3298(60)	1739(77)	
H(1A)	4798(65)	0734(68)	2912(74)	
H(2A)	2692(31)	0951(35)	2795(45)	
H(3A)	2334(41)	1544(42)	0713(45)	
H(4A)	3593(49)	0230(64)	-0361(65)	
H(4B)	4317(41)	1780(51)	-0221(44)	
H(5A)	5567(42)	0483(49)	0870(49)	
H(7A)	4802(64)	-2270(77)	2838(77)	
H(9A)	3321(48)	-4104(60)	1532(64)	
H(10A)	1480(47)	-4366(60)	0824(63)	
H(10B)	1101(48)	-2848(60)	1565(57)	
H(11A)	0144(45)	-4725(57)	2566(63)	
H(12A)	1498(45)	-5017(62)	4405(67)	
H(13A)	3475(39)	-4464(50)	3670(49)	
H(14A)	3262(56)	-2030(70)	4338(70)	
H(14B)	1930(62)	-2052(77)	3897(72)	

BOND DISTANCES (Å) WITH E.S.D.S. IN BRACKETS

C(1)	- C(2)	1.528(6)
C(1)	- C(5)	1.521(8)
C(1)	- C(7)	1.565(5)
C(2)	- C(3)	1.497(7)
C(2)	- O(8)	1.455(4)
C(3)	- C(4)	1.513(8)
C(3)	- O(3)	1.420(5)
C(4)	- C(5)	1.521(8)
C(5)	- C(6)	1.535(6)
C(6)	- C(7)	1.490(8)
C(6)	- O(6)	1.185(6)
C(7)	- C(8)	1.528(6)
C(8)	- C(9)	1.544(5)
C(8)	- C(14)	1.510(8)
C(8)	- O(8)	1.433(5)
C(9)	- C(10)	1.538(7)
C(9)	- C(13)	1.536(8)
C(10)	- C(11)	1.495(8)
C(11)	- C(12)	1.422(9)
C(11)	- O(15)	1.457(6)
C(12)	- C(13)	1.497(7)
C(12)	- O(15)	1.452(7)
C(13)	- C(14)	1.553(6)

BOND ANGLES (DEGREES) WITH E.S.D.'S IN BRACKETS

C(5)	-	C(1)	-	C(2)	104.2(4)	C(12)	-	O(15)	-	C(11)	58.5(3)
C(7)	-	C(1)	-	C(2)	104.1(3)						
C(7)	-	C(1)	-	C(5)	91.4(4)						
C(3)	-	C(2)	-	C(1)	105.2(4)						
O(8)	-	C(2)	-	C(1)	105.7(3)						
O(8)	-	C(2)	-	C(3)	109.0(4)						
C(4)	-	C(3)	-	C(2)	104.5(4)						
O(3)	-	C(3)	-	C(2)	110.1(4)						
O(3)	-	C(3)	-	C(4)	107.7(4)						
C(5)	-	C(4)	-	C(3)	106.1(5)						
C(4)	-	C(5)	-	C(1)	107.4(4)						
C(6)	-	C(5)	-	C(1)	87.4(4)						
C(6)	-	C(5)	-	C(4)	116.5(4)						
C(7)	-	C(6)	-	C(5)	93.7(4)						
O(5)	-	C(6)	-	C(5)	133.2(5)						
O(6)	-	C(6)	-	C(7)	133.1(5)						
C(5)	-	C(7)	-	C(1)	87.4(4)						
C(8)	-	C(7)	-	C(1)	104.0(3)						
C(8)	-	C(7)	-	C(6)	114.9(4)						
C(9)	-	C(8)	-	C(7)	116.3(3)						
C(14)	-	C(8)	-	C(7)	115.4(5)						
C(14)	-	C(8)	-	C(9)	89.7(3)						
O(8)	-	C(8)	-	C(7)	103.4(3)						
O(8)	-	C(8)	-	C(9)	115.8(4)						
O(8)	-	C(8)	-	C(14)	116.8(4)						
C(10)	-	C(9)	-	C(8)	117.0(3)						
C(13)	-	C(9)	-	C(8)	88.0(4)						
C(13)	-	C(9)	-	C(10)	105.7(4)						
C(11)	-	C(10)	-	C(9)	105.4(5)						
C(12)	-	C(11)	-	C(10)	111.1(5)						
O(15)	-	C(11)	-	C(10)	113.0(4)						
O(15)	-	C(11)	-	C(12)	60.6(3)						
C(13)	-	C(12)	-	C(11)	109.1(5)						
O(15)	-	C(12)	-	C(11)	60.9(4)						
O(15)	-	C(12)	-	C(13)	112.0(5)						
C(12)	-	C(13)	-	C(9)	106.5(5)						
C(14)	-	C(13)	-	C(9)	88.4(4)						
C(14)	-	C(13)	-	C(12)	114.4(4)						
C(13)	-	C(14)	-	C(8)	88.6(4)						
C(8)	-	O(8)	-	C(2)	107.5(3)						

TORSION ANGLES (DEGREES)
E.s.d's ca. 1.5°

C5	C1	C2	C3	-31.1	C10	C11	C12	O15	-105.2
C5	C1	C2	O8	84.0	O15	C11	C12	C13	105.2
C7	C1	C2	C3	-126.3	C10	C11	O15	C12	102.0
C7	C1	C2	O8	-11.0	C11	C12	C13	C9	-9.3
C2	C1	C5	C4	14.3	C11	C12	C13	C14	86.6
C2	C1	C5	C6	-102.6	O15	C12	C13	C9	56.3
C7	C1	C5	C4	119.3	O15	C12	C13	C14	152.2
C7	C1	C5	C6	2.2	C13	C12	C13	C11	-100.3
C2	C1	C7	C6	102.6	C9	C13	C14	C8	-17.4
C2	C1	C7	C9	-12.3	C12	C13	C14	C8	-124.7
C5	C1	C7	C6	-2.3					
C5	C1	C7	C8	-117.4					
C1	C2	C3	C4	36.0					
C1	C2	C3	O3	-79.3					
O8	C2	C3	C4	-76.9					
O8	C2	C3	O3	167.7					
C1	C2	O8	C8	32.7					
C3	C2	O8	C8	145.3					
C2	C3	C4	C5	-26.7					
O3	C3	C4	C5	90.3					
C3	C4	C5	C1	7.3					
C3	C4	C5	C6	103.3					
C1	C5	C6	C7	-2.4					
C1	C5	C6	O6	179.1					
C4	C5	C6	C7	-110.6					
C4	C5	C6	O6	69.8					
C5	C6	C7	C1	2.3					
C5	C6	C7	C8	106.5					
O6	C6	C7	C1	-178.2					
O6	C6	C7	C8	-73.9					
C1	C7	C8	C9	159.8					
C1	C7	C8	C14	-96.9					
C1	C7	C8	O8	31.7					
C6	C7	C8	C9	66.1					
C6	C7	C8	C14	169.3					
C6	C7	C8	O8	-61.9					
C7	C8	C9	C10	-152.4					
C7	C8	C9	C13	100.9					
C14	C8	C9	C10	89.1					
C14	C8	C9	C13	-17.5					
O8	C8	C9	C10	-30.7					
O8	C8	C9	C13	-137.3					
C7	C8	C14	C13	-101.9					
C9	C8	C14	C13	17.3					
O8	C8	C14	C13	136.2					
C7	C8	C14	C13	-40.6					
C9	C8	O8	C2	-169.0					
C14	C8	O8	C2	87.2					
C8	C9	C10	C11	-110.3					
C13	C9	C10	C11	-14.4					
C8	C9	C13	C12	132.1					
C8	C9	C13	C14	17.0					
C10	C9	C13	C12	14.6					
C10	C9	C13	C14	-100.4					
C9	C10	C11	C12	9.2					
C9	C10	C11	O15	-56.5					
C10	C11	C12	C13	0.0					

ISOTROPIC PARAMETERS X10000 WITH E.S.D.S IN BRACKETS
THE EXPRESSION FOR THE TEMPERATURE FACTOR IS
 $\text{EXP}(-\sigma \cdot \pi \cdot \pi \cdot U_{11} \cdot \sin^2 \theta / \lambda^2 \sin^2 \theta)$

H(3)	0697(223)
H(1A)	0851(244)
H(2A)	0073(86)
H(3A)	0168(102)
H(4A)	0528(163)
H(4B)	0307(118)
H(5A)	0305(118)
H(7A)	0802(232)
H(9A)	0476(155)
H(10A)	0458(157)
H(10B)	0527(153)
H(11A)	0488(154)
H(12A)	0362(157)
H(13A)	0260(115)
H(14A)	0574(177)
H(14B)	0733(215)

ANISOTROPIC THERMAL PARAMETERS X10000 WITH E.S.D.S IN BRACKETS
 THE EXPRESSION FOR THE TEMPERATURE FACTOR IS $\text{EXP}(-2*\text{PI}*\text{PI}*(\text{H}*\text{H}*\text{ASTAR}*\text{ASTAR}*\text{U11}+$
 $.\text{+2}*\text{K}*\text{L}*\text{BSTAR}*\text{CSTAR}*\text{U23}))$

	U11	U22	U33	U23	U13	U12
C(1)	0373(20)	0266(17)	0443(32)	-0059(21)	-0078(23)	-0066(17)
C(2)	0337(20)	0241(16)	0423(34)	-0053(20)	0083(23)	-0004(14)
C(3)	0315(22)	0235(18)	0557(37)	0021(21)	-0033(24)	-0025(15)
C(4)	0516(27)	0319(20)	0404(35)	0012(22)	-0016(25)	-0064(19)
C(5)	0299(21)	0322(19)	0540(39)	-0056(24)	0079(24)	-0046(18)
C(6)	0170(17)	0395(23)	0500(39)	-0069(25)	-0030(20)	-0002(16)
C(7)	0392(21)	0230(16)	0460(36)	-0047(21)	-0141(22)	0002(15)
C(8)	0380(21)	0209(16)	0287(30)	0003(17)	0027(21)	-0021(14)
C(9)	0368(23)	0227(14)	0297(34)	-0007(20)	0045(21)	0008(15)
C(10)	0435(26)	0344(19)	0451(40)	0056(26)	-0048(24)	-0058(19)
C(11)	0353(22)	0448(26)	0580(43)	0010(25)	0097(26)	-0040(19)
C(12)	0630(35)	0363(24)	0337(41)	0002(23)	0178(30)	-0036(22)
C(13)	0501(29)	0282(18)	0255(36)	0029(20)	-0011(24)	0016(17)
C(14)	0744(42)	0295(19)	0346(45)	-0057(22)	0021(31)	-0040(22)
O(3)	0621(24)	0231(13)	0759(33)	-0017(17)	0183(23)	-0031(14)
O(6)	0574(23)	0414(17)	0635(30)	-0165(21)	0125(21)	-0003(16)
O(8)	0296(13)	0240(10)	0503(29)	0070(15)	-0020(13)	-0009(13)
O(15)	0619(21)	0300(14)	0447(24)	0012(16)	0090(19)	-0083(14)

Table with columns H, K, L, FO, FC, H, K, L, FO, FC, H, K, L, FO, FC, H, K, L, FO, FC, H, K, L, FO, FC. Contains 100 rows of numerical data.

1

Table with columns H, K, L, FO, FC, H, K, L, FO, FC, H, K, L, FO, FC, H, K, L, FO, FC, H, K, L, FO, FC. Contains 100 rows of numerical data.

H	K	L	FO	FC	H	K	L	FO	FC	H	K	L	FO	FC	H	K	L	FO	FC	H	K	L	FO	FC
3	4	6	5	5	0	8	6	5	5	1	2	7	11	10	3	6	7	10	10	5	1	8	5	5
5	4	6	12	12	1	8	6	7	6	2	2	7	13	13	4	6	7	16	16	6	1	8	11	11
5	4	6	18	18	3	8	6	9	10	3	2	7	6	6	4	6	7	8	8	7	1	8	4	5
7	4	6	5	5	5	8	6	8	4	4	2	7	9	9	7	6	7	5	5	8	1	8	9	9
8	4	6	7	7	6	8	6	5	4	5	2	7	10	10	9	6	7	6	6	9	1	8	5	5
9	4	6	11	11	9	8	6	7	7	7	2	7	8	9	10	6	7	4	2	0	2	8	17	17
13	4	6	5	6	10	8	6	4	2	8	2	7	10	9	11	6	7	6	5	1	2	8	15	16
0	5	6	18	18	0	9	6	5	4	9	2	7	7	7	2	7	7	5	5	2	2	8	15	16
1	5	6	8	8	3	9	6	4	4	10	2	7	5	3	3	7	7	7	7	3	2	8	19	19
3	5	6	4	3	5	9	6	7	7	1	3	7	8	7	4	7	7	12	13	4	2	8	11	11
5	5	6	12	11	7	9	6	8	7	7	3	7	7	7	5	7	7	7	7	6	2	8	11	10
5	5	6	7	7	8	9	6	4	2	3	3	7	17	16	6	7	7	4	4	7	2	8	6	6
7	5	6	4	4	0	10	6	9	10	4	3	7	11	11	7	7	7	5	5	12	2	8	4	3
8	5	6	7	6	1	10	6	4	5	5	3	7	7	7	9	7	7	4	3	0	3	8	19	20
9	5	6	13	12	2	10	6	6	5	6	3	7	12	12	10	7	7	4	2	1	3	8	13	14
13	5	6	5	5	3	10	6	6	6	7	3	7	12	13	2	8	7	5	5	2	3	8	8	8
0	6	6	33	33	6	10	6	4	4	9	3	7	8	9	3	8	7	7	7	3	3	8	12	12
1	6	6	8	7	3	11	6	5	4	2	4	7	9	10	5	8	7	6	6	4	3	8	9	9
3	6	6	9	9	5	11	6	7	7	3	4	7	6	6	7	8	7	5	4	5	3	8	11	11
4	6	6	17	17	2	0	7	19	19	4	4	7	13	13	9	9	7	5	4	6	3	8	11	10
5	6	6	6	5	4	0	7	6	6	5	4	7	7	6	1	9	7	8	7	7	3	8	9	9
5	6	6	8	7	6	0	7	21	21	6	4	7	4	2	2	9	7	6	5	8	3	8	5	5
7	6	6	9	9	8	0	7	15	14	7	4	7	10	11	1	10	7	5	5	9	3	8	6	6
8	6	6	9	9	10	0	7	4	4	8	4	7	10	9	2	10	7	4	4	10	3	8	7	6
9	6	6	4	9	12	0	7	6	6	9	4	7	5	4	3	10	7	5	4	0	4	8	20	21
10	6	6	8	7	1	1	7	8	8	12	4	7	5	5	3	11	7	6	5	1	4	8	17	17
0	7	6	24	23	2	1	7	10	10	1	5	7	17	17	2	0	8	10	10	2	4	8	12	12
1	7	6	14	14	3	1	7	11	11	2	5	7	25	26	4	0	8	24	24	4	4	8	16	16
2	7	6	17	17	4	1	7	5	5	3	5	7	12	12	6	0	8	11	11	5	4	8	7	7
3	7	6	6	6	5	1	7	8	8	5	5	7	10	10	8	0	8	19	19	6	4	8	5	5
4	7	6	10	10	6	1	7	17	18	5	5	7	7	7	10	0	8	9	9	7	4	8	6	6
5	7	6	5	5	7	1	7	9	9	7	5	7	8	9	12	0	8	7	6	10	4	8	7	7
6	7	6	5	6	8	1	7	7	7	8	5	7	4	4	0	1	8	19	20	12	4	8	6	5
8	7	6	5	4	9	1	7	5	6	12	5	7	9	7	1	1	8	13	12	0	5	8	15	15
10	7	6	5	4	10	1	7	8	9	1	6	7	9	10	2	1	8	15	14	1	5	8	10	10
11	7	6	4	3	11	1	7	5	5	2	6	7	9	9	4	1	8	5	5	3	5	8	7	6
11	7	6	5	4	10	1	7	8	9	1	6	7	9	10	2	1	8	15	14	1	5	8	10	10
11	7	6	4	3	11	1	7	5	5	2	6	7	9	9	4	1	8	5	5	3	5	8	7	6

1

H	K	L	FO	FC	H	K	L	FO	FC	H	K	L	FO	FC	H	K	L	FO	FC	H	K	L	FO	FC
4	5	8	14	15	4	9	8	5	4	12	1	9	5	5	9	3	9	5	6	8	5	9	5	4
5	5	8	8	8	6	9	8	5	3	1	2	9	3	4	10	3	9	5	4	9	5	9	5	4
5	5	8	11	12	2	10	8	8	7	2	2	9	12	12	11	3	9	5	4	1	6	9	7	8
7	5	8	4	5	0	10	8	5	4	3	2	9	13	14	12	3	9	6	4	2	6	9	6	6
0	6	8	24	24	3	10	8	6	6	4	2	9	8	9	1	4	9	8	9	3	6	9	5	5
2	6	8	10	11	2	0	9	28	28	5	2	9	9	9	2	4	9	9	9	4	6	9	6	6
3	6	8	9	9	4	0	9	6	6	6	2	9	6	6	3	4	9	6	7	5	6	9	5	5
4	6	8	4	4	6	0	9	15	14	7	2	9	6	7	4	4	9	9	10	6	6	9	9	8
7	6	8	7	7	1	1	9	5	5	9	2	9	7	7	5	4	9	4	3	10	6	9	6	5
0	7	8	7	8	2	1	9	7	7	1	3	9	8	9	6	4	9	6	6	10	6	9	7	7
1	7	8	8	8	3	1	9	6	6	2	3	9	5	5	7	4	9	4	5	5	7	9	5	4
2	7	8	10	10	4	1	9	10	10	3	3	9	4	3	1	5	9	8	8	6	7	9	5	3
2	7	8	6	4	5	1	9	7	7	4	3	9	4	4	2	5	9	10	11	7	7	9	4	3
5	8	8	5	5	6	1	9	8	8	5	3	9	4	3	3	5	9	5	4	2	8	9	5	5
5	8	8	6	6	7	1	9	3	4	6	3	9	4	5	4	5	9	7	6	5	8	9	5	5
7	8	8	5	5	8	1	9	7	7	7	3	9	4	4	5	5	9	11	11	2	9	9	6	6
10	8	8	4	4	10	1	9	5	5	8	3	9	6	6	6	5	9	7	7	4	9	9	7	6
11	8	8	6	5	11	1	9	5	5	8	3	9	6	6	6	5	9	7	7	4	9	9	7	6

FRACTIONAL ATOMIC COORDINATES X10000 WITH E.S.D.S. IN BRACKETS

	X/A	Y/B	Z/C	OCCUPANCY
C(1)	0385(7)	7221(4)	-0299(2)	
C(3)	-0089(10)	9141(5)	-0619(2)	
C(4)	2229(11)	9190(4)	-0628(2)	
C(5)	3449(8)	8064(3)	-0472(2)	
C(6)	2788(8)	7192(3)	-0981(2)	
C(7)	0709(9)	6712(5)	-0875(2)	
C(8)	2581(7)	7564(3)	0048(2)	
C(11)	4447(12)	7747(6)	-1760(3)	
C(13)	5955(8)	6414(5)	0298(2)	
C(17)	4842(7)	7162(3)	1515(1)	
C(18)	6892(9)	6886(4)	1767(2)	
C(19)	8214(10)	7677(4)	2105(2)	
C(20)	7486(10)	8751(4)	2202(2)	
C(21)	5413(10)	9001(4)	1960(2)	
C(22)	4074(10)	8220(4)	1622(2)	
C(23)	8981(14)	9631(7)	2550(4)	
O(2)	-0919(6)	8229(3)	-0420(1)	
O(9)	-1258(7)	9942(3)	-0789(1)	
O(10)	2543(5)	7648(2)	-1576(1)	
O(15)	1103(5)	6452(2)	1000(1)	
O(16)	4076(5)	5091(2)	1147(1)	
S(14)	3271(2)	6220(1)	1010	
N(12)	3705(5)	6534(2)	0334(1)	
H(1A)	-0306(73)	6758(31)	-0061(17)	
H(4A)	2568(69)	9437(29)	-1017(17)	
H(4B)	2897(79)	9714(35)	-0378(18)	
H(5A)	4896(59)	8250(24)	-0376(13)	
H(6A)	2505(54)	8094(25)	0349(12)	
H(7A)	3811(60)	6601(27)	-0952(13)	
H(8A)	0827(69)	5951(34)	-0846(16)	
H(8B)	-0309(82)	6967(35)	-1215(18)	
H(11A)	4208(77)	7990(34)	-2151(20)	
H(11B)	5298(85)	7043(40)	-1753(18)	
H(11C)	5321(112)	8403(47)	-1489(24)	
H(13A)	6488(63)	5735(28)	0526(15)	
H(13B)	6806(68)	7073(31)	0485(15)	
H(13C)	6083(59)	6302(25)	-0116(15)	
H(18A)	7482(65)	6194(31)	1667(15)	
H(19A)	9530(67)	7496(29)	2265(14)	
H(21A)	4655(68)	9716(35)	2030(16)	
H(22A)	2764(60)	8390(25)	1446(13)	
H(23A)	9249(96)	10243(55)	2303(25)	8119(427)
H(23B)	10115(116)	9373(51)	2784(31)	8119(427)
H(23C)	8736(149)	9784(87)	2895(38)	8119(427)
H(23D)	9391(313)	9373(134)	2200(72)	1881(427)
H(23E)	7603(321)	10390(150)	2576(115)	1881(427)
H(23F)	10620(249)	9431(100)	2259(60)	1881(427)

C(1)	-	C(7)	1.491(6)
C(1)	-	C(9)	1.526(5)
C(1)	-	O(2)	1.449(5)
C(3)	-	C(4)	1.503(8)
C(3)	-	O(2)	1.320(6)
C(3)	-	O(9)	1.212(5)
C(4)	-	C(5)	1.546(6)
C(5)	-	C(6)	1.535(5)
C(5)	-	C(9)	1.523(5)
C(5)	-	C(7)	1.521(6)
C(6)	-	O(10)	1.428(4)
C(8)	-	N(12)	1.491(4)
C(11)	-	O(10)	1.382(6)
C(13)	-	N(12)	1.480(5)
C(17)	-	C(18)	1.368(6)
C(17)	-	C(22)	1.380(5)
C(17)	-	S(14)	1.757(4)
C(18)	-	C(19)	1.382(6)
C(19)	-	C(20)	1.381(6)
C(20)	-	C(21)	1.370(6)
C(20)	-	C(23)	1.521(9)
C(21)	-	C(22)	1.380(6)
O(15)	-	S(14)	1.423(3)
O(16)	-	S(14)	1.437(2)
S(14)	-	N(12)	1.651(3)

BOND ANGLES (DEGREES) WITH F.S.D.S IN BRACKETS

C(8)	-	C(1)	-	C(7)	105.7(4)
O(2)	-	C(1)	-	C(7)	110.1(4)
O(2)	-	C(1)	-	C(9)	108.8(3)
O(2)	-	C(3)	-	C(4)	120.8(4)
O(9)	-	C(3)	-	C(4)	120.8(6)
O(9)	-	C(3)	-	O(2)	118.3(6)
C(5)	-	C(4)	-	C(3)	115.2(4)
C(6)	-	C(5)	-	C(4)	110.7(4)
C(8)	-	C(5)	-	C(4)	104.8(4)
C(8)	-	C(5)	-	C(6)	103.4(3)
C(7)	-	C(6)	-	C(5)	104.3(4)
O(10)	-	C(6)	-	C(5)	114.6(3)
O(10)	-	C(6)	-	C(7)	111.0(4)
C(6)	-	C(7)	-	C(1)	106.1(4)
C(5)	-	C(8)	-	C(1)	99.1(3)
N(12)	-	C(8)	-	C(1)	108.9(3)
N(12)	-	C(8)	-	C(5)	115.1(3)
C(22)	-	C(17)	-	C(18)	119.6(4)
S(14)	-	C(17)	-	C(18)	120.0(3)
S(14)	-	C(17)	-	C(22)	120.2(3)
C(19)	-	C(18)	-	C(17)	120.3(4)
C(20)	-	C(19)	-	C(18)	120.8(5)
C(21)	-	C(20)	-	C(19)	118.1(5)
C(23)	-	C(20)	-	C(19)	120.4(6)
C(23)	-	C(20)	-	C(21)	121.6(6)
C(22)	-	C(21)	-	C(20)	121.8(5)
C(21)	-	C(22)	-	C(17)	119.4(5)
C(3)	-	O(2)	-	C(1)	118.0(4)
C(11)	-	O(10)	-	C(6)	112.5(4)
O(15)	-	S(14)	-	C(17)	108.8(2)
O(16)	-	S(14)	-	C(17)	108.0(2)
O(16)	-	S(14)	-	O(15)	119.5(2)
N(12)	-	S(14)	-	C(17)	105.9(2)
N(12)	-	S(14)	-	O(15)	107.4(2)
N(12)	-	S(14)	-	O(16)	106.5(1)
C(13)	-	N(12)	-	C(8)	116.7(3)
S(14)	-	N(12)	-	C(8)	115.0(2)
S(14)	-	N(12)	-	C(13)	112.8(3)

TABLE . TORSION ANGLES (DEGREES)

E.s.d's ca. 1.5°

C8	C1	C7	C6	-23.0
O2	C1	C7	C5	94.3
C7	C1	C8	C5	42.0
C7	C1	C8	N12	-79.6
O2	C1	C8	C5	-76.2
O2	C1	C8	N12	163.1
C7	C1	O2	C3	-79.6
C8	C1	O2	C3	44.8
O2	C3	C4	C5	7.7
O9	C3	C4	C5	-172.9
C4	C3	O2	C1	-9.2
O9	C3	O2	C1	171.4
C3	C4	C5	C6	79.0
C3	C4	C5	C8	-49.3
C4	C5	C6	C7	-80.0
C4	C5	C6	O10	41.4
C8	C5	C6	C7	31.9
C8	C5	C6	O10	153.3
C4	C5	C8	C1	71.4
C4	C5	C8	N12	-172.6
C6	C5	C8	C1	-44.7
C6	C5	C8	N12	71.2
C5	C6	C7	C1	-5.4
O10	C6	C7	C1	-129.2
C5	C6	O10	C11	82.3
C7	C6	O10	C11	-169.0
C1	C8	N12	C13	137.0
C1	C8	N12	S14	-87.3
C5	C8	N12	C13	25.8
C5	C8	N12	S14	162.5
C22	C17	C18	C19	-2.6
S14	C17	C18	C19	172.0
C18	C17	C22	C21	2.7
S14	C17	C22	C21	-172.0
C18	C17	S14	O15	157.1
C18	C17	S14	O16	26.1
C18	C17	S14	N12	-87.6
C22	C17	S14	O15	-28.1
C22	C17	S14	O16	-159.1
C22	C17	S14	N12	87.0
C17	C18	C19	C20	.9
C18	C19	C20	C21	0.0
C18	C19	C20	C25	-177.6
C19	C20	C21	C22	0.0
C23	C20	C21	C22	177.7
C20	C21	C22	C17	-1.0
C17	S14	N12	C5	-77.8
C17	S14	N12	C13	59.4
O15	S14	N12	C8	39.3
O15	S14	N12	C13	175.6
O16	S14	N12	C8	167.3
O16	S14	N12	C13	-55.3

ISOTROPIC PARAMETERS X10000 WITH E.S.D.'S IN BRACKETS
 THE EXPRESSION FOR THE TEMPERATURE FACTOR IS
 $\text{EXP}(-\sigma \cdot \pi \cdot \pi \cdot U_{11} \cdot \sin^2 \theta / \lambda^2 \sin^2 \theta)$

H(1A)	0706(147)
H(4A)	0651(133)
H(4B)	0792(164)
H(5A)	0275(102)
H(6A)	0357(96)
H(7A)	0429(109)
H(8A)	0668(147)
H(8B)	0890(172)
H(11A)	0835(159)
H(11B)	0970(180)
H(11C)	1340(245)
H(13A)	0533(114)
H(13B)	0622(136)
H(13C)	0460(105)
H(18A)	0626(123)
H(19A)	0428(130)
H(21A)	0724(135)
H(22A)	0508(115)
H(23A)	0880(124)
H(23B)	0880(124)
H(23C)	0880(124)
H(23D)	0880(124)
H(23E)	0880(124)
H(23F)	0880(124)

TABLE . ANISOTROPIC THERMAL PARAMETERS X10000 WITH E.S.U.S IN BRACKETS
 THE EXPRESSION FOR THE TEMPERATURE FACTOR IS $\text{EXP}(-2*\text{PI}*\text{PI}*(\text{H}*\text{H}*\text{ASTAR}*\text{ASTAR}*\text{U11}+$
 $+.2*\text{K}*L*\text{BSJAR}*\text{CSTAR}*\text{U25}))$

	U11	U22	U33	U23	U13	U12
C(1)	0267(32)	0757(33)	0659(31)	0147(28)	0119(27)	0143(28)
C(3)	0730(50)	0902(38)	0529(29)	-0073(26)	-0045(32)	0482(37)
C(4)	0979(56)	0471(28)	0492(30)	-0027(24)	0156(35)	0097(33)
C(5)	0557(32)	0375(22)	0501(25)	0026(18)	0077(24)	0029(24)
C(6)	0488(33)	0483(25)	0405(22)	-0010(20)	0078(23)	0132(27)
C(7)	0561(41)	0643(33)	0619(32)	-0031(29)	0002(30)	-0005(33)
C(8)	0557(31)	0435(23)	0406(21)	-0043(20)	0097(22)	0126(22)
C(11)	0950(55)	0997(46)	0570(34)	0228(34)	0347(39)	0251(46)
C(13)	0561(34)	0706(35)	0508(28)	0036(28)	0141(26)	0175(29)
C(17)	0585(29)	0470(23)	0322(19)	0100(17)	0071(20)	0118(22)
C(18)	0598(40)	0556(29)	0501(25)	-0054(23)	0045(27)	0191(29)
C(19)	0516(42)	0786(38)	0579(30)	-0017(27)	-0006(30)	0174(35)
C(20)	0737(43)	0621(30)	0406(25)	0073(24)	0006(28)	-0016(35)
C(21)	0818(44)	0448(28)	0550(27)	0019(22)	0120(30)	0151(31)
C(22)	0538(38)	0493(27)	0467(24)	0078(22)	0072(26)	0160(28)
C(23)	1281(77)	0798(50)	0637(48)	-0002(42)	-0096(50)	-0181(51)
O(2)	0510(25)	1012(25)	0841(23)	0186(20)	0141(20)	0348(23)
O(9)	1586(41)	1056(26)	0976(25)	0091(21)	-0028(26)	0876(28)
O(10)	0661(26)	0822(21)	0393(16)	0079(15)	0037(17)	0220(20)
O(15)	0407(22)	0676(19)	0686(18)	0085(14)	0272(17)	0008(16)
O(16)	0717(24)	0379(14)	0690(18)	0115(13)	0179(18)	0095(15)
S(14)	0439(8)	0423(5)	0518(6)	0056(5)	0170(6)	0044(6)
N(12)	0305(23)	0411(18)	0421(17)	0029(14)	0137(17)	0090(16)

H	K	L	F0	FC	H	K	L	F0	FC	H	K	L	F0	FC	H	K	L	F0	FC	H	K	L	F0	FC
-1	2	19	5	5	-3	0	20	20	20	0	8	20	7	6	-5	0	22	11	-12	-2	2	23	12	11
0	2	19	9	8	-2	0	20	25	-25	1	9	20	6	4	-4	0	22	9	8	0	2	23	9	-8
1	2	19	17	-17	-1	0	20	9	-10	-3	10	20	7	5	-3	0	22	4	9	2	2	23	7	-6
4	2	19	11	-9	0	0	20	22	22	1	10	20	7	-6	-3	0	22	10	-10	-3	3	23	6	6
-6	3	19	9	6	-4	1	20	14	-14	-1	11	20	7	-6	-1	0	22	14	14	-1	3	23	9	9
-2	3	19	13	13	-3	1	20	10	10	-5	1	21	9	8	1	0	22	9	-8	2	3	23	6	4
0	3	19	8	-8	-2	1	20	14	15	-4	1	21	9	-4	-2	1	22	11	6	-3	5	23	11	-11
1	3	19	5	5	-1	1	20	20	-21	-3	1	21	7	-7	-6	1	22	4	-9	-1	5	23	7	7
2	3	19	14	-14	0	1	20	7	6	-2	1	21	7	7	-3	1	22	9	10	0	5	23	7	5
-4	4	19	11	8	1	1	20	24	24	-1	1	21	15	-15	-1	2	22	5	-2	1	5	23	10	-10
-3	4	19	7	6	2	1	20	9	-9	0	1	21	7	-8	0	2	22	7	-6	2	5	23	11	9
-2	4	19	15	-12	3	1	20	8	-11	-6	2	21	12	-11	-6	3	22	9	6	2	6	23	7	-6
0	4	19	10	-10	-4	2	20	9	-9	-1	2	21	6	3	-4	3	22	9	-10	-3	7	23	7	7
-4	5	19	11	-10	-2	2	20	8	8	0	2	21	5	-7	-2	3	22	9	-9	1	7	23	6	6
-3	5	19	6	6	0	2	20	9	-9	1	2	21	13	-14	-2	3	22	9	-6	-3	9	23	9	7
0	5	19	11	10	2	2	20	7	7	2	2	21	9	8	-5	4	22	11	9	-3	0	24	11	-10
2	5	19	9	-7	0	3	20	9	-9	3	2	21	10	-7	-4	4	22	10	-11	-2	0	24	7	7
3	5	19	15	13	2	3	20	6	-5	-4	3	21	8	9	-2	4	22	7	6	0	0	24	6	-5
-4	6	19	9	-8	-6	4	20	8	-7	0	3	21	7	8	-1	4	22	12	-11	-5	1	24	3	-9
-3	6	19	9	-10	-5	4	20	11	9	-3	4	21	10	-11	0	4	22	5	-5	-2	1	24	11	-10
-2	6	19	14	18	-4	4	20	13	10	1	4	21	5	3	1	4	22	5	6	-1	1	24	15	15
-1	6	19	12	-12	-3	4	20	7	-9	2	4	21	5	5	-2	5	22	6	5	2	1	24	10	-11
0	6	19	12	-13	-2	4	20	8	-9	-5	5	21	9	-6	-1	5	22	6	-6	-5	2	24	9	-6
1	6	19	9	9	0	4	20	5	-4	-3	5	21	11	-11	1	5	22	7	-5	0	2	24	6	-5
-3	7	19	7	-8	-3	5	20	8	9	-2	5	21	14	-14	1	6	22	8	6	2	2	24	9	7
-2	7	19	6	7	1	5	20	9	-9	0	5	21	6	5	-1	7	22	9	10	-5	3	24	9	-8
0	7	19	9	-9	-1	6	20	13	12	3	5	21	9	8	1	7	22	8	-8	1	3	24	9	-8
1	7	19	8	-7	0	6	20	7	-8	-4	6	21	10	-9	-1	8	22	11	7	-2	4	24	7	-3
-3	9	19	4	-6	2	6	20	6	5	2	6	21	11	-10	-2	8	22	7	-6	0	4	24	10	11
-1	9	19	10	9	-1	7	20	11	11	-3	7	21	7	-8	-1	9	22	10	10	2	4	24	9	-9
0	9	19	10	-9	0	7	20	5	5	-2	7	21	6	5	1	9	22	9	-7	-2	6	24	7	8
1	9	19	8	8	1	7	20	5	-5	-1	7	21	6	-4	-3	10	22	6	4	-1	6	24	8	-7
-2	10	19	10	-10	2	7	20	6	5	0	8	21	6	7	-4	1	23	10	-9	0	6	24	6	6
-1	10	19	9	9	-5	8	20	9	-5	-2	9	21	13	12	-1	1	23	10	-10	1	6	24	9	7
-6	0	20	11	7	-3	8	20	7	8	0	9	21	6	-4	-5	2	23	14	13	-2	7	24	12	12
-3	0	20	14	-17	-2	8	20	7	-9	-1	10	21	7	7	-1	2	23	8	-8	0	7	24	6	-6
-6	0	20	11	7	-3	8	20	7	8	0	9	21	6	-4	-6	2	23	14	13	-2	7	24	12	12
-3	0	20	14	-17	-2	8	20	7	-9	-1	10	21	7	7	-3	2	23	8	-8	0	7	24	6	-6

H	K	L	F0	FC	H	K	L	F0	FC	H	K	L	F0	FC	H	K	L	F0	FC	H	K	L	F0	FC
-1	8	24	8	8	1	2	25	5	5	-1	0	26	6	-5	-1	5	26	7	-5	0	0	28	6	5
0	4	24	6	-5	-5	3	25	10	7	-4	1	26	11	9	1	5	26	9	10	-3	1	28	9	-7
0	1	25	6	3	-3	3	25	6	-5	0	1	26	7	-7	-1	7	26	6	-4	-1	4	28	9	9
1	1	25	6	-6	0	3	25	11	-10	-3	3	26	9	-8	-1	1	27	9	8	-1	1	29	5	3
-4	2	25	12	-11	-1	6	25	6	6	-1	3	26	7	9	0	2	27	10	10	-2	2	29	7	-7
-2	2	25	6	5	-3	0	26	9	-7	0	3	26	5	-4	-2	3	27	6	5	-1	2	29	7	5
-1	2	25	11	-10	-2	0	26	10	10	1	3	26	6	-5	-3	0	28	6	4	-2	3	29	6	-5

2-exo-bromo-3-endo-hydroxy-7,7-dichlorobicyclo[3.2.0]-
heptan-6-one (29).

Label	Value	Label	Value
C1	0.000000	C2	0.000000
C3	0.000000	C4	0.000000
C5	0.000000	C6	0.000000
C7	0.000000	C8	0.000000
C9	0.000000	C10	0.000000
C11	0.000000	C12	0.000000
C13	0.000000	C14	0.000000
C15	0.000000	C16	0.000000
C17	0.000000	C18	0.000000
C19	0.000000	C20	0.000000
C21	0.000000	C22	0.000000
C23	0.000000	C24	0.000000
C25	0.000000	C26	0.000000
C27	0.000000	C28	0.000000
C29	0.000000	C30	0.000000
C31	0.000000	C32	0.000000
C33	0.000000	C34	0.000000
C35	0.000000	C36	0.000000
C37	0.000000	C38	0.000000
C39	0.000000	C40	0.000000
C41	0.000000	C42	0.000000
C43	0.000000	C44	0.000000
C45	0.000000	C46	0.000000
C47	0.000000	C48	0.000000
C49	0.000000	C50	0.000000
C51	0.000000	C52	0.000000
C53	0.000000	C54	0.000000
C55	0.000000	C56	0.000000
C57	0.000000	C58	0.000000
C59	0.000000	C60	0.000000
C61	0.000000	C62	0.000000
C63	0.000000	C64	0.000000
C65	0.000000	C66	0.000000
C67	0.000000	C68	0.000000
C69	0.000000	C70	0.000000
C71	0.000000	C72	0.000000
C73	0.000000	C74	0.000000
C75	0.000000	C76	0.000000
C77	0.000000	C78	0.000000
C79	0.000000	C80	0.000000
C81	0.000000	C82	0.000000
C83	0.000000	C84	0.000000
C85	0.000000	C86	0.000000
C87	0.000000	C88	0.000000
C89	0.000000	C90	0.000000
C91	0.000000	C92	0.000000
C93	0.000000	C94	0.000000
C95	0.000000	C96	0.000000
C97	0.000000	C98	0.000000
C99	0.000000	C100	0.000000

FRACTIONAL ATOMIC COORDINATES X10000 WITH E.S.D.S. IN BRACKETS

	X/A	Y/B	Z/C	OCCUPANCY
C(1A)	0859(4)	1464(8)	4705(7)	
C(1B)	1195(4)	4240(8)	-0823(7)	
C(2A)	0965(4)	0273(8)	4984(7)	
C(2B)	0758(5)	3793(9)	0133(8)	
C(3A)	1579(4)	0298(8)	5201(8)	
C(3B)	1159(6)	3024(10)	0489(9)	
C(4A)	1610(6)	1438(10)	5618(9)	
C(4B)	1731(6)	3669(15)	0371(12)	
C(5A)	1316(4)	2200(9)	5056(8)	
C(5B)	1834(4)	3905(9)	-0711(9)	
C(6A)	1672(5)	2412(8)	4009(8)	
C(6B)	1713(5)	2753(8)	-1116(8)	
C(7A)	1191(4)	1829(8)	3650(8)	
C(7B)	1295(4)	3320(8)	-1609(8)	
O(1A)	2058(2)	0264(6)	4300(5)	
O(1B)	1345(3)	2193(5)	-0284(5)	
O(2A)	2138(3)	2878(6)	3584(6)	
O(2B)	2157(5)	1985(9)	-1593(9)	
BR(1A)	0320	-0103(1)	6184(1)	
BR(1B)	0428	5000(1)	1069(1)	
CL(1A)	1420(1)	0840(2)	2701(2)	
CL(1B)	1728(1)	3899(3)	-2756(2)	
CL(2A)	0763(1)	2904(2)	3270(2)	
CL(2B)	0674(1)	2558(3)	-1759(3)	
H(1A)	0410(40)	1678(69)	4879(62)	
H(1B)	1138(38)	5074(70)	-0914(67)	
H(2A)	0948(34)	-0331(64)	4416(62)	
H(2B)	0421(42)	3440(74)	0016(68)	
H(3A)	1649(47)	-0380(91)	5667(83)	
H(3B)	1050(42)	2619(76)	1143(79)	
H(5A)	1136(35)	2849(66)	5368(58)	
H(5B)	2166(32)	4417(63)	-1042(55)	
H(4A1)	2003(37)	1609(65)	5642(61)	
H(4A2)	1386(38)	1461(68)	6289(73)	
H(4B1)	1828(48)	4147(89)	0677(84)	
H(4B2)	2090(52)	3287(87)	0453(90)	
HU(1A)	1976(37)	-0451(76)	4079(66)	
HU(2B)	2222(66)	2210(114)	8042(98)	

BOND DISTANCES (\AA) WITH E.S.U.S IN BRACKETS

C(1A)	-	C(2A)	1.529(12)
C(1A)	-	C(5A)	1.572(13)
C(1A)	-	C(7A)	1.543(13)
C(1B)	-	C(2B)	1.534(13)
C(1B)	-	C(5B)	1.578(13)
C(1B)	-	C(7B)	1.551(13)
C(2A)	-	C(3A)	1.535(12)
C(2A)	-	BR(1A)	1.957(8)
C(2B)	-	C(3B)	1.503(15)
C(2B)	-	BR(1B)	1.971(10)
C(3A)	-	C(4A)	1.509(14)
C(3A)	-	O(1A)	1.424(11)
C(3B)	-	C(4B)	1.491(17)
C(3B)	-	O(1B)	1.460(12)
C(4A)	-	C(5A)	1.513(15)
C(4B)	-	C(5B)	1.531(18)
C(5A)	-	C(6A)	1.503(14)
C(5B)	-	C(6B)	1.564(13)
C(6A)	-	C(7A)	1.528(13)
C(6A)	-	O(2A)	1.198(10)
C(6B)	-	C(7B)	1.521(13)
C(6B)	-	O(1B)	1.410(10)
C(6B)	-	O(2B)	1.393(13)
C(7A)	-	CL(1A)	1.769(10)
C(7A)	-	CL(2A)	1.810(9)
C(7B)	-	CL(1B)	1.784(10)
C(7B)	-	CL(2B)	1.764(10)

BOND ANGLES (DEGREES) WITH E.S.D.'S IN BRACKETS

C(5A) - C(1A) - C(2A)	105.7(8)	CL(2A) - C(7A) - CL(1A)	108.0(5)
C(7A) - C(1A) - C(2A)	117.1(8)	C(6B) - C(7B) - C(1B)	87.3(8)
C(7A) - C(1A) - C(5A)	88.8(7)	CL(1B) - C(7B) - C(1B)	108.5(6)
C(5B) - C(1B) - C(2B)	101.1(8)	CL(1B) - C(7B) - C(6B)	110.6(6)
C(7B) - C(1B) - C(2B)	108.4(7)	CL(2B) - C(7B) - C(1B)	121.1(6)
C(7B) - C(1B) - C(5B)	87.6(7)	CL(2B) - C(7B) - C(6B)	118.2(7)
C(3A) - C(2A) - C(1A)	105.3(7)	CL(2B) - C(7B) - CL(1B)	109.3(6)
BR(1A) - C(2A) - C(1A)	108.1(6)	C(6B) - O(1B) - C(2B)	106.3(7)
BR(1A) - C(2A) - C(3A)	108.7(6)		
C(3B) - C(2B) - C(1B)	102.7(8)		
BR(1B) - C(2B) - C(1B)	111.4(7)		
BR(1B) - C(2B) - C(3B)	111.8(8)		
C(4A) - C(3A) - C(2A)	104.9(8)		
O(1A) - C(3A) - C(2A)	108.5(8)		
O(1A) - C(3A) - C(4A)	105.7(8)		
C(4B) - C(3B) - C(2B)	104.5(10)		
O(1B) - C(3B) - C(2B)	103.3(9)		
O(1B) - C(3B) - C(4B)	103.2(10)		
C(5A) - C(4A) - C(3A)	104.8(9)		
C(5B) - C(4B) - C(3B)	94.0(11)		
C(4A) - C(5A) - C(1A)	106.3(8)		
C(6A) - C(5A) - C(1A)	89.1(8)		
C(6A) - C(5A) - C(4A)	116.4(9)		
C(4B) - C(5B) - C(1B)	107.0(9)		
C(6B) - C(5B) - C(1B)	84.9(7)		
C(6B) - C(5B) - C(4B)	103.1(10)		
C(7A) - C(6A) - C(5A)	91.9(8)		
O(2A) - C(6A) - C(5A)	136.1(10)		
O(2A) - C(6A) - C(7A)	132.0(11)		
C(7B) - C(6B) - C(5B)	89.2(7)		
O(1B) - C(6B) - C(5B)	103.6(8)		
O(1B) - C(6B) - C(7B)	108.2(8)		
O(2B) - C(6B) - C(5B)	125.9(9)		
O(2B) - C(6B) - C(7B)	122.7(9)		
O(2B) - C(6B) - O(1B)	105.1(9)		
C(6A) - C(7A) - C(1A)	89.3(8)		
CL(1A) - C(7A) - C(1A)	120.7(7)		
CL(1A) - C(7A) - C(6A)	119.7(6)		
CL(2A) - C(7A) - C(1A)	110.6(6)		
CL(2A) - C(7A) - C(6A)	106.9(6)		

TOPSION ANGLES (DEGREES)

E.s.d.'s ca. 1.5°

C5A	C1A	C2A	C3A	-15.7	01R	C3B	C43	C5B	53.0
C5A	C1A	C2A	RR1A	100.2	C2B	C33	01B	C6B	66.1
C7A	C1A	C2A	C3A	81.0	C4B	C3B	01B	C6B	-42.5
C7A	C1A	C2A	BR1A	-162.9	C3A	C4A	C5A	C1A	26.3
C2A	C1A	C5A	C4A	-6.3	C3A	C4A	C5A	C6A	-71.0
C7A	C1A	C5A	C6A	111.0	C3R	C4B	C5B	C1B	43.6
C7A	C1A	C5A	C4A	-124.2	C3B	C4B	C5B	C6B	-44.9
C7A	C1A	C5A	C6A	-6.9	C1A	C5A	C6A	C7A	5.9
C2A	C1A	C7A	C6A	-100.2	C1A	C5A	C6A	02A	-175.3
C2A	C1A	C7A	CL1A	24.5	C4A	C5A	C6A	C7A	114.7
C2A	C1A	C7A	CL2A	151.9	C4A	C5A	C6A	02A	-67.5
C5A	C1A	C7A	C6A	6.7	C1R	C5B	C6B	C7B	24.7
C5A	C1A	C7A	CL1A	131.5	C1R	C5B	C6B	01B	-83.9
C5A	C1A	C7A	CL2A	-101.0	C1B	C5B	C6B	02B	155.7
C5B	C1B	C2B	C3B	-15.5	C4B	C5B	C6B	C7B	130.9
C5R	C1B	C2B	RR1B	104.2	C4B	C5B	C6B	01B	22.4
C7R	C1B	C2B	C3B	75.6	C4R	C5B	C6B	02B	-97.9
C7B	C1B	C2B	RR1R	-164.5	C5A	C6A	C7A	C1A	-7.1
C2R	C1B	C5B	C4R	-18.1	C5A	C6A	C7A	CL1A	-132.6
C2B	C1B	C5B	C6B	84.0	C5A	C6A	C7A	CL2A	104.2
C7B	C1B	C5B	C4B	-126.3	02A	C6A	C7A	C1A	175.0
C7B	C1B	C5B	C6B	-24.2	02A	C6A	C7A	CL1A	49.5
C2B	C1B	C7B	C6B	-76.0	02A	C6A	C7A	CL2A	-73.5
C2B	C1B	C7B	CL1B	173.1	C5B	C6B	C7B	C1B	-25.0
C2B	C1B	C7B	CL2B	45.6	C5B	C6B	C7B	CL1B	83.7
C5B	C1B	C7B	C6B	24.8	C5B	C6B	C7B	CL2B	-149.3
C5B	C1B	C7B	CL1B	-85.9	01B	C6B	C7B	C1B	79.0
C5B	C1B	C7B	CL2B	145.5	01B	C6B	C7B	CL1B	-172.2
C1A	C2A	C3A	C4A	32.4	01B	C6B	C7B	CL2B	-45.2
C1A	C2A	C3A	01A	-80.2	02B	C6B	C7B	C1B	-158.5
BR1A	C2A	C3A	C4A	-83.2	02B	C6B	C7B	CL1B	-49.7
BR1A	C2A	C3A	01A	164.1	02B	C6B	C7B	CL2B	77.2
C1B	C2B	C3B	C4B	46.2	C5R	C6B	01B	C3B	11.1
C1B	C2B	C3B	01B	-61.4	C7B	C6B	01B	C3B	-82.5
PR1B	C2B	C3B	C4B	-73.3	02B	C6B	01B	C3B	144.8
BR1B	C2B	C3B	01B	178.9					
C2A	C3A	C4A	C5A	-36.4					
01A	C3A	C4A	C5A	78.0					
C2B	C3B	C4B	C5B	-54.7					

ISOTROPIC PARAMETERS X1000 WITH E.S.D.'S IN BRACKETS

THE EXPRESSION FOR THE TEMPERATURE FACTOR IS

EXP(-B*PI*PI*U11*SINSQTHETA/LAMBDAQ)

H(1A)	0449(274)
H(1B)	0528(280)
H(2A)	0343(255)
H(2B)	0566(323)
H(3A)	1003(411)
H(3B)	0470(307)
H(5A)	0270(230)
H(5B)	0184(205)
H(4A1)	0409(255)
H(4A2)	0443(299)
H(4B1)	0586(417)
H(4B2)	0693(395)
H(1A)	1146(288)
H(2B)	0315(585)

ANISOTROPIC THERMAL PARAMETERS X10000 WITH E.S.O.S IN BRACKETS
 THE EXPRESSION FOR THE TEMPERATURE FACTOR IS $\text{EXP}(-2*\text{PI}*\text{PI}*(\text{H}*\text{H}*\text{ASTAR}*\text{ASTAR}*\text{U11} +$
 $+2*\text{K}*\text{L}*\text{BSTAR}*\text{CSTAR}*\text{U23}))$

	U11	U22	U33	U23	U13	U12
C(1A)	0334(56)	0496(56)	0287(71)	-0045(51)	-0051(51)	0106(50)
C(1B)	0369(53)	0278(57)	0459(76)	0099(53)	-0031(50)	-0058(44)
C(2A)	0274(44)	0441(65)	0220(64)	0001(48)	-0001(41)	-0050(42)
C(2B)	0412(60)	0437(64)	0374(76)	-0134(54)	-0032(54)	-0024(52)
C(3A)	0405(52)	0465(72)	0290(70)	-0072(53)	-0086(48)	0026(49)
C(3B)	0814(94)	0576(74)	0254(84)	0106(66)	-0062(68)	0087(70)
C(4A)	0467(71)	0732(85)	0290(84)	-0053(64)	-0201(64)	-0119(63)
C(4B)	0517(84)	0924(121)	0738(143)	-0255(100)	-0319(85)	0182(83)
C(5A)	0407(57)	0502(71)	0244(75)	-0175(55)	-0025(54)	0150(52)
C(5B)	0292(57)	0561(79)	0550(99)	0061(66)	0007(55)	-0098(55)
C(6A)	0418(61)	0340(60)	0510(83)	-0082(54)	-0147(61)	0054(48)
C(6B)	0451(62)	0380(65)	0351(74)	0039(52)	-0061(55)	0050(50)
C(7A)	0326(52)	0532(70)	0339(74)	-0033(53)	-0144(50)	0091(47)
C(7B)	0352(57)	0464(69)	0453(79)	0028(56)	0049(53)	0020(47)
0(1A)	0314(51)	0479(52)	0492(49)	-0031(39)	0013(30)	0035(33)
0(1B)	0799(55)	0371(43)	0347(52)	0115(37)	0094(43)	0024(37)
0(2A)	0405(43)	0555(46)	0614(56)	-0046(41)	-0075(41)	-0095(38)
0(2B)	0696(59)	0529(56)	0507(79)	0089(58)	0003(55)	0251(45)
BR(1A)	0388(5)	0834(9)	0417(9)	0174(7)	-0009(5)	-0057(6)
BR(1B)	0561(7)	0588(7)	0563(9)	-0217(7)	-0013(6)	-0015(6)
CL(1A)	0617(17)	0702(20)	0355(19)	-0144(15)	-0089(14)	-0003(15)
CL(1B)	0767(20)	0722(21)	0388(21)	0172(16)	0009(16)	0157(17)
CL(2A)	0568(17)	0622(19)	0572(22)	0142(16)	-0203(16)	0085(15)
CL(2B)	0478(17)	1105(27)	0717(26)	-0437(21)	-0145(17)	-0073(16)

Table with 10 columns: H, K, L, FO, FC for five groups. Each group contains multiple rows of numerical data.

Table with 10 columns: H, K, L, FO, FC for five groups. Each group contains multiple rows of numerical data.

